ESCUELA DE DOCTORADO
INTERNACIONAL DE LA USC

Pablo
Ventoso Osorio

Tesis doctoral

Análisis transcriptómico de la respuesta frente a la exposición al ácido domoico (toxina de tipo amnésico, ASP), y a *Pseudo-nitzschia* productora de ácido domoico, en la glándula digestiva de moluscos bivalvos

Santiago de Compostela, 2024

Programa de doctorado en Ciencias Marinas, Tecnología y Gestión

ESCOLA DE DOUTORAMENTO INTERNACIONAL DA USC

TESIS DOCTORAL

ANÁLISIS TRANSCRIPTÓMICO DE LA RESPUESTA FRENTE A LA EXPOSICIÓN AL ÁCIDO DOMOICO (TOXINA DE TIPO AMNÉSICO, ASP), Y A *PSEUDO-NITZSCHIA* PRODUCTORA DE ÁCIDO DOMOICO, EN LA GLÁNDULA DIGESTIVA DE MOLUSCOS BIVALVOS

Autor

Pablo Ventoso Osorio

Director: Antonio Juan Pazos Castelos

Tutor/a: Antonio Juan Pazos Castelos

PROGRAMA DE DOCTORADO EN CIENCIAS MARINAS, TECNOLOGÍA Y GESTIÓN

SANTIAGO DE COMPOSTELA

FINANCIACIÓN

Parte del trabajo de esta tesis ha sido financiado por el Ministerio de Economía y Competitividad (MINECO) del Gobierno de España y los fondos FEDER (Fondo Europeo de Desarrollo Regional) de la Unión Europea en el marco del proyecto AGL2012-39972-C02.

AGRADECIMIENTOS

Este proyecto de tesis no sería posible sin la inestimable contribución de mi director Antonio J. Pazos Castelos. Gracias Antonio por la guía, el constante apoyo y la paciencia durante todo este proyecto.

Es importante destacar el papel fundamental desempeñado por Juan Blanco, responsable de realizar los ensayos de intoxicación y cuantificación de la concentración de ácido domoico y en cuya obra se sostiene esta tesis.

También quiero agradecer a José L. Sánchez y M. Luz Pérez-Parallé, la oportunidad de unirme al departamento de Biología Molecular y toda la ayuda y orientación recibida.

Otro de los actores clave en este proyecto es Roi Martínez-Escauriaza, cuyo soporte en el desarrollo de los experimentos de laboratorio fue determinante.

Finalmente, agradecer a Jina y a mis padres su constante aliento y, al pequeño Pablo en camino, que se porte tan bien mientras escribo estas últimas líneas.

RESUMEN

La intoxicación amnésica por mariscos (ASP) es causada por diatomeas del género *Pseudo-nitzschia*, que producen la toxina ácido domoico. Los bivalvos son organismos filtradores que pueden acumular biotoxinas en sus tejidos durante los episodios tóxicos fitoplanctónicos por floraciones de algas nocivas (*Harmful Algal Blooms*), siendo la glándula digestiva el órgano en el que se acumula la mayor parte del ácido domoico. El conocimiento a nivel molecular de los efectos del ácido domoico y de los mecanismos implicados su captación y excreción es limitado en los moluscos bivalvos. Para ayudar a esclarecer estos procesos se ha empleado un enfoque basado en la secuenciación (Illumina *paired-end*) y ensamblaje *de novo* del transcriptoma en la glándula digestiva de tres especies de moluscos bivalvos: el mejillón (*Mytilus galloprovincialis*), la volandeira (*Aequipecten opercularis*) y la vieira (*Pecten maximus*). Posteriormente se analizó la expresión génica diferencial tras la inyección de ácido domoico (en la vieira) o la exposición a *Pseudo-nitzschia* productora de ácido domoico (en el mejillón y en la volandeira), en comparación con animales no expuestos. La hipótesis de partida es que las alteraciones en la expresión génica son útiles para ayudar a esclarecer los posibles efectos de la toxina, los mecanismos moleculares implicados y los mecanismos de desintoxicación. Para este fin, tras la anotación funcional de los genes (con Blastx), el estudio del enriquecimiento funcional (de términos GO de ontología génica y de dominios PFAM) y de las redes de interacciones proteína-proteína (obtenidas con el algoritmo String) permite analizar qué procesos (biológicos, celulares y moleculares) están alterados por la exposición al ácido domoico. Algunos resultados son coincidentes en las especies estudiadas (sobre todo en *M. galloprovincialis* y *A. opercularis*): la sobreexpresión de genes que codifican para enzimas implicadas en el metabolismo de xenobióticos (citocromos P450, aldo/ceto reductasas, glutatión S-transferasas y sulfotransferasas) y para transportadores transmembrana de la superfamilia SLC (transportadores de solutos), la expresión diferencial de genes relacionados con la respuesta inmune (generalmente infraexpresados), la respuesta frente al estrés y la apoptosis. Los resultados indican que uno de los principales efectos en estos bivalvos de la exposición al ácido domoico, y a *Pseudo-nitzschia* productora de ácido domoico, es el estrés oxidativo y una parte de los genes diferencialmente expresados están implicados en la respuesta frente a dicho estrés. Esto es especialmente claro en *A. opercularis* con la sobreexpresión de genes que codifican para proteínas mitocondriales, componentes del proteasoma y enzimas antioxidantes. En *P. maximus* las redes de interacciones entre proteínas obtenidas con los genes sobreexpresados están enriquecidas en términos de GO tales como transporte mediado por vesículas, respuesta frente al estrés, transducción de señales, procesos del sistema inmune, procesos metabólicos del ARN, autofagia, lisosoma y actividad oxidorreductasa, evidenciando una respuesta de estrés tras la inyección de ácido domoico. En la glándula digestiva de las tres especies hay expresión de genes que codifican para receptores de glutamato, tanto ionotrópicos como metabotrópicos, por lo que parte de las acciones del ácido domoico pueden estar mediadas por estos receptores.

ÍNDICE

1 INTRODUCCIÓN

La clase Bivalvia es una de las ocho clases del *phylum Mollusca* (Gosling, 2015). Dentro de los moluscos bivalvos se encuentran algunas especies importantes en acuicultura como los mejillones, ostras, vieiras, almejas y berberechos. La acuicultura de los moluscos bivalvos tiene especial importancia en Galicia, como se detalla más adelante. Los bivalvos tienen también gran importancia ecológica en el medio marino, pues impactan el ciclo de nutrientes, crean y modifican el hábitat y afectan a las redes alimentarias directa e indirectamente (Vaughn and Hoellein, 2018). Una gran parte de los bivalvos son animales filtradores sésiles o sedentarios, que están en constante contacto con el agua, por ello los materiales acumulados en los tejidos blandos y en la concha se utilizan como centinelas e indicadores de los cambios ambientales (Vaughn and Hoellein, 2018). Por ser filtradores, los bivalvos pueden acumular biotoxinas en sus tejidos durante los episodios tóxicos fitoplanctónicos por floraciones de algas nocivas (Harmful Algal Blooms). Las toxinas de origen fitoplanctónico se acumulan en los tejidos de los moluscos bivalvos, sobre todo en la glándula digestiva, y cuando estos mariscos son consumidos por los humanos pueden tener efectos adversos en la salud humana causando intoxicaciones alimentarias (FAO, 2004; Lawrence et al., 2011; Paredes et al., 2011). Esta acumulación de biotoxinas tiene también un impacto económico adverso en la explotación de los recursos acuícolas, debido a la prohibición de la extracción y comercialización de los bivalvos (FAO, 2004; Lawrence et al., 2011; Paredes et al., 2011).

Los aspectos que van a ser tratados brevemente en esta introducción son: la importancia de la acuicultura en general, pero especialmente la acuicultura de los moluscos bivalvos en el mundo, en España y en Galicia, la biología de los moluscos bivalvos, sobre todo en lo que concierne a los procesos de alimentación y de excreción; los episodios tóxicos de origen fitoplanctónico y las biotoxinas e intoxicaciones asociadas, especialmente aquellas en las que los bivalvos son el principal vector; el metabolismo de los xenobióticos y, por último, la justificación de la unidad y coherencia temática y metodológica de la tesis.

1.1 LA ACUICULTURA EN ESPAÑA Y EL MUNDO

La acuicultura a nivel mundial está adquiriendo en los últimos años una importancia cada vez mayor en la producción de alimentos de origen acuático, así en 2021 se ha alcanzado una cifra récord, pues el 50% de la producción de especies acuáticas provino de la acuicultura (FAO, 2024), el otro 50% corresponde a la pesca o captura. Parece además que esta tendencia se va a mantener en los próximos años.

La producción mundial de la acuicultura alcanzó un récord de producción en 2021 de alrededor de 126 millones de toneladas de peso vivo, de los cuales 91 millones de toneladas corresponden a animales acuáticos y 35 millones a algas (FAO, 2024). Los principales productores mundiales de animales acuáticos mediante acuicultura son los países asiáticos, pues China ocupa el primer lugar seguida de India e Indonesia. La producción de China

supone un 56% del total mundial. Si nos referimos a la producción per cápita (kg por persona) Asia ocupa también el primer lugar con algo más de 15 kg por persona, estando Europa en la tercera posición con unos 5 kg por persona (FAO, 2024).

Dentro de Europa, España ocupaba en 2021 el tercer puesto en la acuicultura de animales acuáticos con 280000 toneladas, (que suponen un 7,8% del total europeo) situándose tras Noruega y la Federación Rusa (FAO, 2024). España es dentro de Europa el primer importador y el cuarto exportador de animales acuáticos (calculado por el valor expresado en dólares de EE. UU.). El consumo per cápita de alimentos de origen acuático en España fue en 2019 de unos 40,4 kg/año, ocupando el quinto puesto en Europa, este consumo es aproximadamente el doble de la media europea (21,7 kg/año) y de la media mundial (20,5 kg/año) (FAO, 2024).

El cultivo de moluscos bivalvos ocupa un lugar importante en la producción acuícola mundial, de hecho, si nos referimos a la producción de animales marinos en 2021 el primer lugar lo ocupan los moluscos con unos 18,5 millones de toneladas de peso vivo, seguidos de peces y crustáceos (FAO, 2024). La producción acuícola de moluscos creció un 34% desde 2011, cuando la producción acuícola de moluscos era de 13,8 millones de toneladas. Dentro de los moluscos el primer puesto corresponde a las ostras seguidas de las almejas y los mejillones.

En España la producción total de animales acuáticos (por acuicultura) en 2021 fue de 279880 toneladas, repartida de la siguiente manera: moluscos 206371, peces marinos 51752, Peces diádromos 18477, crustáceos 3273, y peces de agua dulce 7 (FAO, 2024). Por tanto, el primer puesto corresponde claramente a los moluscos bivalvos. Dentro de los moluscos el primer puesto corresponde a los mejillones (203226 toneladas) seguidos a gran distancia por el grupo de almejas y berberechos (1703 toneladas) y ostras (1432 toneladas) y pectínidos (5 toneladas) (FAO, 2024).

Según la Asociación Empresarial de Acuicultura de España (APROMAR, 2023) en 2021 había 5.182 establecimientos de acuicultura en España (4.928 de moluscos y 254 de peces). (APROMAR, 2023) cifra la producción de la acuicultura en España en 2022 en 326.520 toneladas con un valor en primera venta de 760,7 millones de euros, siendo la especie más abundante el mejillón con 255.218 toneladas y con un valor estimado de 159,3 millones de euros. El siguiente grupo de moluscos en cantidad producida son las ostras, pues la producción conjunta de ostra plana (*Ostrea edulis*) y ostra japonesa (*Magallana gigas*) en 2022 ascendió a 1.463 toneladas (APROMAR, 2023), siendo Galicia la principal comunidad autónoma productora. Por su parte, la producción conjunta de almejas fina (*Ruditapes decussatus*), japonesa (*Ruditapes philippinarum*) y babosa (*Venerupis corrugata*) en 2022 fue de 993 toneladas (APROMAR, 2023), de las que la mayor parte corresponde a la almeja japonesa (725 toneladas). En la producción de almejas se evidenció un notable descenso respecto al año anterior (2021) en el que la producción total fue de 1.752 toneladas (APROMAR, 2022). La producción europea de moluscos de acuicultura está liderada por España y ha permanecido prácticamente constante en la última década, dentro de España Galicia es la principal comunidad autónoma productora (APROMAR, 2023).

Los datos anteriormente citados evidencian la importancia de la producción acuícola de moluscos bivalvos en España, siendo también destacable que el principal productor dentro de

España es Galicia, así, por ejemplo, la producción gallega de mejillón representa el 97 % del total nacional (APROMAR, 2023).

1.2 LOS MOLUSCOS BIVALVOS

Los moluscos son animales de cuerpo blando pero protegido en la mayor parte de los casos por una concha dura. El *phylum Mollusca* es uno de los más grandes y diversos del reino animal, en concreto es el segundo más extenso tras el *phylum Arthropoda*. La clase *Bivalvia* es una de las ocho clases de moluscos, y es la segunda mayor clase dentro del *phylum Mollusca* (Gosling, 2015). Los bivalvos tienen dos valvas conectadas por un ligamento elástico, los músculos aductores mantienen unidas las valvas, y la relajación del ligamento y la contracción de estos músculos abren y cierran las valvas, respectivamente (Gosling, 2015). Pertenecen a esta clase especies importantes desde el punto de vista de la alimentación humana como los mejillones, ostras, almejas, berberechos o vieiras. Una parte de los bivalvos son sésiles (mejillones y ostras, por ejemplo) mientras que otros tienen una cierta capacidad de movimiento (almejas y pectínidos por ejemplo).

Entre las partes que componen el cuerpo de los bivalvos podemos citar la concha, el manto, las branquias, el pie y los músculos aductores; además están los órganos internos menos visibles como el aparato circulatorio (corazón y vasos hemolinfáticos), aparato excretor (riñones y glándulas pericárdicas), aparato digestivo (palpos labiales, boca, esófago, estómago, intestino, glándula digestiva), aparato reproductor (gónadas) y sistema nervioso (ganglios y nervios).

La concha de los bivalvos contiene un 95% de materia inorgánica (carbonato cálcico principalmente), el 5 % restante está formado por proteínas y el polisacárido quitina(Gosling, 2015). En los mejillones, las dos valvas son de tamaño similar y tienen una forma aproximadamente triangular mientras que en los pectínidos tienen una forma casi circular.

Por su importancia para el proceso de intoxicación-desintoxicación describiremos a continuación los procesos de alimentación y de excreción en los bivalvos. En cuanto a su alimentación, aunque algunos bivalvos son detritívoros, la mayoría utiliza superficies branquiales para filtrar las partículas de alimento del agua circundante, son por tanto filtradores (o suspensívoros). Esto implica que bombean grandes volúmenes de agua para alimentarse, lo que puede conducir a que se produzca, en determinadas circunstancias, una acumulación de microorganismos (bacterias, virus), contaminantes antropogénicos y organismos tóxicos (Gosling, 2015). La comida de los bivalvos se compone de una variedad de partículas en suspensión, fitoplancton principalmente, pero también bacterias, microzooplancton y detritos. La materia orgánica disuelta (aminoácidos, azúcares…) también es utilizada como alimento.

Las branquias además de su función respiratoria tienen también un papel en la alimentación de los moluscos bivalvos (Gosling, 2015; Morton, 1983) pues filtran y seleccionan las partículas de alimento del medio (principalmente fitoplancton y materia orgánica en suspensión) y pueden también absorber sustancias disueltas. En los moluscos lamelibranquios las branquias reemplazan a los palpos como órganos de alimentación pues se alimentan utilizando la corriente entrante como fuente de alimento (Gosling, 2015). Es lo que se denomina alimentación por suspensión o filtración pues las branquias captan las partículas

suspendidas del agua bombeada a través de la cavidad del manto ayudándose de los diversos tractos ciliares.

Las branquias, o ctenidia, son dos estructuras grandes en forma de cortina formadas por numerosos filamentos en forma de W y dividen la cavidad del manto en las cámaras exhalante e inhalante (Gosling, 2015). Con la ayuda de los cilios laterales, frontales y latero-frontales de las branquias las partículas de alimento son captadas, seleccionadas y conducidas hacia los surcos alimentarios ciliados (Gosling, 2015) que a su vez las dirigen hacia los palpos labiales y la boca. Cada branquia termina en un par de palpos labiales triangulares situados a cada lado de la boca. La función principal de los palpos labiales es eliminar continuamente material de los tractos alimentarios de las branquias para evitar la saturación de las branquias. Cuando la concentración de partículas es alta una parte de éstas son envueltas en mucus y expulsadas al exterior en forma de pseudoheces, mientras que el resto de las partículas son dirigidas hacia la boca. Pero las pseudoheces pueden proceder también de una selección cualitativa y de tamaño (eliminar partículas en función de su tamaño o composición), así los bivalvos son capaces de seleccionar preferentemente partículas nutritivas, como las microalgas, y rechazar las partículas de poco valor nutritivo en sus pseudoheces. Las partículas que entran por la boca, tras un corto paso por el esófago, alcanzan el estómago. Tanto la boca como el esófago son ciliados, y estos cilios contribuyen al movimiento de los alimentos hacia el estómago (Gosling, 2015).

El estómago tiene generalmente una forma oval y está rodeado por la glándula digestiva. La digestión tiene lugar en dos fases, una fase extracelular en el estómago, y otra intracelular en los divertículos digestivos que se abren lateralmente desde el estómago (Morton, 1983). En la digestión extracelular interviene el estilo cristalino, una varilla gelatinosa secretada por el saco del estilo. La acción de los cilios del saco hace que el estilo cristalino rote sobre el escudo gástrico, compuesto por quitina, este proceso por una parte tritura las partículas de alimento, y por otra libera las enzimas digestivas contenidas en el estilo (que actúan principalmente sobre los carbohidratos), produciéndose así la digestión extracelular. Tras ésta, parte del material (las partículas más grandes y las más densas) pasa directamente al intestino para ser eliminado como heces, mientras que otra parte (las partículas más finas y la materia digerida) se mantienen en suspensión con la ayuda de los cilios y se transfiere a través de un sistema de conductos hasta los divertículos digestivos (de la glándula digestiva) donde tiene lugar la digestión intracelular.

La glándula digestiva se compone de numerosos túbulos digestivos de fondo ciego, que se conectan con el estómago a través de conductos ciliados en los que hay un flujo en las dos direcciones, desde el estómago hacia la glándula digestiva para la digestión intracelular y los productos de desecho de dicha digestión van hacia el estómago e intestino para su eliminación en las heces (Beninger and Le Pennec, 2016; Gosling, 2015; Owen, 1955). Los productos finales de la digestión se absorben en la glándula digestiva. Los túbulos digestivos se componen principalmente de dos tipos de células: las digestivas y las secretoras, también denominadas basófilas (Beninger and Le Pennec, 2016; Blanco et al., 2020; Gosling, 2015; Morton, 1983; Weinstein, 1995).

Las células digestivas captan las partículas de alimento por endocitosis y las almacenan en vesículas (fagosomas) hasta que son digeridas en los lisosomas, que contienen numerosas enzimas hidrolíticas y los productos finales de la digestión pasan al sistema hemolinfático

(Beninger and Le Pennec, 2016; Gosling, 2015; Morton, 1983; Weinstein, 1995). Los productos de desecho se retienen en cuerpos residuales que luego se liberan en la luz de los túbulos (Gosling, 2015). Las células digestivas juegan un papel importante también en los procesos de desintoxicación y en la biotransformación de los xenobióticos. Las células secretoras (basófilas) tienen su citoplasma ocupado en gran medida por el retículo endoplásmico rugoso y el aparato de Golgi, lo que indica un nivel alto de síntesis de proteínas, probablemente implicado en la secreción de enzimas para la digestión extracelular (Gosling, 2015; Weinstein, 1995).

Tanto las partículas rechazadas en el estómago como el material de desecho procedente de la glándula digestiva se eliminan a través del ano tras su paso por el intestino. Éste no es únicamente un lugar de paso, sino que puede jugar un papel activo en la digestión extracelular y en la absorción de nutrientes (Beninger and Le Pennec, 2016).

El aparato excretor de los bivalvos está formado por las glándulas pericárdicas y dos riñones. Los productos de desecho se acumulan en determinadas células de las glándulas pericárdicas y periódicamente se transfieren a la cavidad pericárdica, desde donde fluyen hacia los riñones. La hemolinfa se filtra desde las aurículas hasta la cavidad pericárdica a través de numerosos podocitos presentes en las glándulas pericárdicas (Beninger and Le Pennec, 2016; Jones, 1983). Este filtrado pasa de la cavidad pericárdica al riñón, donde tienen lugar los procesos de secreción y reabsorción, el producto final de estos procesos es la orina (Andrews, 1988; Andrews and Jennings, 1993; Gosling, 2015; Pirie and George, 1979).

1.3 LAS PROLIFERACIONES ALGALES NOCIVAS Y LAS BIOTOXINAS MARINAS

De las en torno a 5.000 especies marinas de fitoplancton existentes, aproximadamente 300 pueden, a veces, presentarse en cantidades tan elevadas (floraciones) para producir las denominadas “mareas rojas” (FAO, 2004; Hallegraeff, 2003; Hallegraeff et al., 1995), pero solo unas 80 especies son capaces de producir toxinas potentes que pueden afectar a los humanos tras el paso por mariscos y peces (Hallegraeff, 2003). El término marea roja puede resultar confuso, pues el color no siempre es rojo, por ello se generalizó a episodios de especies tóxicas, que no implican dar color al agua, pues el hecho de la coloración y la toxicidad no están siempre unidos. Posteriormente una nueva generalización condujo a la denominación empleada actualmente de proliferaciones algales nocivas (*Harmful Algal Blooms*, HABs*)* que se refiere a proliferaciones que producen daños a las personas, a sus actividades (pesca, marisqueo y acuicultura entre otras) o a los ecosistemas acuáticos. Así la Environmental Protection Agency de los EE. UU. dice que las proliferaciones algales nocivas representan un riesgo para las personas, los animales, los ecosistemas acuáticos, la economía, los suministros de agua potable, los valores de las propiedades, la pesca comercial e industrial y las actividades recreativas como la natación.

Algunas de estas proliferaciones algales nocivas son tóxicas, se acumulan en los organismos que las consumen y pueden producir efectos adversos en la salud humana. Los bivalvos que se alimentan por filtración acumulan las toxinas en sus tejidos y, por lo tanto, son los principales vectores de las toxinas que produce el fitoplancton. Estas proliferaciones también son nocivas porque pueden afectar a las explotaciones acuícolas y a las poblaciones naturales de organismos marinos. En los últimos años la aparición de este tipo de episodios ha aumentado en frecuencia, intensidad y distribución geográfica (Gobler, 2020).

En función de los efectos biológicos que producen, y de su estructura química, las biotoxinas marinas responsables de los episodios tóxicos se pueden clasificar en varios grupos, que se describen brevemente a continuación tomando como referencia principalmente algunas de las revisiones publicadas sobre el tema en los últimos 20 años (Basti et al., 2018; Brown et al., 2020; EFSA, 2009; FAO, 2004; Farabegoli et al., 2018; Hallegraeff, 2003; Lawrence et al., 2011; Louzao et al., 2022; Paredes et al., 2011; Pinto et al., 2023; Pulido, 2016; Rasmussen et al., 2016; Visciano et al., 2016; Young et al., 2020). En la descripción las separamos en dos categorías, las toxinas reglamentadas en la Unión Europea y las toxinas emergentes.

1.3.1 Toxinas reglamentadas

Se incluyen aquí las toxinas que están reguladas en la Unión Europea: las saxitoxinas (STX), el ácido domoico (DA), el ácido okadaico (OA) y análogos (dinofisistoxinas, DTX), los azaspirácidos (AZA) y las yesotoxinas (YTX).

1.3.1.1 Toxinas responsables de las intoxicaciones paralizantes (PSP, Paralytic Shellfish Poisoning)

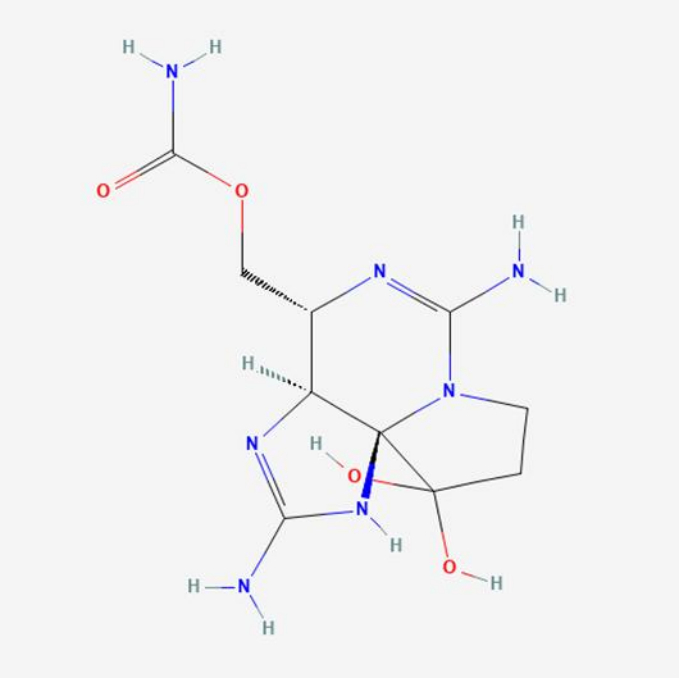

Figura 1.1. Estructura de la saxitoxina. Obtenida de PubChem, Identifier: CID 56947150; URL: https://pubchem.ncbi.nlm.nih.gov/compound/56947150#section=2D-Structure

Son un grupo de tetrahidropurinas siendo su principal representante la saxitoxina (STX) que fue también la primera toxina de este grupo caracterizada (FAO, 2004; Schantz et al., 1958, 1957). Las toxinas causantes de PSP son producidas principalmente por dinoflagelados del género *Alexandrium* y en menor medida de los géneros *Gymnodinium* y *Pyrodinium*. También pueden ser producidas por algunos géneros de cianobacterias de agua dulce (Basti et al., 2018; FAO, 2004). Los síntomas leves de la PSP incluyen el hormigueo o entumecimiento en labios, boca, cara y cuello junto a dolor de cabeza y mareos, pudiendo evolucionar a debilidad

muscular, ataxia, dificultad respiratoria y en los casos más graves muerte por parálisis respiratoria (Basti et al., 2018; Lawrence et al., 2011). Las saxitoxinas provocan un bloqueo de los canales de sodio dependientes de voltaje y, por lo tanto, un bloqueo de la despolarización de la membrana que impide la transmisión de los impulsos nerviosos.

1.3.1.2 Toxinas responsables de las intoxicaciones amnésicas (ASP, Amnesic Shellfish Poisoning)

El ácido domoico, un aminoácido tricarboxílico análogo del neurotransmisor glutamato (ácido glutámico), es la principal toxina de este grupo. Hay varios isómeros del ácido domoico, pero la mayoría de ellos son menos tóxicos que éste (Blanco et al., 2021b; Munday et al., 2008). Aunque fue aislado inicialmente a partir de un alga roja *Chondria armata* (Takemoto and Daigo, 1958) lo producen también diversas especies de los géneros *Pseudo-nitzschia* y *Nitzschia* (Bates et al., 2018, 1989). Por ser la toxina implicada en esta tesis la tratamos de forma más extensa en una sección posterior.

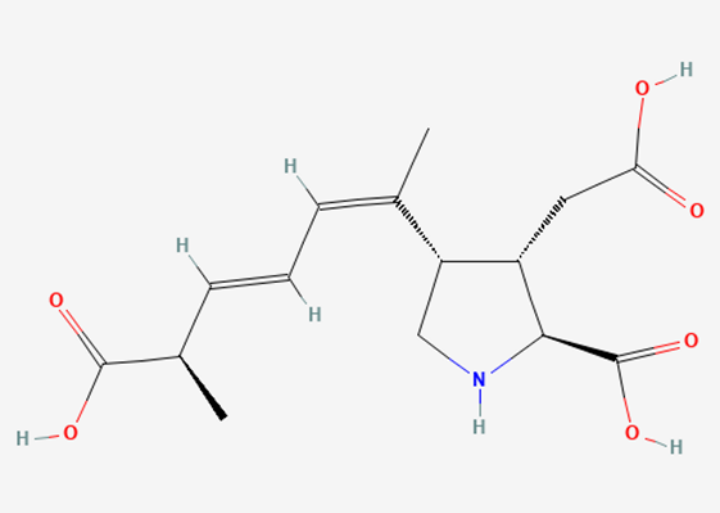

Figura 1.2. Estructura del ácido domoico. Obtenida de PubChem, Identifier: CID 5282253; URL: https://pubchem.ncbi.nlm.nih.gov/compound/5282253#section=2D-Structure

1.3.1.3 Toxinas lipofílicas responsables de las intoxicaciones diarreicas (DSP, Diarrhetic Shellfish Poisoning)

Los principales responsables son el ácido okadaico (OA) (Tachibana et al., 1981), primer compuesto identificado como causante de este tipo de toxicidad, y sus derivados las dinofisistoxinas (DTX). Los principales productores son dinoflagelados de los géneros *Dinophysis* y *Prorocentrum* (Blanco, 2018; Lawrence et al., 2011). Este grupo originalmente estaba compuesto a su vez por tres grupos de toxinas lipofílicas: el ácido okadaico (OA) y sus análogos las dinofisistoxinas (DTX), las yesotoxinas (YTX) y las pectenotoxinas (PTX) (Basti et al., 2018) aunque actualmente tanto las yesotoxinas como las pectenotoxinas ya no forman parte del grupo de toxinas diarreicas ya que nunca se ha informado de intoxicación diarreica humana asociada con estas toxinas (Lawrence et al., 2011). Las toxinas del grupo del ácido okadaico son producidas principalmente por dinoflagelados pertenecientes a los géneros *Dinophysis* y *Prorocentrum* (FAO, 2004).

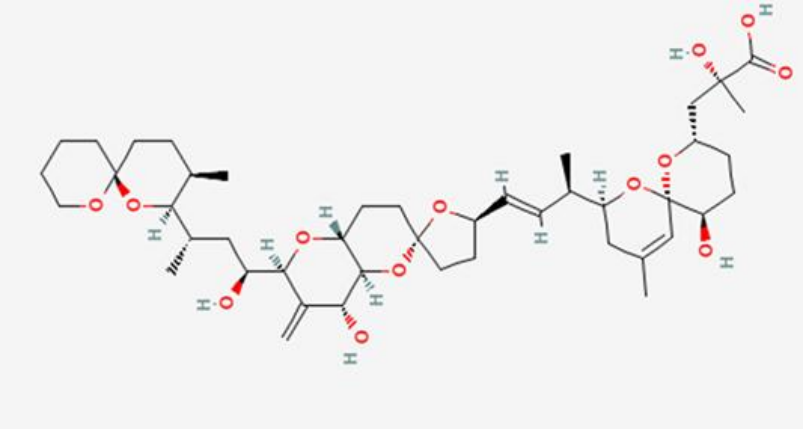

Figura 1.3. Estructura del ácido okadaico. Obtenida de PubChem, Identifier: 446512; URL: https://pubchem.ncbi.nlm.nih.gov/compound/446512#section=2D-Structure

Los síntomas de la intoxicación diarreica por mariscos (DSP) aparecen en una hora tras la ingestión de mariscos contaminados y afectan el tracto gastrointestinal con náuseas, vómitos, calambres abdominales y diarrea (FAO, 2004), estos síntomas generalmente desaparecen a los pocos días. No se ha registrado ninguna muerte a causa de DSP. En cuanto al mecanismo de acción, el ácido okadaico inhibe fuertemente las serina/treonina fosfatasas 1 (PP1) y 2A (PP2A) (Paredes et al., 2011), estas enzimas catalizan la desfosforilación de numerosas proteínas y juegan por ello un papel importante en la regulación de diversos procesos celulares (metabolismo, transporte transmembrana, apoptosis…), pues los procesos de fosforilación/desfosforilación son una forma de regular la actividad de dichas proteínas.

1.3.1.4 Intoxicación por azaspirácidos (AZP, Azaspiracid Shellfish Poisoning)

Los azaspirácidos son poliéteres lipófilos que contienen anillos de tipo espiro, una amina heterocíclica y un ácido carboxílico (Otero and Silva, 2022). Son producidos por dinoflagelados de los géneros *Azadinium* y *Amphidoma* (Basti et al., 2018; Krock et al., 2012; Otero and Silva, 2022; Tillmann et al., 2012, 2009; Visciano et al., 2016). Los síntomas de la intoxicación por azaspirácidos (AZP) son muy similares a los descritos para DSP, incluyendo náuseas, vómitos, calambres abdominales y diarrea, que desaparecen a los pocos días (Lawrence et al., 2011). El mecanismo de acción de estas toxinas todavía no se ha dilucidado.

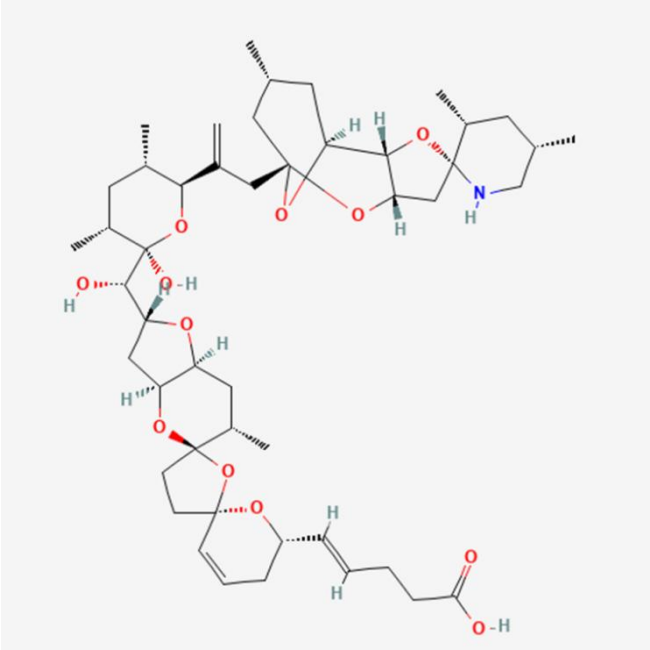

Figura 1.4. Estructura del azaspirácido 1. Obtenida de PubChem, Identifier: 21593892; URL: https://pubchem.ncbi.nlm.nih.gov/compound/21593892#section=2D-Structure

1.3.1.5 Yesotoxinas (YTX)

La yesotoxina (YTX) y sus análogos son un grupo de poliéteres sulfatados aislados a partir de la glándula digestiva de la vieira *Mizuhopecten yessoensis* (Murata et al., 1987). Son producidos dinoflagelados de los géneros *Gonyaulax*, *Protoceratium* y *Lingulaulax* (Lawrence et al., 2011). Son tóxicas en ratones por inyección intraperitoneal y muestran también citotoxicidad (Paz et al., 2008) pero el mecanismo de acción no se conoce bien.

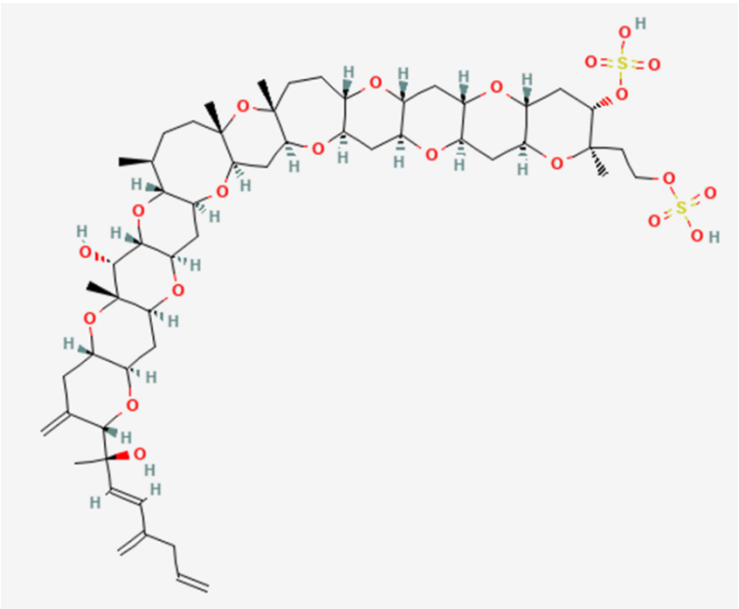

Figura 1.5. Estructura de la yesotoxina. Obtenida de PubChem, Identifier: 6440821 URL: https://pubchem.ncbi.nlm.nih.gov/compound/6440821#section=2D-Structure

1.3.2 Toxinas emergentes

En este apartado están recogidas algunas de las toxinas emergentes de origen fitoplanctónico.

1.3.2.1 Toxinas responsables de las intoxicaciones neurotóxicas (NSP, Neurotoxic Shellfish Poisoning)

Los principales responsables de la intoxicación neurotóxica por mariscos (NSP) son un grupo de poliéteres policíclicos liposolubles denominados brevetoxinas (Lin et al., 1981; Shimizu et al., 1986), producidos principalmente por dinoflagelados de la especie *Karenia brevis.* Los síntomas de NSP incluyen dolor abdominal, náuseas, vómitos, diarrea, dolor de cabeza, vértigo, parestesia, calambres, broncoconstricción, parálisis, convulsiones y coma (Basti et al., 2018; Paredes et al., 2011). Las brevetoxinas son sustancias despolarizantes pues abren los canales iónicos de sodio (Na^+) dependientes de voltaje en las membranas celulares (FAO, 2004) lo que incrementa el flujo de iones Na^+ hacia la célula.

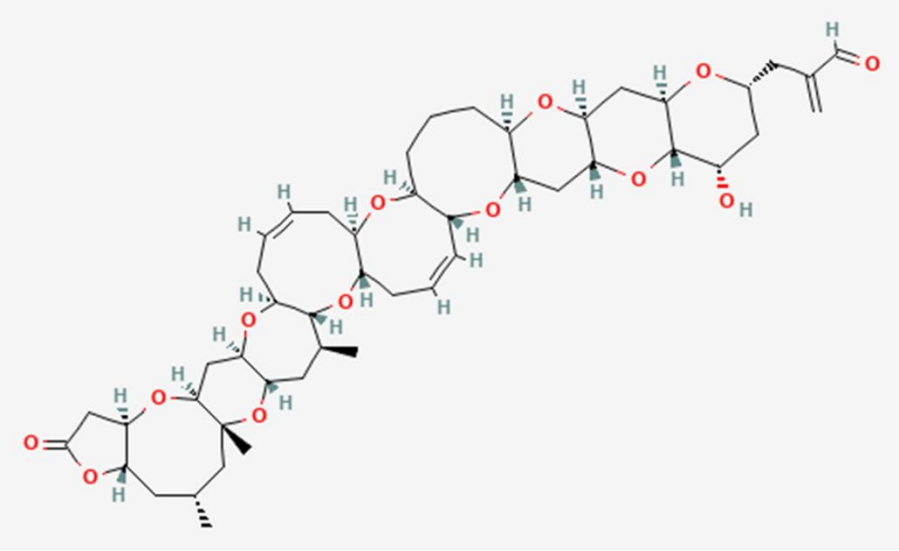

Figura 1.6. Estructura de la brevetoxina 1. Obtenida de PubChem, Identifier: 56841987; URL: https://pubchem.ncbi.nlm.nih.gov/compound/56841987#section=2D-Structure

1.3.2.2 Ciguatera (CFP, Ciguatera Fish Poisoning)

Las ciguatoxinas (CTX) son poliéteres liposolubles que se originan debido a la biotransformación de sus precursores, las gambiertoxinas (Lehane and Lewis, 2000) producidas por dinoflagelados del género *Gambierdiscus* (Miyahara et al., 1979; Murata et al., 1990; Visciano et al., 2016). Los vectores de transmisión habitual de las ciguatoxinas son los peces y no los moluscos bivalvos.

Las ciguatoxinas se acumulan a lo largo de la cadena alimentaria, desde pequeños peces herbívoros hasta peces carnívoros que se alimentan de ellos (FAO, 2004). Su mecanismo de acción es análogo al de las brevetoxinas, pues se unen a los canales de sodio sensibles al voltaje y los abren, lo que incrementa el flujo de iones Na^+ hacia la célula y provoca la despolarización de las membranas.

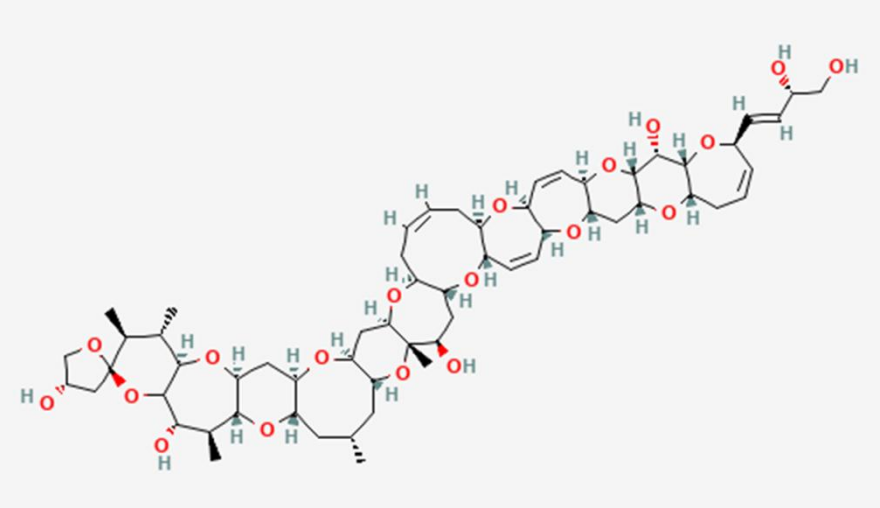

Figura 1.7. Estructura de la ciguatoxina. Obtenida de PubChem, Identifier: 129627864
URL: https://pubchem.ncbi.nlm.nih.gov/compound/129627864#section=2D-Structure

1.3.2.3 Palitoxinas (PLTX)

La palitoxina es un poliéter de gran tamaño con partes hidrofílicas y partes lipofílicas que fue aislado por primera vez de un coral del género *Palythoa*, pero luego se han encontrado la palitoxina o derivados (PLTX) en diversos organismos marinos que van desde dinoflagelados del género *Ostreopsis* hasta crustáceos y peces, que son los principales vectores de su consumo en humanos (Ciminiello et al., 2011, 2010, 2008, 2006; Farabegoli et al., 2018; Franchini et al., 2010). El principal problema de las palitoxinas parecen ser los aerosoles. Es una toxina que afecta las funciones celulares mediante la unión selectiva a la bomba Na^+-K^+ ATPasa, que es esencial para mantener los gradientes iónicos, la palitoxina inhibe el transporte activo de Na^+ y K^+ a través de la membrana pues convierte a esta bomba en un canal iónico no selectivo permanentemente abierto (Deeds and Schwartz, 2010; Patocka et al., 2018).

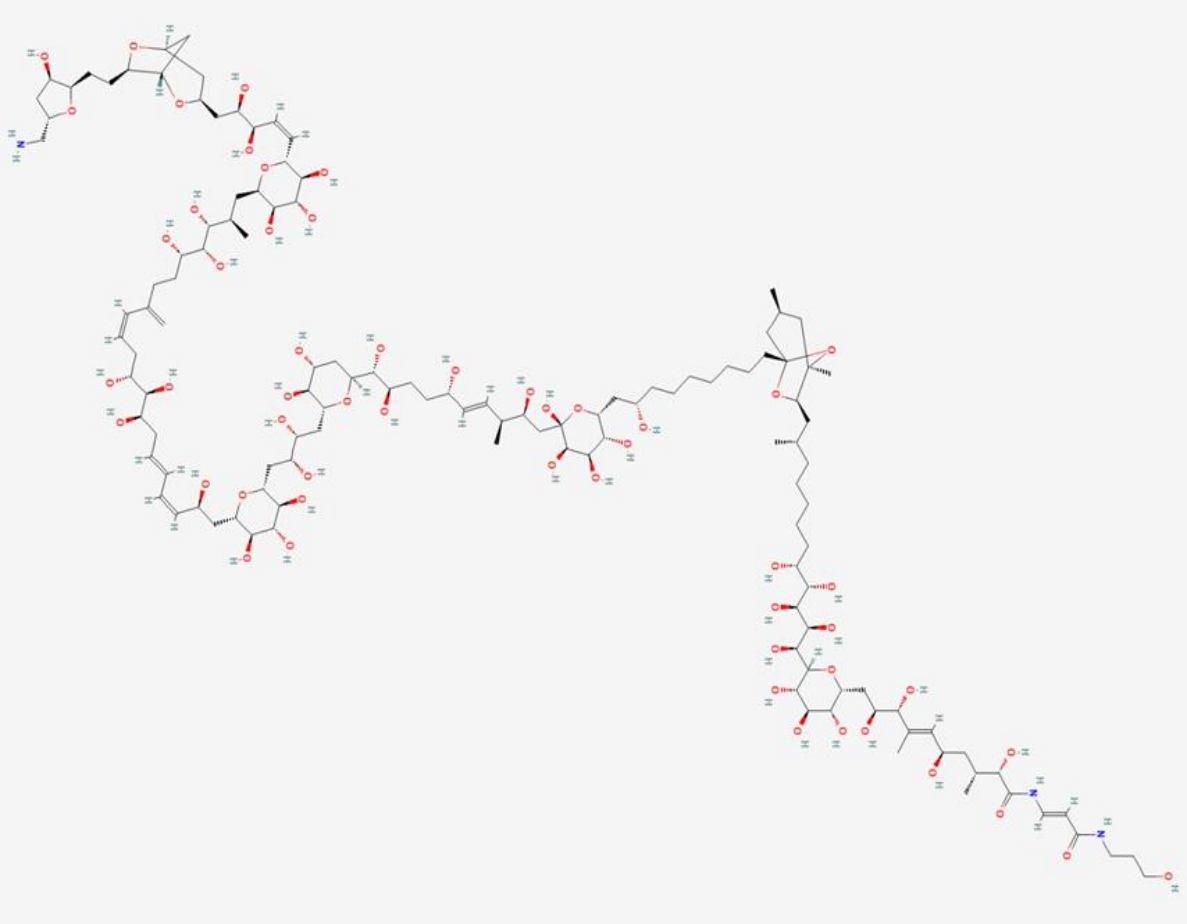

Figura 1.8. Estructura de la palitoxina. Obtenida de PubChem, Identifier: 11105289; URL: https://pubchem.ncbi.nlm.nih.gov/compound/11105289#section=2D-Structure

1.4 EL ÁCIDO DOMOICO Y SU PRESENCIA EN MOLUSCOS BIVALVOS

Como decíamos anteriormente, las toxinas del grupo del ácido domoico son las responsables de la intoxicación amnésica por mariscos (ASP). En el año 1987, en la Isla del Príncipe Eduardo (Canadá), más de cien personas resultaron intoxicadas debido al consumo de mejillones (*Mytilus edulis*) que contenían ácido domoico (Perl et al., 1990; Wright et al., 1989). La toxina había sido producida por diatomeas de la especie *Pseudo-nitzschia multiseries* (Bates et al., 1989). Además de ésta, hay otras especies de diatomeas de los géneros *Pseudo-nitzschia* y *Nitzschia* con capacidad para producir el ácido domoico (Bates et al., 2019, 2018; Lelong et al., 2012; Trainer et al., 2012). Las especies del género *Pseudo-nitzschia* pueden encontrarse a lo largo de la mayoría de las costas del mundo, pero los impactos de la toxina, el ácido domoico, son más frecuentes en los sistemas de afloramiento (Trainer et al., 2012). La prevalencia del ácido domoico y las diatomeas tóxicas parece haber aumentado en todo el mundo (Bates et al., 2018) y algunos estudios recientes indican que el aumento de los afloramientos de *Pseudo-nitzschia* tóxica puede ser debido al cambio climático (Cabrera et al., 2020; McKibben et al., 2017). El control de la producción del ácido domoico en *Pseudo-nitzschia* es complejo y parece que está influenciado por toda una serie de factores como los niveles de nutrientes nitrogenados, la adquisición de metales traza o la salinidad (Trainer et al., 2012). Entre los factores que incrementan la producción de ácido

domoico en *Pseudo-nitzschia* están la limitación de silicatos y fosfatos, bajas concentraciones de hierro o altas concentraciones de cobre (Lelong et al., 2012), pero todavía no se conocen bien todos los mecanismos que conducen al incremento o a la disminución de la producción de ácido domoico.

Los síntomas debidos a la intoxicación con ácido domoico aparecen dentro de las primeras horas tras la ingestión e inicialmente afectan el tracto gastrointestinal con náuseas, vómitos, calambres abdominales y diarrea (Lawrence et al., 2011). Más tarde aparecen dolores de cabeza y otros síntomas neurológicos, provocando frecuentemente alteraciones de la memoria, de ahí el nombre de intoxicación amnésica por mariscos, y en los casos más graves puede causar la muerte (Lawrence et al., 2011). El ácido domoico es un aminoácido excitador, análogo del neurotransmisor glutamato, que actúa como agonista de los receptores ionotrópicos de glutamato (iGluRs) e induce excitotoxicidad (Pulido, 2008). Existen 3 tipos de receptores ionotrópicos de glutamato: kainato (KA), AMPA (α-amino-3-hydroxy-5-methylisoxazole4-propionate) y NMDA (N-methyl-D-aspartate). La principal causa de neurotoxicidad parece ser la activación de los iGluRs y la subsiguiente liberación de glutamato endógeno, lo que conduce a una cascada de eventos que provocan el daño celular y tisular (Pulido, 2008). Estos eventos están mediados predominantemente por una entrada excesiva de Ca^{2+} en las neuronas a través de canales iónicos, causada por la activación de los iGluRs (Lefebvre and Robertson, 2010).

El ácido domoico es excitotóxico (Lefebvre and Robertson, 2010; Pulido, 2008) y causa estrés oxidativo (Giordano et al., 2007, 2006; Hiolski et al., 2014; Xu et al., 2008) en el sistema nervioso central de mamíferos y también de otros, pero los posibles efectos en invertebrados han sido mucho menos estudiados. Aunque parece que el ácido domoico no es tóxico para los moluscos bivalvos (o por lo menos no es altamente tóxico) sí hay varios trabajos en los que se indica que puede ejercer varios efectos fisiológicos y subletales en los bivalvos marinos. Algunos de estos efectos son crecimiento larvario reducido y disminución en la tasa de crecimiento y en la supervivencia de juveniles de *P. maximus* (Liu et al., 2008, 2007), daños en el DNA en *M. edulis* (Dizer et al., 2001), cierre de la concha, acidosis en la hemolinfa, hipoxia, aumento en el número y la actividad de los hemocitos en la ostra *Magallana gigas* como resultado de una respuesta al estrés (Jones et al., 1995a, 1995b). Sin embargo, los mecanismos moleculares por los que el ácido domoico provoca los efectos descritos en los bivalvos han sido poco estudiados. Algunos autores han sugerido que varias toxinas de origen fitoplanctónico aunque no afectan la supervivencia de los moluscos bivalvos, provocan estrés oxidativo (González and Puntarulo, 2016; Hégaret et al., 2011; Malanga et al., 2016).

En los bivalvos el ácido domoico en su mayor parte no se metaboliza y se excreta sin cambios (Novaczek et al., 1991). En una gran parte de los bivalvos, incluida la vieira, el ácido domoico se acumula sobre todo en la glándula digestiva (Álvarez et al., 2020; Blanco et al., 2020, 2006, 2002a, 2002b; Madhyastha et al., 1991; Novaczek et al., 1991; Wright et al., 1989).

El principal problema del ácido domoico en Europa, en cuanto a la explotación de los recursos marinos, se debe a su acumulación en la vieira (*P. maximus*). Este pectínido es una especie de alto valor económico y por ello es un recurso pesquero valioso (Duncan et al., 2016). En la vieira la tasa de depuración de ácido domoico es muy baja (Blanco et al., 2006, 2002a), a diferencia de lo que sucede en otros bivalvos que tienen altas tasas de depuración

del ácido domoico como sucede en los mejillones *M. edulis* (Novaczek et al., 1992, 1991) y *M. galloprovincialis* (Blanco et al., 2002b), las ostras de la especie *Crassostrea virginica* (Mafra Jr. et al., 2010) o pectínidos como *Argopecten purpuratus* (Álvarez et al., 2020). Debido a las floraciones de especies productoras de ácido domoico del género *Pseudo-nitzschia* y a la baja tasa de depuración para el ácido domoico de las vieiras (*P. máximus*), éstas presentan frecuentemente niveles superiores a los permitidos para su consumo (Blanco et al., 2021b, 2020, 2006, 2002a) que son de 20 mg kg^{-1} (EFSA, 2009). Es decir, la lenta depuración hace que entre dos floraciones de *Pseudo-nitzschia* productora de ácido domoico no dé tiempo a que el contenido de esta toxina en los tejidos de la vieira descienda a valores que permitan su comercialización. Cuando se supera el nivel permitido de ácido domoico la comercialización de esa especie debe interrumpirse, lo que provoca una pérdida de ingresos para la pesca y la acuicultura. (Blanco et al., 2021b) indican, refiriéndose a un período de 25 años de monitoreo del ácido domoico en Galicia, que el 100% de las muestras de *P. maximus* contenían ácido domoico y el 97,4% mostraban niveles por encima del límite regulatorio. Si se excluía a la vieira, en el 13,3% de las muestras de bivalvos se detectaba el ácido domoico y solo el 1,3% estaban por encima del límite regulatorio (Blanco et al., 2021b). Queda claro, por tanto, que el principal impacto causado por el ácido domoico en el marisqueo y la acuicultura en Galicia se produce sobre la explotación de la vieira y que se debe en gran medida a la muy lenta depuración de esta toxina en *P. maximus*.

1.5 METABOLISMO DE XENOBIÓTICOS.

El término xenobiótico hace referencia a aquellos compuestos químicos o sustancias extrañas o ajenas a las que proceden de la composición o metabolismo normal de un organismo. Estos compuestos pueden ser tóxicos para el organismo por lo que normalmente son metabolizados como paso previo a su eliminación. Las biotoxinas marinas y los contaminantes antropogénicos son xenobióticos, tanto para los moluscos bivalvos como para el hombre. Cuando un xenobiótico llega a un organismo vivo los procesos que tienen lugar son: la absorción (donde juega un papel importante el aparato digestivo), la distribución en distintos órganos y tejidos (con participación del aparato circulatorio), el metabolismo (generalmente tiene lugar sobre todo en el hígado en los vertebrados y en la glándula digestiva en los bivalvos) y finalmente la excreción (con la participación del aparato excretor). Los xenobióticos experimentan generalmente en el organismo un metabolismo en tres fases (Oesch and Arand, 1999; Oesch and Hengstler, 2021; Xu et al., 2005): fase I (funcionalización) y fase II (conjugación) y fase III (transporte activo).

Los objetivos de las fases I y II son: disminuir la toxicidad del xenobiótico y transformarlo en un derivado más hidrófilo para facilitar su excreción. Las principales características de las enzimas que participan en el metabolismo de xenobióticos son: una especificidad amplia por el sustrato y que generalmente pueden ser inducidas por compuestos exógenos.

La fase I sirve para la conversión de compuestos apolares (lipófilos) en compuestos más polares (más hidrófilos) y también para la introducción o liberación de grupos funcionales que puedan ser usados para la conjugación en la fase II.

El principal tipo de reacción de la fase I es la oxidación, otros tipos son la reducción y la hidrólisis (de ésteres, amidas y epóxidos). El principal grupo de enzimas que catalizan reacciones de fase I son una familia de monooxigenasas, los citocromos P450 (CYP), otros

grupos son las monooxigenasas dependientes de flavina (FMO) las monoaminooxidasas (MAO) o las ciclooxigenasas (COX). Las monooxigenasas dependientes del citocromo P450 representan una superfamilia de enzimas con 57 genes en humanos (Esteves et al., 2021) que catalizan generalmente reacciones de hidroxilación en las que se incorpora un átomo de oxígeno a partir de oxígeno molecular.

El sistema de fase II cataliza la conjugación de los xenobióticos o sus metabolitos de fase I con moléculas endógenas. Los productos resultantes son generalmente más hidrofílicos que los sustratos correspondientes y por ello más fáciles de excretar. Para la conjugación se requiere la presencia de un grupo reactivo. Los principales tipos de grupos reactivos son hidroxilo, tiol, amino, halógeno, carboxilo y epóxido. Los principales tipos de reacciones de fase II, catalizadas por transferasas, son: la conjugación con ácido glucurónico (las UDP-glucuronosiltransferasas, UGT, catalizan la conjugación con el ácido glucurónico de muchos compuestos para formar glucurónidos), la conjugación con glutatión (las glutatión S-transferasas, GST, conjugan las moléculas con un tripéptido, el glutatión, lo que incrementa mucho su solubilidad, las proteínas maduras son homodímeros), conjugación con aminoácidos, conjugación con sulfato (catalizada por sulfotransferasas), acilación, metilación.

El grupo más importante de enzimas de fase II son las GST. La actividad glutatión transferasa (GST) aparece en al menos cuatro familias de enzimas estructuralmente distintas (Board and Menon, 2013): las GST citosólicas; las GST mitocondriales de clase Kappa; las enzimas MAPEG y las proteínas de resistencia a la fosfomicina. Hay 7 clases de GST citosólicas (Blanchette et al., 2007; Board and Menon, 2013): GSTA (alfa, α), GSTM (mu, μ), GSTP (pi, π), GSTT (theta, θ), GSTS (sigma, σ), GSTZ (zeta, ζ), GSTO (omega, ω).

El sistema de fase III está formado por transportadores de la familia de las proteínas ABC (ATP-binding cassette) que bombean de forma activa (con el consumo de energía en forma de ATP) los xenobióticos hacia fuera de las células. Estructuralmente el transportador funcional contiene dos dominios de unión al ATP y dos dominios transmembrana. En humanos estas proteínas se han clasificado en 7 familias que se denominan con los nombres ABCA, ABCB, ABCC, ABCD, ABCE, ABCF y ABCG (Alam and Locher, 2023; Ferreira et al., 2014).

La multirresistencia frente a xenobióticos (MXR) en organismos acuáticos expuestos a toxinas o contaminantes es un fenómeno análogo a la multirresistencia frente a fármacos (MDR) observada en líneas celulares tumorales resistentes a antitumorales (Bard, 2000; Eufemia et al., 2002; Jeong et al., 2017; Lozano et al., 2015; Martínez-Escauriaza et al., 2021; Whalen et al., 2010). Esta multirresistencia se debe en parte al elevado nivel de expresión de ciertas proteínas transportadoras ABC: ABCB (denominada también MDR, por "*multidrug resistance"* y P-glucoproteína, ABCC (denominada también MRP, por "*multidrug resistance protein*") y la ABCG2.

Aunque en la fase III de transporte transmembrana de los xenobióticos o de sus metabolitos hacia el exterior de las células intervienen generalmente transportadores de la familia ABC, también pueden participar ahí proteínas pertenecientes a la mayor superfamilia de transportadores transmembrana, la de los transportadores de solutos (SLC, *solute carriers*) (Xun et al., 2020). Esta superfamilia incluye 52 familias y 395 genes en el genoma humano según (Hediger et al., 2013) aunque se ha actualizado a 65 familias ("SLC tables," n.d.)(SLC tables, https://www.bioparadigms.org/slc/).

Es importante destacar que el metabolismo de los xenobióticos es un sistema inducible. Los xenobióticos por intermedio de los receptores nucleares (NR) o del receptor de hidrocarburos aromáticos (AhR) inducen la síntesis de enzimas de las fases I y II y de transportadores de la fase III (Xu et al., 2005).

1.6 JUSTIFICACIÓN RAZONADA DE LA UNIDAD Y COHERENCIA TEMÁTICA Y METODOLÓGICA DE LA TESIS.

La presente tesis pretende profundizar en la comprensión de los procesos de intoxicación y desintoxicación frente al ácido domoico en moluscos bivalvos, así como en los posibles efectos de esta toxina sobre los bivalvos, empleando para ello herramientas transcriptómicas: RNA-seq y transcripción inversa acoplada a PCR en tiempo real cuantitativa (RT-qPCR). Con todo ello se pretende encontrar aquellos genes implicados tanto en el proceso de depuración del ácido domoico como en la respuesta de los moluscos bivalvos frente a la toxina y a las *Pseudo-nitzschia* productoras de ácido domoico.

En los últimos años se ha producido un gran desarrollo de las técnicas "ómicas" (genómica, transcriptómica, proteómica y metabolómica), lo que ha permitido que se apliquen en numerosos campos científicos relacionados con la biología (Dai and Shen, 2022; Sundaray et al., 2022; Thind et al., 2021). Entre estas aplicaciones están el estudio de los mecanismos moleculares de los procesos de intoxicación y desintoxicación y el estudio de los efectos de las toxinas sobre los organismos vivos. Las alteraciones en la expresión génica inducidas por la presencia de una determinada toxina ayudan a averiguar y esclarecer los posibles efectos de dichas toxinas, los mecanismos moleculares implicados y los mecanismos de desintoxicación. Este enfoque puede proporcionar algunas pistas sobre los procesos biológicos, celulares y moleculares alterados por el ácido domoico.

Una de las mejores formas de estudiar los efectos de las toxinas sobre la expresión génica es analizando la expresión diferencial mediante las técnicas transcriptómicas (RNA-seq, RT-qPCR). Este enfoque transcriptómico ha permitido la identificación de genes potencialmente implicados en la respuesta a toxinas en vertebrados (Bodero et al., 2018; Hiolski et al., 2014; Lefebvre et al., 2009; Ryan et al., 2005; Wang et al., 2008) y también en moluscos bivalvos (Chi et al., 2019, 2018; Detree et al., 2016; Dong et al., 2022; Dou et al., 2020; Gerdol et al., 2014; Prego-Faraldo et al., 2018; Wang et al., 2022; Zhang et al., 2023). Así, los genes desregulados por la exposición al ácido domoico podrían proporcionar información sobre los procesos de desintoxicación de los bivalvos frente a la toxina y sobre los procesos celulares, moleculares y biológicos alterados por la acción de la toxina.

Como se decía en el apartado dedicado al ácido domoico la tasa de depuración de éste en los bivalvos es especie específica y puede diferir mucho de una especie a otra (Blanco et al., 2021b, 2006, 2002a, 2002b; Mafra Jr. et al., 2010; Novaczek et al., 1992; Trainer and Bill, 2004). Los mejillones del género Mytilus (Blanco et al., 2002b; Mafra Jr. et al., 2010; Novaczek et al., 1992) y la ostra *Crassostrea virginica* (Mafra Jr. et al., 2010) eliminan rápidamente el ácido domoico, mientras que la vieira *Pecten maximus* (Blanco et al., 2006, 2002a) y la navaja *Siliqua patula* (Trainer and Bill, 2004) depuran muy lentamente el ácido domoico. En la volandeira (*Aequipecten opercularis*) la tasa de depuración es mayor que en la vieira (Mauriz and Blanco, 2010), aunque resultados recientes parecen indicar que la

depuración en la volandeira es relativamente lenta (García-Corona et al., 2024a). Tanto en los mejillones como en las vieiras y en las volandeiras el ácido domoico se acumula sobre todo en la glándula digestiva (Blanco et al., 2002a; Madhyastha et al., 1991; Novaczek et al., 1992; Wright et al., 1989).

En esta tesis se estudia la respuesta frente al ácido domoico y frente a *Pseudo-nitzschia* productora de ácido domoico en los moluscos bivalvos Los hechos descritos en el párrafo anterior nos han llevado a elegir tres especies para realizar este trabajo: el mejillón, *Mytilus galloprovincialis*, abordado en la primera publicación, (Pazos et al., 2017); la volandeira, *Aequipecten opercularis*, abordado en la segunda publicación (Ventoso et al., 2019); la vieira, *Pecten maximus*, abordado en la tercera publicación (Ventoso et al., 2021). El mejillón, *M. galloprovincialis*, es un depurador rápido frente al ácido domoico y es además el principal recurso de la acuicultura en Galicia (por cantidad de producción, tal como se recoge en esta introducción). La vieira, *P. maximus*, es una especie de alto valor económico en el mercado y es un depurador muy lento, por ello es la especie más afectada por la acumulación de ácido domoico. Debido a la proliferación de especies productoras de ácido domoico del género *Pseudo-nitzschia* y a la baja tasa de depuración de *P. maximus* la concentración de ácido domoico en esta especie suele estar en Galicia por encima de los límites reglamentarios (20 mg de ácido domoico kg^{-1}) en muchas áreas (Blanco et al., 2020, 2006, 2002a). Por su parte la volandeira, *A. opercularis*, tiene una tasa de depuración mayor que la de la vieira, pero inferior a la del mejillón, pero además es un pectínido como la vieira y por ello está evolutivamente más próxima de ésta que el mejillón.

2 OBJETIVOS

La hipótesis de partida es que las alteraciones en la expresión génica en los bivalvos expuestos al ácido domoico o a *Pseudo-nitzschia* productora de ácido domoico son útiles para ayudar a esclarecer los posibles efectos de dichas toxinas, los mecanismos moleculares implicados y los mecanismos de desintoxicación. Una de las informaciones que se pretende obtener es qué procesos, a nivel biológico, celular y molecular, están alterados por la exposición al ácido domoico. Para ello se utilizan herramientas transcriptómicas.

En los moluscos bivalvos se sabe poco sobre las bases moleculares de los procesos de desintoxicación frente al ácido domoico, el objetivo principal es profundizar en la comprensión de dicho proceso y buscar aquellos genes potencialmente implicados en él. Nos planteamos para ello varios objetivos parciales:

1. Secuenciar y ensamblar *de novo* el transcriptoma de la glándula digestiva de varias especies de moluscos bivalvos con distintas tasas de depuración frente al ácido domoico: el mejillón (*Mytilus galloprovincialis*), la vieira (*Pecten maximus*) y la volandeira (*Aequipecten opercularis*). Una vez ensamblado el transcriptoma, hacer la anotación funcional de los genes. Este primer objetivo es necesario para poder acometer el siguiente objetivo.

2. Estudiar la expresión diferencial de los genes en las especies de bivalvos citadas en el punto anterior (*M. galloprovincialis*, *P. maximus* y *A. opercularis*) al exponerlas al ácido domoico (durante una floración tóxica natural de *Pseudo-nitzschia* o por exposición directa al compuesto). Los genes diferencialmente expresados pueden proporcionar información acerca de los procesos de desintoxicación en los moluscos bivalvos, así como del efecto del ácido domoico sobre estos animales.

3. A partir de los resultados obtenidos en el punto anterior, comparando los datos en las tres especies, y de la bibliografía disponible, evaluar cuáles son los genes potencialmente implicados tanto en la desintoxicación como en la respuesta de los bivalvos frente al ácido domoico. Apoyándose en los datos de expresión diferencial obtenidos, describir los principales procesos alterados por la acción del ácido domoico.

Los objetivos parciales uno y dos se abordan en las tres publicaciones, estando cada una de ellas circunscrita a una de las especies utilizadas: el mejillón (*Mytilus galloprovincialis*), la vieira (*Pecten maximus*) y la volandeira (*Aequipecten opercularis*). El tercer objetivo parcial se aborda, además de en las tres publicaciones, en la discusión general.

3 MÉTODOS

Una descripción detallada de la metodología empleada puede verse en el **ANEXO I TRABAJOS PUBLICADOS** (Pazos et al., 2017; Ventoso et al., 2021, 2019) para el mejillón, la vieira y la volandeira.

Para el estudio de la respuesta frente al ácido domoico en los moluscos bivalvos, y la búsqueda de genes implicados en la eliminación de dicha toxina, se utilizó un enfoque transcriptómico basado en la secuenciación del transcriptoma (RNA-seq) y la PCR en tiempo real cuantitativa (RT-qPCR).

3.1 EXPOSICIÓN AL ÁCIDO DOMOICO

La exposición al ácido domoico de los mejillones (*M. galloprovincialis*) y las volandeiras (*A. opercularis*) se realizó en el medio natural durante episodios tóxicos de *Pseudo-nitzschia*. En el mejillón se utilizaron 12 animales: 6 controles y 6 intoxicados con ácido domoico (Figura 3.1). En la volandeira se utilizaron 18 animales: 6 controles y 12 con ácido domoico, de éstos 6 con un nivel más bajo (grupo DB) y 6 con un nivel más alto (grupo DA) de ácido domoico.

Debido a su muy baja tasa de depuración frente al ácido domoico es imposible encontrar vieiras en Galicia que no contengan la toxina en su glándula digestiva, por ello en esta especie lo que se hizo fue inyectar 6 animales con 62.5 µL de solución de ácido domoico de 8µg/µL en agua de mar, repitiéndose el tratamiento cada 2 días hasta un total de 6 inyecciones (Figura 3.1). Otras 6 vieiras, a las que se les inyecta únicamente agua de mar, sirvieron de control.

Otros enfoques que se hubieran centrado más en el ácido domoico excluyendo otros compuestos que pueden tener algún efecto sobre la expresión génica (el efecto de la *Pseudo-nitzschia*) se descartaron debido a problemas metodológicos. El suministro de ácido domoico disuelto a los bivalvos no fue posible debido a su baja eficiencia de absorción, y la exposición diferencial a *Pseudo-nitzschia* tóxica (productora de ácido domoico) y no tóxica también fue inviable por la dificultad de obtener cepas tóxicas y no tóxicas de la misma especie de *Pseudo-nitzschia* y la rápida pérdida de toxicidad de algunas cepas.

3.2 DETERMINACIÓN DEL CONTENIDO DE ÁCIDO DOMOICO

La determinación de los niveles de ácido domoico en las muestras se realizó mediante cromatografía líquida de alta resolución acoplada con espectrometría de masas (LC-MS/MS) en el Centro de Investigaciones Marinas de la Xunta de Galicia (Pedras de Corón, Vilanova de Arousa). El método utilizado se describe de forma detallada en las tres publicaciones que forman parte de esta tesis (Pazos et al., 2017; Ventoso et al., 2021, 2019).

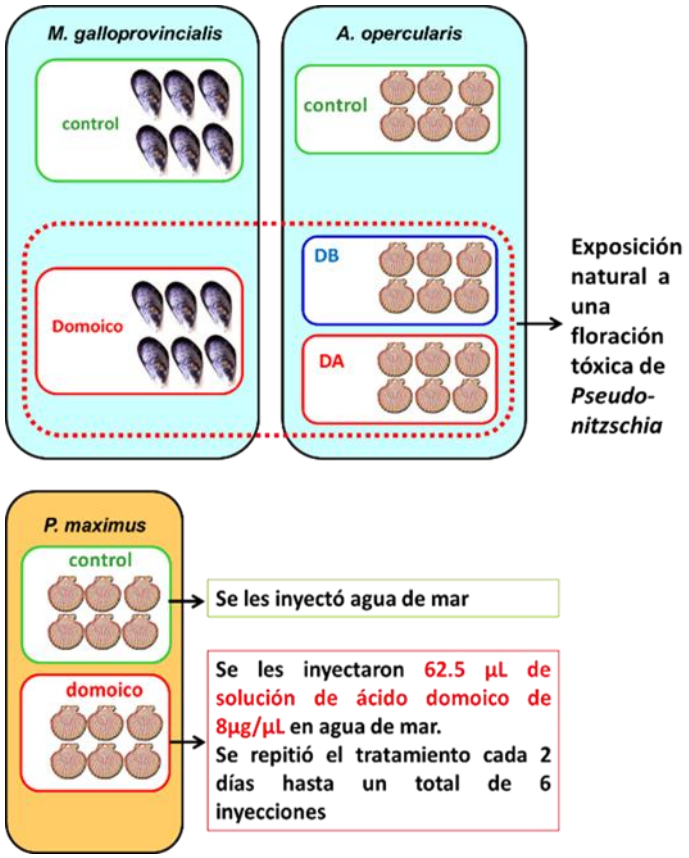

Figura 3.1. Exposición al ácido domoico. La exposición de los mejillones (*M. galloprovincialis*) y las volandeiras (*A. opercularis*) se realizó en el medio natural durante floraciones tóxicas de *Pseudo-nitzschia* que contenía ácido domoico. Mientras que la exposición de las vieiras (*P. maximus*) se realizó mediante inyecciones de ácido domoico en el músculo aductor

3.3 SECUENCIACIÓN DEL TRANSCRIPTOMA (RNA-SEQ)

La RNA-seq es una técnica de secuenciación de nueva generación (Conesa et al., 2016; Goodwin et al., 2016; Hornett and Wheat, 2012; Hu et al., 2021; Thind et al., 2021; Van den Berge et al., 2019; Vijay et al., 2013) que permite analizar de forma conjunta la expresión de todos los genes en una muestra mediante la secuenciación de todo el transcriptoma (es decir, todo el RNA producido en la transcripción de los genes).

Esta técnica permite, entre otras cosas, evaluar los efectos de una toxina (el ácido domoico en este caso) en la expresión génica mediante la comparación entre muestras de animales expuestos a la toxina y de animales control. Se analizan los genes diferencialmente expresados por la exposición al ácido domoico en todo el transcriptoma. Los genes que posean diferencias significativas en su expresión son candidatos para estar implicados en los mecanismos de desintoxicación y en la respuesta frente a la toxina.

La aplicación de métodos de anotación y enriquecimiento funcionales permite identificar las rutas metabólicas, los procesos biológicos, las funciones moleculares y los componentes celulares alterados por la exposición al ácido domoico o a *Pseudo-nitzschia* productora de ácido domoico. El enfoque transcriptómico ha sido empleado con éxito para descubrir la respuesta de los bivalvos frente a las biotoxinas marinas y también para identificar genes

presuntamente implicados en los procesos de desintoxicación (Chi et al., 2018; Detree et al., 2016; Gerdol et al., 2014; Li et al., 2017; Prego-Faraldo et al., 2018).

Dentro de los métodos de secuenciación de nueva generación (Next-generation sequencing, NGS) hemos utilizado uno de los denominados métodos de segunda generación de lectura corta (short-read sequencing) cuya característica común es la secuenciación masiva de moléculas de DNA cortas (100-800 pb) amplificadas clonalmente y secuenciadas en paralelo (Hu et al., 2021). De entre los métodos de secuenciación de lectura corta hemos utilizado el de Illumina (https://www.illumina.com/), que es la tecnología de secuenciación más precisa del mercado (Hu et al., 2021), con una tasa de error del 0,1 % (principalmente errores de sustitución, y muy raramente inserciones/deleciones) cuando se utiliza el *paired-end sequencing* (secuenciación que se produce desde ambos extremos de un fragmento de DNA). El principio de la secuenciación de la plataforma Illumina es la "secuenciación por síntesis" (SBS), que implica la incorporación de nucleótidos dependiente de la DNA polimerasa (Goodwin et al., 2016) y una determinada señal, un fluoróforo, identifica la incorporación de un nucleótido en la cadena de DNA en elongación. La plataforma de secuenciación puede recopilar información de muchos millones de centros de reacción simultáneamente, secuenciando así muchos millones de moléculas de DNA en paralelo (Goodwin et al., 2016).

La secuenciación masiva en paralelo produce grandes cantidades de datos, esto implica que el análisis bioinformático posterior de dichos datos es esencial para poder implementar estas tecnologías.

Los pasos que hay que seguir para la secuenciación del transcriptoma son (Figura 3.2):

Extracción del RNA (NucleoSpin RNA kit MachereyNagel, Düren, Germany). La determinación de la concentración y pureza del RNA se realizó mediante espectrofotometría en Nanodrop ND-1000 (un valor en la ratio A260/A230 en torno a 2-2,2 y en la ratio A260/A280 de aproximadamente 2, indican una adecuada pureza). La cantidad de RNA total se determinó también por fluorometría con Qubit 2.0 (Invitrogen). La integridad del RNA se determinó mediante una electroforesis desnaturalizante en gel de agarosa (D1 low EEO, Pronadisa) al 1% en TBE (Tris-Borato-EDTA) 0,5X y también utilizando el Agilent 2100 Bioanalyzer (Agilent Technologies).

Purificación del RNA mensajero (mRNA) y preparación de librerías de cDNA.

Secuenciación utilizando la tecnología Illumina (paired-end sequencing, 100 x 2 bp), en secuenciador Illumina HiSeq 2000. Control de calidad de las lecturas obtenidas realizado con FastQC (https://www.bioinformatics.babraham.ac.uk/projects/fastqc/).

Ensamblaje *de novo* del transcriptoma con Oases, versión 0.2.09 (Schulz et al., 2012) y Trinity, versión 2.1.1 (Grabherr et al., 2011). Los métodos de ensamblaje *de novo* ensamblan las secuencias directamente a partir de las lecturas obtenidas. Este paso es imprescindible cuando no se cuenta con un genoma de referencia.

Agrupamiento (clustering) con CD-hit versión 4.6. (al 90% de homología) para reducir la redundancia.

Mapeo de cada muestra frente al transcriptoma de referencia obtenido en el paso anterior con Bowtie2, versión 2.2.6 (Langmead and Salzberg, 2012). Pues para analizar la expresión diferencial mediante el recuento de lecturas, primero hay que mapear dichas lecturas frente al genoma de referencia o, como en nuestro caso, al transcriptoma ensamblado anteriormente y cuantificarlas.

Estudio de la expresión génica diferencial con DESeq2 versión 1.8.2 (http://www.bioconductor.org/packages/devel/ bioc/html/DESeq2.html)

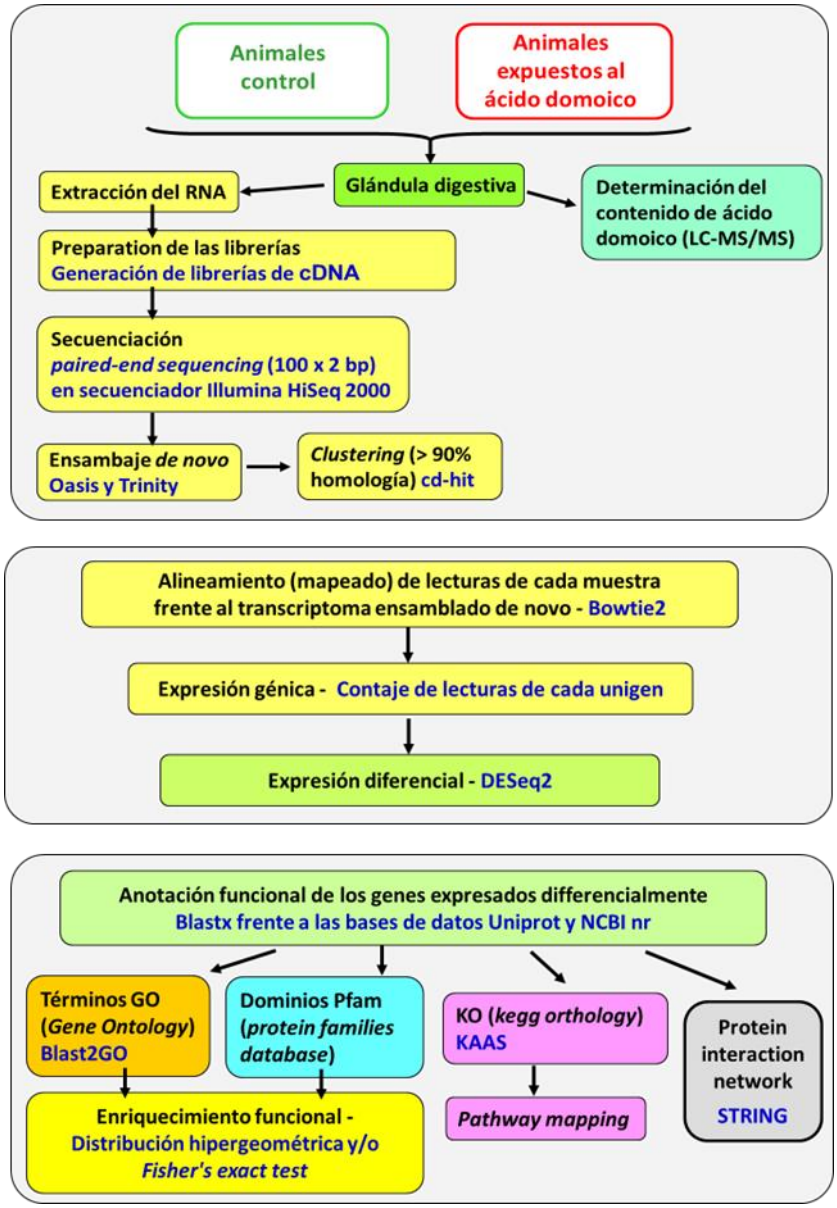

Figura 3.2. Esquema de la metodología empleada para el estudio transcriptómico: ensamblaje *de novo* del transcriptoma, análisis de la expresión génica por RNA-seq, anotación funcional de los genes y enriquecimiento funcional

Una vez obtenidos los resultados del análisis de la expresión génica diferencial se hace la anotación de los genes, utilizando el programa Blast (Altschul et al., 1990) frente a bases de datos como NCBI-nr, Uniprot o Swiss-Prot, utilizando para ello el programa OmicsBox (BioBam Bioinformatics) (Conesa et al., 2005; Götz et al., 2008). La anotación se amplía

mediante la incorporación de información de la especie, el nombre del gen y las funciones utilizando la ontología del gen (GO), los dominios estructurales de proteínas (PFAM) (Finn et al., 2016) asociados con el transcrito utilizando InterPro, la asignación de ortólogos y el mapeo de rutas en KAAS (KEGG Automatic Annotation Server) (Moriya et al., 2007). Esto permitirá seleccionar aquellos genes que en base a su función y expresión diferencial se considere que pueden estar implicados en la depuración del ácido domoico y en la respuesta frente a dicha toxina.

Después de la anotación se hace un estudio de enriquecimiento funcional para ver qué términos GO y qué motivos de proteínas PFAM están más representados en los genes diferencialmente expresados en relación con el total del transcriptoma utilizando la distribución hipergeométrica o la prueba exacta de Fisher (Fisher, 1922).

Con las proteínas codificadas por los genes diferencialmente expresados también se hace un estudio de las redes de interacciones proteína-proteína (Protein Network Analysis) con el algoritmo String (Franceschini et al., 2013; Szklarczyk et al., 2015), para buscar las relaciones e interacciones entre las proteínas codificadas por los genes expresados diferencialmente. Este análisis es más eficiente utilizando bases de datos de los organismos más estudiados (Artigaud et al., 2015). Por lo tanto, los homólogos humanos de las proteínas codificadas por los genes expresados diferencialmente en la glándula digestiva de las tres especies de bivalvos se identificaron mediante una búsqueda blastx (Altschul et al., 1997) frente la base de datos de proteínas humanas de String (9606.protein.sequences.v10.fa), con valor $E \leq 10^{-5}$. Los mejores resultados de la búsqueda blastx se utilizaron como entrada en el programa String.

3.4 PCR EN TIEMPO REAL CUANTITATIVA (RT-qPCR)

La expresión génica ha sido validada mediante PCR en tiempo real cuantitativa (RT-qPCR) para confirmar la expresión diferencial obtenida mediante RNA-seq. La RT-qPCR (Figura 3.3) cuantifica la expresión de un gen determinado (el mRNA correspondiente a dicho gen) tras su transformación en DNA complementario (cDNA) mediante transcripción inversa.

El cDNA se sintetizó a partir de 0,5 μg de RNA total con el kit iScript™cDNA Synthesis kit (ref. 170-8891, BioRad, Hercules, CA, USA) en un volumen de reacción de 20 μL y las condiciones fueron 5 min a 25 ◦C, 30 min a 42 ◦C y 5 min a 85 ◦C.

El cDNA se cuantificó por RT-qPCR midiendo en cada ciclo de amplificación la fluorescencia emitida por un fluorocromo (SYBR Green), pues esta fluorescencia es proporcional a la cantidad o concentración del amplicón. El fluorocromo empleado está contenido en el reactivo comercial SsoFastTM EvaGreen® Supermix (BioRad). Éste se une a fragmentos de DNA de doble cadena emitiendo fluorescencia a 522 nm. El equipo iCycler iQ® Real-time System (BioRad) consta de un termociclador convencional que tiene acoplado una cámara que permite registrar la fluorescencia en cada pocillo, de esta forma se asocia cada ciclo con un valor de fluorescencia medido en RFU (Relative Fluorescence Units).

La representación gráfica de la fluorescencia emitida respecto a cada ciclo en escala semilogarítmica permite obtener una representación lineal de la fase exponencial de amplificación. A partir de estos datos se determina el Cq (ciclo de cuantificación) que es el número de ciclos necesarios para alcanzar un determinado umbral de fluorescencia (Figura 3.4). Este umbral puede fijarse manualmente (que es lo que hemos hecho en nuestro caso) o calcularse mediante diversos algoritmos.

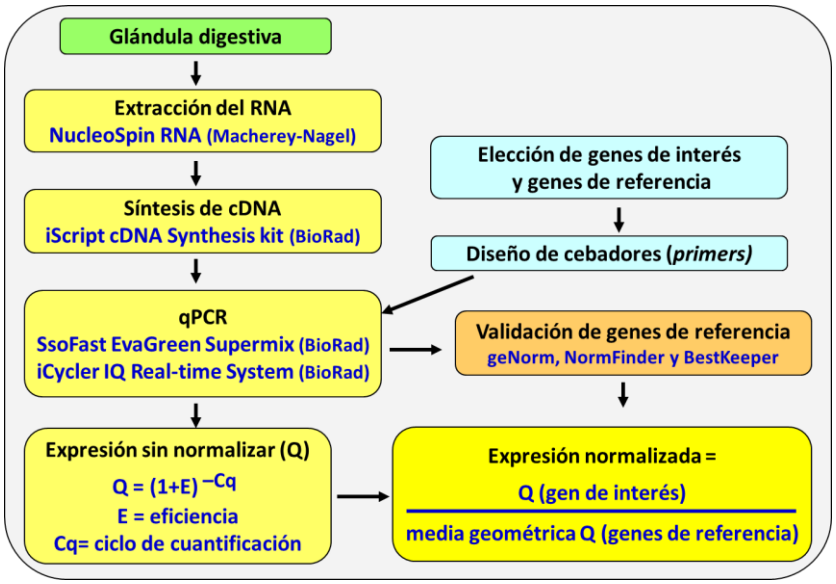

Figura 3.3. Estudio de la expresión génica por RT-qPCR

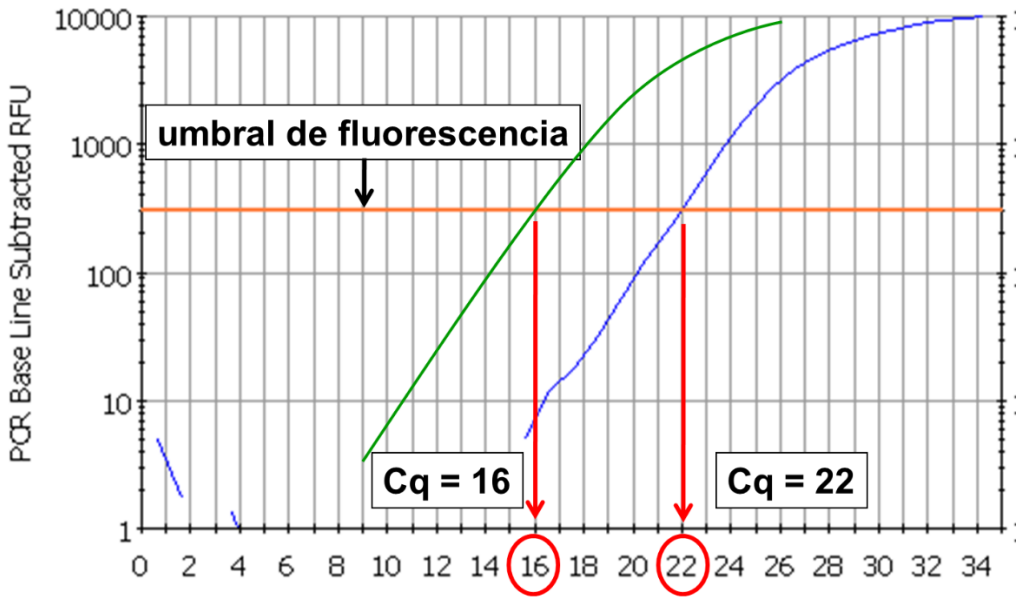

Figura 3.4. Ejemplo del cálculo del ciclo de cuantificación (Cq) en el análisis de la expresión génica por RT-qPCR. El Cq es el número de ciclos necesarios (representados en el eje X) para alcanzar un determinado nivel o umbral de fluorescencia (representado en el eje Y, RFU = Relative Fluorescence Units)

Los cebadores de oligonucleótidos necesarios para las amplificaciones de cada gen se diseñaron con el OligoAnalyzer 3.1 (https://eu.idtdna.com/pages/tools/oligoanalyzer) a partir de las secuencias obtenidas en la RNA-seq o de secuencias disponibles en las bases de datos

del NCBI. Los cebadores tienen entre 19 y 23 nucleótidos con una temperatura de fusión (Tm) de 60ºC. Las longitudes de los amplicones están comprendidas entre 80 y 200 pares de bases (bp). Los oligonucleótidos fueron sintetizados por Thermo Scientific (Thermo Fisher Scientific) y por Integrated DNA Technologies (Leuven, Bélgica).

La especificidad de los cebadores se confirmó por la presencia de un único pico en la curva de fusión y por la presencia de una única banda del tamaño esperado cuando los productos de PCR se corrieron en un gel de agarosa al 2%. También se confirmó la identidad de los amplicones mediante secuenciación.

Cada reacción de PCR estuvo compuesta por 4 µl de cDNA diluido 1:5 que equivalen a 20 ng de cDNA (esta dilución reduce las variaciones en el pipeteo al utilizar un mayor volumen manteniendo constante la cantidad de cDNA añadida), 10 µl de SsoFastTM EvaGreen® Supermix (BioRad) que contiene la Taq polimerasa, los desoxirribonucleótidos trifosfato (dNTPs), un tampón con todos los cofactores necesarios para la función de la polimerasa y SYBR Green, 0,8 µl de cada cebador con una concentración de 10 µM (concentración final 400 nM) y agua libre de DNAsas y de inhibidores de PCR (PCR-grade wáter, Roche), hasta completar un volumen final de 20 µl. Las muestras se analizaron por duplicado y, además, se contó con 2 controles negativos (solamente reactivo y cebadores, sin cDNA) para identificar una posible contaminación con una fuente externa y un control de RNA (a la mezcla de la reacción se añadió un volumen de RNA equivalente a la cantidad de cDNA añadido en las muestras) para verificar que no quedan trazas de DNA genómico.

El programa de termociclado empleado constó de una desnaturalización inicial de 95ºC durante 30 segundos, seguida de 40 ciclos de tres pasos: desnaturalización inicial a 95ºC 5 segundos; hibridación y extensión a 60ºC 10 segundos; medida de la fluorescencia a 75ºC 10 segundos. Finalmente, un paso para la realización de la curva de fusión, con una desnaturalización a 95ºC 20 segundos, una hibridación a 60ºC durante 20 segundos, tras la cual se llevan a cabo 80 ciclos de incremento de temperatura de 0,5ºC cada 10 segundos hasta alcanzar los 100ºC. La curva de fusión permite comprobar la especificidad de la amplificación.

La eficiencia de amplificación (E) de cada par de cebadores se calculó mediante la aplicación Real-time PCR Miner (Zhao and Fernald, 2005). Este algoritmo calcula las eficiencias a partir de los denominados datos brutos (raw data) de las amplificaciones (fluorescencia registrada y ciclo asociado en cada medición). Estos parámetros son necesarios para calcular la expresión génica. Es bueno que las eficiencias se aproximen al 100% (E =1).

Los valores de expresión obtenidos para los genes de interés es necesario normalizarlos con respecto a la expresión de genes de referencia para permitir una comparación entre muestras (Bustin et al., 2009; Huggett et al., 2013). Los genes de referencia son genes que se expresan de forma estable en todas las condiciones (muestras de animales control y muestras de animales expuestos a la toxina en nuestro caso). La correcta elección de estos genes es de crucial importancia para una adecuada normalización, ya que no existen genes de referencia universales.

Para la selección de los mejores genes de referencia se emplearon los programas geNorm 3.5 (Vandesompele et al., 2002), NormFinder v. 0.953 (Andersen et al., 2004) y BestKeeper v.1

(Pfaffl et al., 2004) (Pfaffl et al., 2004). Cada uno de ellos emplea un algoritmo determinado para calcular la estabilidad de la expresión de los genes de referencia entre las muestras analizadas. El programa geNorm clasifica los genes con el parámetro "M", que es la variación media por parejas de cada gen. Menores valores de M indican mayor estabilidad. El cálculo se hace con todos los genes ensayados, tras esta operación, eliminará el gen con una M más elevada y se vuelve a realizar el cálculo con los restantes. Este proceso se repite sucesivamente hasta que solo queda el par más estable. Este programa también calcula un factor de normalización que informa del número óptimo de genes de referencia a emplear. NormFinder evalúa la estabilidad de expresión mediante la estimación de la variación total de los genes y la variación entre los subgrupos de la muestra. Por su parte, el programa BestKeeper calcula un coeficiente de correlación entre cada gen y la media geométrica de los valores de Cq de todos los genes agrupados (índice BestKeeper). La estabilidad se deduce del valor del coeficiente de correlación (r) y la desviación estándar (SD). Se tiene en cuenta la información aportada por los tres algoritmos para elegir los mejores genes de referencia en cada caso.

Para el cálculo de la expresión normalizada los valores de Cq se transformaron en cantidades (Q, expresión no normalizada) utilizando la ecuación $Q = (1+E)^{-Cq}$ (Mauriz et al., 2012) donde E es la eficiencia. La expresión génica normalizada se calculó como la relación entre Q y el factor de normalización. El factor de normalización utilizado fue la media geométrica de las cantidades (Q) de los genes de referencia seleccionados (Figura 3.3) según la fórmula que aparece a continuación:

$$\text{Media geométrica de la expresión de los genes de referencia} = \sqrt[n]{(1+E_{ref1})^{-Cq_{ref1}} \times (1+E_{ref2})^{-Cq_{ref2}} \times \ldots \times (1+E_{refn})^{-Cq_{refn}}}$$

Los análisis estadísticos de la expresión normalizada se realizaron con el paquete estadístico IBM SPSS Statistics 20.0 o 24.0 (IBM SPSS, Chicago, IL, EE. UU.). Los datos se sometieron a pruebas de normalidad (prueba de Shapiro-Wilk) y de homogeneidad de varianzas (prueba de Levene). La expresión génica se transformó logarítmicamente (log base 2) para cumplir con los requisitos de normalidad y homogeneidad de varianzas. La expresión de los genes en los animales expuestos al ácido domoico en relación con el grupo de control se comparó mediante la prueba t de Student o mediante ANOVA seguida de la prueba t de Dunnett. Se consideró estadísticamente significativo un valor de $p < 0,05$.

4 DISCUSIÓN

Se ha analizado la respuesta transcriptómica en la glándula digestiva de 3 especies de moluscos bivalvos tras la exposición a *Pseudo-nitzschia* productora de ácido domoico o la inyección de ácido domoico. En el mejillón *Mytilus galloprovincialis* y la volandeira *Aequipecten opercularis*, los animales tratados fueron expuestos a una floración tóxica natural de *Pseudo-nitzschia* (Pazos et al., 2017; Ventoso et al., 2019). Mientras que en la vieira *Pecten maximus* la exposición al ácido domoico fue directa mediante inyección del mismo en el músculo aductor (Ventoso et al., 2021), por lo que no puede descartarse que los resultados obtenidos en *M. galloprovincialis* y *A. opercularis* también se deban a la interacción con la propia diatomea. Mientras que en la vieira *Pecten maximus*, los efectos del ácido domoico sobre la glándula digestiva pueden deberse a la interacción directa con la toxina transportada mediante la hemolinfa o indirectamente a través de la interacción del ácido domoico en el sistema nervioso (ganglios cerebrales, parietoviscerales y pedales). La unión a receptores en estos ganglios puede tener un efecto en la glándula digestiva mediado por los sistemas nervioso y neuroendocrino.

Las evidencias obtenidas aportan información sobre un proceso poco estudiado, los efectos del ácido domoico y su metabolismo en moluscos bivalvos, hallándose varios puntos en la misma línea de estudios previos.

Algunos genes que codifican para enzimas que forman parte de los mecanismos de defensa frente al daño oxidativo (glutatión S-transferasas, sulfotransferasas) se encuentran diferencialmente expresados en *M. galloprovincialis* y *A. opercularis* tras la exposición a *Pseudo-nitzschia* productora de ácido domoico y en *P. maximus* tras la inyección de éste (Pazos et al., 2017; Ventoso et al., 2021, 2019).

En las tres especies de bivalvos se ha observado, por tanto, una respuesta transcriptómica al daño causado por el estrés oxidativo, pero esta respuesta es mucho más clara en la volandeira (Ventoso et al., 2019) tras la exposición a *Pseudo-nitzschia* productora de ácido domoico, en la que se sobreexpresan distintos grupos de enzimas antioxidantes (glutatión S-transferasas, tiorredoxinas, glutarredoxinas y cobre/zinc superóxido dismutasas). También se observa en *A. opercularis* una respuesta frente a la genotoxicidad del ácido domoico, pues entre los términos GO enriquecidos para los genes sobreexpresados se encuentran la "reparación del DNA" y el "estímulo de respuesta celular frente al daño en el DNA" (Ventoso et al., 2019). Esto concuerda con resultados de otros autores (Dizer et al., 2001) que encontraron en *M. edulis* que el daño en el DNA es significativamente superior tras la inyección de ácido domoico.

Varios estudios encontraron que el ácido domoico induce estrés oxidativo en el sistema nervioso central de vertebrados. (Giordano et al., 2007, 2006; Hiolski et al., 2014; Pérez-Gómez and Tasker, 2014; Pulido, 2008; Xu et al., 2008) y en bivalvos (Dizer et al., 2001; González and Puntarulo, 2016; Hégaret et al., 2011; Jones et al., 1995a, 1995b; Liu et al., 2007, 2008;

Malanga et al., 2016). También otras biotoxinas marinas inducen estrés oxidativo en los bivalvos (Chi et al., 2018; Freitas et al., 2020; González and Puntarulo, 2016; Hégaret et al., 2011; Huang et al., 2015; Malanga et al., 2016; Pinto et al., 2023; Prego-Faraldo et al., 2016).

La generación de estrés oxidativo es el mecanismo a través del cual el ácido domoico ejerce su efecto tóxico. Se trata de un aminoácido tricarboxílico estructuralmente análogo al ácido glutámico, por lo que actúa como agonista de receptores ionotrópicos de glutamato causando un flujo descontrolado de Ca^{+2} y Na^{+} al interior celular lo que deriva en la generación de especies reactivas del oxígeno (ROS), peroxidación de lípidos, daño mitocondrial, daño en el DNA y muerte celular. (Zabaglo et al., 2016)

En *A. opercularis* (Ventoso et al., 2019), para los genes sobreexpresados, 2 de los términos GO más enriquecidos dentro de la categoría "componente celular" fueron "complejo proteasoma "y "núcleo del proteasoma". Además, el dominio Pfam proteasoma (PF00227) también se encuentra enriquecido y proteínas implicadas en la función del proteasoma forman un grupo con nodos altamente conectados en la red de interacciones proteína-proteína elaborada con el algoritmo String. El daño causado por las especies reactivas del oxígeno afecta a la integridad de diversas proteínas, una consecuencia del aumento de proteínas no funcionales es la sobreexpresión de genes implicados en el sistema proteasoma (Livneh et al., 2016). Éste es un complejo proteico encargado de la degradación de proteínas, entre ellas las proteínas dañadas por procesos oxidativos (Shang and Taylor, 2011).

Estos resultados se encuentran alineados con el estudio realizado por Manfrin et al. (2010) en *M. galloprovincialis*, donde se observó una sobreexpresión de transcritos de RNAm implicados en la actividad del proteasoma tras exposición al ácido okadaico.

La respuesta frente al daño proteico causado por diversos tipos de estrés (altas temperaturas, toxinas, patógenos e hipoxia) también está mediada por proteínas de choque térmico (HSP) que están implicadas en el correcto plegado de proteínas (Cheng et al., 2016).

En *M. galloprovincialis* (Pazos et al., 2017) se observa una infraexpresión de genes que codifican para proteínas HSP mientras que en *A. opercularis* (Ventoso et al., 2019), aunque principalmente se encuentran infraexpresados (14 sobreexpresados y 35 infraexpresados), la mitad de los genes sobreexpresados se corresponden con formas mitocondriales. La sobreexpresión de algunas HSP mitocondriales es probablemente una respuesta frente al daño mitocondrial observado en *A. opercularis*, del que hablamos más adelante, estas chaperonas moleculares contribuyen al correcto plegado proteico evitando el fallo funcional causado por el estrés oxidativo inducido por el ácido domoico. Entre los genes infraexpresados predominan los que codifican para HSP70 (proteínas de choque térmico de 70kDa). Por su parte, en *P. maximus*, se sobreexpresa el gen *heat shock 70 kDa protein 12A-like* de la subfamilia *Hspa12* que codifica para proteínas HSP70 (Ventoso et al., 2021). Es interesante señalar que en otro pectínido (*Mizuhopecten yessoensis*) una duplicación en tándem de genes *Hsp70* ha dado lugar a una expansión de los genes de la subfamilia *Hspa12* (Cheng et al., 2016) debido probablemente a una evolución adaptativa al estrés causado por la exposición a algas nocivas.

Varias publicaciones reportan un aumento de la expresión de genes que codifican para proteínas HSP tras la exposición a algas nocivas productoras de toxinas. En *M. chilensis* expuesto a saxitoxina. (Núñez-Acuña et al., 2013), en hemocitos de *C. gigas* expuestos a brevetoxina

(Mello et al., 2012), en la glándula digestiva de *C. gigas* y *C. farreri* tras exposición a saxitoxina (Cao et al., 2018), en branquias de *A. irradians* expuestas a ácido okadaico (Chi et al., 2018), en hemocitos de *A. irradians* tras exposición al ácido domoico (Chi et al., 2019), en la glándula digestiva de *A. irradians* tras exposición al ácido domoico (Song et al., 2020), en la glándula digestiva de *Mizuhopecten yessoensis* tras exposición a *Alexandrium catenella* productora de Saxitoxina (Cheng et al., 2016).

El sentido de la expresión diferencial de los genes que codifican para proteínas HSP (sobreexpresión o infraexpresión) evaluada en las publicaciones anteriormente mencionadas, depende de la concentración de la toxina y del tiempo al que fueron expuestos los animales. Chi et al. (2019) observaron que bajas concentraciones de ácido domoico disuelto (10 µg/L) inducen la expresión de genes *Hsp* en el corto plazo, pero largas exposiciones o la exposición a concentraciones de 100µg/L reducen la expresión génica, sugiriendo que el ácido domoico puede agotar la capacidad antioxidante de las células y su efecto sobre la integridad proteica es dependiente de la dosis y el tiempo.

En *A. opercularis* (Ventoso et al., 2019) se encuentran sobreexpresados genes que codifican para proteínas ribosomales mitocondriales, así como para translocasas de la membrana externa e interna. El análisis de interacciones proteicas elaborado con el algoritmo String (Szklarczyk et al., 2015) también muestra una alta conexión en nodos para estas proteínas. Esto es indicativo de un aumento en la biogénesis mitocondrial como respuesta frente al daño mitocondrial provocado probablemente por el estrés oxidativo.

Los resultados comentados en el párrafo anterior concuerdan con los obtenidos por otros autores (Hiolski et al., 2014) en el pez cebra. Estos autores evaluaron la respuesta transcriptómica en el cerebro del pez cebra tras la exposición crónica a bajas concentraciones de ácido domoico, y sugieren que la respuesta frente a la disfunción mitocondrial causada por el estrés oxidativo es una biogénesis mitocondrial compensatoria del daño donde evaluaron la respuesta transcriptómica en el cerebro del pez cebra tras exposición crónica a bajas concentraciones de ácido domoico.

En relación a estos mecanismos compensatorios del daño, Anderson et al. (2015), a través de un metaanálisis de los efectos del estrés ambiental en ostras, proponen un modelo de respuesta intracelular según el cual, si los mecanismos de protección frente al estrés oxidativo (sobreexpresión de enzimas antioxidantes y chaperonas moleculares) no logran limitar el daño, se produciría un daño celular que conduce a la apoptosis. Diversos autores destacaron la implicación del ácido domoico en la inducción de la apoptosis (Giordano et al., 2008, 2007; Pinto-Silva et al., 2008; Tsunekawa et al., 2013). Es de esperar, por lo tanto, la sobreexpresión de genes implicados en la apoptosis. En las 3 especies estudiadas *M. galloprovincialis*, *A. opercularis* y *P. maximus*, la catepsina D, una proteasa lisosomal que inicia la apoptosis dependiente de Caspasa 8 (Lein et al., 2018) se encuentra sobreexpresada (Pazos et al., 2017; Ventoso et al., 2021, 2019).

En *P. maximus*, se pueden destacar otros 2 procesos potencialmente relacionados con la protección frente al estrés oxidativo: la sobreexpresión de los genes que codifican para la glutamina sintetasa y la pirrolina-5-carboxilato reductasa 2.

La glutamina sintetasa puede jugar un papel protector frente a la toxicidad del glutamato al catalizar la reacción de transformación de glutamato en glutamina (Vardimon et al., 2001; Zou et al., 2010). (Fleischer-Lambropoulos et al., 1996; Lehmann et al., 2009) observaron un aumento de la actividad de la glutamina sintetasa en cultivo de astrocitos por acción del glutamato y agonistas de receptores de glutamato. Además, la glutamina sintetasa también participa en la producción de GABA, un neurotransmisor inhibidor que ha demostrado prevenir los efectos del ácido domoico en las células gliales de rata.

La pirrolina-5-carboxilato reductasa 2, está implicada en el metabolismo del glutamato y la prolina y ha demostrado tener una función protectora frente al estrés oxidativo (Krishnan et al., 2008).

Otra posible respuesta para evitar el efecto del ácido domoico es la infraexpresión de receptores de glutamato. Esta infraexpresión se observa en la glándula digestiva de *A. opercularis* con 7 genes que codifican para receptores de glutamato (2 de receptores NMDA y 5 de ácido kaínico) infraexpresados (Ventoso et al., 2019). En *M. galloprovincialis* y *P. maximus*, no se observa expresión diferencial para ninguno de estos genes (Pazos et al., 2017; Ventoso et al., 2021), pero sí se observa en estas dos especies la expresión de genes que codifican para receptores de glutamato. El número de transcritos que codifican para posibles receptores de glutamato es bastante mayor en la glándula digestiva de las dos especies de pectínidos que en la del mejillón.

En una línea similar a nuestros resultados Hiolski et al. (2014) observaron una infraexpresión de genes que codifican para receptores de glutamato tras la exposición crónica a concentraciones bajas de ácido domoico en el pez cebra. Esta infrarregulación de los receptores de glutamato, puede compensar el aumento de la actividad glutamatérgica causada por el ácido domoico, y con ello, sus efectos nocivos.

El sistema inmune de los moluscos bivalvos es sensible a los contaminantes ambientales (Renault, 2015). La expresión diferencial de genes que codifican para proteínas implicadas en el sistema inmune fue observada en las 3 especies (Pazos et al., 2017; Ventoso et al., 2021, 2019).

En *M. galloprovincialis*, un gen que codifica para una proteína que contiene el dominio C1q se encuentra entre los 25 genes más sobreexpresados y el dominio Pfam C1q (*PF00386.16//C1q_domain*) se encuentra funcionalmente enriquecido con 18 genes diferencialmente expresados. Este dominio está implicado en procesos inmunológicos como la activación de la vía clásica del complemento y el reconocimiento bacteriano (Gerdol et al., 2015, 2011). En el análisis de enriquecimiento funcional Pfam, también se encuentran enriquecidas proteínas que contienen el dominio C-terminal globular del fibrinógeno. A su vez, las lectinas tipo C, se encuentran principalmente sobreexpresadas (Pazos et al., 2017).

En *A. opercularis*, se observa de forma generalizada una infraexpresión de genes implicados en la respuesta inmune. La "respuesta inmune" y los "procesos del sistema inmune" son 2 de los términos GO más enriquecidos entre los genes infraexpresados. En el mismo sentido, las familias Pfam "proteínas portadoras del dominio C1q", "dominio C-terminal globular del fibrinógeno", "dominio de inmunoglobulina" y "factor de necrosis tumoral (TNF)" se encuentran significativamente enriquecidas (Ventoso et al., 2019).

En cambio, los genes que codifican para lectinas tipo C se encuentran principalmente sobreexpresados en *A. opercularis*. La sobrerregulación de las lectinas tipo C es común en las tres especies estudiadas (Pazos et al., 2017; Ventoso et al., 2021, 2019). Los estudios realizados por diversos autores (Astuya et al., 2015; Detree et al., 2016; Núñez-Acuña et al., 2013) evidencian una expresión diferencial de genes implicados en procesos inmunológicos, entre los cuales se encuentra la sobrerregulación de lectinas tipo C en *M. chilensis* tras exposición a saxitoxinas. Las lectinas tipo C son especialmente abundantes en la glándula digestiva de los moluscos bivalvos. Se caracterizan por presentar un dominio de reconocimiento de carbohidratos dependiente de calcio y participan en el reconocimiento de patógenos y en el sistema inmune innato (Gerdol and Venier, 2015).

Pales Espinosa and Allam (2018) encontraron una función no inmune de las lectinas tipo C. En la ostra *Crassostrea virginica*, estas proteínas están implicadas en la eficiencia del reconocimiento de partículas de alimento, permitiendo descartar la ingestión de líneas toxigénicas de algas nocivas. Esta función en la selección del alimento es de gran interés, la sobreexpresión de lectinas tipo C, permitiría potencialmente un mejor descarte de células de líneas toxigénicas en el sistema digestivo de moluscos bivalvos.

En *P. maximus*, aparte de la sobreexpresión de genes que codifican para lectinas tipo C, proteínas implicadas en "procesos del sistema inmune" muestran interacciones funcionales en la red obtenida mediante el algoritmo String, tanto para los genes sobreexpresados como para los infraexpresados (Ventoso et al., 2021).

Diversos estudios muestran una infrarregulación de procesos del sistema inmune tras la exposición a biotoxinas marinas. Chi et al. (2018) observaron una infraexpresión de genes que codifican para lectinas tipo C en *A. irradians* en respuesta al ácido okadaico. Gerdol et al. (2014) observaron en *M. galloprovincialis* una infraexpresión de genes que codifican para proteínas que contienen el dominio C1q tras ser alimentado con líneas toxigénicas de *Alexandrium minutum*. Hégaret et al. (2011) evaluaron *in vitro* las interacciones entre varias algas nocivas y hemocitos de moluscos bivalvos, observando que algunas especies de algas actuaban como inmunoestimulantes mientras que otras como inmunosupresores.

En resumen, las publicaciones disponibles hasta la fecha, muestran tanto la sobrerregulación como la infrarregulación de procesos del sistema inmune en moluscos bivalvos tras exposición a algas nocivas productoras de toxinas, lo que concuerda con nuestros resultados.

Hemos encontrado transportadores de las familias SLC5, SLC16, SLC17, SLC21, SLC22, SLC26, SLC39 y SLC49 que están sobreexpresados tanto en el mejillón como en la volandeira (Pazos et al., 2017; Ventoso et al., 2019). Así entre los genes que hemos encontrado sobreexpresados tras la exposición in vivo a *Pseudo-nitzschia* productora de ácido domoico en *M. galloprovincialis* (Pazos et al., 2017) están el *SLC5A1*, el *SLC17A5*, y genes de las familias *SLC6* y *SLC16* y en *A. opercularis* (Ventoso et al., 2019) el *SLC5A1*, el *SLC16A10* y el *SLC17A5*. Esto concuerda con los resultados de García-Corona (2023) que muestran que la exposición *in vitro* al ácido domoico en la glándula digestiva de *M. edulis*, causa una sobreexpresión de genes que codifican para transportadores de membrana de la familia de los SLC (SLC5, SLC5A1, SLC17A5, SLC16A10, SLC6A9).

Es interesante señalar que tres transcritos que codifican para la sialina (SLC17A5), se encuentran sobreexpresados en *M galloprovincialis* (Pazos et al., 2017) y uno en *A. opercularis* (Ventoso et al., 2019). La familia SLC17 media el transporte transmembrana de aniones orgánicos, entre los cuales, se encuentra el transporte vesicular de glutamato (Miyaji et al., 2011; Reimer, 2013). Estos transportadores podrían estar implicados en el transporte de ácido domoico, el cual es estructuralmente análogo al glutamato. La actividad de los transportadores de la familia SLC17 es dependiente de Cl^- (Miyaji et al., 2011; Reimer, 2013), en línea con los resultados obtenidos por Blanco et al. (2021a) para los transportadores implicados en los mecanismos de captación de ácido domoico en la glándula digestiva de *M. galloprovincialis*. La dirección del flujo del transporte depende frecuentemente de la diferencia de concentración intra/extracelular, por lo que los transportadores SLC17 son candidatos para participar en el proceso de captación y/o excreción del ácido domoico.

Entre los genes sobreexpresados en *M. galloprovincialis* (Pazos et al., 2017) se encuentran 2 transcritos que codifican para miembros de la familia SLC6 (transportadores de neurotransmisores dependientes de sodio y cloruro). En la vieira (Ventoso et al., 2021) está también sobreexpresado un gen de la familia *SLC6* que codifica para un posible transportador de glicina dependiente de sodio y cloruro (*SLC6A9*). La sobrerregulación de este transportador podría reducir la activación de receptores de glutamato NMDA, ya que la glicina es co-agonista de los receptores de glutamato NMDA y esta sería recaptada del espacio extracelular reduciendo su disponibilidad para actuar sobre los receptores. Este mecanismo es el que se observa en el sistema nervioso central de vertebrados, el transportador de glicina 1 regula la unión de la glicina a los receptores NMDA mediante su recaptación del espacio sináptico (Aragón and López-Corcuera, 2005; Zafra et al., 2017). Varias publicaciones relacionan a la familia SLC6 con la toxicidad de diversas especies del género *Pseudo-nitzschia*. Di Dato et al. (2015) encontraron un transcrito que codifica para un transportador de la familia SLC6 que se encuentra sobreexpresado en *P. multistriata* en relación con 2 especies no productoras de ácido domoico *P. arenysensis* y *P. delicatissima*. En la misma línea Boissonneault et al. (2013) encontraron la sobreexpresión de un gen de esta familia en *P. multiseries* en condiciones de producción de toxina en relación con condiciones de no toxicidad. En vertebrados, Lefebvre et al. (2009) mostraron la sobreexpresión del gen *slc6a8* (transportador de creatina 1 dependiente de sodio y cloruro) en el cerebro del pez cebra tras la exposición al ácido domoico.

Por el contrario en *A. opercularis* (Ventoso et al., 2019) aunque la mayoría de los genes *SLC* se encuentran sobreexpresados, la familia SLC6 es una excepción con 48 genes infraexpresados. Además, el término GO "actividad simporte de neurotransmisores dependiente de sodio", es uno de los más enriquecidos entre los genes infraexpresados. El elevado número de transcritos que codifican para transportadores SLC6 en *A. opercularis*, está en línea con los resultados obtenidos por Li et al. (2017) y Xun et al. (2020), que observaron una expansión de genes de la familia *SLC6* en *C. farreri* y *M. yessoensis* respectivamente.

Otras familias *SLC* sobreexpresadas en mejillón y volandeira a destacar son *SLC16* (transportadores monocarboxilato) y *SLC22* (transportadores de cationes orgánicos/aniones/zwitteriones). Se tratan de las familias con mayor número de genes sobreexpresados en *M. galloprovincialis* y *A. opercularis* (Pazos et al., 2017; Ventoso et al., 2019). En concordancia con esto Lefebvre et al. (2009) encontraron 2 transcritos que codifican para el transportador SLC16A9 sobreexpresados en el cerebro del pez cebra tras la exposición al ácido domoico. La familia *SLC22* participa en la absorción (intestino delgado) y excreción

(riñón e hígado) de xenobióticos y sustancias endógenas (Koepsell, 2013) por lo que podría tener un papel en la depuración del ácido domoico.

Una situación similar en cuanto al papel de los transportadores SLC en el transporte de una toxina es la descrita por Xun et al. (2020) que encontraron que en *P. yessoensis* hay una expansión significativa de las familias *SLC5*, *SLC6*, *SLC16*, *SLC23* y *SLC46*, y que tras alimentar los pectínidos con dinoflagelados productores de toxina paralizante (PST) se sobreexpresaron 102 genes de la superfamilia *SLC* en la glándula digestiva, por lo que sugieren la participación de algunos de estos transportadores en el transporte de PST.

Uno de los problemas a la hora de abordar el presente trabajo es que desconocemos la identidad del transportador específico del ácido domoico (o los transportadores específicos), tanto hacia dentro como hacia fuera de las células, pero no solo lo desconocemos en los bivalvos, sino en cualquier organismo. Los resultados que hemos obtenido, junto con la bibliografía disponible (Blanco et al., 2021a; Kimura et al., 2011; Madhyastha et al., 1991; Pazos et al., 2017; Ventoso et al., 2019), sugieren que lo más probable es que intervenga un transportador (o varios) de la superfamilia de los SLC (solute carriers), que comprende unas 66 familias con en torno a 450 genes en humanos (Dvorak and Superti-Furga, 2023) (https://www.bioparadigms.org/slc/intro.htm), mientras que en el pectínido *Mizuhopecten yessoensis* se identificaron 673 genes *SLC* pertenecientes a 48 familias (Xun et al., 2020).

En vertebrados, Kimura et al. (2011) mostraron que intercambiadores de aniones están implicados en el transporte apical-basolateral del ácido domoico a través de monocapas de células Caco-2 (las cuales representan la barrera intestinal humana). Los intercambiadores de aniones pertenecen a la familia SLC (transportadores de solutos), por lo que estos resultados indican que los transportadores SLC son, probablemente, los responsables del transporte transmembrana del ácido domoico en mamíferos.

El ácido domoico es una molécula polar y necesita de un transportador para atravesar la membrana plasmática. Mauriz and Blanco (2010) determinaron la distribución subcelular del ácido domoico en la glándula digestiva de la vieira *P. maximus* mediante centrifugaciones en serie, ultrafiltración y cromatografía por exclusión de tamaño (SEC) observando que la mayor parte de ácido domoico, >90 %, se encuentra libre en el citosol. A raíz de estos resultados, establecieron la hipótesis de que la causa de la larga acumulación de toxina en *P. maximus* es la ausencia de un transportador de membrana eficiente.

Blanco et al. (2021a) encontraron que la entrada de ácido domoico en la glándula digestiva de *M. galloprovincialis*, es dependiente de Cl^- (aunque puede realizar su actividad empleando otros aniones), independiente de ATP y ligeramente sensible al pH. Estas características las presentan transportadores miembros de la familia SLC, lo que supone una prueba de la implicación de miembros de esta familia en el transporte transmembrana del ácido domoico en moluscos bivalvos. En *M. edulis* el ácido kaínico, el ácido glutámico y la prolina inhibían la captación in vitro de ácido domoico disuelto por el tejido de la glándula digestiva, lo que indica competencia por el mismo sitio transportador (Madhyastha et al., 1991), como los transportadores de ácido glutámico y de prolina en mamíferos pertenecen al grupo de los SLC (*solute carriers*), esto es un dato más en favor de la hipótesis de que el o los transportadores transmembrana de ácido domoico pertenecen a la familia de los SLC. Los transportadores SLC median el transporte de azúcares, aminoácidos, neurotransmisores, nucleótidos, iones inorgánicos y xenobióticos a

través de la membrana plasmática. Los transportadores de esta familia pueden realizar un transporte pasivo (denominado también transporte facilitado) o un transporte activo secundario (Hoglund et al., 2011).

Es importante señalar que el campo de los transportadores de membrana es complejo y en comparación con otras familias de genes de importancia similar, los SLC están relativamente poco estudiados (César-Razquin et al., 2015), pues todavía hay muchos transportadores de los que se desconoce la identidad de las moléculas que transportan. En torno a un 10% del genoma humano codifica proteínas transportadoras y un tercio de dichos transportadores son huérfanos, es decir, no se conoce cuál es la molécula transportada (Dvorak and Superti-Furga, 2023; Meixner et al., 2020). En otros, se conoce alguno de los posibles sustratos, pero no se sabe cuál es el sustrato real en condiciones fisiológicas. La situación se complica además porque hay transportadores que transportan diversos sustratos, y también hay moléculas que pueden ser transportadas por más de un transportador. Así por ejemplo hay más de 10 transportadores (SLC1A1; SLC1A2; SLC1A3; SLC1A5; SLC1A6; SLC1A7; SLC7A11; SLC17A6; SLC17A8; SLC22A7; SLC25A18; SLC25A22) que pueden transportar el ácido glutámico (Meixner et al., 2020) (https://opendata.cemm.at/gsflab/slcontology/; http://slc.bioparadigms.org/).

Aparte de la familia SLC, otra de las principales superfamilias de transportadores de membrana es la superfamilia de transportadores dependientes de ATP (superfamilia de transportadores ABC) (Dean et al., 2022), pero a diferencia de lo que sucede con los transportadores SLC hemos encontrado muy pocos genes sobreexpresados que codifiquen para transportadores ABC (Pazos et al., 2017; Ventoso et al., 2021, 2019). Jansen et al. (2015) a través de un ensayo de transporte vesicular, encontraron que el transporte de ácido domoico podría estar mediado por transportadores ABC. Schultz et al. (2013) estableció la hipótesis de que la absorción del ácido domoico desde el intestino anterior y su transferencia a la glándula digestiva y la hemolinfa, es regulada por transportadores ABC unidos a la membrana plasmática en el cangrejo *Metacarcinus magister*. Huang et al. (2014); Lozano et al. (2015); Martínez-Escauriaza et al. (2021); Xu et al. (2014) encontraron que transportadores ABC están probablemente implicados en la eliminación de otra biotoxina, el ácido okadaico, en moluscos bivalvos.

Diversas enzimas implicadas en el metabolismo de xenobióticos, tanto de la fase I (funcionalización) como de la fase II (conjugación), se encuentran diferencialmente expresadas en *M. galloprovincialis*, *A. opercularis* y *P. maximus* (Pazos et al., 2017; Ventoso et al., 2021, 2019). Los genes que codifican para citocromos P450, glutation S-transferasas y sulfotransferasas se encuentran mayoritariamente sobreexpresados (Pazos et al., 2017; Ventoso et al., 2021, 2019) en las tres especies. En *A. opercularis*, además, los dominios Pfam citocromo P450, aldo-ceto reductasas, glutation S-transferasa y sulfotransferasa se encuentran funcionalmente enriquecidos y estas mismas enzimas constituyen nodos altamente conectados en la red de interacciones proteína-proteína elaborada con el algoritmo String (Ventoso et al., 2019). También se observa en la volandeira un alto número de transcritos que codifican para sulfotransferasas (Ventoso et al., 2019), lo que es indicativo de una expansión de esta familia, la cual, se encuentra expandida en el genoma de *C. farreri* (Li et al., 2017).

Peña-Llopis et al. (2014) demostraron que el tratamiento con N-acetilcisteína, permite expulsar más eficazmente el ácido domoico en la vieira *P. maximus* por un incremento de la actividad glutation S-transferasa y la inducción del anabolismo de glutation. Por lo tanto, la glutation S-

transferasa puede participar en el proceso de excreción del ácido domoico. Aunque un trabajo reciente encontró que el tratamiento con N-acetilcisteína no reduce de forma significativa la cantidad de ácido domoico en la glándula digestiva de la vieira (Vanmaldergem et al., 2023).

En *P. maximus* hemos encontrado una sobreexpresión de genes relacionados con la autofagia y el transporte mediado por vesículas junto con un enriquecimiento funcional de los términos GO "autofagia", "lisosoma" y "transporte mediado por vesículas" (Ventoso et al., 2021). En línea con estos resultados, García-Corona (2023) tras una exposición in vitro al ácido domoico de la glándula digestiva de *P. maximus*, observó una sobreexpresión de genes que codifican proteínas relacionadas con la autofagia (*ATG13*, *ATG16* y *ATG101*), así como la acumulación de ácido domoico en autofagosomas, mientras que tras esa misma exposición en *M. edulis* no se sobreexpresan los genes relacionados con autofagia ni se acumula ácido domoico en los autofagosomas.

La autofagia es un proceso autodegradativo muy conservado evolutivamente en los eucariotas que permite la degradación de componentes sobre todo intracelulares (proteínas, ácidos nucleicos, lípidos, organelas...), pero también extracelulares (Aman et al., 2021; Glick et al., 2010; Parzych and Klionsky, 2014; Yu et al., 2018). La autofagia desempeña varias funciones, en condiciones normales el nivel constitutivo de autofagia permite mantener la homeostasia celular degradando moléculas y organelas dañadas (Parzych and Klionsky, 2014). En condiciones de estrés nutricional (falta de alimento) la autofagia se activa y la degradación de componentes celulares permite producir energía para permitir la supervivencia celular (Boya et al., 2013; Parzych and Klionsky, 2014). La autofagia también se puede activar en otros tipos de estrés (por toxinas o por contaminantes antropogénicos por ejemplo) y es un medio de eliminación de patógenos como bacterias o virus (Boya et al., 2013; Pesonen and Vähäkangas, 2019; Rahman et al., 2023). El estrés oxidativo es uno de los tipos de estrés que puede activar la autofagia. Los resultados de Song et al. (2023) sugieren que un estrés oxidativo elevado activa la autofagia, pero falla en la eliminación de la lipofuscina, dejando una gran cantidad de autolisosomas llenos de lipofuscina, denominados cuerpos residuales.

Varios trabajos recientes, García-Corona et al. (2024c, 2024b, 2024a, 2022), utilizando técnicas inmunohistoquímicas con anticuerpos frente al ácido domoico han estudiado la acumulación y la localización subcelular del ácido domoico en moluscos bivalvos. En *P. maximus* el ácido domoico se detecta sobre todo en vesículas autofagosómicas de tamaño pequeño (1-2,5 μm) distribuidas por todo el citoplasma de las células digestivas habiendo también una pequeña fracción de inmunorreactividad en cuerpos residuales (García-Corona et al., 2024c, 2022). En el caso de *A. opercular*is García-Corona et al. (2024c) detectaron el ácido domoico sobre todo en los cuerpos residuales de los divertículos digestivos, pero no en vesículas de tipo autofagosoma. Los autofagosomas que contienen el ácido domoico formarían cuerpos residuales que pueden permanecer en el citoplasma de las células digestivas indefinidamente contribuyendo a la baja tasa de depuración del ácido domoico en la vieira (García-Corona et al., 2024c). En *P. maximus*, García-Corona et al. (2024c, 2022) plantean la hipótesis de que una parte del ácido domoico acumulado permanece en la glándula digestiva debido a la ausencia de transportador eficiente como propusieron Mauriz and Blanco (2010), y a que su desintoxicación es más lenta debido a la formación de autofagosomas que lo retienen.

García-Corona et al. (2024a, 2024b, 2024c) encontraron diferencias temporales en la formación de cuerpos residuales (autofagia tardía) entre *A. opercularis* (inmediatamente después de los

afloramientos tóxicos de *Pseudo-nitzschia*) y *P. maximus* (un mes después de los afloramientos tóxicos de *Pseudo-nitzschia*), esto les llevó a plantear la hipótesis de que el ácido domoico permanece atrapado dentro de estas estructuras menos tiempo en las volandeiras que en las vieiras, porque las volandeiras procesan el ácido domoico más rápido. Estos autores García-Corona et al. (2024a, 2024b, 2024c) sugieren que la autofagia tardía (cuerpos residuales) podría explicar, en parte, la baja tasa de depuración del ácido domoico en *P. maximus* y *A. opercularis*.

Es interesante señalar que los resultados obtenidos por García-Corona et al. (2024c) muestran que, aunque el contenido en ácido domoico en la glándula digestiva de *P. maximus* (638,6 mg kg^{-1} de media) es unas 28 veces superior al de *A. opercularis* (22,7 mg kg^{-1} de media) esa diferencia tan grande no se ve en el porcentaje de superficie cubierta con señal cromogénica frente al ácido domoico que es del 4,8 % en *P. maximus* y del 3,2 % en *A. opercularis*, es decir, solo es 1,5 veces superior en la vieira. Esta diferencia se debe probablemente a que parte del ácido domoico se pierde durante el tratamiento histológico de la glándula digestiva (hay que tener en cuenta que el ácido domoico es una molécula muy hidrosoluble que puede ser parcialmente extraída por algunos de los solventes utilizados en el procesamiento histológico). García-Corona et al. (2024c) indican que una parte del ácido domoico podría perderse por lavado durante el procesado histológico. Es lógico pensar que el ácido domoico que se pierde corresponde al que Mauriz and Blanco (2010) encontraron que está presente de forma "libre" en el citosol de las células de la glándula digestiva de *P. maximus* empleando centrifugaciones en serie, ultrafiltración y cromatografía de exclusión por tamaño (SEC). Los resultados de García-Corona et al. (2024c) también muestran que en la coquina (*Donax trunculus*) el contenido medio en ácido domoico es de 12 mg kg^{-1}, aproximadamente la mitad del de la volandeira (22,7 mg kg^{-1}) mientras que el porcentaje de superficie cubierta con señal cromogénica frente al ácido domoico es de solo el 0,2 %, es decir, es unas 16 veces inferior en la coquina en relación a la volandeira. La mejor explicación posible es que la mayor parte del ácido domoico de la coquina no se detecta por medio de las técnicas inmunohistoquímicas, probablemente porque se pierde en el procesamiento histológico.

En resumen, quedan todavía muchos aspectos por resolver, por lo que hay más preguntas que respuestas. De los resultados de la presente memoria, junto con los de la bibliografía, podemos decir que lo más probable es que el transporte transmembrana del ácido domoico (tanto hacia el interior como hacia el exterior de las células) lo realicen uno o varios transportadores de la familia de los SLC, sin que se pueda descartar la existencia también de un transporte mediante vesículas. Una posible hipótesis para explicar la diferencia entre depuradores rápidos como los mejillones (*M. edulis* y *M. galloprovincialis*) y lentos como las vieiras (*P. maximus*), es que en los depuradores rápidos la presencia de transportadores eficientes permite la expulsión rápida de la toxina, que por ello no se acumula en el interior de las células ni en autofagosomas (no se activaría la autofagia), mientras que en los depuradores lentos la baja eficiencia de los transportadores (o la baja expresión de los genes que los codifican, es decir, que el número de transportadores presentes sea bajo) conduce a una acumulación del ácido domoico en el interior de las células y éste activa la autofagia. Esto conduce a que una parte de la toxina se acumule en autofagosomas, autolisosomas y cuerpos residuales, pero la mayor parte estaría libre en el citosol como encontraron Mauriz y Blanco (2010). Por tanto, la acción de la autofagia no sería suficiente para explicar la lenta depuración, pues no explica por qué la toxina que está libre en el citosol no es transportada hacia fuera de las células. Según esta hipótesis habría dos mecanismos de eliminación del ácido domoico en la vieira uno principal o más importante (mediante transportadores de membrana) y otro secundario o menos importante (de tipo

vesicular relacionado con la autofagia). Otras opciones o hipótesis son también posibles, pues el estado actual de los conocimientos es todavía insuficiente para conocer bien el papel jugado por los transportadores de membrana, la autofagia, el transporte vesicular y otros posibles factores en la dinámica de acumulación y eliminación del ácido domoico en los moluscos bivalvos.

5 CONCLUSIONES

La secuenciación y el ensamblaje *de novo* de los transcriptomas de la glándula digestiva de tres moluscos bivalvos, el mejillón (*Mytilus galloprovincialis*), la vieira (*Pecten maximus*) y la volandeira (*Aequipecten opercularis*) dio lugar a la obtención de 69294, 72673 y 142137 unigenes respectivamente. Una vez ensamblados se realizó la anotación funcional de los transcriptomas frente a diferentes bases de datos: Uniprot, NCBI-nr, PFAM (Protein Families Database), GO (Gene Ontology), KEGG (Kyoto Encyclopedia of Genes and Genomes).

Los resultados obtenidos demuestran la participación del ácido domoico en la expresión diferencial en la vieira, mientras que, tanto en el mejillón como en la volandeira, además del efecto del ácido domoico un papel de la *Pseudo-nitzschia* en sí misma y de otros factores no puede descartarse. El análisis de la expresión génica diferencial entre animales control y animales expuestos a una floración natural de *Pseudo-nitzschia* productora de ácido domoico, en *Mytilus galloprovincialis* y en *A. opercularis*, permitió obtener 1158 y 10144 genes diferencialmente expresados respectivamente. Por su parte el número de genes expresados diferencialmente en la glándula digestiva de *P. maximus* después de la inyección de ácido domoico en el músculo aductor fue de 535.

Algunos resultados de expresión diferencial son coincidentes en las especies estudiadas (sobre todo en *M. galloprovincialis* y *A. opercularis*): la sobreexpresión de genes que codifican para enzimas implicadas en el metabolismo de xenobióticos (citocromos P450, aldo/ceto reductasas, glutatión S-transferasas y sulfotransferasas) y para transportadores de la superfamilia SLC (*solute carriers*), la expresión diferencial de genes relacionados con la respuesta inmune (generalmente infraexpresados), la respuesta frente al estrés (especialmente el estrés oxidativo) y la apoptosis.

Los resultados obtenidos en las tres especies de bivalvos junto con la bibliografía disponible indican que uno de los principales efectos de la exposición al ácido domoico, y a *Pseudo-nitzschia* productora de ácido domoico, es el estrés oxidativo y una parte de los genes diferencialmente expresados están implicados en la respuesta frente a dicho estrés. Esto es especialmente claro en *A. opercularis* donde los resultados del análisis de las redes de proteínas (*protein network analysis*) sugieren que la exposición a *Pseudo-nitzschia* productora de ácido domoico provoca estrés oxidativo y disfunción mitocondrial. La respuesta transcriptómica intenta contrarrestar estos efectos con la sobreexpresión de genes que codifican algunas proteínas mitocondriales, componentes del proteasoma y enzimas antioxidantes (glutatión S-transferasas, tiorredoxinas, glutarredoxinas y cobre/zinc superóxido dismutasas).

En *P. maximus* la alteración de varios procesos biológicos, celulares y moleculares evidencian una respuesta de estrés a nivel de expresión génica, probablemente causada por la inyección de ácido domoico. Así, las redes de proteínas obtenidas con los genes sobreexpresados están enriquecidas en términos de ontología génica (GO), tales como transporte mediado por

vesículas, respuesta frente al estrés, transducción de señales, procesos del sistema inmune, procesos metabólicos del ARN, autofagia, lisosoma y actividad oxidorreductasa. Mientras que las redes obtenidas con los genes infraexpresados están enriquecidas en términos tales como respuesta frente al estrés, procesos del sistema inmune, biogénesis de ribosomas, transducción de señales, procesamiento del ARNm y actividad oxidorreductasa.

En la glándula digestiva de las tres especies hay expresión de genes que codifican para receptores de glutamato, tanto ionotrópicos como metabotrópicos. Parte de las acciones del ácido domoico pueden estar mediadas por estos receptores. Además, en *A. opercularis* algunos genes que codifican receptores ionotrópicos de glutamato (dos genes que codifican receptores NMDA y cinco que codifican receptores de kainato) están infraexpresados tras la exposición a *Pseudo-nitzschia* productora de ácido domoico, siendo posible que esta infraexpresión sea una respuesta compensatoria a la actividad glutamatérgica elevada causada por el ácido domoico.

De los resultados de la presente memoria, junto con los de la bibliografía, se deduce que lo más probable es que el transporte transmembrana del ácido domoico (tanto hacia el interior como hacia el exterior de las células) lo realicen uno o varios transportadores de la familia de los SLC (solute carriers), varios de los cuales están sobreexpresados tras la exposición al ácido domoico o a *Pseudo-nitzschia* productora de ácido domoico. La ausencia de transportadores transmembrana de ácido domoico eficientes y/o el bajo nivel de expresión de dichos transportadores podrían estar implicados en la baja tasa de depuración del ácido domoico en *P. maximus*. Desafortunadamente, el desconocimiento sobre la identidad de los transportadores transmembrana de ácido domoico en otras especies hace que sea difícil identificarlos en los moluscos bivalvos.

6 REFERENCIAS BIBLIOGRÁFICAS

Alam, A., Locher, K.P., 2023. Structure and Mechanism of Human ABC Transporters. Annual Review of Biophysics 52, 275–300. https://doi.org/10.1146/annurev-biophys-111622-091232

Altschul, S.F., Gish, W., Miller, W., Myers, E.W., Lipman, D.J., 1990. Basic local alignment search tool. Journal of Molecular Biology 215, 403–410. https://doi.org/10.1016/S0022-2836(05)80360-2

Altschul, S.F., Madden, T.L., Schäffer, A.A., Zhang, J., Zhang, Z., Miller, W., Lipman, D.J., 1997. Gapped BLAST and PSI-BLAST: a new generation of protein database search programs. Nucleic Acids Res 25, 3389–3402.

Álvarez, G., Rengel, J., Araya, M., Álvarez, F., Pino, R., Uribe, E., Díaz, P.A., Rossignoli, A.E., López-Rivera, A., Blanco, J., 2020. Rapid Domoic Acid Depuration in the Scallop Argopecten purpuratus and Its Transfer from the Digestive Gland to Other Organs. Toxins 12, 698. https://doi.org/10.3390/toxins12110698

Aman, Y., Schmauck-Medina, T., Hansen, M., Morimoto, R.I., Simon, A.K., Bjedov, I., Palikaras, K., Simonsen, A., Johansen, T., Tavernarakis, N., Rubinsztein, D.C., Partridge, L., Kroemer, G., Labbadia, J., Fang, E.F., 2021. Autophagy in healthy aging and disease. Nat Aging 1, 634–650. https://doi.org/10.1038/s43587-021-00098-4

Andersen, C.L., Jensen, J.L., Ørntoft, T.F., 2004. Normalization of Real-Time Quantitative Reverse Transcription-PCR Data: A Model-Based Variance Estimation Approach to Identify Genes Suited for Normalization, Applied to Bladder and Colon Cancer Data Sets. Cancer Res 64, 5245–5250. https://doi.org/10.1158/0008-5472.CAN-04-0496

Anderson, K., Taylor, D.A., Thompson, E.L., Melwani, A.R., Nair, S.V., Raftos, D.A., 2015. Meta-Analysis of Studies Using Suppression Subtractive Hybridization and Microarrays to Investigate the Effects of Environmental Stress on Gene Transcription in Oysters. PLOS ONE 10, e0118839. https://doi.org/10.1371/journal.pone.0118839

Andrews, E.B., 1988. 13 - Excretory Systems of Molluscs, in: Trueman, E.R., Clarke, M.R. (Eds.), Form and Function, The Mollusca. Academic Press, San Diego, pp. 381–448. https://doi.org/10.1016/B978-0-12-751411-6.50020-5

Andrews, E.B., Jennings, K.H., 1993. The anatomical and ultrastructural basis of primary urine formation in Bivalve Molluscs. J. Mollus. Stud. 59, 223–257. https://doi.org/10.1093/mollus/59.2.223

APROMAR, 2023. La Acuicultura en España 2023.

APROMAR, 2022. La Acuicultura en España 2022.

Aragón, C., López-Corcuera, B., 2005. Glycine transporters: crucial roles of pharmacological interest revealed by gene deletion. Trends in Pharmacological Sciences 26, 283–286. https://doi.org/10.1016/j.tips.2005.04.007

Artigaud, S., Richard, J., Thorne, M.A., Lavaud, R., Flye-Sainte-Marie, J., Jean, F., Peck, L.S., Clark, M.S., Pichereau, V., 2015. Deciphering the molecular adaptation of the king scallop (Pecten maximus) to heat stress using transcriptomics and proteomics. BMC Genomics 16, 988. https://doi.org/10.1186/s12864-015-2132-x

Astuya, A., Carrera, C., Ulloa, V., Aballay, A., Núñez-Acuña, G., Hégaret, H., Gallardo-Escárate, C., 2015. Saxitoxin Modulates Immunological Parameters and Gene Transcription in Mytilus chilensis Hemocytes. International Journal of Molecular Sciences 16, 15235–15250. https://doi.org/10.3390/ijms160715235

Bard, S.M., 2000. Multixenobiotic resistance as a cellular defense mechanism in aquatic organisms. Aquatic Toxicology 48, 357–389. https://doi.org/10.1016/S0166-445X(00)00088-6

Basti, L., Hégaret, H., Shumway, S.E., 2018. Harmful Algal Blooms and Shellfish, in: Harmful Algal Blooms. John Wiley & Sons, Ltd, pp. 135–190. https://doi.org/10.1002/9781118994672.ch4

Bates, S.S., Bird, C.J., Freitas, A.S.W. de, Foxall, R., Gilgan, M., Hanic, L.A., Johnson, G.R., McCulloch, A.W., Odense, P., Pocklington, R., Quilliam, M.A., Sim, P.G., Smith, J.C., Rao, D.V.S., Todd, E.C.D., Walter, J.A., Wright, J.L.C., 1989. Pennate Diatom Nitzschia pungens as the Primary Source of Domoic Acid, a Toxin in Shellfish from Eastern Prince Edward Island, Canada. Can. J. Fish. Aquat. Sci. 46, 1203–1215. https://doi.org/10.1139/f89-156

Bates, S.S., Hubbard, K.A., Lundholm, N., Montresor, M., Leaw, C.P., 2018. Pseudo-nitzschia, Nitzschia, and domoic acid: New research since 2011. Harmful Algae 79, 3–43. https://doi.org/10.1016/j.hal.2018.06.001

Bates, S.S., Lundholm, N., Hubbard, K.A., Montresor, M., Leaw, C.P., 2019. Toxic and Harmful Marine Diatoms, in: Diatoms: Fundamentals and Applications. John Wiley & Sons, Ltd, pp. 389–434. https://doi.org/10.1002/9781119370741.ch17

Beninger, P.G., Le Pennec, M., 2016. Chapter 3 - Scallop Structure and Function, in: Shumway, S.E., Parsons, G.J. (Eds.), Developments in Aquaculture and Fisheries Science, Scallops. Elsevier, pp. 85–159. https://doi.org/10.1016/B978-0-444-62710-0.00003-1

Blanchette, B., Feng, X., Singh, B.R., 2007. Marine Glutathione S-Transferases. Mar Biotechnol 9, 513–542. https://doi.org/10.1007/s10126-007-9034-0

Blanco, J., 2018. Accumulation of Dinophysis Toxins in Bivalve Molluscs. Toxins 10, 453. https://doi.org/10.3390/toxins10110453

Blanco, J., Acosta, C.P., Bermúdez De La Puente, M., Salgado, C., 2002a. Depuration and anatomical distribution of the amnesic shellfish poisoning (ASP) toxin domoic acid in the king scallop Pecten maximus. Aquatic Toxicology 60, 111–121.

Blanco, J., Acosta, C.P., Mariño, C., Muñiz, S., Martín, H., Moroño, Á., Correa, J., Arévalo, F., Salgado, C., 2006. Depuration of domoic acid from different body compartments of the king scallop *Pecten maximus* grown in raft culture and natural bed. Aquatic Living Resources 19, 257–265. https://doi.org/10.1051/alr:2006026

Blanco, J., de la Puente, M.B., Arévalo, F., Salgado, C., Moroño, Á., 2002b. Depuration of mussels (Mytilus galloprovincialis) contaminated with domoic acid. Aquatic Living Resources 15, 53–60.

Blanco, J., Mariño, C., Martín, H., Álvarez, G., Rossignoli, A.E., 2021a. Characterization of the Domoic Acid Uptake Mechanism of the Mussel (Mytilus galloprovincialis) Digestive Gland. Toxins 13, 458. https://doi.org/10.3390/toxins13070458

Blanco, J., Mauríz, A., Álvarez, G., 2020. Distribution of Domoic Acid in the Digestive Gland of the King Scallop Pecten maximus. Toxins 12, 371. https://doi.org/10.3390/toxins12060371

Blanco, J., Moroño, Á., Arévalo, F., Correa, J., Salgado, C., Rossignoli, A.E., Lamas, J.P., 2021b. Twenty-Five Years of Domoic Acid Monitoring in Galicia (NW Spain): Spatial, Temporal and Interspecific Variations. Toxins 13, 756. https://doi.org/10.3390/toxins13110756

Board, P.G., Menon, D., 2013. Glutathione transferases, regulators of cellular metabolism and physiology. Biochimica et Biophysica Acta (BBA) - General Subjects, Cellular functions of glutathione 1830, 3267–3288. https://doi.org/10.1016/j.bbagen.2012.11.019

Bodero, M., Hoogenboom, R.L.A.P., Bovee, T.F.H., Portier, L., de Haan, L., Peijnenburg, A., Hendriksen, P.J.M., 2018. Whole genome mRNA transcriptomics analysis reveals different modes of action of the diarrheic shellfish poisons okadaic acid and dinophysis toxin-1 versus azaspiracid-1 in Caco-2 cells. Toxicology in Vitro 46, 102–112. https://doi.org/10.1016/j.tiv.2017.09.018

Boissonneault, K.R., Henningsen, B.M., Bates, S.S., Robertson, D.L., Milton, S., Pelletier, J., Hogan, D.A., Housman, D.E., 2013. Gene expression studies for the analysis of domoic acid production in the marine diatom Pseudo-nitzschia multiseries. BMC molecular biology 14, 25.

Boya, P., Reggiori, F., Codogno, P., 2013. Emerging regulation and functions of autophagy. Nat Cell Biol 15, 713–720. https://doi.org/10.1038/ncb2788

Brown, A.R., Lilley, M., Shutler, J., Lowe, C., Artioli, Y., Torres, R., Berdalet, E., Tyler, C.R., 2020. Assessing risks and mitigating impacts of harmful algal blooms on mariculture and marine fisheries. Reviews in Aquaculture 12, 1663–1688. https://doi.org/10.1111/raq.12403

Bustin, S.A., Benes, V., Garson, J.A., Hellemans, J., Huggett, J., Kubista, M., Mueller, R., Nolan, T., Pfaffl, M.W., Shipley, G.L., Vandesompele, J., Wittwer, C.T., 2009. The MIQE Guidelines: Minimum Information for Publication of Quantitative Real-Time PCR Experiments. Clinical Chemistry 55, 611–622. https://doi.org/10.1373/clinchem.2008.112797

Cabrera, J., González, P.M., Puntarulo, S., 2020. The Phycotoxin Domoic Acid as a Potential Factor for Oxidative Alterations Enhanced by Climate Change. Front Plant Sci 11. https://doi.org/10.3389/fpls.2020.576971

Cao, R., Wang, D., Wei, Q., Wang, Q., Yang, D., Liu, H., Dong, Z., Zhang, X., Zhang, Q., Zhao, J., 2018. Integrative Biomarker Assessment of the Influence of Saxitoxin on Marine Bivalves: A Comparative Study of the Two Bivalve Species Oysters, Crassostrea gigas, and Scallops, Chlamys farreri. Front Physiol 9. https://doi.org/10.3389/fphys.2018.01173

César-Razquin, A., Snijder, B., Frappier-Brinton, T., Isserlin, R., Gyimesi, G., Bai, X., Reithmeier, R.A., Hepworth, D., Hediger, M.A., Edwards, A.M., Superti-Furga, G., 2015. A Call for Systematic Research on Solute Carriers. Cell 162, 478–487. https://doi.org/10.1016/j.cell.2015.07.022

Cheng, J., Xun, X., Kong, Y., Wang, Shuyue, Yang, Z., Li, Y., Kong, D., Wang, Shi, Zhang, L., Hu, X., Bao, Z., 2016. Hsp70 gene expansions in the scallop Patinopecten yessoensis and their expression regulation after exposure to the toxic dinoflagellate Alexandrium catenella. Fish & Shellfish Immunology 58, 266–273. https://doi.org/10.1016/j.fsi.2016.09.009

Chi, C., Giri, S.S., Jun, J.W., Kim, S.W., Kim, H.J., Kang, J.W., Park, S.C., 2018. Detoxification- and Immune-Related Transcriptomic Analysis of Gills from Bay Scallops (Argopecten irradians) in Response to Algal Toxin Okadaic Acid. Toxins 10, 308. https://doi.org/10.3390/toxins10080308

Chi, C., Zhang, C., Liu, J., Zheng, X., 2019. Effects of Marine Toxin Domoic Acid on Innate Immune Responses in Bay Scallop Argopecten irradians. Journal of Marine Science and Engineering 7, 407. https://doi.org/10.3390/jmse7110407

Ciminiello, P., Dell'Aversano, C., Fattorusso, E., Forino, M., Grauso, L., Tartaglione, L., 2011. A 4-decade-long (and still ongoing) hunt for palytoxins chemical architecture. Toxicon, Palytoxin-group toxins 57, 362–367. https://doi.org/10.1016/j.toxicon.2010.09.005

Ciminiello, P., Dell'Aversano, C., Fattorusso, E., Forino, M., Magno, G.S., Tartaglione, L., Grillo, C., Melchiorre, N., 2006. The Genoa 2005 Outbreak. Determination of Putative Palytoxin in Mediterranean Ostreopsis ovata by a New Liquid Chromatography Tandem Mass Spectrometry Method. Anal. Chem. 78, 6153–6159. https://doi.org/10.1021/ac060250j

Ciminiello, P., Dell'Aversano, C., Fattorusso, E., Forino, M., Tartaglione, L., Grillo, C., Melchiorre, N., 2008. Putative Palytoxin and Its New Analogue, Ovatoxin-a, in *Ostreopsis ovata* Collected Along the Ligurian Coasts During the 2006 Toxic Outbreak. Journal of the American Society for Mass Spectrometry 19, 111–120. https://doi.org/10.1016/j.jasms.2007.11.001

Ciminiello, P., Dell'Aversano, C., Iacovo, E.D., Fattorusso, E., Forino, M., Grauso, L., Tartaglione, L., Guerrini, F., Pistocchi, R., 2010. Complex palytoxin-like profile of Ostreopsis ovata. Identification of four new ovatoxins by high-resolution liquid chromatography/mass spectrometry. Rapid Communications in Mass Spectrometry 24, 2735–2744. https://doi.org/10.1002/rcm.4696

Conesa, A., Götz, S., García-Gómez, J.M., Terol, J., Talón, M., Robles, M., 2005. Blast2GO: a universal tool for annotation, visualization and analysis in functional genomics research. Bioinformatics 21, 3674–3676. https://doi.org/10.1093/bioinformatics/bti610

Conesa, A., Madrigal, P., Tarazona, S., Gomez-Cabrero, D., Cervera, A., McPherson, A., Szcześniak, M.W., Gaffney, D.J., Elo, L.L., Zhang, X., Mortazavi, A., 2016. A survey of best practices for RNA-seq data analysis. Genome Biology 17, 13. https://doi.org/10.1186/s13059-016-0881-8

Dai, X., Shen, L., 2022. Advances and Trends in Omics Technology Development. Frontiers in Medicine 9.

Dean, M., Moitra, K., Allikmets, R., 2022. The human ATP-binding cassette (ABC) transporter superfamily. Human Mutation 43, 1162–1182. https://doi.org/10.1002/humu.24418

Deeds, J.R., Schwartz, M.D., 2010. Human risk associated with palytoxin exposure. Toxicon, Toxins in Seafood 56, 150–162. https://doi.org/10.1016/j.toxicon.2009.05.035

Detree, C., Núñez-Acuña, G., Roberts, S., Gallardo-Escárate, C., 2016. Uncovering the Complex Transcriptome Response of Mytilus chilensis against Saxitoxin: Implications of Harmful Algal Blooms on Mussel Populations. PLOS ONE 11, e0165231. https://doi.org/10.1371/journal.pone.0165231

Di Dato, V., Musacchia, F., Petrosino, G., Patil, S., Montresor, M., Sanges, R., Ferrante, M.I., 2015. Transcriptome sequencing of three *Pseudo-nitzschia* species reveals comparable gene sets and the presence of Nitric Oxide Synthase genes in diatoms. Scientific Reports 5, 12329. https://doi.org/10.1038/srep12329

Dizer, H., Fischer, B., Harabawy, A.S.A., Hennion, M.-C., Hansen, P.-D., 2001. Toxicity of domoic acid in the marine mussel Mytilus edulis. Aquatic Toxicology 55, 149–156. https://doi.org/10.1016/S0166-445X(01)00178-3

Dong, C., Wu, H., Zheng, G., Peng, J., Guo, M., Tan, Z., 2022. Transcriptome Analysis Reveals MAPK/AMPK as a Key Regulator of the Inflammatory Response in PST Detoxification in Mytilus galloprovincialis and Argopecten irradians. Toxins 14, 516. https://doi.org/10.3390/toxins14080516

Dou, M., Jiao, Y., Zheng, J., Zhang, G., Li, H., Liu, J., Yang, W., 2020. De novo transcriptome analysis of the mussel Perna viridis after exposure to the toxic dinoflagellate Prorocentrum lima. Ecotoxicology and Environmental Safety 192, 110265. https://doi.org/10.1016/j.ecoenv.2020.110265

Duncan, P.F., Brand, A.R., Strand, Ø., Foucher, E., 2016. Chapter 19 - The European Scallop Fisheries for Pecten maximus, Aequipecten opercularis, Chlamys islandica, and Mimachlamys varia, in: Shumway, S.E., Parsons, G.J. (Eds.), Developments in Aquaculture and Fisheries Science, Scallops. Elsevier, pp. 781–858. https://doi.org/10.1016/B978-0-444-62710-0.00019-5

Dvorak, V., Superti-Furga, G., 2023. Structural and functional annotation of solute carrier transporters: implication for drug discovery. Expert Opinion on Drug Discovery 18, 1099–1115. https://doi.org/10.1080/17460441.2023.2244760

EFSA, E.F.S., 2009. Marine biotoxins in shellfish – Summary on regulated marine biotoxins. EFSA Journal 7, 1306. https://doi.org/10.2903/j.efsa.2009.1306

Esteves, F., Rueff, J., Kranendonk, M., 2021. The Central Role of Cytochrome P450 in Xenobiotic Metabolism—A Brief Review on a Fascinating Enzyme Family. Journal of Xenobiotics 11, 94–114. https://doi.org/10.3390/jox11030007

Eufemia, N., Clerte, S., Girshick, S., Epel, D., 2002. Algal products as naturally occurring substrates for p-glycoprotein in Mytilus californianus. Marine Biology 140, 343–353. https://doi.org/10.1007/s002270100693

FAO, 2024. Fishery and Aquaculture Statistics – Yearbook 2021, FAO Yearbook of Fishery and Aquaculture Statistics. FAO, Rome, Italy. https://doi.org/10.4060/cc9523en

FAO, 2004. Marine biotoxins, FAO Food and Nutrition Paper. FAO, Rome, Italy.

Farabegoli, F., Blanco, L., Rodríguez, L.P., Vieites, J.M., Cabado, A.G., 2018. Phycotoxins in Marine Shellfish: Origin, Occurrence and Effects on Humans. Marine Drugs 16, 188. https://doi.org/10.3390/md16060188

Ferreira, M., Costa, J., Reis-Henriques, M.A., 2014. ABC transporters in fish species: a review. Front Physiol 5. https://doi.org/10.3389/fphys.2014.00266

Finn, R.D., Coggill, P., Eberhardt, R.Y., Eddy, S.R., Mistry, J., Mitchell, A.L., Potter, S.C., Punta, M., Qureshi, M., Sangrador-Vegas, A., Salazar, G.A., Tate, J., Bateman, A., 2016. The Pfam protein families database: towards a more sustainable future. Nucleic Acids Res 44, D279–D285. https://doi.org/10.1093/nar/gkv1344

Fisher, R.A., 1922. On the Interpretation of $\chi 2$ from Contingency Tables, and the Calculation of P. Journal of the Royal Statistical Society 85, 87–94. https://doi.org/10.2307/2340521

Fleischer-Lambropoulos, E., Kazazoglou, T., Geladopoulos, T., Kentroti, S., Stefanis, C., Vernadakis, A., 1996. Stimulation of glutamine synthetase activity by excitatory amino acids in astrocyte cultures derived from aged mouse cerebral hemispheres may be associated with non-n-methyl-d-aspartate receptor activation. International Journal of Developmental Neuroscience 14, 523–530. https://doi.org/10.1016/0736-5748(95)00098-4

Franceschini, A., Szklarczyk, D., Frankild, S., Kuhn, M., Simonovic, M., Roth, A., Lin, J., Minguez, P., Bork, P., von Mering, C., Jensen, L.J., 2013. STRING v9.1: protein-protein interaction networks, with increased coverage and integration. Nucleic Acids Res 41, D808–D815. https://doi.org/10.1093/nar/gks1094

Franchini, A., Malagoli, D., Ottaviani, E., 2010. Targets and Effects of Yessotoxin, Okadaic Acid and Palytoxin: A Differential Review. Marine Drugs 8, 658–677. https://doi.org/10.3390/md8030658

Freitas, R., Marques, F., De Marchi, L., Vale, C., Botelho, M.J., 2020. Biochemical performance of mussels, cockles and razor shells contaminated by paralytic shellfish toxins. Environmental Research 188, 109846. https://doi.org/10.1016/j.envres.2020.109846

García-Corona, J.L., 2023. Physiological mechanisms involved in the contamination and long retention of the amnesic shellfish poisoning toxin, domoic acid, in the king scallop Pecten maximus (phdthesis). Université de Bretagne occidentale - Brest.

García-Corona, J.L., Fabioux, C., Hégaret, H., 2024a. The queen scallop *Aequipecten opercularis*: A slow domoic acid depurator? Harmful Algae 138, 102708. https://doi.org/10.1016/j.hal.2024.102708

García-Corona, J.L., Fabioux, C., Vanmaldergem, J., Petek, S., Derrien, A., Terre-Terrillon, A., Bressolier, L., Breton, F., Hegaret, H., 2024b. The amnesic shellfish poisoning toxin, domoic acid: The tattoo of the king scallop *Pecten maximus*. Harmful Algae 133, 102607. https://doi.org/10.1016/j.hal.2024.102607

García-Corona, J.L., Hégaret, H., Deléglise, M., Marzari, A., Rodríguez-Jaramillo, C., Foulon, V., Fabioux, C., 2022. First subcellular localization of the amnesic shellfish toxin, domoic acid, in bivalve tissues: Deciphering the physiological mechanisms involved in its long-retention in the king scallop Pecten maximus. Harmful Algae 116, 102251. https://doi.org/10.1016/j.hal.2022.102251

García-Corona, J.L., Hegaret, H., Lassudrie, M., Derrien, A., Terre-Terrillon, A., Delaire, T., Fabioux, C., 2024c. Comparative study of domoic acid accumulation, isomer content and associated digestive subcellular processes in five marine invertebrate species. Aquatic Toxicology 266, 106793. https://doi.org/10.1016/j.aquatox.2023.106793

Gerdol, M., Manfrin, C., De Moro, G., Figueras, A., Novoa, B., Venier, P., Pallavicini, A., 2011. The C1q domain containing proteins of the Mediterranean mussel Mytilus galloprovincialis: A widespread and diverse family of immune-related molecules. Developmental & Comparative Immunology 35, 635–643. https://doi.org/10.1016/j.dci.2011.01.018

Gerdol, M., Moro, G.D., Manfrin, C., Milandri, A., Riccardi, E., Beran, A., Venier, P., Pallavicini, A., 2014. RNA sequencing and de novo assembly of the digestive gland transcriptome in Mytilus galloprovincialis fed with toxinogenic and non-toxic strains of Alexandrium minutum. BMC Research Notes 7, 722. https://doi.org/10.1186/1756-0500-7-722

Gerdol, M., Venier, P., 2015. An updated molecular basis for mussel immunity. Fish & Shellfish Immunology 46, 17–38. https://doi.org/10.1016/j.fsi.2015.02.013

Gerdol, M., Venier, P., Pallavicini, A., 2015. The genome of the Pacific oyster Crassostrea gigas brings new insights on the massive expansion of the C1q gene family in Bivalvia. Developmental & Comparative Immunology 49, 59–71. https://doi.org/10.1016/j.dci.2014.11.007

Giordano, G., Klintworth, H.M., Kavanagh, T.J., Costa, L.G., 2008. Apoptosis induced by domoic acid in mouse cerebellar granule neurons involves activation of p38 and JNK MAP kinases. Neurochemistry International 52, 1100–1105. https://doi.org/10.1016/j.neuint.2007.11.004

Giordano, G., White, C.C., McConnachie, L.A., Fernandez, C., Kavanagh, T.J., Costa, L.G., 2006. Neurotoxicity of Domoic Acid in Cerebellar Granule Neurons in a Genetic Model of Glutathione Deficiency. Mol Pharmacol 70, 2116–2126. https://doi.org/10.1124/mol.106.027748

Giordano, G., White, C.C., Mohar, I., Kavanagh, T.J., Costa, L.G., 2007. Glutathione Levels Modulate Domoic Acid–Induced Apoptosis in Mouse Cerebellar Granule Cells. Toxicol. Sci. 100, 433–444. https://doi.org/10.1093/toxsci/kfm236

Glick, D., Barth, S., Macleod, K.F., 2010. Autophagy: cellular and molecular mechanisms. J Pathol 221, 3–12. https://doi.org/10.1002/path.2697

Gobler, C.J., 2020. Climate Change and Harmful Algal Blooms: Insights and perspective. Harmful Algae, Climate change and harmful algal blooms 91, 101731. https://doi.org/10.1016/j.hal.2019.101731

González, P.M., Puntarulo, S., 2016. Seasonality and toxins effects on oxidative/nitrosative metabolism in digestive glands of the bivalve Mytilus edulis platensis. Comparative Biochemistry and Physiology Part A: Molecular & Integrative Physiology, Special Issue: Second International Conference on Oxidative Stress in Aquatic Ecosystems 200, 79–86. https://doi.org/10.1016/j.cbpa.2016.04.011

Goodwin, S., McPherson, J.D., McCombie, W.R., 2016. Coming of age: ten years of next-generation sequencing technologies. Nat Rev Genet 17, 333–351. https://doi.org/10.1038/nrg.2016.49

Gosling, E., 2015. Marine Bivalve Molluscs, 2nd ed. John Wiley & Sons, Ltd. https://doi.org/10.1002/9781119045212

Götz, S., García-Gómez, J.M., Terol, J., Williams, T.D., Nagaraj, S.H., Nueda, M.J., Robles, M., Talón, M., Dopazo, J., Conesa, A., 2008. High-throughput functional annotation and data mining with the Blast2GO suite. Nucleic Acids Res 36, 3420–3435. https://doi.org/10.1093/nar/gkn176

Grabherr, M.G., Haas, B.J., Yassour, M., Levin, J.Z., Thompson, D.A., Amit, I., Adiconis, X., Fan, L., Raychowdhury, R., Zeng, Q., Chen, Z., Mauceli, E., Hacohen, N., Gnirke, A., Rhind, N., di Palma, F., Birren, B.W., Nusbaum, C., Lindblad-Toh, K., Friedman, N., Regev, A., 2011. Full-length transcriptome assembly from RNA-Seq data without a reference genome. Nature Biotechnology 29, 644–652. https://doi.org/10.1038/nbt.1883

Hallegraeff, G.M., 2003. Harmful algal blooms: A global overview, in: Manual on Harmful Marine Microalgae, Monographs on Oceanographic Methodology. IOC-UNESCO, Paris, pp. 25–49.

Hallegraeff, G.M., Anderson, D.M., Cembella, A., 1995. Manual on Harmful Marine Microalgae, IOC Manuals and Guides No. 33, UNESCO, Paris.

Hediger, M.A., Clémençon, B., Burrier, R.E., Bruford, E.A., 2013. The ABCs of membrane transporters in health and disease (SLC series): Introduction. Molecular Aspects of Medicine 34, 95–107. https://doi.org/10.1016/j.mam.2012.12.009

Hégaret, H., Da Silva, P.M., Wikfors, G.H., Haberkorn, H., Shumway, S.E., Soudant, P., 2011. In vitro interactions between several species of harmful algae and haemocytes of bivalve molluscs. Cell Biol Toxicol 27, 249–266. https://doi.org/10.1007/s10565-011-9186-6

Hiolski, E.M., Kendrick, P.S., Frame, E.R., Myers, M.S., Bammler, T.K., Beyer, R.P., Farin, F.M., Wilkerson, H., Smith, D.R., Marcinek, D.J., Lefebvre, K.A., 2014. Chronic low-level domoic acid exposure alters gene transcription and impairs mitochondrial function in the CNS. Aquatic Toxicology 155, 151–159. https://doi.org/10.1016/j.aquatox.2014.06.006

Hoglund, P.J., Nordstrom, K.J.V., Schioth, H.B., Fredriksson, R., 2011. The Solute Carrier Families Have a Remarkably Long Evolutionary History with the Majority of the Human Families Present before Divergence of Bilaterian Species. Molecular Biology and Evolution 28, 1531–1541. https://doi.org/10.1093/molbev/msq350

Hornett, E.A., Wheat, C.W., 2012. Quantitative RNA-Seq analysis in non-model species: assessing transcriptome assemblies as a scaffold and the utility of evolutionary divergent genomic reference species. BMC genomics 13, 361.

Hu, T., Chitnis, N., Monos, D., Dinh, A., 2021. Next-generation sequencing technologies: An overview. Human Immunology, Next Generation Sequencing and its Application to Medical Laboratory Immunology 82, 801–811. https://doi.org/10.1016/j.humimm.2021.02.012

Huang, L., Wang, J., Chen, W.-C., Li, H.-Y., Liu, J.-S., Tao Jiang, Yang, W.-D., 2014. P-glycoprotein expression in Perna viridis after exposure to Prorocentrum lima, a dinoflagellate producing DSP toxins. Fish & Shellfish Immunology 39, 254–262. https://doi.org/10.1016/j.fsi.2014.04.020

Huang, L., Zou, Y., Weng, H., Li, H.-Y., Liu, J.-S., Yang, W.-D., 2015. Proteomic profile in Perna viridis after exposed to Prorocentrum lima, a dinoflagellate producing DSP toxins. Environmental Pollution 196, 350–357. https://doi.org/10.1016/j.envpol.2014.10.019

Huggett, J.F., Foy, C.A., Benes, V., Emslie, K., Garson, J.A., Haynes, R., Hellemans, J., Kubista, M., Mueller, R.D., Nolan, T., Pfaffl, M.W., Shipley, G.L., Vandesompele, J., Wittwer, C.T., Bustin, S.A., 2013. The Digital MIQE Guidelines: Minimum Information for Publication of Quantitative Digital PCR Experiments. Clinical Chemistry 59, 892–902. https://doi.org/10.1373/clinchem.2013.206375

Jansen, R.S., Mahakena, S., Haas, M. de, Borst, P., Wetering, K. van de, 2015. ATP-binding Cassette Subfamily C Member 5 (ABCC5) Functions as an Efflux Transporter of Glutamate Conjugates and Analogs. J. Biol. Chem. 290, 30429–30440. https://doi.org/10.1074/jbc.M115.692103

Jeong, C.-B., Kim, H.-S., Kang, H.-M., Lee, J.-S., 2017. ATP-binding cassette (ABC) proteins in aquatic invertebrates: Evolutionary significance and application in marine ecotoxicology. Aquatic Toxicology 185, 29–39. https://doi.org/10.1016/j.aquatox.2017.01.013

Jones, H.D., 1983. 4 - The Circulatory Systems of Gastropods and Bivalves, in: Saleuddin, A.S.M., Wilbur, K.M. (Eds.), The Mollusca, The Mollusca. Academic Press, San Diego, pp. 189–238. https://doi.org/10.1016/B978-0-12-751405-5.50012-9

Jones, T.O., Whyte, J.N.C., Ginther, N.G., Townsend, L.D., Iwama, G.K., 1995a. Haemocyte changes in the pacific oyster, crassostrea gigas, caused by exposure to domoic acid in the diatom pseudonitzschia pungens f. multiseries. Toxicon 33, 347–353. https://doi.org/10.1016/0041-0101(94)00170-D

Jones, T.O., Whyte, J.N.C., Townsend, L.D., Ginther, N.G., Iwama, G.K., 1995b. Effects of domoic acid on haemolymph pH, PCO2 and PO2 in the Pacific oyster, Crassostrea gigas and the California mussel, Mytilus californianus. Aquatic Toxicology 31, 43–55. https://doi.org/10.1016/0166-445X(94)00057-W

Kimura, O., Kotaki, Y., Hamaue, N., Haraguchi, K., Endo, T., 2011. Transcellular transport of domoic acid across intestinal Caco-2 cell monolayers. Food and Chemical Toxicology 49, 2167–2171. https://doi.org/10.1016/j.fct.2011.06.001

Koepsell, H., 2013. The SLC22 family with transporters of organic cations, anions and zwitterions. Molecular Aspects of Medicine, The ABCs of membrane transporters in health and disease (SLC series) 34, 413–435. https://doi.org/10.1016/j.mam.2012.10.010

Krishnan, N., Dickman, M.B., Becker, D.F., 2008. Proline modulates the intracellular redox environment and protects mammalian cells against oxidative stress. Free Radical Biology and Medicine 44, 671–681. https://doi.org/10.1016/j.freeradbiomed.2007.10.054

Krock, B., Tillmann, U., Voß, D., Koch, B.P., Salas, R., Witt, M., Potvin, É., Jeong, H.J., 2012. New azaspiracids in Amphidomataceae (Dinophyceae). Toxicon 60, 830–839. https://doi.org/10.1016/j.toxicon.2012.05.007

Langmead, B., Salzberg, S.L., 2012. Fast gapped-read alignment with Bowtie 2. Nat Methods 9, 357–359. https://doi.org/10.1038/nmeth.1923

Lawrence, J., Loreal, H., Toyofuku, H., Hess, P., Karunasagar, I., Ababouch, L., Fishery and Aquaculture Economics and Policy Division, 2011. Assessment and management of biotoxin risks in bivalve molluscs, FAO Fisheries and Aquaculture Technical Paper. FAO, Rome, Italy.

Lefebvre, K.A., Robertson, A., 2010. Domoic acid and human exposure risks: A review. Toxicon 56, 218–230. https://doi.org/10.1016/j.toxicon.2009.05.034

Lefebvre, K. A., Tilton, S.C., Bammler, T.K., Beyer, R.P., Srinouanprachan, S., Stapleton, P.L., Farin, F.M., Gallagher, E.P., 2009. Gene Expression Profiles in Zebrafish Brain after Acute Exposure to Domoic Acid at Symptomatic and Asymptomatic Doses. Toxicological Sciences 107, 65–77. https://doi.org/10.1093/toxsci/kfn207

Lehane, L., Lewis, R.J., 2000. Ciguatera: recent advances but the risk remains. International Journal of Food Microbiology 61, 91–125. https://doi.org/10.1016/S0168-1605(00)00382-2

Lehmann, C., Bette, S., Engele, J., 2009. High extracellular glutamate modulates expression of glutamate transporters and glutamine synthetase in cultured astrocytes. Brain Research 1297, 1–8. https://doi.org/10.1016/j.brainres.2009.08.070

Lein, P.J., Supasai, S., Guignet, M., 2018. Chapter 9 - Apoptosis as a Mechanism of Developmental Neurotoxicity. DEVELOPMENTAL NEUROBIOLOGY 2nd ed, 91–112.

Lelong, A., Hégaret, H., Soudant, P., Bates, S.S., 2012. Pseudo-nitzschia (Bacillariophyceae) species, domoic acid and amnesic shellfish poisoning: revisiting previous paradigms. Phycologia 51, 168–216. https://doi.org/10.2216/11-37.1

Li, Yuli, Sun, X., Hu, X., Xun, X., Zhang, J., Guo, X., Jiao, W., Zhang, Lingling, Liu, W., Wang, J., Li, J., Sun, Y., Miao, Y., Zhang, X., Cheng, T., Xu, G., Fu, X., Wang, Y., Yu, X., Huang, X., Lu, W., Lv, J., Mu, C., Wang, D., Li, X., Xia, Y., Li, Yajuan, Yang, Z., Wang, F., Zhang, Lu, Xing, Q., Dou, H., Ning, X., Dou, J., Li, Yangping, Kong, D., Liu, Y., Jiang, Z., Li, R., Wang, S., Bao, Z., 2017. Scallop genome reveals molecular adaptations to semi-sessile life and neurotoxins. Nature Communications 8, 1721. https://doi.org/10.1038/s41467-017-01927-0

Lin, Y.-Y., Risk, M., Ray, S.M., Van Engen, D., Clardy, J., Golik, J., James, J.C., Nakanishi, K., 1981. Isolation and structure of brevetoxin B from the “red tide” dinoflagellate Ptychodiscus brevis (Gymnodinium breve). J. Am. Chem. Soc. 103, 6773–6775. https://doi.org/10.1021/ja00412a053

Liu, H, Kelly, M., Campbell, D., Dong, S., Zhu, J., Wang, S., 2007. Exposure to domoic acid affects larval development of king scallop Pecten maximus (Linnaeus, 1758). Aquatic Toxicology 81, 152–158. https://doi.org/10.1016/j.aquatox.2006.11.012

Liu, H., Kelly, M.S., Campbell, D.A., Fang, J., Zhu, J., 2008. Accumulation of domoic acid and its effect on juvenile king scallop Pecten maximus (Linnaeus, 1758). Aquaculture 284, 224–230. https://doi.org/10.1016/j.aquaculture.2008.07.003

Livneh, I., Cohen-Kaplan, V., Cohen-Rosenzweig, C., Avni, N., Ciechanover, A., 2016. The life cycle of the 26S proteasome: from birth, through regulation and function, and onto its death. Cell Res 26, 869–885. https://doi.org/10.1038/cr.2016.86

Louzao, M.C., Vilariño, N., Vale, C., Costas, C., Cao, A., Raposo-Garcia, S., Vieytes, M.R., Botana, L.M., 2022. Current Trends and New Challenges in Marine Phycotoxins. Marine Drugs 20, 198. https://doi.org/10.3390/md20030198

Lozano, V., Martínez-Escauriaza, R., Pérez-Parallé, M.L., Pazos, A.J., Sánchez, J.L., 2015. Two novel multidrug resistance associated protein (MRP/ABCC) from the Mediterranean mussel (*Mytilus galloprovincialis*): characterization and expression patterns in detoxifying tissues. Canadian Journal of Zoology 93, 567–578. https://doi.org/10.1139/cjz-2015-0011

Madhyastha, M.S., Novaczek, I., Ablett, R.F., Johnson, G., Nijjar, M.S., Sims, D.E., 1991. In vitro study of domoic acid uptake by gland tissue of blue mussel (Mytilus L.). Aquatic Toxicology 20, 73–81. https://doi.org/10.1016/0166-445X(91)90042-8

Mafra Jr., L.L., Bricelj, V.M., Fennel, K., 2010. Domoic acid uptake and elimination kinetics in oysters and mussels in relation to body size and anatomical distribution of toxin. Aquatic Toxicology 100, 17–29. https://doi.org/10.1016/j.aquatox.2010.07.002

Malanga, G., GONZÁLEZ, P.M., OSTERA, J.M., PUNTARULO, S., 2016. Oxidative stress in the hydrophilic medium of algae and invertebrates. BIOCELL 40, 35–38.

Manfrin, C., Dreos, R., Battistella, S., Beran, A., Gerdol, M., Varotto, L., Lanfranchi, G., Venier, P., Pallavicini, A., 2010. Mediterranean Mussel Gene Expression Profile Induced by Okadaic Acid Exposure. Environ. Sci. Technol. 44, 8276–8283. https://doi.org/10.1021/es102213f

Martínez-Escauriaza, R., Lozano, V., Pérez-Parallé, M.L., Blanco, J., Sánchez, J.L., Pazos, A.J., 2021. Expression Analyses of Genes Related to Multixenobiotic Resistance in Mytilus galloprovincialis after Exposure to Okadaic Acid-Producing Dinophysis acuminata. Toxins 13, 614. https://doi.org/10.3390/toxins13090614

Mauriz, A., Blanco, J., 2010. Distribution and linkage of domoic acid (amnesic shellfish poisoning toxins) in subcellular fractions of the digestive gland of the scallop Pecten maximus. Toxicon 55, 606–611. https://doi.org/10.1016/j.toxicon.2009.10.017

Mauriz, O., Maneiro, V., Pérez-Parallé, M.L., Sánchez, J.L., Pazos, A.J., 2012. Selection of reference genes for quantitative RT-PCR studies on the gonad of the bivalve mollusc Pecten maximus L. Aquaculture 370–371, 158–165. https://doi.org/10.1016/j.aquaculture.2012.10.020

McKibben, S.M., Peterson, W., Wood, A.M., Trainer, V.L., Hunter, M., White, A.E., 2017. Climatic regulation of the neurotoxin domoic acid. Proceedings of the National Academy of Sciences 114, 239–244. https://doi.org/10.1073/pnas.1606798114

Meixner, E., Goldmann, U., Sedlyarov, V., Scorzoni, S., Rebsamen, M., Girardi, E., Superti-Furga, G., 2020. A substrate-based ontology for human solute carriers. Molecular Systems Biology 16, e9652. https://doi.org/10.15252/msb.20209652

Mello, D.F., De Oliveira, E.S., Vieira, R.C., Simoes, E., Trevisan, R., Dafre, A.L., Barracco, M.A., 2012. Cellular and Transcriptional Responses of Crassostrea gigas Hemocytes Exposed in Vitro to Brevetoxin (PbTx-2). Marine Drugs 10, 583–597. https://doi.org/10.3390/md10030583

Miyahara, J.T., Akau, C.K., Yasumoto, T., 1979. Effects of ciguatoxin and maitotoxin on the isolated guinea pig atria. Res Commun Chem Pathol Pharmacol 25, 177–180.

Miyaji, T., Omote, H., Moriyama, Y., 2011. Functional characterization of vesicular excitatory amino acid transport by human sialin. Journal of Neurochemistry 119, 1–5. https://doi.org/10.1111/j.1471-4159.2011.07388.x

Moriya, Y., Itoh, M., Okuda, S., Yoshizawa, A.C., Kanehisa, M., 2007. KAAS: an automatic genome annotation and pathway reconstruction server. Nucleic Acids Res 35, W182–W185. https://doi.org/10.1093/nar/gkm321

Morton, B., 1983. 2 - Feeding and Digestion in Bivalvia, in: Saleuddin, A.S.M., Wilbur, K.M. (Eds.), The Mollusca, The Mollusca. Academic Press, San Diego, pp. 65–147. https://doi.org/10.1016/B978-0-12-751405-5.50010-5

Munday, R., Holland, P.T., McNabb, P., Selwood, A.I., Rhodes, L.L., 2008. Comparative toxicity to mice of domoic acid and isodomoic acids A, B and C. Toxicon 52, 954–956. https://doi.org/10.1016/j.toxicon.2008.10.005

Murata, M., Kumagai, M., Lee, J.S., Yasumoto, T., 1987. Isolation and structure of yessotoxin, a novel polyether compound implicated in diarrhetic shellfish poisoning. Tetrahedron Letters 28, 5869–5872. https://doi.org/10.1016/S0040-4039(01)81076-5

Murata, M., Legrand, A.M., Ishibashi, Y., Fukui, M., Yasumoto, T., 1990. Structures and configurations of ciguatoxin from the moray eel Gymnothorax javanicus and its likely precursor from the dinoflagellate Gambierdiscus toxicus. J. Am. Chem. Soc. 112, 4380–4386. https://doi.org/10.1021/ja00167a040

Novaczek, I., Madhyastha, M.S., Ablett, R.F., Donald, A., Johnson, G., Nijjar, M.S., Sims, D.E., 1992. Depuration of Domoic Acid from Live Blue Mussels (*Mytilus edulis*). Canadian Journal of Fisheries and Aquatic Sciences 49, 312–318. https://doi.org/10.1139/f92-035

Novaczek, I., Madhyastha, M.S., Ablett, R.F., Johnson, G., Nijjar, M.S., Sims, D.E., 1991. Uptake, disposition and depuration of domoic acid by blue mussels (Mytilus edulis). Aquatic Toxicology 21, 103–118. https://doi.org/10.1016/0166-445X(91)90009-X

Núñez-Acuña, G., Aballay, A.E., Hégaret, H., Astuya, A.P., Gallardo-Escárate, C., 2013. Transcriptional responses of Mytilus chilensis exposed in vivo to saxitoxin (STX). J Molluscan Stud 79, 323–331. https://doi.org/10.1093/mollus/eyt030

Oesch, F., Arand, M., 1999. Chapter 4 - Xenobiotic Metabolism, in: Marquardt, H., Schäfer, S.G., McClellan, R., Welsch, F. (Eds.), Toxicology. Academic Press, San Diego, pp. 83–109. https://doi.org/10.1016/B978-012473270-4/50063-8

Oesch, F., Hengstler, J.G., 2021. Importance of Xenobiotic Metabolism: Mechanistic Considerations Relevant for Regulation, in: Reichl, F.-X., Schwenk, M. (Eds.), Regulatory Toxicology. Springer International Publishing, Cham, pp. 745–758. https://doi.org/10.1007/978-3-030-57499-4_71

Otero, P., Silva, M., 2022. Emerging Marine Biotoxins in European Waters: Potential Risks and Analytical Challenges. Marine Drugs 20, 199. https://doi.org/10.3390/md20030199

Owen, G., 1955. Observations on the Stomach and Digestive Diverticula of the Lamellibranchia: I. The Anisomyaria and Eulamellibranchia. J Cell Sci s3-96, 517–537. https://doi.org/10.1242/jcs.s3-96.36.517

Pales Espinosa, E., Allam, B., 2018. Reverse genetics demonstrate the role of mucosal C-type lectins in food particle selection in the oyster *Crassostrea virginica*. Journal of Experimental Biology jeb.174094. https://doi.org/10.1242/jeb.174094

Paredes, I., Rietjens, I.M.C.M., Vieites, J.M., Cabado, A.G., 2011. Update of risk assessments of main marine biotoxins in the European Union. Toxicon 58, 336–354. https://doi.org/10.1016/j.toxicon.2011.07.001

Parzych, K.R., Klionsky, D.J., 2014. An Overview of Autophagy: Morphology, Mechanism, and Regulation. Antioxid Redox Signal 20, 460–473. https://doi.org/10.1089/ars.2013.5371

Patocka, J., Nepovimova, E., Wu, Q., Kuca, K., 2018. Palytoxin congeners. Arch Toxicol 92, 143–156. https://doi.org/10.1007/s00204-017-2105-8

Paz, B., Daranas, A.H., Norte, M., Riobó, P., Franco, J.M., Fernández, J.J., 2008. Yessotoxins, a Group of Marine Polyether Toxins: an Overview. Mar Drugs 6, 73–102. https://doi.org/10.3390/md20080005

Pazos, A.J., Ventoso, P., Martínez-Escauriaza, R., Pérez-Parallé, M.L., Blanco, J., Triviño, J.C., Sánchez, J.L., 2017. Transcriptional response after exposure to domoic acid-producing Pseudo-nitzschia in the digestive gland of the mussel Mytilus galloprovincialis. Toxicon 140, 60–71. https://doi.org/10.1016/j.toxicon.2017.10.002

Peña-Llopis, S., Serrano, R., Pitarch, E., Beltrán, E., Ibáñez, M., Hernández, F., Peña, J.B., 2014. N-Acetylcysteine boosts xenobiotic detoxification in shellfish. Aquatic Toxicology 154, 131–140. https://doi.org/10.1016/j.aquatox.2014.05.006

Pérez-Gómez, A., Tasker, R.A., 2014. Domoic Acid as a Neurotoxin, in: Kostrzewa, R.M. (Ed.), Handbook of Neurotoxicity. Springer New York, New York, NY, pp. 399–419. https://doi.org/10.1007/978-1-4614-5836-4_87

Perl, T.M., Bédard, L., Kosatsky, T., Hockin, J.C., Todd, E.C., McNutt, L.A., Remis, R.S., 1990. Amnesic shellfish poisoning: a new clinical syndrome due to domoic acid. Can Dis Wkly Rep 16 Suppl 1E, 7–8.

Pesonen, M., Vähäkangas, K., 2019. Autophagy in exposure to environmental chemicals. Toxicology Letters 305, 1–9. https://doi.org/10.1016/j.toxlet.2019.01.007

Pfaffl, M.W., Tichopad, A., Prgomet, C., Neuvians, T.P., 2004. Determination of stable housekeeping genes, differentially regulated target genes and sample integrity: BestKeeper – Excel-based tool using pair-wise correlations. Biotechnology Letters 26, 509–515. https://doi.org/10.1023/B:BILE.0000019559.84305.47

Pinto, A., Botelho, M.J., Churro, C., Asselman, J., Pereira, P., Pereira, J.L., 2023. A review on aquatic toxins - Do we really know it all regarding the environmental risk posed by phytoplankton neurotoxins? Journal of Environmental Management 345, 118769. https://doi.org/10.1016/j.jenvman.2023.118769

Pinto-Silva, C.R.C., Moukha, S., Matias, W.G., Creppy, E.E., 2008. Domoic acid induces direct DNA damage and apoptosis in Caco-2 cells: Recent advances. Environmental Toxicology 23, 657–663. https://doi.org/10.1002/tox.20361

Pirie, B.J.S., George, S.G., 1979. Ultrastructure of the heart and excretory system of Mytilus edulis (L.). Journal of the Marine Biological Association of the United Kingdom 59, 819–829. https://doi.org/10.1017/S0025315400036869

Prego-Faraldo, M., Martínez, L., Méndez, J., 2018. RNA-Seq Analysis for Assessing the Early Response to DSP Toxins in Mytilus galloprovincialis Digestive Gland and Gill. Toxins 10, 417. https://doi.org/10.3390/toxins10100417

Prego-Faraldo, M.V., Valdiglesias, V., Laffon, B., Mendez, J., Eirin-Lopez, J.M., 2016. Early Genotoxic and Cytotoxic Effects of the Toxic Dinoflagellate Prorocentrum lima in the Mussel Mytilus galloprovincialis. Toxins 8, 159. https://doi.org/10.3390/toxins8060159

Pulido, O.M., 2016. Phycotoxins by harmful algal blooms (HABS) and human poisoning: an overview. Int Clin Pathol J. 2, 145–152. https://doi.org/10.15406/icpjl.2016.02.00062

Pulido, O.M., 2008. Domoic Acid Toxicologic Pathology: A Review. Marine Drugs 6, 180–219. https://doi.org/10.3390/md20080010

Rahman, M.A., Rahman, M.S., Parvez, M.A.K., Kim, B., 2023. The Emerging Role of Autophagy as a Target of Environmental Pollutants: An Update on Mechanisms. Toxics 11, 135. https://doi.org/10.3390/toxics11020135

Rasmussen, S.A., Andersen, A.J.C., Andersen, N.G., Nielsen, K.F., Hansen, P.J., Larsen, T.O., 2016. Chemical Diversity, Origin, and Analysis of Phycotoxins. J. Nat. Prod. 79, 662–673. https://doi.org/10.1021/acs.jnatprod.5b01066

Reimer, R.J., 2013. SLC17: A functionally diverse family of organic anion transporters. Molecular Aspects of Medicine, The ABCs of membrane transporters in health and disease (SLC series) 34, 350–359. https://doi.org/10.1016/j.mam.2012.05.004

Renault, T., 2015. Immunotoxicological effects of environmental contaminants on marine bivalves. Fish & Shellfish Immunology 46, 88–93. https://doi.org/10.1016/j.fsi.2015.04.011

Ryan, J.C., Morey, J.S., Ramsdell, J.S., van Dolah, F.M., 2005. Acute phase gene expression in mice exposed to the marine neurotoxin domoic acid. Neuroscience 136, 1121–1132. https://doi.org/10.1016/j.neuroscience.2005.08.047

Schantz, E.J., McFarren, E.F., Schafer, M.L., Lewis, K.H., 1958. Purified Shellfish Poison for Bioassay Standardization. Journal of Association of Official Agricultural Chemists 41, 160–168. https://doi.org/10.1093/jaoac/41.1.160

Schantz, E.J., Mold, J.D., Stanger, D.W., Shavel, J., Riel, F.J., Bowden, J.P., Lynch, J.M., Wyler, R.S., Riegel, B., Sommer, H., 1957. Paralytic Shellfish Poison. VI. A Procedure for the Isolation and Purification of the Poison from Toxic Clam and Mussel Tissues. J. Am. Chem. Soc. 79, 5230–5235. https://doi.org/10.1021/ja01576a044

Schultz, I.R., Skillman, A., Sloan-Evans, S., Woodruff, D., 2013. Domoic acid toxicokinetics in Dungeness crabs: New insights into mechanisms that regulate bioaccumulation. Aquatic Toxicology 140–141, 77–88. https://doi.org/10.1016/j.aquatox.2013.04.011

Schulz, M.H., Zerbino, D.R., Vingron, M., Birney, E., 2012. Oases: robust de novo RNA-seq assembly across the dynamic range of expression levels. Bioinformatics 28, 1086–1092. https://doi.org/10.1093/bioinformatics/bts094

Shang, F., Taylor, A., 2011. Ubiquitin-proteasome pathway and cellular responses to oxidative stress. Free Radic Biol Med 51, 5–16. https://doi.org/10.1016/j.freeradbiomed.2011.03.031

Shimizu, Yuzuru., Chou, H.Nong., Bando, Hideo., Van Duyne, Gregory., Clardy, Jon., 1986. Structure of brevetoxin A (GB-1 toxin), the most potent toxin in the Florida red tide organism Gymnodinium breve (Ptychodiscus brevis). J. Am. Chem. Soc. 108, 514–515. https://doi.org/10.1021/ja00263a031

SLC tables URL https://www.bioparadigms.org/slc/ (accessed 12.15.18).

Song, J.A., Choi, C.Y., Park, H.-S., 2020. Exposure to domoic acid causes oxidative stress in bay scallops Argopecten irradians. Fish Sci 86, 701–709. https://doi.org/10.1007/s12562-020-01431-3

Song, S.B., Shim, W., Hwang, E.S., 2023. Lipofuscin Granule Accumulation Requires Autophagy Activation. Molecules and Cells 46, 486–495. https://doi.org/10.14348/molcells.2023.0019

Sundaray, J.K., Dixit, S., Rather, A., Rasal, K.D., Sahoo, L., 2022. Aquaculture omics: An update on the current status of research and data analysis. Marine Genomics 64, 100967. https://doi.org/10.1016/j.margen.2022.100967

Szklarczyk, D., Franceschini, A., Wyder, S., Forslund, K., Heller, D., Huerta-Cepas, J., Simonovic, M., Roth, A., Santos, A., Tsafou, K.P., Kuhn, M., Bork, P., Jensen, L.J., von Mering, C., 2015. STRING v10: protein–protein interaction networks, integrated over the tree of life. Nucleic Acids Res 43, D447–D452. https://doi.org/10.1093/nar/gku1003

Tachibana, K., Scheuer, P.J., Tsukitani, Y., Kikuchi, H., Van Engen, D., Clardy, J., Gopichand, Y., Schmitz, F.J., 1981. Okadaic acid, a cytotoxic polyether from two marine sponges of the genus Halichondria. J. Am. Chem. Soc. 103, 2469–2471. https://doi.org/10.1021/ja00399a082

Takemoto, T., Daigo, K., 1958. Constituents of Chondria armata. Chemical & Pharmaceutical Bulletin 6, 578b–5580. https://doi.org/10.1248/cpb.6.578b

Thind, A.S., Monga, I., Thakur, P.K., Kumari, P., Dindhoria, K., Krzak, M., Ranson, M., Ashford, B., 2021. Demystifying emerging bulk RNA-Seq applications: the application and utility of bioinformatic methodology. Briefings in Bioinformatics 22, bbab259. https://doi.org/10.1093/bib/bbab259

Tillmann, U., Elbrächter, M., Krock, B., John, U., Cembella, A., 2009. Azadinium spinosum gen. et sp. nov. (Dinophyceae) identified as a primary producer of azaspiracid toxins. European Journal of Phycology 44, 63–79. https://doi.org/10.1080/09670260802578534

Tillmann, U., Salas, R., Gottschling, M., Krock, B., O'Driscoll, D., Elbrächter, M., 2012. *Amphidoma languida* sp. nov. (Dinophyceae) Reveals a Close Relationship between *Amphidoma* and *Azadinium*. Protist 163, 701–719. https://doi.org/10.1016/j.protis.2011.10.005

Trainer, V.L., Bates, S.S., Lundholm, N., Thessen, A.E., Cochlan, W.P., Adams, N.G., Trick, C.G., 2012. Pseudo-nitzschia physiological ecology, phylogeny, toxicity, monitoring and impacts on ecosystem health. Harmful Algae, Harmful Algae--The requirement for species-specific information 14, 271–300. https://doi.org/10.1016/j.hal.2011.10.025

Trainer, V.L., Bill, B.D., 2004. Characterization of a domoic acid binding site from Pacific razor clam. Aquatic Toxicology 69, 125–132. https://doi.org/10.1016/j.aquatox.2004.04.012

Tsunekawa, K., Kondo, F., Okada, T., Feng, G.-G., Huang, L., Ishikawa, N., Okada, S., 2013. Enhanced expression of WD repeat-containing protein 35 (WDR35) stimulated by domoic acid in rat hippocampus: involvement of reactive oxygen species generation and p38 mitogen-activated protein kinase activation. BMC Neuroscience 14, 4. https://doi.org/10.1186/1471-2202-14-4

Van den Berge, K., Hembach, K.M., Soneson, C., Tiberi, S., Clement, L., Love, M.I., Patro, R., Robinson, M.D., 2019. RNA Sequencing Data: Hitchhiker's Guide to Expression Analysis. Annu. Rev. Biomed. Data Sci. https://doi.org/10.1146/annurev-biodatasci-072018-021255

Vandesompele, J., De Preter, K., Pattyn, F., Poppe, B., Van Roy, N., De Paepe, A., Speleman, F., 2002. Accurate normalization of real-time quantitative RT-PCR data by geometric averaging of multiple internal control genes. Genome Biol 3, research0034.1-research0034.11.

Vanmaldergem, J., García-Corona, J.L., Deléglise, M., Fabioux, C., Hegaret, H., 2023. Effect of the antioxidant N-acetylcysteine on the depuration of the amnesic shellfish poisoning toxin, domoic acid, in the digestive gland of the king scallop Pecten maximus. Aquat. Living Resour. 36, 14. https://doi.org/10.1051/alr/2023011

Vardimon, L., Dror, I.B., Avisar, N., Shiftan, L., Kruchkova, Y., Oren, A., 2001. Regulation of glutamine synthetase in normal and injured neural tissues. Gene Function & Disease 2, 83–88. https://doi.org/10.1002/1438-826X(200110)2:2/3<83::AID-GNFD83>3.0.CO;2-W

Vaughn, C.C., Hoellein, T.J., 2018. Bivalve Impacts in Freshwater and Marine Ecosystems. Annual Review of Ecology, Evolution, and Systematics 49, 183–208. https://doi.org/10.1146/annurev-ecolsys-110617-062703

Ventoso, P., Pazos, A.J., Blanco, J., Pérez-Parallé, M.L., Triviño, J.C., Sánchez, J.L., 2021. Transcriptional Response in the Digestive Gland of the King Scallop (Pecten maximus) After the Injection of Domoic Acid. Toxins 13, 339. https://doi.org/10.3390/toxins13050339

Ventoso, P., Pazos, A.J., Pérez-Parallé, M.L., Blanco, J., Triviño, J.C., Sánchez, J.L., 2019. RNA-Seq Transcriptome Profiling of the Queen Scallop (Aequipecten opercularis) Digestive Gland after Exposure to Domoic Acid-Producing Pseudo-nitzschia. Toxins 11, 97. https://doi.org/10.3390/toxins11020097

Vijay, N., Poelstra, J.W., Künstner, A., Wolf, J.B.W., 2013. Challenges and strategies in transcriptome assembly and differential gene expression quantification. A comprehensive *in silico* assessment of RNA-seq experiments. Molecular Ecology 22, 620–634. https://doi.org/10.1111/mec.12014

Visciano, P., Schirone, M., Berti, M., Milandri, A., Tofalo, R., Suzzi, G., 2016. Marine Biotoxins: Occurrence, Toxicity, Regulatory Limits and Reference Methods. Frontiers in Microbiology 7.

Wang, L., Liang, X.-F., Huang, Y., Li, S.-Y., Ip, K.-C., 2008. Transcriptional responses of xenobiotic metabolizing enzymes, HSP70 and Na+/K+-ATPase in the liver of rabbitfish (Siganus oramin) intracoelomically injected with amnesic shellfish poisoning toxin. Environ. Toxicol. 23, 363–371. https://doi.org/10.1002/tox.20350

Wang, Yujue, Li, M., Lou, J., Xun, X., Chang, L., Wang, Yangrui, Zhang, Q., Lu, L., Wang, H., Hu, J., Bao, Z., Hu, X., 2022. Transcriptome and Network Analyses Reveal the Gene Set Involved in PST Accumulation and Responses to Toxic Alexandrium minutum Exposure in the Gills of Chlamys farreri. International Journal of Molecular Sciences 23, 7912. https://doi.org/10.3390/ijms23147912

Weinstein, J.E., 1995. Fine structure of the digestive tubule of the eastern oyster, Crassostrea virginica (Gmelin 1791). Journal of Shellfish Research 97–103.

Whalen, K.E., Sotka, E.E., Goldstone, J.V., Hahn, M.E., 2010. The role of multixenobiotic transporters in predatory marine molluscs as counter-defense mechanisms against dietary allelochemicals. Comparative Biochemistry and Physiology Part C: Toxicology & Pharmacology 152, 288–300. https://doi.org/10.1016/j.cbpc.2010.05.003

Wright, J.L.C., Boyd, R.K., Freitas, A.S.W. de, Falk, M., Foxall, R.A., Jamieson, W.D., Laycock, M.V., McCulloch, A.W., McInnes, A.G., Odense, P., Pathak, V.P., Quilliam, M.A., Ragan, M.A., Sim, P.G., Thibault, P., Walter, J.A., Gilgan, M., Richard, D.J.A., Dewar, D., 1989. Identification of domoic acid, a neuroexcitatory amino acid, in toxic mussels from eastern Prince Edward Island. Can. J. Chem. 67, 481–490. https://doi.org/10.1139/v89-075

Xu, C., Li, C.Y.-T., Kong, A.-N.T., 2005. Induction of phase I, II and III drug metabolism/transport by xenobiotics. Arch Pharm Res 28, 249–268. https://doi.org/10.1007/BF02977789

Xu, R., Tao, Y., Wu, C., Yi, J., Yang, Y., Yang, R., Hong, D., 2008. Domoic acid induced spinal cord lesions in adult mice: Evidence for the possible molecular pathways of excitatory amino acids in spinal cord lesions. NeuroToxicology 29, 700–707. https://doi.org/10.1016/j.neuro.2008.04.011

Xu, Y.-Y., Liang, J.-J., Yang, W.-D., Wang, J., Li, H.-Y., Liu, J.-S., 2014. Cloning and expression analysis of P-glycoprotein gene in Crassostrea ariakensis. Aquaculture 418–419, 39–47. https://doi.org/10.1016/j.aquaculture.2013.10.004

Xun, X., Cheng, J., Wang, J., Li, Y., Li, X., Li, M., Lou, J., Kong, Y., Bao, Z., Hu, X., 2020. Solute carriers in scallop genome: Gene expansion and expression regulation after exposure to toxic dinoflagellate. Chemosphere 241, 124968. https://doi.org/10.1016/j.chemosphere.2019.124968

Young, N., Sharpe, R.A., Barciela, R., Nichols, G., Davidson, K., Berdalet, E., Fleming, L.E., 2020. Marine harmful algal blooms and human health: A systematic scoping review. Harmful Algae 98, 101901. https://doi.org/10.1016/j.hal.2020.101901

Yu, L., Chen, Y., Tooze, S.A., 2018. Autophagy pathway: Cellular and molecular mechanisms. Autophagy 14, 207–215. https://doi.org/10.1080/15548627.2017.1378838

Zabaglo, K., Chrapusta, E., Bober, B., Kaminski, A., Adamski, M., Bialczyk, J., 2016. Environmental roles and biological activity of domoic acid: A review. Algal Research 13, 94–101. https://doi.org/10.1016/j.algal.2015.11.020

Zafra, F., Ibáñez, I., Bartolomé-Martín, D., Piniella, D., Arribas-Blázquez, M., Giménez, C., 2017. Glycine Transporters and Its Coupling with NMDA Receptors, in: Ortega, A., Schousboe, A. (Eds.), Glial Amino Acid Transporters, Advances in Neurobiology. Springer International Publishing, Cham, pp. 55–83. https://doi.org/10.1007/978-3-319-55769-4_4

Zhang, X., Xun, X., Meng, D., Li, M., Chang, L., Shi, J., Ding, W., Sun, Y., Wang, H., Bao, Z., Hu, X., 2023. Transcriptome Analysis Reveals the Genes Involved in Oxidative Stress Responses of Scallop to PST-Producing Algae and a Candidate Biomarker for PST Monitoring. Antioxidants 12, 1150. https://doi.org/10.3390/antiox12061150

Zhao, S., Fernald, R.D., 2005. Comprehensive Algorithm for Quantitative Real-Time Polymerase Chain Reaction. J Comput Biol 12, 1047–1064. https://doi.org/10.1089/cmb.2005.12.1047

Zou, J., Wang, Y.-X., Dou, F.-F., Lü, H.-Z., Ma, Z.-W., Lu, P.-H., Xu, X.-M., 2010. Glutamine synthetase down-regulation reduces astrocyte protection against glutamate excitotoxicity to neurons. Neurochemistry International 56, 577–584. https://doi.org/10.1016/j.neuint.2009.12.021

ANEXO I TRABAJOS PUBLICADOS

A1.1 TRANSCRIPTIONAL RESPONSE AFTER EXPOSURE TO DOMOIC ACID-PRODUCING *PSEUDO-NITZSCHIA* IN THE DIGESTIVE GLAND OF THE MUSSEL *MYTILUS GALLOPROVINCIALIS*

A1.1.1 Características de la publicación

Estado: Publicado
Título: Transcriptional response after exposure to domoic acid-producing *Pseudo-nitzschia* in the digestive gland of the mussel *Mytilus galloprovincialis*
Nombre de la revista: Toxicon
Editorial: Elsevier Ltd
Autores: Pazos Antonio J., Pablo Ventoso, Roi Martínez-Escauriaza, M. Luz Pérez-Parallé, Juan Blanco, Juan C. Triviño y José L. Sánchez
Contribución específica del doctorado: Investigación, redacción (revisión y edición)
Año publicación: 2017
Volumen: 140 (60-71)
DOI: https://doi.org/10.1016/j.toxicon.2017.10.002
Autorización de la revista: No es necesaria autorización de la editorial y/o revista. Elsevier Ltd permite el libre uso de artículos para la elaboración de tesis doctorales.
(https://www.elsevier.com/about/policies-and-standards/copyright/permissions)

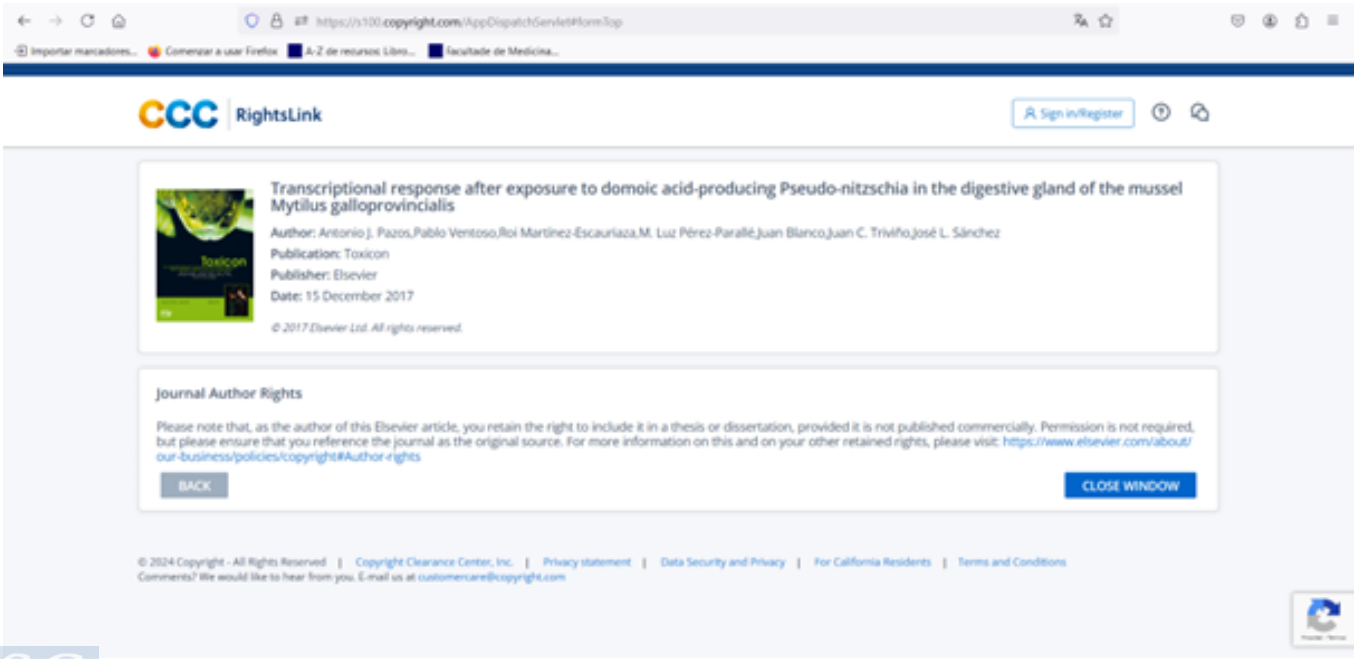

A1.1.2 Indicios de calidad de la revista

Scientific Journal Rankings (SJR): 0,692
Cuartil (2017): 2 - Área: Toxicology
Journal Impact Factor (JCF): 2,352
Cuartil (2017): 3 - Área: Pharmacology & Pharmacy; Toxicology
Journal Citation Indicator (JCI): 0,83
Cuartil (2017): 2 - Área: Toxicology; Pharmacology & Pharmacy

A1.1.3 Impacto de la publicación

Citas: 23 (Scopus), 28 (Google Scholar), 21 (Web of Science)

Toxicon 140 (2017) 60–71

Contents lists available at ScienceDirect

Toxicon

journal homepage: www.elsevier.com/locate/toxicon

Transcriptional response after exposure to domoic acid-producing *Pseudo-nitzschia* in the digestive gland of the mussel *Mytilus galloprovincialis*

Antonio J. Pazos [a, *], Pablo Ventoso [a], Roi Martínez-Escauriaza [a], M. Luz Pérez-Parallé [a], Juan Blanco [b], Juan C. Triviño [c], José L. Sánchez [a]

[a] Departamento de Bioquímica y Biología Molecular, Instituto de Acuicultura, Universidade de Santiago de Compostela, Santiago de Compostela, 15782, Spain
[b] Centro de Investigacións Mariñas, Xunta de Galicia, Pedras de Corón s/n Apdo 13, Vilanova de Arousa, 36620, Spain
[c] Sistemas Genómicos, Ronda G. Marconi 6, Paterna, Valencia, 46980, Spain

ARTICLE INFO

Article history:
Received 16 May 2017
Received in revised form
28 July 2017
Accepted 8 October 2017
Available online 12 October 2017

Keywords:
Amnesic shellfish poisoning (ASP)
Domoic acid
RNA-seq
Transcriptome
Differential expression
Mytilus galloprovincialis

ABSTRACT

Bivalve molluscs are filter feeding species that can accumulate biotoxins in their body tissues during harmful algal blooms. Amnesic Shellfish Poisoning (ASP) is caused by species of the diatom genus *Pseudo-nitzschia*, which produces the toxin domoic acid. The *Mytilus galloprovincialis* digestive gland transcriptome was *de novo* assembled based on the sequencing of 12 cDNA libraries, six obtained from control mussels and six from mussels naturally exposed to domoic acid-producing diatom *Pseudo-nitzschia australis*. After *de novo* assembly 94,727 transcripts were obtained, with an average length of 1015 bp and a N50 length of 761 bp. The assembled transcripts were clustered (homology > 90%) into 69,294 unigenes. Differential gene expression analysis was performed (DESeq2 algorithm) in the digestive gland following exposure to the toxic algae. A total of 1158 differentially expressed unigenes (absolute fold change > 1.5 and p-value < 0.05) were detected: 686 up-regulated and 472 down-regulated. Several membrane transporters belonging to the family of the SLC (solute carriers) were over-expressed in exposed mussels. Functional enrichment was performed using Pfam annotations obtained from the genes differentially expressed, 37 Pfam families were found to be significantly (FDR adjusted p-value < 0.1) enriched. Some of these families (sulfotransferases, aldo/keto reductases, carboxylesterases, C1q domain and fibrinogen C-terminal globular domain) could be putatively involved in detoxification processes, in the response against of the oxidative stress and in immunological processes. Protein network analysis with STRING algorithm found alteration of the Notch signaling pathway under the action of domoic acid-producing *Pseudo-nitzschia*. In conclusion, this study provides a high quality reference transcriptome of *M. galloprovincialis* digestive gland and identifies potential genes involved in the response to domoic acid.

1. Introduction

Bivalve molluscs are filter feeding species that filter large amounts of water and can accumulate biotoxins in their body tissues during harmful algal blooms. The accumulation of biotoxins in shellfish has adverse economic impacts, leading to harvesting closures, because the consumption of these shellfish can cause human health problems. Amnesic Shellfish Poisoning (ASP) is caused by species of the diatom genus *Pseudo-nitzschia* (Bates et al., 1989, 1998), which produces the toxin domoic acid. Domoic acid is an amino acid with three carboxyl groups and one imino group, and structurally resembles glutamic acid and kainic acid. Domoic acid is a potent glutamate receptor agonist and is excitotoxic in the vertebrate central nervous system (Lefebvre and Robertson, 2010). Domoic acid accumulated in mussels caused a human intoxication outbreak in Canada in 1987 (Wright et al., 1989). Although it seems that domoic acid is not toxic to shellfish, there are some

* Corresponding author.
E-mail address: antonioj.pazos@usc.es (A.J. Pazos).

https://doi.org/10.1016/j.toxicon.2017.10.002
0041-0101/

publications about the effects of domoic acid on marine bivalves (Dizer et al., 2001; Jones et al., 1995).

There are important interspecific differences in domoic acid accumulation and elimination in bivalves. Mussels (*Mytilus*) and oysters (*Crassostrea gigas*) are fast domoic acid depurators (Blanco et al., 2002b; Mafra et al., 2010; Novaczek et al., 1991, 1992), while the king scallop *Pecten maximus* and the razor clam *Siliqua patula* showed the slowest depuration rates among bivalves (Drum et al., 1993; Blanco et al., 2002a). Most of the domoic acid in the mussels was accumulated in the digestive gland (Madhyastha et al., 1991; Novaczek et al., 1991; Wright et al., 1989), which is the main site of detoxification of xenobiotics (Livingstone and Farrar, 1984; Livingstone, 1998). In *Mytilus edulis,* domoic acid retained in the digestive gland was intracellular and predominantly cytosolic (Madhyastha et al., 1991). Domoic acid is slightly or not metabolized and is excreted unchanged from mussels, mainly in dissolved form (Novaczek et al., 1991). However, in bivalves, little is known about the molecular basis of domoic acid detoxification (biotoxin absorption, distribution, metabolism and excretion).

The king scallop *Pecten maximus* and the razor clam *Siliqua patula* are the most affected species by domoic acid among those with commercial interest. Notwithstanding, they do not share the same accumulation mechanism. While in *S. patula* domoic acid is bound to receptors (Trainer and Bill, 2004), the toxin seems to be free in the cytosol of the king scallop (Mauriz and Blanco, 2010). The extremely slow depuration of this latter species, which has a highly commercial value and can be cultured, has been hypothesized to be due to the lack of an efficient efflux transporter (Mauriz and Blanco, 2010), presumably of the same type as those that would carry out this function in fast depurating bivalves, such as *M. galloprovincialis*. It could be expected, consequently, that finding the route responsible for the domoic acid depuration in *M. galloprovincialis* would also make it possible to identify the cause of the slow depuration of *P. maximus*.

In bivalve molluscs, whole genomes are only available in the Pacific oyster, *Crassostrea gigas* (Zhang et al., 2012), the pearl oyster, *Pinctada fucata* (Takeuchi et al., 2012), and the mussel *M. galloprovincialis* (Murgarella et al., 2016), but the last two are low-coverage studies (at low-level sequencing depth). Nevertheless, several transcriptomes are publicly available for marine bivalve species, including the mussel *M. galloprovincialis* (Craft et al., 2010; Gerdol et al., 2014; Moreira et al., 2015; Rosani et al., 2011; Suárez-Ulloa et al., 2013). The best way to study the effects of toxins on gene expression is analyzing the differential expression through the technique of RNA-seq. This transcriptomic approach has enabled the identification of genes putatively involved in the response to toxins and pollutants in bivalve molluscs (Deng et al., 2014; Gerdol et al., 2014; Lüchmann et al., 2015; Meng et al., 2013; Rondon et al., 2016). The genes dysregulated by exposure to domoic acid could provide insights into the detoxification processes in the mussels during the *Pseudo-nitzschia* blooms.

In this work the whole transcriptome of *M. galloprovincialis* digestive gland was *de novo* assembled and the genes differentially expressed after exposure to domoic acid-producing *Pseudo-nitzschia australis* were investigated, in order to examine those potentially altered by the action of domoic acid and identify transcripts which could participate in detoxification processes or affect the physiological state of the mussels. Previous studies have characterized gene expression changes associated with exposure to domoic acid in vertebrates (Hiolski et al., 2014; Lefebvre et al., 2009; Ryan et al., 2005), but to our knowledge, this is the first report on transcriptome profiling and differential gene expression in an invertebrate under the exposure to a domoic acid-producing species.

2. Material and methods

2.1. Animals

The mussels (*M. galloprovincialis*) were obtained from the same rope and depth of a raft in the culture area of Redondela (42°17′36.3″N, 8°38′30.7″W, Ría de Vigo, Spain). Six mussels naturally exposed to toxic *Pseudo-nitzschia australis* were collected on May 23, 2013 (toxin group) and another six mussels (control group) were collected on June 3, 2013 (when the toxin in mussels had decreased substantially). During that period, the environmental conditions in the area had only small variations. Water temperature and salinity at 4.6 m depth had an inter-day CV% of 2.6% (14.39 ± 0.37 °C) and 1.3% (34.31 ± 0.45) respectively (from continuous record by an hydrographic buoy in the area, Pilar de Rande, http://www2.meteogalicia.gal/galego/observacion/plataformas/plataformas.asp?idEst=15100). Superficial *in vivo* fluorescence and light transmittance, which are indexes of phytoplankton and seston concentration, respectively, only varied from 16.5 to 16.9 relative units, in the first case and from 61.3 to 62.8% in the second (http://www.intecmar.gal/Ctd/Default.aspx). The *Pseudo-nitzschia* concentrations varied from 35640 cells·L^{-1} on May 20th to 7425 on May 27th and increased again (without any increase of toxicity) to 57915 cells·L^{-1} on June 3rd (Intecmar, preliminary reports, www.intecmar.gal). Even when the routine monitoring does not discriminate the *Pseudo-nitzschia* species, it was clear that the populations that developed after May 27th were not toxic as no increase in domoic acid concentration in mussels was detected.

Mussels were dissected to separate the digestive gland (DG), gills and the remaining tissues. Each digestive gland was divided into two parts. One part was treated with RNAlater (ref. AM7021, Ambion, Life Technologies) according to the manufacturer's instructions and then stored at −80 °C prior to the RNA extraction, whereas the second part was used in the determination of the domoic acid content.

Other approaches that would have been more focused on domoic acid by excluding other compounds that could have some effect on gene transcription had to be discarded because of methodological problems. Supplying domoic acid to mussels was not possible because of their low absorption efficiency for this toxin, and differential exposure to toxic and not toxic *Pseudo-nitzschia* was also inviable because of the same reason, the difficulty of obtaining toxic and not toxic strains of the same species and the quick loss of toxicity of some strains.

2.2. Chemicals and reagents for toxin extraction and LC-MS/MS

Methanol for HPLC and formic acid were purchased from Labscan and Sigma Aldrich, respectively. Ultrapure water was obtained using a Milli-Q Gradient system, coupled to an Elix Advantage 10, both from Millipore.

2.3. Determination of the domoic acid content

To extract the toxin, each digestive gland was placed in aqueous methanol (50%) in a proportion of 1:2 w:v and homogenized with an Ultraturrax T25 (IKA). The extract was clarified using centrifugation at 18000*g* at 4 °C for ten minutes, retaining the supernatant that was immediately analyzed.

Domoic acid in the obtained extracts was analyzed using LC-MS/MS. The chromatographic separation was carried out using a Thermo Accela chromatographic system, with a high pressure pump and autosampler. The stationary phase was a solid core Kinetex C18, 50 × 2.1 mm 2.6 μm column (Phenomenex). An elution

gradient, with a flow of 280 μL/min, was used with mobile phase A (formic acid 0.2%) and B (50% MeOH with formic acid 0.2%). The gradient started at 100% A, maintained this condition for one minute, linearly changed until reaching 55% B in minute 5, held for 2 min and reverted to initial conditions to equilibrate before the next injection. 5 μL of extract, previously filtered through a PES 0.2 μm syringe filter (MFS), were injected.

After the chromatographic separation, domoic acid was detected and quantified by means of a Thermo TSQ Quantum Access MAX triple quadrupole mass spectrometer, equipped with a HESI-II electrospray interface, using positive polarization and SRM mode. The transition 312.18 > 266.18 m/z was used to quantify the response and 312.18 > 248.18 for confirmation. The spectrometer was operated under the following conditions: spray voltage 3400 V, capillary temperature 270 °C, HESI-II temperature 110 °C, Sheet gas (Nitrogen) 20 (nominal pressure), auxiliary gas (Nitrogen) 10 (nominal pressure). A collision energy of 15 V and a collision gas (Argon) pressure of 1.5 mTorr were used.

Concentrations of domoic acid were obtained by comparing the response of the quantification transition in the sample extracts with that of a reference solution obtained from NRC Canada. The limit of quantification of the method for tissue analysis is less than 20 ng/mL of extract, well below the concentrations of the extracts in this study.

2.4. RNA extraction

Total RNA was extracted from 20 mg of digestive gland tissue using the NucleoSpin RNA (ref. 740955, Macherey-Nagel, Germany) according to the manufacturer's instructions. A step of RNA precipitation with 0.5 vol of lithium chloride (LiCl 7.5 M, LICl precipitation solution, Ambion) was added and the RNA pellet was dissolved in 50 μl of RNA storage solution (ref. AM7000, Ambion, Life Technologies). Total RNA was treated with Turbo DNA-free (ref. AM1907M, Ambion, Life Technologies) to remove any DNA contamination. The integrity and quality of RNA samples were measured using agarose gel electrophoresis, an Agilent 2100 Bioanalyzer (Agilent Technologies) and a Nanodrop ND-1000 spectrophotometer (NanoDrop Technologies). The quantity of the total RNA was determined using Qubit 2.0 (Invitrogen). As the majority of Protostomes have 28S rRNA with a so-called “hidden break” (Dheilly et al., 2011; Ishikawa, 1977), we cannot use the RIN (RNA integrity number). Under denaturing conditions the two fragments of 28S rRNA separate and migrate with the 18S rRNA. The results of the Agilent 2100 Bioanalyzer (Supplementary file 1) showed the absence of RNA degradation.

2.5. Library preparation and sequencing

Twelve cDNA libraries were generated from the digestive gland of the mussels (six obtained from control mussels and six from mussels naturally exposed to domoic acid). Poly(A)+ mRNA fraction was isolated from total RNA and cDNA libraries were obtained following Illumina's recommendations. Briefly, poly(A)+ RNA was isolated on poly-T oligoattached magnetic beads and chemically fragmented prior to reverse transcription and cDNA generation. The cDNA fragments then went through an end repair process, the addition of a single ‘A’ base to the 3′ end and after that ligation of the adapters. Finally, the products were purified and enriched with PCR to create the indexed final double stranded cDNA library. The quality of the libraries was analyzed using a Bioanalyzer 2100, High Sensitivity assay; the quantity of the libraries was determined by real-time PCR in LightCycler 480 (Roche). Prior to cluster generation in cbot (Illumina), an equimolar pooling of the libraries was performed. The pool of the cDNA libraries was sequenced by paired-end sequencing (100 × 2 bp) on Illumina HiSeq 2000 sequencer.

2.6. De novo assembly

Quality control checks of raw sequencing data were performed with FastQC. The technical adapters were eliminated using Trimgalore software version 0.3.3 (http://www.bioinformatics.babraham.ac.uk/projects/trim_galore/). Additionally, the reads with a mean phred score >30 were selected.

Subsequently, all samples were combined and the complexity of the reads was reduced by removing duplicates reads. Then, *de novo* assembly was performed using the Oases, version 0.2.09 (Schulz et al., 2012) and Trinity, version 2.1.1 (Grabherr et al., 2011) programs. For the transcriptome assembly odd kmer sizes between 55 and 95 were evaluated and the kmer size that achieved the highest N50 value was selected. The use of different *de novo* assembly programs and a range of different Kmers sizes allow to combine and maximize the diversity and completeness of *de novo* assembled transcripts. The assembled transcripts were clustered (>90% homology) to reduce redundancy, this process was performed using cd-hit software, version 4.6. For each sequence the potential ORFs were detected using Transdecoder software, version 2.0, with standard parameters.

Each sample was then mapped with Bowtie2 version 2.2.6 (Langmead and Salzberg, 2012) against the reference transcriptome obtained in the previous step. The reads of good quality (Mapping Quality ≥ 20) were selected to increase the resolution of the count expression. Finally, the expression inference was evaluated by means of the counts of properly paired reads by transcript.

2.7. Differential expression

For the differential expression analysis, the transcriptome expression for each sample was normalized by library size, following the DESeq2 protocols (Supplementary file 2). For identifying possible samples outliers, a study of correlation and Euclidean distance between samples was performed using the statistical software R, version 3.2.3, and considering the whole normalized transcriptome.

For the study of differential gene expression, the DESeq2 algorithm was used (http://www.bioconductor.org/packages/devel/bioc/html/DESeq2.html), version 1.8.2, this method is based in a negative binomial distribution. The genes with a fold change of less than −1.5 or greater than 1.5, and a not adjusted p-value < 0.05 were considered differentially expressed, although p-values adjusted using the Benjamini and Hochberg (1995) method for controlling False Discovery Rate (FDR) were also calculated.

2.8. Functional annotation

Differentially expressed genes (DEGs) were annotated using blastx against Uniprot database and blastn against NCBI nucleotide database (Altschul et al., 1990), in both cases using an E-value threshold of 0.01. Later on, annotation was expanded by incorporating information from species, gene name and functions using Gene Ontology (http://www.geneontology.org/GO.refgenome.shtml) and protein structure domains associated with the transcript using InterPro (https://www.ebi.ac.uk/interpro/). Differentially expressed genes were also annotated with Blast2GO software (Conesa et al., 2005; Götz et al., 2008), using blastx 2.2.30 against NCBI nr database (E-value threshold of 10^{-3}). Ortholog assignment and pathway mapping in KAAS (KEGG Automatic Annotation Server) was performed (Moriya et al., 2007) using the BBH (bidirectional best hit) method (http://www.genome.jp/tools/kaas/).

2.9. Functional enrichment

A functional enrichment study was performed using the Pfam (Finn et al., 2016) functional information. This study is based on a hypergeometric distribution (Johnson et al., 1992) using the statistical software R version 3.2.3.

2.10. Network analysis

To search for the relationships between proteins coded by the differentially expressed genes identified in the present study, network analyses using the String 10.0 algorithm (Szklarczyk et al., 2015) were performed. The STRING (Search Tool for the Retrieval of Interacting Genes/Proteins) database (http://string-db.org) provides a critical assessment and integration of protein-protein interactions, including direct (physical) as well as indirect (functional) associations (Szklarczyk et al., 2015). Known and predicted associations are scored and integrated, resulting in comprehensive protein networks. This network analysis is more efficient using databases from the most studied organisms (Artigaud et al., 2015). Therefore, putative human homologs of proteins coded by the differentially expressed genes in *M. galloprovincialis* DG (after filtering using a p-value < 0.002) were identified by means of a blastx search (Altschul et al., 1997) against the STRING human protein database (9606.protein.sequences.v10.fa), with an E-value threshold of 10^{-5}. The top blastx search results were used as input in the STRING program.

2.11. Real time RT-qPCR validation

cDNA was synthesized using 0.5 μg of RNA with the iScript™cDNA Synthesis kit (ref. 170–8891, BioRad, CA, USA) in a 20 μl reaction volume containing 5X iScript Reaction Mix, 1 μl iScript Reverse Transcriptase; the reaction was allowed to continue for 5 min at 25 °C, 30 min at 42 °C and 5 min at 85 °C.

Six reference gene candidates (Table 1, Lozano et al., 2015), *glyceraldehyde-3-phosphate dehydrogenase* (*gapdh*), *cytochrome c oxidase subunit I* (*cox1*), *ubiquitin-ribosomal protein S27 fusion protein* (*rps27*), *eukaryotic translation initiation factor 5A* (*tif5a*), *40S ribosomal protein S4* (*rps4*), *actin* (*act*), and six target genes (Table 1) were used in the study of gene expression. Oligonucleotide primers were designed with the OligoAnalyzer 3.1 (http://eu.idtdna.com/analyzer/Applications/OligoAnalyzer/) from the sequences of Table 1. Oligonucleotides were synthesized by Thermo Scientific (Thermo Fisher Scientific). The primer sequences and amplicon lengths are listed in Table 1. The specificity of the primers was confirmed by the presence of a single peak in the melting curve and by the presence of a single band of the expected size when PCR products were run in a 2% agarose gel. The identity of the amplicons was also confirmed by sequencing. PCR amplification efficiency (E) of each transcript was determined by means of Real Time PCR Miner software (http://www.miner.ewindup.info/, Zhao and Fernald, 2005). The mean amplification efficiency (E) of each amplicon (Table 1) was used in the calculation of gene expression.

A quantitative real-time reverse transcription polymerase chain reaction (RT-qPCR) was conducted in 96-well reaction plates on an iCycler iQ® Real-time System (BioRad, CA, U.S.A.). The PCR final volume was 20 μl, containing 4 μl of 1:5 diluted cDNA (20 ng of cDNA), 10 μl SsoFast EvaGreen Supermix (ref. 172–5201, Bio-Rad), 400 nM forward and reverse primers, and 4.4 μl PCR-grade water. Real-time qPCR analysis was conducted in technical duplicates and 6 biological replicates. The cycling conditions were as follows: 30 s at 95 °C (initial template, denaturation), and 40 cycles of 5 s at 95 °C (denaturation) followed by 10 s at 60 °C (annealing and elongation) and 10 s at 75 °C for fluorescence measurement. At the end of each run a melting curve was carried out: 95 °C for 20 s and 60 °C for 20 s followed by an increase in temperature from 60 to 100 °C (with temperature increases in steps of 0.5 °C every 10 s). Baseline values were automatically determined for all plates using the Bio-Rad iCycler iQ software V3.1 (IQ™ Real-Time PCR Detection System). The threshold value was set manually at 70 RFU to calculate the Cq values. As a control for genomic DNA contamination, an equivalent amount of total RNA without reverse transcription was tested for each gene (non-reverse transcriptase control). Non-template controls (NTC) were also included in each run.

For accurate relative quantification of gene expression, a normalization must be performed using internal reference genes whose expression levels are stable (Andersen et al., 2004; Bustin et al., 2009; Cubero-Leon et al., 2012; Mauriz et al., 2012; Pfaffl et al., 2004; Vandesompele et al., 2002). The data obtained were analyzed using three Microsoft Excel based software applications, geNorm V3.5 (Vandesompele et al., 2002), NormFinder V0.953 (Andersen et al., 2004) and BestKeeper V1 (Pfaffl et al., 2004).

The Cq values were transformed to quantities (Q, non-normalized expression) by using the equation $Q = (1 + E)^{-Cq}$ (Mauriz et al., 2012). The normalized gene expression was calculated as the ratio between Q and the normalization factor. The normalization factor used was the geometric mean of the quantities (Q) of the selected reference genes.

Statistical analyses were performed with IBM SPSS Statistics 20.0 package. Data were tested for normality (Shapiro–Wilk test) and for homogeneity of variance (Levene's test). Gene expression was log-transformed (base 2) to meet the requirements of normality and homogeneity of variances. The expression of target genes in control and toxin (domoic acid-contaminated mussels) groups was compared using a Student's-t test. $P < 0.05$ was considered statistically significant.

Table 1
Gene symbols, GenBank accession number or sequence name, gene name/description, primers, amplicon length (bp) for each primer pair and average efficiency (E).

Symbol	Accession number or sequence name	Gene name/description	Sense primer (5′ - 3′)	Antisense primer (5′ - 3′)	bp	E
gapdh	AJ625093, FL593798, FL496349	*Glyceraldehyde-3-phosphate dehydrogenase*	AGGAATGGCCTTCAGGGTAC	TCAGATGCTGCTTTAATGGCTG	114	0.8269
cox1	NC_006886	*Cytochrome c oxidase subunit I*	TGCTCATTGGCATTGGGTGTC	AGTTCCTGCTCAGTCCATCTCAC	151	0.7730
rps27	AJ625324, AJ516561, AJ625501	*Ubiquitin-ribosomal protein S27 fusion protein*	CGTGAATGTCCCAACGAAGAG	TGTTGCCTCTGGTTTGTTGA	114	0.8143
tif5a	FL593258	*Eukaryotic translation initiation factor 5A*	ACGCTACTTGACATTAACGATG	AGCTAGTTCTTCTCCCATAGC	171	0.8399
rps4	FL492874	*40S ribosomal protein S4*	TGGGTTATCGAGGGCGTAG	TCCCTTAGTTTGTGAGGACCTG	121	0.7950
act	AF157491	*Actin*	TCTTGATTTCGAGCAGGAAATG	GGATGGTTGGAATAATGATTCTG	138	0.8372
rtn4	*68516_Contig63488*	*Reticulon-4-like isoform X3*	GCACTGTTGTTATGGGTGTTG	TGGTCACAAGCCATTGACAC	152	0.8610
slc46a3	*87569_Contig19100*	*Solute carrier family 46 member 3*	CAATGTCGGCACTGACTGTT	ACTCCGCCTATGTTCCACAG	136	0.8256
pcat	*29165_comp41484_c0_seq1*	*Proton coupled amino acid transporter*	AGGCGATCTCTCTGAGCAAA	GAATGTGGAGGAGCACCATT	114	0.8285
faxc	*34052_Contig60530*	*Failed axon connections homolog*	AAGTTCCTGCTCGGAGACAA	CGAAAGATTGCCAGTAAGCA	82	0.8093
abcg1	*22476_Contig64139*	*ATP-binding cassette transporter G1*	CCAATCCTGTAACCACGACA	GCTCTCCATGTTAGGCTTCC	94	0.8264
cola1	*87907_Contig57568*	*Collagen alpha1 chain - cola1*	ACAAAGGGCGTTTACAGTGG	TTGTTTGGGCAGGTCTTCTC	137	0.8430

3. Results and discussion

3.1. Biometrical characteristics and domoic acid content

The digestive glands had a mean domoic acid content of 3884 ng/g in the toxin group and 130 ng/g in the control group (Table 2 and Supplementary file 3). Mussels were collected from rafts, this approach was chosen because of the difficulty of supplying toxic *Pseudo-nitzschia* under controlled conditions in the laboratory, due to the relatively low absorption efficiency of the mussels and the loss of toxicity of the *Pseudo-nitzschia* cultures. Therefore some of the differences between the two conditions (control and toxin) should be due mainly to domoic acid, but a role of *Pseudo-nitzschia* itself or other factors could not be discarded. The two groups of mussels had very similar biometrical characteristics (Table 2 and Supplementary file 3) and no significant differences (GLM ANOVA) were detected in total weight ($p = 0.44$), digestive gland weight ($p = 0.18$) or other tissues weight ($p = 0.88$), neither in the relationship other tissues weight/digestive gland weight ($p = 0.70$), indicating that no disrupting event, such as spawning for example, could have affected one of the groups (Supplementary file 4).

In many RNA-seq experiments, samples are pooled and there are no true biological replicates. Rajkumar et al. (2015) showed the limited utility of sample pooling strategies for differential gene expression analysis using RNA-seq. Pooled samples identified differentially expressed genes (DEGs) with high false positivity rates and low positive predictive values. Rajkumar et al. (2015) proposed increasing the number of biological replicate samples. Six biological replicates for each condition (control and toxin) were used in the present work.

3.2. Sequencing and de novo assembly

After *de novo* assembly with Trinity and Oases, 94,727 transcripts were obtained. The length of the transcripts ranged from 450 to 15,385 bp, with an average length of 1015 bp and a N50 length of 761 bp, (Table 3). The assembled transcripts were clustered (homology > 90%) to reduce redundancy, thus 69,294 unigenes were obtained (Table 3). The raw data are accessible from the NCBI Sequence Read Archive (BioProject PRJNA326100, BioSample accession numbers from SAMN05824318 to SAMN05824329).

3.3. Differential expression, functional annotation and functional enrichment analysis of the differentially expressed genes (DEGs)

A total of 1158 differentially expressed unigenes (absolute fold change > 1.5 and p-value < 0.05) were detected in the digestive gland of *M. galloprovincialis* (Supplementary files 5 and 6, Tables 4 and 5): 686 up-regulated and 472 down-regulated. Some of the differentially expressed genes could be considered as candidates to participate in detoxification of domoic acid. Functional annotation results for the assembled unigenes and for differentially expressed unigenes are summarized in Table 6. KO orthologs and level 2 GO annotation of the differentially expressed unigenes are shown in Supplementary Files 7 and 8, respectively.

A study of functional enrichment was performed using Pfam annotations obtained from the differentially expressed genes. 37 Pfam families were found to be significantly (FDR adjusted p-value < 0.1) enriched (Supplementary file 9, Table 7). Among these enriched domains, we found genes coding for proteins involved in the metabolism of toxins and detoxification processes (short chain dehydrogenases, sulfotransferases, aldo/keto reductases and carboxylesterases), and genes coding for proteins involved in immunological processes (C1q domain containing proteins and fibrinogen C-terminal globular domain containing proteins).

Domoic acid is a zwitterionic compound that is mainly excreted unchanged in mussels (Novaczek et al., 1991). Presumably, therefore, it needs a transport protein to cross the cell membrane. Taking these facts into account, the most important genes involved in its excretion are expected to be those related to membrane transport. The over-expression in *M. galloprovincialis* of a number of genes coding for membrane transporters belonging to the family of the SLC (solute carrier transporters) is of great interest, some of which could be involved in the absorption and/or excretion of domoic acid. The SLC gene series include 52 families and 395 transporter genes in the human genome (Hediger et al., 2013; http://slc.bioparadigms.org/). The SLC families populate three clans of Pfam (a clan is a compilation of Pfam entries that are judged likely to be homologous), one of these clans is the major facilitator superfamily (MFS) clan (Höglund et al., 2011). We found 54 (45 up and 9 down) differentially expressed unigenes that code for putative SLC transporters. These genes belong to 19 families (Supplementary file 10).

Most studies on domoic acid have focused on the mechanisms of neurotoxicity and there is little information about the absorption and excretion mechanisms at the molecular level. In the scallop *Pecten maximus*, Mauriz and Blanco (2010) found that domoic acid is free in the cytosol of the digestive gland and hypothesize that the lack of membrane transporters could be the cause of the long retention time of domoic acid in this species. Madhyastha et al. (1991) found that kainic acid, glutamic acid and proline inhibited the *in vitro* uptake of dissolved domoic acid by the digestive gland tissue of the blue mussel indicating competition for the same carrier site. Kimura et al. (2011) showed that diisothiocyanostilbene-2,2′-disulfonic acid (DIDS, an anion exchange inhibitor) sensitive anion exchangers were involved in the apical-to-basolateral transport of DA across the Caco-2 cell monolayers (which represent the intestinal barrier). These results point to the SLC

Table 2
Wet weight (g) of the soft tissues (Total weight), wet weight (g) of the digestive gland (DG weight) and domoic acid (DA) concentration (ng/g) in the digestive gland (DG) in sampled mussels (*Mytilus galloprovincialis*).

	Total weight (g)		DG weight (g)		DA in the DG (ng/g)	
	mean	SD	mean	SD	mean	SD
Control	7.289	1.755	1.031	0.388	130	68
Toxin	6.480	1.345	0.720	0.133	3884	1567

Table 3
Summary of Illumina transcriptome sequencing an assembly for *M. galloprovincialis* digestive gland.

Summary of raw reads data	
Throughput (Mb)	64,919
Number of reads	705,558,488
Filtered reads	676,169,399
Average read length alter filtering (bp)	100
Sequence quality ≥ Q30 (%)	95.04
Mean quality score	34.82
GC%	38
Summary of the assembled transcriptome	
Total number of filtered reads	676,169,399
Number of assembled transcripts	94,727
Number of assembled unigenes	69,294
Contig N50 Length (bp)	761
Minimum contig length (bp)	450
Maximum contig length (bp)	15,385
Average contig length (bp)	1015
Total length in contigs (bp)	70,321,015

Table 4
List of the 25 top up-regulated genes (ordered by p-value) in the digestive gland of *M. galloprovincialis*.

Seq. Name	Seq. Description	Seq. Length	baseMean	log2FC	FC	p-value	Adjusted p-value*
24701_Contig7063	Sialin (SLC17A5)	728	76.89	1.77	3.41	6.12E-14	2.41E-09
85094_Contig61251	zinc finger protein fyve domain-containing	502	333.2	1.18	2.27	3.87E-11	7.61E-07
54762_Contig2397	lateral signaling target protein 2-like protein	1246	599.63	1.4	2.64	1.43E-10	1.88E-06
74724_Contig35290	—NA—	521	86.94	2.36	5.14	9.45E-09	6.19E-05
11393_Contig15071	heavy metal-binding protein hip	978	9.37	4.19	18.31	9.82E-08	3.22E-04
78489_Contig56437	transmembrane protein 144	1401	258.33	1.18	2.27	6.37E-07	1.57E-03
86546_Locus_23710_Transcript_1/1	endothelin-converting enzyme 1-like	560	5.94	3.53	11.56	1.24E-06	2.43E-03
13759_Contig25056	protein jagged-1b-like	1018	128.52	2.23	4.68	1.56E-06	2.58E-03
19377_Contig66244	alpha subunit	1164	26.28	3.24	9.42	1.95E-06	3.07E-03
49206_Contig15207	scavenger receptor cysteine-rich protein	593	28.94	2.11	4.33	2.05E-06	3.09E-03
93621_Locus_43041_Transcript_1/1	c-binding protein	532	47.47	3.34	10.15	6.77E-06	6.34E-03
57531_Contig61115	transmembrane protein 184c	1703	505.72	0.72	1.65	1.35E-05	1.04E-02
87378_Contig58008	c1q domain containing protein 1q3	1351	201.59	2.93	7.63	1.50E-05	1.07E-02
47234_Contig30292	loc100145110 protein	997	53.58	1.61	3.05	2.11E-05	1.43E-02
82068_Contig36412	hypothetical protein BRAFLDRAFT_106563	880	43.46	3.24	9.42	2.34E-05	1.54E-02
62155_Locus_6630_Transcript_1/1	mechanosensory protein 2	523	96.85	0.68	1.6	2.87E-05	1.69E-02
46175_comp26962_c0_seq1	marginal zone b- and b1-cell-specific protein	918	158.75	0.89	1.86	3.15E-05	1.79E-02
73482_Contig24179	—NA—	988	471.73	2.04	4.11	4.55E-05	2.41E-02
37888_comp8580_c0_seq1	sodium potassium calcium exchanger mitochondrial	966	95.47	1.08	2.11	4.60E-05	2.41E-02
82224_Locus_19707_Transcript_1/1	major facilitator superfamily domain-containing protein 7-a	569	20.18	2.06	4.18	4.95E-05	2.56E-02
53454_Contig56461	15-hydroxyprostaglandin dehydrogenase	1118	756.17	1.23	2.34	5.54E-05	2.76E-02
23765_Contig58660	parkinson disease 7 domain-containing protein 1 isoform ×2	1131	81.88	0.97	1.96	6.45E-05	2.95E-02
55199_Contig56628	2 -5 -oligoadenylate synthase 3	1368	999.31	2.52	5.75	7.12E-05	3.15E-02
84837_Locus_47119_Transcript_1/1	—NA—	712	11.12	2.71	6.56	7.44E-05	3.25E-02

*p-value adjusted using the Benjamini and Hochberg (1995) method for controlling False Discovery Rate (FDR).

Table 5
List of the 25 top down-regulated genes (ordered by p-value) in the digestive gland of *M. galloprovincialis*.

Seq. Name	Seq. Description	Seq. Length	baseMean	log2FC	FC	p-value	Adjusted p-value*
27153_Contig16105	carbohydrate sulfotransferase 15	654	29.41	−1.2	−2.3	1.23E-08	6.90E-05
87907_Contig57568	collagen alpha-1 chain	2488	794.56	−2.22	−4.66	2.64E-08	1.30E-04
74134_Locus_9533_Transcript_1/1	toll-like receptor c	513	5.39	−3.46	−11.03	1.42E-06	2.58E-03
45972_Contig55102	—NA—	1361	333.34	−1.47	−2.77	1.58E-06	2.58E-03
85706_Contig273	—NA—	525	21.1	−3.58	−11.92	2.13E-06	3.10E-03
13085_Contig49628	heat shock 70 kda protein 12a	1256	139.32	−3	−8	3.59E-06	4.43E-03
56622_comp42876_c0_seq2	—NA—	734	358.62	−0.7	−1.62	3.60E-06	4.43E-03
78732_comp31145_c0_seq1	dual oxidase 2	981	218.88	−1.58	−3	3.88E-06	4.62E-03
63287_Locus_18884_Transcript_2/2	toll-like receptor 3	679	4.88	−3.53	−11.54	4.50E-06	4.91E-03
73327_Locus_29686_Transcript_1/1	e3 ubiquitin-protein ligase mib2	825	4.6	−3.64	−12.43	5.82E-06	5.72E-03
54892_Contig63791	dual oxidase 1-like	2992	407.78	−1.55	−2.93	6.97E-06	6.38E-03
79748_comp41472_c0_seq14	—NA—	657	18.4	−3.27	−9.67	7.75E-06	6.77E-03
90443_comp42682_c0_seq1	hypothetical protein CGI_10028730	996	343.02	−1.6	−3.03	7.68E-06	6.77E-03
24973_Contig62834	glutamine–fructose-6-phosphate aminotransferase	4437	263.46	−2.49	−5.63	1.06E-05	8.69E-03
13499_Contig52999	—NA—	1362	104.69	−1.4	−2.64	1.36E-05	1.04E-02
43098_Contig51186	replication factor c subunit 1-like	1402	171.91	−0.94	−1.92	1.38E-05	1.04E-02
90678_Contig56928	copine family protein 2-like	1957	88.5	−2.77	−6.83	1.47E-05	1.07E-02
35783_Contig56453	ankyrin-1- partial	1273	140.68	−1.16	−2.24	1.97E-05	1.36E-02
33566_Locus_23397_Transcript_1/1	protocadherin gamma-a11	1344	141.35	−2.86	−7.26	2.49E-05	1.55E-02
20543_Contig67588	ankyrin repeat domain-containing protein 46	628	48.83	−1	−2	2.98E-05	1.72E-02
31859_Locus_31794_Transcript_1/1	magnesium chelatase	783	4.01	−3.37	−10.36	3.30E-05	1.85E-02
31273_Contig33124	tripartite motif-containing protein 45	561	42.1	−2.88	−7.37	3.70E-05	2.04E-02
23893_Contig22062	Poly [ADP-ribose] polymerase 14-like	737	18.91	−1.72	−3.29	4.58E-05	2.41E-02
23614_Contig3522	protein phosphatase mitochondrial	1541	72.31	−2.14	−4.4	5.33E-05	2.68E-02
74966_Contig65675	dual oxidase	881	77.22	−1.56	−2.95	7.72E-05	3.34E-02

*p-value adjusted using the Benjamini and Hochberg (1995) method for controlling False Discovery Rate (FDR).

Table 6
Summary of the functional annotation results.

	number	%
Differentially expressed unigenes	**1158**	
With Blastx hit (nr)	1008	87.05
With GO terms	921	79.53
With enzyme code	172	14.85
With KO ortholog	397	34.28
With PFAM domains	772	66.67
All unigenes	**69294**	
With KO ortholog	6941	10.02
With PFAM domains	20295	29.29

transporters as those responsible for the transmembrane transport of domoic acid in mammals.

The top (Table 4, Supplementary file 6) differentially expressed gene (ordered by p-value) is *SLC17A5* (sialin), and among the overexpressed genes there are three transcripts encoding for sialin. The SLC17 family mediate the transmembrane transport of organic anions (Reimer, 2013) and include type I phosphate transporters (SLC17A1–4), sialin (SLC17A5), vesicular glutamate transporters (VGLUT1–3, SLC17A7, SLC17A6, and SLC17A8, respectively), and a vesicular nucleotide transporter (VNUT; SLC17A9). In mammals, sialin transports sialic acid to lysosomes, but may also function as a

Table 7
Pfam families significantly enriched (FDR adjusted p-value < 0.1) with four or more differentially expressed genes.

Category	Number of genes	p-value	Adjusted p-value
PF00386.16//C1q_domain	18	3.89E-07	8.75E-05
PF01926.18//50S_ribosome-binding_GTPase	4	2.44E-06	0.0002745
PF11790.3//Glycosyl_hydrolase_catalytic_core	8	3.92E-05	0.00294
PF13561.1//Enoyl-(Acyl_carrier_protein)_reductase	17	0.000135057	0.006077552
PF01699.19//Sodium/calcium_exchanger_protein	4	0.000454684	0.01473678
PF00106.20//short_chain_dehydrogenase	19	0.000458478	0.01473678
PF00685.22//Sulfotransferase_domain	10	0.000702494	0.019757649
PF05175.9//Methyltransferase_small_domain	4	0.000804908	0.020122708
PF02157.10//Mannose-6-phosphate_receptor	4	0.002008836	0.037665675
PF00147.13//Fibrinogen_beta_and_gamma_chains,_C-terminal_globular_domain	5	0.00424775	0.060439627
PF08659.5//KR_domain	13	0.004276715	0.060439627
PF00248.16//Aldo/keto_reductase_family	6	0.007431077	0.069666347
PF00135.23//Carboxylesterase_family	8	0.01607136	0.097731243

vesicular transporter for aspartic acid and glutamic acid (Miyaji et al., 2008, 2011; Reimer, 2013). Sialin might be involved in the transport of domoic acid, which shares some structural characteristics with glutamic acid.

There were genes belonging to the *SLC6* family (sodium- and chloride-dependent neurotransmitter transporter family) that were overexpressed in *M. galloprovincialis* DG (Supplementary file 10). It is interesting to note that Di Dato et al. (2015) found a transcript of this family that is overexpressed in a domoic acid-producing *Pseudo-nitzschia* species (*P. multistriata*) in relation to two other species that do not produce domoic acid (*P. arenysensis* and *P. delicatissima*), suggesting that this gene is expressed more in toxin-producing species (Di Dato et al., 2015). In addition, a gene of this family is up-regulated in *Pseudo-nitzschia multiseries* under toxin-producing conditions (Boissonneault et al., 2013). Moreover, a gene belonging to the *SLC6* family (*sodium- and chloride-dependent creatine transporter 1*, *SLC6A8*) was overexpressed in zebrafish brain after exposure to domoic acid (Lefebvre et al., 2009).

Several genes from the *SLC16* family, coding for monocarboxylate transporters, were also overexpressed in *M. galloprovincialis* DG (Supplementary file 10). The human *SLC16* gene family comprises 14 members, four encode monocarboxylate transporters but the substrates of eight members are unknown (Halestrap, 2013). The members overexpressed in *M. galloprovincialis* DG (*SLC16A4*, *SLC16A9*, *SLC16A12* and *SLC16A13*) are part of those that do not have a known substrate. Lefebvre et al. (2009) found two *SLC16A9* genes up-regulated in zebrafish brain after exposure to domoic acid.

Besides SLC, the other major superfamily of transmembrane transporters is the ATP-binding cassette (ABC) transporter superfamily (Dean et al., 2001). ABC transporters (MDRs and MRPs) could be involved in the excretion of some biotoxins in bivalves (Huang et al., 2014; Lozano et al., 2015; Xu et al., 2014). Jansen et al. (2015), using a vesicular membrane transport assay, found that domoic acid could be transported by an ATP-binding cassette (ABC) transporter (human ABCC5 or MRP5). Schultz et al. (2013) hypothesized that the absorption of domoic acid from the foregut and transfer into the hepatopancreas and hemolymph is regulated by membrane bound, unidirectional transporters of the ABC transporter family in Dungeness crabs. In *M. galloprovincialis* DG we have found only two up-regulated ABC transporters (Supplementary files 5 and 6): 4042_comp19047_c0_seq1 (*ABCD4*) and 22476_Contig64139 (*ABCG1*).

Even when biotransformation, as already commented, is not the main route of domoic acid elimination from mussels, some effect cannot be discarded. Some genes coding for enzymes involved in biotransformation have been found to be differentially expressed in this work (short-chain dehydrogenases/reductases, sulfotransferases, aldo-keto reductases, carboxylesterases, cytochromes P450 and glutathione S-transferases).

The exposure of the organisms to harmful algae toxins has been found to produce an increase of oxidative stress and some immunological reactions. Those processes have probably no or little effect on the elimination of the toxin from the mussels but the genes related to them are expected to be differentially expressed. Domoic acid causes an increase in oxidative stress in mouse as indicated by increases in reactive oxygen species and lipid peroxidation (Giordano et al., 2006, 2007) and several authors (González and Puntarulo, 2016; Hégaret et al., 2011; Malanga et al., 2016) showed that harmful algae toxins provoke oxidative stress in bivalves. Some of the genes induced in *M. galloprovincialis* (Supplementary file 6) could be involved in the response against the oxidative stress (aldo-keto reductases and GSTs for example). It is interesting to point that the gene coding for glutamate-cysteine ligase regulatory subunit is up-regulated in *M. galloprovincialis* digestive gland. This protein is the first enzyme of glutathione (GSH) synthesis, and GSH protects against oxidative stress. Peña-Llopis et al. (2014) demonstrated that treatment of scallops (*P. maximus*) with N-acetylcysteine allowed them to remove more efficiently the ASP toxin domoic acid by increasing the glutathione S-transferase (GST) activity and inducing the glutathione (GSH) anabolism.

Some of the functionally enriched Pfam families are putatively involved in immunological processes. The immune system of marine bivalves is sensitive to environmental contaminants (Renault, 2015) and it is possible that domoic acid, as some other biotoxins do, could also disturb the immune system (Hégaret et al., 2011). The C1q domain is involved in the activation of the classical complement pathway and in other functions, such as apoptosis, bacterial recognition, cell adhesion and cell differentiation (Gerdol et al., 2011, 2015). There is an expansion of proteins containing the C1q domain in several bivalve molluscs. Thus, a large number of C1q domain proteins have been identified in the *C. virginica* (Zhang et al., 2014), *C. gigas* (Gerdol et al., 2015) *M. galloprovincialis* (Gerdol et al., 2011; Venier et al., 2011) and *M. edulis* (Philipp et al., 2012) transcriptomes.

3.4. Protein network analysis (STRING)

Protein–protein associations can be employed to group and organize all protein-coding genes in a genome (Franceschini et al., 2013). The complete set of associations can be assembled into a large network. Protein network information can help in the interpretation of functional genomics data. After filtering by a p-value < 0.002, 175 unigenes were found to be differentially expressed and a blastx search found 95 homologs in the STRING database. 32

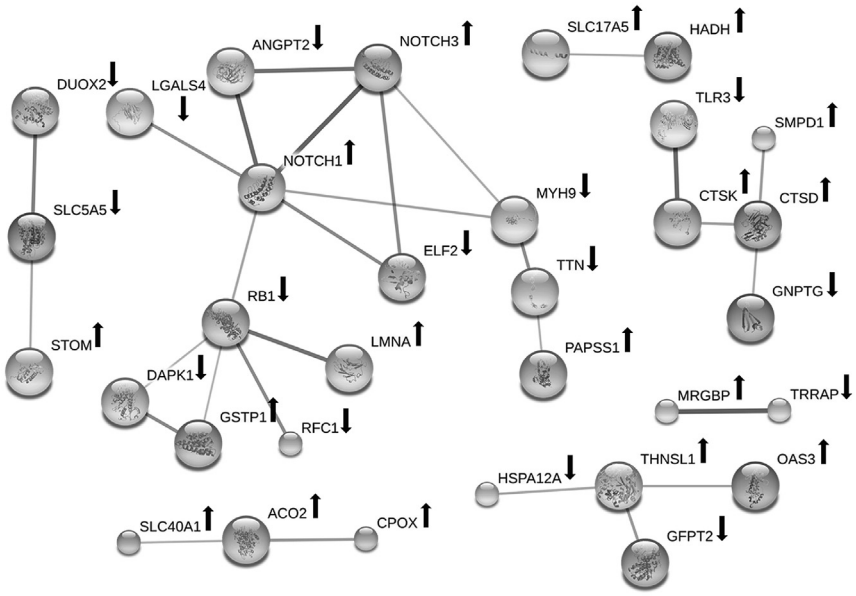

Fig. 1. Network showing interactions of proteins (n = 95) coded by genes differentially expressed in the present study. Network was constructed using the String 10.0 algorithm. Proteins were named according to the human gene/protein name. They are shown in the confidence view (stronger associations are represented by thicker lines). A full list of gene symbols is available in Supplementary file 11. ↑ = up-regulated; ↓ = down-regulated.

proteins showed interactions (Fig. 1, Supplementary file 11), and the network is enriched in interactions (p-value = 0.0141): interactions observed 29, interactions expected 18. There is a central node around NOTCH1 which showed 6 interactions: LGALS4 (lectin, galactoside-binding, soluble 4), ANGPT2 (angiopoietin 2), NOTCH3, MYH9 (myosin, heavy chain 9, cellular myosin), ELF2 (E74-like factor 2), and RB1 (retinoblastoma 1).

The Notch genes encode receptors that interact with ligands (Jagged1, Jagged2 and Delta1) on surrounding cells. Receptors and ligands are both transmembrane proteins, thus, the Notch signaling pathway is involved in cell-cell communications that regulate cell-fate determinations in several tissues. Notch signals can either promote or suppress proliferation, cell death and specification of cell fates depending of the cellular context (Kopan and Ilagan, 2009; Schwanbeck et al., 2011). This pathway has diverse roles in the maintenance of normal gut function in mammals (Sander and Powell, 2004) and in liver development and repair (Geisler and Strazzabosco, 2015).

3.5. Real time RT-qPCR validation

We used 6 biological replicates for each condition (control and toxin). Six putative reference genes (Table 1, Lozano et al., 2015) were analyzed and their ranking in order of expression stability is displayed in Table 8. The most stable reference genes identified by the three different analysis methods (geNorm, NormFinder and BestKeeper) were *rps27*, *cox1*, *rps4* and *gapdh*. These four genes were used for normalization of the gene expression. We selected six genes (Table 1): four up-regulated, one down-regulated and one not differentially expressed and their expression was quantified using RT-qPCR. The results of normalized expression (Fig. 2) were similar to those obtained using RNA-seq. Four genes were significantly up-regulated and one gene is not differentially expressed. The down-regulated gene in RNA-seq is also down-regulated in RT-qPCR but the result is not significant at $P < 0.05$.

4. Conclusions

The present study represents the first analysis of *M. galloprovincialis* transcriptome after exposure to a domoic acid-producing species. After *de novo* assembly, 69,294 unigenes were obtained and 1158 differentially expressed genes (DEGs) were identified. Functional enrichment was performed using Pfam annotations and 37 families were found to be significantly enriched for DEGs. Although the results obtained suggest the involvement of domoic acid in the differential expression, a role of *Pseudo-nitzschia* itself or other factors could not be totally discarded. The over-expression of membrane transporters belonging to the family of the SLC (solute carrier transporters) is of great interest because some of them could be involved in the absorption and/or excretion of domoic acid. Some of the DEGs and some of the enriched Pfam families (sulfotransferases, aldo/keto reductases, carboxylesterases,

Table 8
Rank of six candidate reference genes in quantitative real-time reverse transcription–polymerase chain reaction (RT–qPCR), calculated by geNorm, NormFinder, and BestKeeper analysis.

Rank	GeNorm	average M	Normfinder	Stability	BestKeeper	SD	BestKeeper	*r*
1	*rps4-gapdh*	0.91	*rps27*	0.100	*rps4*	0.74	*rps27*	0.91
2	*rps4-gapdh*	0.91	*cox1*	0.159	*cox1*	0.78	*cox1*	0.64
3	*rps27*	0.97	*rps4*	0.241	*gapdh*	0.84	*gapdh*	0.53
4	*cox1*	1.04	*gapdh*	0.276	*tif5a*	0.94	*act*	0.52
5	*tif5a*	1.17	*tif5a*	0.287	*rps27*	1.11	*tif5a*	0.48
6	*act*	1.37	*act*	0.499	*act*	1.45	*rps4*	0.45

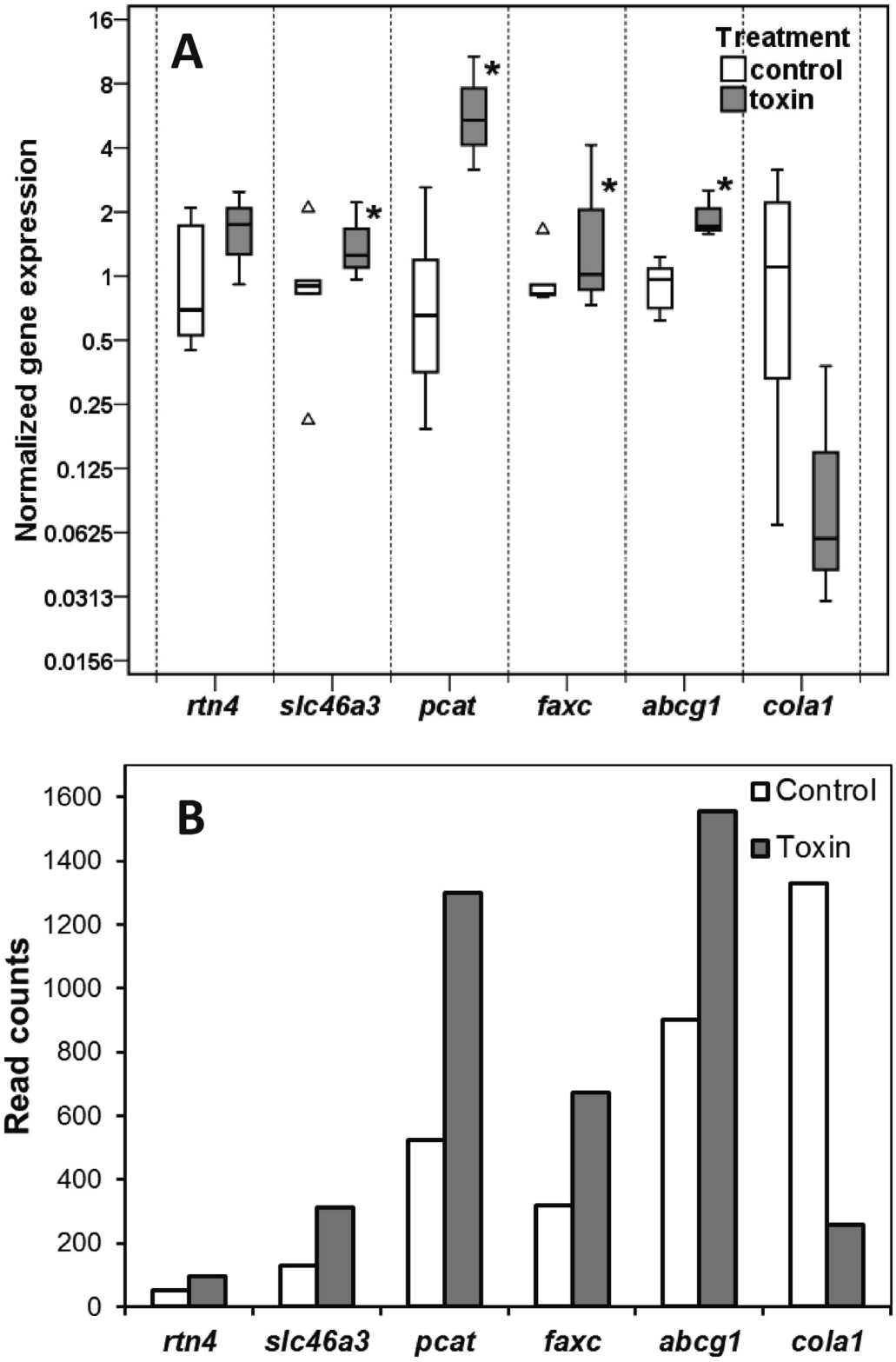

Fig. 2. Gene expression. (A) Normalized gene expression in the digestive gland of *Mytilus galloprovincialis* in the presence of domoic acid, as determined by RT-qPCR analyses. The box and whisker plots were obtained using IBM SPSS version 20.0 software. Boxes represent the lower and upper quartiles with medians. Bars represent the ranges for the data (n = 6 for control, 6 for toxin). Triangles represent extreme values (more than three box lengths from the end of a box). Statistical analysis was performed using Student's *t*-test: $^{*}P < 0.05$. (B) Mean read counts obtained by RNA-seq.

C1q domain and fibrinogen C-terminal globular domain) could be putatively involved in detoxification processes, in the response against of the oxidative stress and in immunological processes. Considering the absence of previous studies in the literature, the present work is a starting point for further researches.

Acknowledgements

This work has been supported by the Spanish Ministry MINECO (Ministerio de Economía y Competitividad) and the FEDER Funds (European Regional Development Fund) of the European Union under the project AGL2012-39972-C02. We acknowledge Carmen Mariño and Helena Martín (CIMA) for their technical assistance in toxin determination, and the Biotoxins and Sampling departments of INTECMAR for sharing the information required to choose the place and time to carry out the experiment and supplying the biological samples. We thank Mary Vázquez for helpful comments on the English version of the manuscript.

Transparency document

Transparency document related to this article can be found online at https://doi.org/10.1016/j.toxicon.2017.10.002.

Appendix A. Supplementary data

Supplementary data related to this article can be found at https://doi.org/10.1016/j.toxicon.2017.10.002.

References

Altschul, S.F., Gish, W., Miller, W., Myers, E.W., Lipman, D.J., 1990. Basic local alignment search tool. J. Mol. Biol. 215, 403–410.

Altschul, S.F., Madden, T.L., Schäffer, A.A., Zhang, J., Zhang, Z., Miller, W., Lipman, D.J., 1997. Gapped BLAST and PSI-BLAST: a new generation of protein database search programs. Nucleic Acids Res. 25, 3389–3402.

Andersen, C.L., Jensen, J.L., Orntoft, T.F., 2004. Normalization of real-time quantitative reverse transcription-PCR data: a model-based variance estimation approach to identify genes suited for normalization, applied to bladder and colon cancer data sets. Cancer Res. 64, 5245–5250.

Artigaud, S., Richard, J., Thorne, M.A., Lavaud, R., Flye-Sainte-Marie, J., Jean, F., Peck, L.S., Clark, M.S., Pichereau, V., 2015. Deciphering the molecular adaptation of the king scallop (Pecten maximus) to heat stress using transcriptomics and proteomics. BMC Genomics 16, 988. https://doi.org/10.1186/s12864-015-2132-x.

Bates, S.S., Bird, C.J., de Freitas, A.S.W., Foxall, R., Gilgan, M., Hanic, L.A., Johnson, G.R., McCulloch, A.W., Odense, P., Pocklington, R., Quilliam, M.A., Sim, P.G., Smith, J.C., Subba Rao, D.V., Todd, E.C.D., Walter, J.A., Wright, J.L.C., 1989. Pennate diatom *Nitzschia pungens* as the primary source of domoic acid, a toxin in shellfish from eastern Prince Edward Island, Canada. Can. J. Fish. Aquat. Sci. 46, 1203–1215.

Bates, S.S., Garrison, D.L., Horner, R.A., 1998. Bloom dynamics and physiology of domoic-acid-producing *Pseudo-nitzschia* species. In: Anderson, D.M., Hallegraeff, G.M., Cembella, A.D. (Eds.), The Physiological Ecology of Harmful Algal Blooms-NATO Advanced Study Institute Series. Springer-Verlag, Heidelberg, Germany, pp. 267–292.

Benjamini, Y., Hochberg, Y., 1995. Controlling the false discovery rate: a practical and powerful approach to multiple testing. J. R. Stat. Soc. B 57, 289–300. https://doi.org/10.2307/2346101.

Blanco, J., Acosta, C.P., Bermúdez De La Puente, M., Salgado, C., 2002a. Depuration and anatomical distribution of the amnesic shellfish poisoning (ASP) toxin domoic acid in the king scallop *Pecten maximus*. Aquat. Toxicol. 60, 111–121.

Blanco, J., de la Puente, M.B., Arévalo, F., Salgado, C., Moroño, Á., 2002b. Depuration of mussels (*Mytilus galloprovincialis*) contaminated with domoic acid. Aquat. Living Resour. 15, 53–60.

Boissonneault, K.R., Henningsen, B.M., Bates, S.S., Robertson, D.L., Milton, S., Pelletier, J., Hogan, D.A., Housman, D.E., 2013. Gene expression studies for the analysis of domoic acid production in the marine diatom *Pseudo-nitzschia multiseries*. BMC Mol. Biol. 14, 25. https://doi.org/10.1186/1471-2199-14-25.

Bustin, S.A., Benes, V., Garson, J.A., Hellemans, J., Huggett, J., Kubista, M., Mueller, R., Nolan, T., Pfaffl, M.W., Shipley, G.L., Vandesompele, J., Wittwer, C., 2009. The MIQE guidelines - minimum information for publication of quantitative real-time PCR experiments. Clin. Chem. 55, 611–622.

Conesa, A., Götz, S., Garcia-Gomez, J.M., Tero, J.l, Talon, M., Robles, M., 2005. Blast2GO: a universal tool for annotation, visualization and analysis in functional genomics research. Bioinformatics 21, 3674–3676.

Craft, J.A., Gilbert, J.A., Temperton, B., Dempsey, K.E., Ashelford, K., Tiwari, B., Hutchinson, T.H., Chipman, J.K., 2010. Pyrosequencing of *Mytilus galloprovincialis* cDNAs: tissue-specific expression patterns. PLoS ONE 5, e8875. https://doi.org/10.1371/journal.pone.0008875.

Cubero-Leon, E., Ciocan, C.M., Minier, C., Rotchell, J.M., 2012. Reference gene selection for qPCR in mussel, *Mytilus edulis*, during gametogenesis and exogenous estrogen exposure. Environ. Sci. Pollut. Res. 19, 2728–2733.

Dean, M., Rzhetsky, A., Allikmets, R., 2001. The human ATP-binding cassette (ABC) transporter superfamily. Genome Res. 11, 1156–1166. https://doi.org/10.1101/gr.GR-1649R.

Deng, X., Pan, L., Miao, J., Cai, Y., Hu, F., 2014. Digital gene expression analysis of reproductive toxicity of benzo[a]pyrene in male scallop *Chlamys farreri*. Ecotox. Environ. Saf. 110, 190–196. https://doi.org/10.1016/j.ecoenv.2014.09.002.

Dheilly, N.M., Lelong, C., Huvet, A., Favrel, P., 2011. Development of a Pacific Oyster (Crassostrea gigas) 31,918-feature microarray: identification of reference genes and tissue-enriched expression patterns. BMC Genomics 12, 468. https://doi.org/10.1186/1471-2164-12-468.

Di Dato, V., Musacchia, F., Petrosino, G., Patil, S., Montresor, M., Sanges, R., Ferrante, M.I., 2015. Transcriptome sequencing of three *Pseudo-nitzschia* species reveals comparable gene sets and the presence of Nitric Oxide Synthase genes in diatoms. Sci. Rep. 5, 12329. https://doi.org/10.1038/srep12329.

Dizer, H., Fischer, B., Harabawy, A.S.A., Hennion, M.-C., Hansen, P.-D., 2001. Toxicity of domoic acid in the marine mussel *Mytilus edulis*. Aquat. Toxicol. 55, 149–156. https://doi.org/10.1016/S0166-445X(01)00178-3.

Drum, A.S., Siebens, T.L., Crecelius, E.A., Elston, R.A., 1993. Domoic acid in the Pacific razor clam Siliqua patula (Dixon, 1789). J. Shellfish Res. 12, 443–450.

Finn, R.D., Coggill, P., Eberhardt, R.Y., Eddy, S.R., Mistry, J., Mitchell, A.L., Potter, S.C., Punta, M., Qureshi, M., Sangrador-Vegas, A., Salazar, G.A., Tate, J., Bateman, A., 2016. The Pfam protein families database: towards a more sustainable future. Nucleic Acids Res. 44 (D1), D279–D285. https://doi.org/10.1093/nar/gkv1344.

Franceschini, A., Szklarczyk, D., Frankild, S., Kuhn, M., Simonovic, M., Roth, A., Lin, J., Minguez, P., Bork, P., von Mering, C., Jensen, L.J., 2013. STRING v9.1: protein-protein interaction networks, with increased coverage and integration. Nucleic Acids Res. 41 (Database issue), D808–D815. https://doi.org/10.1093/nar/gks1094.

Geisler, F., Strazzabosco, M., 2015. Emerging roles of Notch signaling in liver disease. Hepatology 61, 382–392. https://doi.org/10.1002/hep.27268.

Gerdol, M., Manfrin, C., De Moro, G., Figueras, A., Novoa, B., Venier, P., Pallavicini, A., 2011. The C1q domain containing proteins of the Mediterranean mussel *Mytilus galloprovincialis*: a widespread and diverse family of immune-related molecules. Dev. Comp. Immunol. 35, 635–643. https://doi.org/10.1016/j.dci.2011.01.018.

Gerdol, M., Moro, G.D., Manfrin, C., Milandri, A., Riccardi, E., Beran, A., Venier, P., Pallavicini, A., 2014. RNA sequencing and de novo assembly of the digestive gland transcriptome in *Mytilus galloprovincialis* fed with toxinogenic and non-toxic strains of Alexandrium minutum. BMC Res. Notes 7, 722. https://doi.org/10.1186/1756-0500-7-722.

Gerdol, M., Venier, P., Pallavicini, A., 2015. The genome of the Pacific oyster Crassostrea gigas brings new insights on the massive expansion of the C1q gene family in Bivalvia. Dev. Comp. Immunol. 49 (1), 59–71. https://doi.org/10.1016/j.dci.2014.11.007.

Giordano, G., White, C.C., McConnachie, L.A., Fernandez, C., Kavanagh, T.J., Costa, L.G., 2006. Neurotoxicity of domoic acid in cerebellar granule neurons in a genetic model of glutathione deficiency. Mol. Pharmacol. 70, 2116–2126. https://doi.org/10.1124/mol.106.027748.

Giordano, G., White, C.C., Mohar, I., Kavanagh, T.J., Costa, L.G., 2007. Glutathione levels modulate domoic acid–induced apoptosis in mouse cerebellar granule cells. Toxicol. Sci. 100, 433–444. https://doi.org/10.1093/toxsci/kfm236.

González, P.M., Puntarulo, S., 2016. Seasonality and toxins effects on oxidative/nitrosative metabolism in digestive glands of the bivalve Mytilus edulis platensis. Comp. Biochem. Physiol. A 200, 79–86. https://doi.org/10.1016/j.cbpa.2016.04.011.

Götz, S., García-Gómez, J.M., Terol, J., Williams, T.D., Nagaraj, S.H., Nueda, M.J., Robles, M., Talón, M., Dopazo, J., Conesa, A., 2008. High-throughput functional annotation and data mining with the Blast2GO suite. Nucleic Acids Res. 36, 3420–3435. https://doi.org/10.1093/nar/gkn176.

Grabherr, M.G., Haas, B.J., Yassour, M., Levin, J.Z., Thompson, D.A., Amit, I., Adiconis, X., Fan, L., Raychowdhury, R., Zeng, Q., Chen, Z., Mauceli, E., Hacohen, N., Gnirke, A., Rhind, N., di Palma, F., Birren, B.W., Nusbaum, C., Lindblad-Toh, K., Friedman, N., Regev, A., 2011. Full-length transcriptome assembly from RNA-Seq data without a reference genome. Nat. Biotechnol. 29, 644–652. https://doi.org/10.1038/nbt.1883.

Halestrap, A.P., 2013. The SLC16 gene family - structure, role and regulation in health and disease. Mol. Asp. Med. 34, 337–349. https://doi.org/10.1016/j.mam.2012.05.003.

Hediger, M.A., Clémençon, B., Burrier, R.E., Bruford, E.A., 2013. The ABCs of membrane transporters in health and disease (SLC series): introduction. Mol. Asp. Med. 34, 95–107. https://doi.org/10.1016/j.mam.2012.12.009.

Hégaret, H., Silva, P.M., Wikfors, G.H., Haberkorn, H., Shumway, S.E., Soudant, P., 2011. In vitro interactions between several species of harmful algae and haemocytes of bivalve molluscs. Cell Biol. Toxicol. 27, 249–266. https://doi.org/10.1007/s10565-011-9186-6.

Hiolski, E.M., Kendrick, P.S., Frame, E.R., Myers, M.S., Bammler, T.K., Beyer, R.P., Farin, F.M., Wilkerson, H., Smith, D.R., Marcinek, D.J., Lefebvre, K.A., 2014. Chronic low-level domoic acid exposure alters gene transcription and impairs

mitochondrial function in the CNS. Aquat. Toxicol. 155, 151–159. https://doi.org/10.1016/j.aquatox.2014.06.006.
Höglund, P.J., Nordström, K.J., Schiöth, H.B., Fredriksson, R., 2011. The solute carrier families have a remarkably long evolutionary history with the majority of the human families present before divergence of Bilaterian species. Mol. Biol. Evol. 28, 1531–1541. https://doi.org/10.1093/molbev/msq350.
Huang, L., Wang, J., Chen, W.-C., Li, H.-Y., Liu, J.-S., Jiang, T., Yang, W.-D., 2014. P-glycoprotein expression in *Perna viridis* after exposure to *Prorocentrum lima*, a dinoflagellate producing DSP toxins. Fish Shellfish Immunol. 39, 254–262. https://doi.org/10.1016/j.fsi.2014.04.020.
Ishikawa, H., 1977. Evolution of ribosomal RNA. Comp. Biochem. Physiol. B 58, 1–7.
Jansen, R.S., Mahakena, S., Haas, M. de, Borst, P., Wetering, K. van de, 2015. ATP-binding cassette subfamily C member 5 (ABCC5) functions as an efflux transporter of glutamate conjugates and analogs. J. Biol. Chem. 290, 30429–30440. https://doi.org/10.1074/jbc.M115.692103.
Johnson, N.L., Kotz, S., Kemp, A.W., 1992. Univariate Discrete Distributions, second ed. Wiley, New York.
Jones, T.O., Whyte, J.N.C., Townsend, L.D., Ginther, N.G., Iwama, G.K., 1995. Effects of domoic acid on haemolymph pH, PCO2 and PO2 in the Pacific oyster, *Crassostrea gigas* and the California mussel, *Mytilus californianus*. Aquat. Toxicol. 31, 43–55. https://doi.org/10.1016/0166-445X(94)00057-W.
Kimura, O., Kotaki, Y., Hamaue, N., Haraguchi, K., Endo, T., 2011. Transcellular transport of domoic acid across intestinal Caco-2 cell monolayers. Food Chem. Toxicol. 49, 2167–2171. https://doi.org/10.1016/j.fct.2011.06.001.
Kopan, R., Ilagan, M.X., 2009. The canonical Notch signaling pathway: unfolding the activation mechanism. Cell 137, 216–233. https://doi.org/10.1016/j.cell.2009.03.045.
Langmead, B., Salzberg, S.L., 2012. Fast gapped-read alignment with Bowtie 2. Nat. Methods 9, 357–359. https://doi.org/10.1038/nmeth.1923.
Lefebvre, K.A., Robertson, A., 2010. Domoic acid and human exposure risks: a review. Toxicon 56, 218–230. https://doi.org/10.1016/j.toxicon.2009.05.034.
Lefebvre, K.A., Tilton, S.C., Bammler, T.K., Beyer, R.P., Srinouanprachan, S., Stapleton, P.L., Farin, F.M., Gallagher, E.P., 2009. Gene expression profiles in zebrafish brain after acute exposure to domoic acid at symptomatic and asymptomatic doses. Toxicol. Sci. 107, 65–77. https://doi.org/10.1093/toxsci/kfn207.
Livingstone, D.R., 1998. The fate of organic xenobiotics in aquatic ecosystems: quantitative and qualitative differences in biotransformation by invertebrates and fish. Comp. Biochem. Physiol. 120A, 43–49.
Livingstone, D.R., Farrar, S.V., 1984. Tissue and subcellular distribution of enzyme activities of mixed function oxygenase and benzo *a* pyrene metabolism in the common mussel *Mytilus edulis*. L. Sci. Total Environ. 39, 209–235.
Lozano, V., Martínez-Escauriaza, R., Pérez-Parallé, M.L., Pazos, A.J., Sánchez, J.L., 2015. Two novel multidrug resistance associated protein (MRP/ABCC) from the Mediterranean mussel (*Mytilus galloprovincialis*): characterization and expression patterns in detoxifying tissues. Can. J. Zool. 93, 567–578. https://doi.org/10.1139/cjz-2015-0011.
Lüchmann, K.H., Clark, M.S., Bainy, A.C.D., Gilbert, J.A., Craft, J.A., Chipman, J.K., Thorne, M.A.S., Mattos, J.J., Siebert, M.N., Schroeder, D.C., 2015. Key metabolic pathways involved in xenobiotic biotransformation and stress responses revealed by transcriptomics of the mangrove oyster *Crassostrea brasiliana*. Aquat. Toxicol. 166, 10–20. https://doi.org/10.1016/j.aquatox.2015.06.012.
Madhyastha, M.S., Novaczek, I., Ablett, R.F., Johnson, G., Nijjar, M.S., Sims, D.E., 1991. In vitro study of domoic acid uptake by digestive gland tissue of blue mussel (Mytilus edulis L.). Aquat. Toxicol. 20, 73–82.
Mafra Jr., L.L., Bricelj, V.M., Fennel, K., 2010. Domoic acid uptake and elimination kinetics in oysters and mussels in relation to body size and anatomical distribution of toxin. Aquat. Toxicol. 100, 17–29. https://doi.org/10.1016/j.aquatox.2010.07.002.
Malanga, G., González, P.M., Ostera, J.M., Puntarulo, S., 2016. Oxidative stress in the hydrophilic medium of algae and invertebrates. Biocell 40, 35–38.
Mauriz, A., Blanco, J., 2010. Distribution and linkage of domoic acid (amnesic shellfish poisoning toxins) in subcellular fractions of the digestive gland of the scallop *Pecten maximus*. Toxicon 55, 606–611. https://doi.org/10.1016/j.toxicon.2009.10.017.
Mauriz, O., Maneiro, V., Pérez-Parallé, M.L., Sánchez, J.L., Pazos, A.J., 2012. Selection of reference genes for quantitative RT-PCR studies on the gonad of the bivalve mollusc *Pecten maximus* L. Aquaculture 370–371, 158–165.
Meng, X., Liu, M., Jiang, K., Wang, B., Tian, X., Sun, S., Luo, Z., Qiu, C., Wang, L., 2013. De novo characterization of Japanese scallop mizuhopecten yessoensis transcriptome and analysis of its gene expression following cadmium exposure. PLoS ONE 8, e64485. https://doi.org/10.1371/journal.pone.0064485.
Miyaji, T., Echigo, N., Hiasa, M., Senoh, S., Omote, H., Moriyama, Y., 2008. Identification of a vesicular aspartate transporter. Proc. Natl. Acad. Sci. U. S. A. 105, 11720–117244. https://doi.org/10.1073/pnas.0804015105.
Miyaji, T., Omote, H., Moriyama, Y., 2011. Functional characterization of vesicular excitatory amino acid transport by human sialin. J. Neurochem. 119, 1–5. https://doi.org/10.1111/j.1471-4159.2011.07388.x.
Moreira, R., Pereiro, P., Canchaya, C., Posada, D., Figueras, A., Novoa, B., 2015. RNA-Seq in *Mytilus galloprovincialis*: comparative transcriptomics and expression profiles among different tissues. BMC Genomics 16, 728. https://doi.org/10.1186/s12864-015-1817-5.
Moriya, Y., Itoh, M., Okuda, S., Yoshizawa, A., Kanehisa, M., 2007. KAAS: an automatic genome annotation and pathway reconstruction server. Nucleic Acids Res. 35, W182–W185.
Murgarella, M., Puiu, D., Novoa, B., Figueras, A., Posada, D., Canchaya, C., 2016. A first insight into the genome of the filter-feeder mussel *Mytilus galloprovincialis*. PLOS ONE 11, e0151561. https://doi.org/10.1371/journal.pone.0151561.
Novaczek, I., Madhyastha, M.S., Ablett, R.F., Johnson, G., Nijjar, M.S., Sims, D.E., 1991. Uptake, disposition and depuration of domoic acid by blue mussels (*Mytilus edulis*). Aquat. Toxicol. 21, 103–118.
Novaczek, I., Madhyastha, M.S., Ablett, R.F., Donald, A., Johnson, G., Nijjar, M.S., Sims, D.E., 1992. Depuration of domoic acid from live blue mussels (*Mytilus edulis*). Can. J. Fish. Aquat. Sci. 49, 312–318.
Peña-Llopis, S., Serrano, R., Pitarch, E., Beltrán, E., Ibáñez, M., Hernández, F., Peña, J.B., 2014. N-Acetylcysteine boosts xenobiotic detoxification in shellfish. Aquat. Toxicol. 154, 131–140. https://doi.org/10.1016/j.aquatox.2014.05.006.
Pfaffl, M.W., Tichopad, A., Prgomet, C., Neuvians, T.P., 2004. Determination of stable housekeeping genes, differentially regulated target genes and sample integrity: BestKeeper–Excel-based tool using pair-wise correlations. Biotechnol. Lett. 26, 509–515.
Philipp, E.E.R., Kraemer, L., Melzner, F., Poustka, A.J., Thieme, S., Findeisen, U., Schreiber, S., Rosenstiel, P.I., 2012. Massively parallel RNA sequencing identifies a complex immune gene repertoire in the lophotrochozoan *Mytilus edulis*. PLoS ONE 7, e33091. https://doi.org/10.1371/journal.pone.0033091.
Rajkumar, A.P., Qvist, P., Lazarus, R., Lescai, F., Ju, J., Nyegaard, M., Mors, O., Børglum, A.D., Li, Q., Christensen, J.H., 2015. Experimental validation of methods for differential gene expression analysis and sample pooling in RNA-seq. BMC Genomics 16, 548. https://doi.org/10.1186/s12864-015-1767-y.
Reimer, R.J., 2013. SLC17: a functionally diverse family of organic anion transporters. Mol. Asp. Med. 34 (2–3), 350–359. https://doi.org/10.1016/j.mam.2012.05.004.
Renault, T., 2015. Immunotoxicological effects of environmental contaminants on marine bivalves. Fish Shellfish Immunol. 46, 88–93. https://doi.org/10.1016/j.fsi.2015.04.011.
Rondon, R., Akcha, F., Alonso, P., Menard, D., Rouxel, J., Montagnani, C., Mitta, G., Cosseau, C., Grunau, C., 2016. Transcriptional changes in Crassostrea gigas oyster spat following a parental exposure to the herbicide diuron. Aquat. Toxicol. 175, 47–55. https://doi.org/10.1016/j.aquatox.2016.03.007.
Rosani, U., Varotto, L., Rossi, A., Roch, P., Novoa, B., Figueras, A., Pallavicini, A., Venier, P., 2011. Massively parallel amplicon sequencing reveals isotype-specific variability of antimicrobial peptide transcripts in *Mytilus galloprovincialis*. PLoS One 6, e26680. https://doi.org/10.1371/journal.pone.0026680.
Ryan, J.C., Morey, J.S., Ramsdell, J.S., Van Dolah, F.M., 2005. Acute phase gene expression in mice exposed to the marine neurotoxin domoic acid. Neuroscience 136, 1121–1132.
Sander, G.R., Powell, B.C., 2004. Expression of notch receptors and ligands in the adult gut. J. Histochem. Cytochem. 52, 509–516. https://doi.org/10.1177/002215540405200409.
Schwanbeck, R., Martini, S., Bernoth, K., Just, U., 2011. The Notch signaling pathway: molecular basis of cell context dependency. Eur. J. Cell Biol. 90, 572–581. https://doi.org/10.1016/j.ejcb.2010.10.004.
Schultz, I.R., Skillman, A., Sloan-Evans, S., Woodruff, D., 2013. Domoic acid toxicokinetics in Dungeness crabs: new insights into mechanisms that regulate bioaccumulation. Aquat. Toxicol. 140–141, 77–88. https://doi.org/10.1016/j.aquatox.2013.04.011.
Schulz, M.H., Zerbino, D.R., Vingron, M., Birney, E., 2012. Oases: robust de novo RNA-seq assembly across the dynamic range of expression levels. Bioinformatics 28, 1086–1092. https://doi.org/10.1093/bioinformatics/bts094.
Suárez-Ulloa, V., Fernández-Tajes, J., Aguiar-Pulido, V., Rivera-Casas, C., González-Romero, R., Ausio, J., Méndez, J., Dorado, J., Eirín-López, J.M., 2013. The CHROMEVALOA database: a resource for the evaluation of okadaic acid contamination in the marine environment based on the chromatin-associated transcriptome of the mussel *Mytilus galloprovincialis*. Mar. Drugs 11, 830–841. https://doi.org/10.3390/md11030830.
Szklarczyk, D., Franceschini, A., Wyder, S., Forslund, K., Heller, D., Huerta-Cepas, J., Simonovic, M., Roth, A., Santos, A., Tsafou, K.P., Kuhn, M., Bork, P., Jensen, L.J., von Mering, C., 2015. STRING v10: protein-protein interaction networks, integrated over the tree of life. Nucleic Acids Res. 43 (Database issue), D447–D452. https://doi.org/10.1093/nar/gku1003.
Takeuchi, T., Kawashima, T., Koyanagi, R., Gyoja, F., Tanaka, M., Ikuta, T., et al., 2012. Draft genome of the pearl oyster *Pinctada fucata*: a platform for understanding bivalve biology. DNA Res. 19, 117–130.
Trainer, V.L., Bill, B.D., 2004. Characterization of a domoic acid binding site from Pacific razor clam. Aquat. Toxicol. 69, 125–132.
Vandesompele, J., De Preter, K., Pattyn, F., Poppe, B., Van Roy, N., De Paepe, A., Speleman, F., 2002. Accurate normalization of real-time quantitative RT-PCR data by geometric averaging of multiple internal control genes. Genome Biol. 3. RESEARCH0034.
Venier, P., Varotto, L., Rosani, U., Millino, C., Celegato, B., Bernante, F., Lanfranchi, G., Novoa, B., Roch, P., Figueras, A., Pallavicini, A., 2011. Insights into the innate immunity of the Mediterranean mussel *Mytilus galloprovincialis*. BMC Genomics 12, 69. https://doi.org/10.1186/1471-2164-12-69.
Wright, J.L.C., Boyd, R.K., de Freitas, A.S.W., Falk, M., Foxall, R.A., Jamieson, W.D., Laycock, M.V., McCulloch, A.W., McInnes, A.G., 1989. Identification of domoic acid, a neuroexcitatory amino acid, in toxic mussels from eastern Prince Edward Island. Can. J. Chem. 67, 481–490.
Xu, Y.-Y., Liang, J.-J., Yang, W.-D., Wang, J., Li, H.-Y., Liu, J.-S., 2014. Cloning and expression analysis of P-glycoprotein gene in *Crassostrea ariakensis*. Aquaculture 418–419, 39–47. https://doi.org/10.1016/j.aquaculture.2013.10.004.
Zhang, G., Fang, X., Guo, X., Li, L., Luo, R., Xu, F., et al., 2012. The oyster genome

reveals stress adaptation and complexity of shell formation. Nature 490, 49–54. https://doi.org/10.1038/nature11413.
Zhang, L., Li, L., Zhu, Y., Zhang, G., Guo, X., 2014. Transcriptome analysis reveals a rich gene set related to innate immunity in the Eastern oyster (*Crassostrea virginica*). Mar. Biotechnol. (NY) 16, 17–33. https://doi.org/10.1007/s10126-013-9526-z.
Zhao, S., Fernald, R.D., 2005. Comprehensive algorithm for quantitative real-time polymerase chain reaction. J. Comput. Biol. 12, 1047–1064.

A1.2 RNA-Seq Transcriptome Profiling of the Queen Scallop (*Aequipecten opercularis*) Digestive Gland after Exposure to Domoic Acid-Producing *Pseudo-nitzschia*

A1.2.1 Características de la publicación

Estado: Publicado
Título: RNA-Seq Transcriptome Profiling of the Queen Scallop (*Aequipecten opercularis*) Digestive Gland after Exposure to Domoic Acid-Producing *Pseudo-nitzschia*
Nombre de la revista: Toxins
Editorial: MDPI
Autores: Ventoso Pablo, Antonio J. Pazos, M. Luz Pérez-Parallé, Juan Blanco, Juan C. Triviño, y José L. Sánchez
Contribución específica del doctorado: Realización de la extracción del RNA, experimentos RT-qPCR y varios análisis bioinformáticos. Redacción del manuscrito
Año publicación: 2019
Volumen: 11 (97)
DOI: https://doi.org/10.3390/toxins11020097
Autorización de la revista: No es necesaria autorización de la editorial y/o revista. Al tratarse de una revista de acceso abierto se permite su uso para la elaboración de tesis doctorales. (https://www.mdpi.com/openaccess)

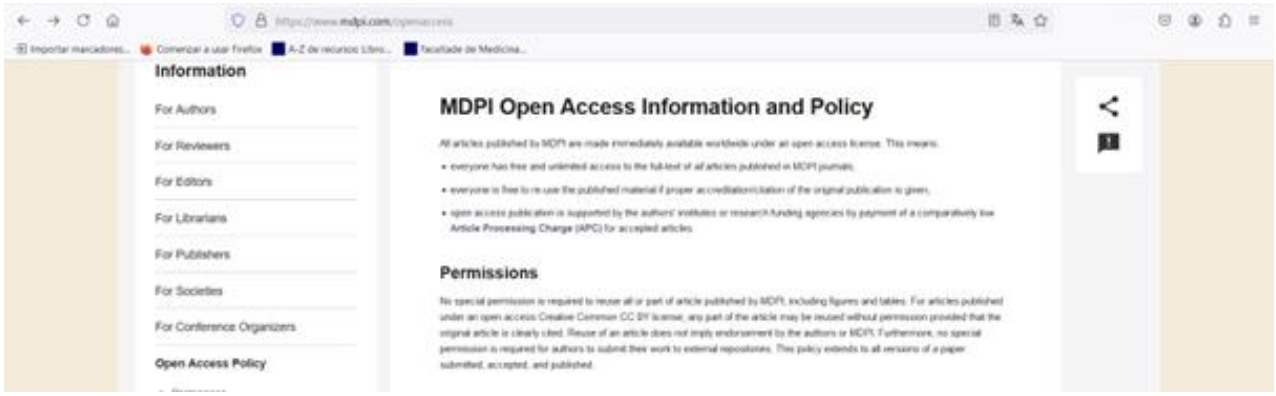

A1.2.2 Indicios de calidad de la revista

Scientific Journal Rankings (SJR): 1,034
Cuartil (2019): 1- Área: Health, Toxicology and Mutagenesis; Toxicology
Journal Impact Factor (JIF): 3,531
Cuartil (2019): 1 - Área: Food Science & Technology; Toxicology
Journal Citation Indicator (JCI): 0,98
Cuartil (2019): 1 - Área: Food Science & Technology; Toxicology

A1.2.3 Impacto de la publicación

Citas: 17 (Scopus), 22 (Google Scholar), 17 (Web of Science)

toxins

MDPI

Article

RNA-Seq Transcriptome Profiling of the Queen Scallop (*Aequipecten opercularis*) Digestive Gland after Exposure to Domoic Acid-Producing *Pseudo-nitzschia*

Pablo Ventoso [1], Antonio J. Pazos [1,*], M. Luz Pérez-Parallé [1], Juan Blanco [2], Juan C. Triviño [3] and José L. Sánchez [1]

1 Departamento de Bioquímica y Biología Molecular, Instituto de Acuicultura, Universidade de Santiago de Compostela, 15782 Santiago de Compostela, Spain; pabloventoso24@hotmail.com (P.V.); luz.perez-paralle@usc.es (M.L.P.-P.); joseluis.sanchez@usc.es (J.L.S.)

2 Centro de Investigacións Mariñas, Xunta de Galicia, Pedras de Corón s/n Apdo 13, 36620 Vilanova de Arousa, Spain; juan.carlos.blanco.perez@xunta.gal

3 Sistemas Genómicos, Ronda G. Marconi 6, Paterna, 46980 Valencia, Spain; jc.trivino@sistemasgenomicos.com

* Correspondence: antonioj.pazos@usc.es; Tel.: +34-881-816-056

Received: 28 December 2018; Accepted: 3 February 2019; Published: 6 February 2019

Abstract: Some species of the genus *Pseudo-nitzschia* produce the toxin domoic acid, which causes amnesic shellfish poisoning (ASP). Given that bivalve mollusks are filter feeders, they can accumulate these toxins in their tissues. To elucidate the transcriptional response of the queen scallop *Aequipecten opercularis* after exposure to domoic acid-producing *Pseudo-nitzschia*, the digestive gland transcriptome was de novo assembled using an Illumina HiSeq 2000 platform. Then, a differential gene expression analysis was performed. After the assembly, 142,137 unigenes were obtained, and a total of 10,144 genes were differentially expressed in the groups exposed to the toxin. Functional enrichment analysis found that 374 Pfam (protein families database) domains were significantly enriched. The C1q domain, the C-type lectin, the major facilitator superfamily, the immunoglobulin domain, and the cytochrome P450 were among the most enriched Pfam domains. Protein network analysis showed a small number of highly connected nodes involved in specific functions: proteasome components, mitochondrial ribosomal proteins, protein translocases of mitochondrial membranes, cytochromes P450, and glutathione S-transferases. The results suggest that exposure to domoic acid-producing organisms causes oxidative stress and mitochondrial dysfunction. The transcriptional response counteracts these effects with the up-regulation of genes coding for some mitochondrial proteins, proteasome components, and antioxidant enzymes (glutathione S-transferases, thioredoxins, glutaredoxins, and copper/zinc superoxide dismutases).

Keywords: amnesic shellfish poisoning (ASP); domoic acid; bivalves; *Aequipecten opercularis*; scallop; RNA-seq; transcriptome; differential expression; qPCR; oxidative stress

Key Contribution: To our knowledge, this is the first report on de novo transcriptome assembly and differential gene expression in a scallop under domoic acid exposure. The results reveal the transcriptional response of the queen scallop after exposure to domoic acid-producing *Pseudo-nitzschia* and suggest that some of the up-regulated genes code for proteins involved in protection against oxidative stress and mitochondrial impairment: proteasome components, mitochondrial ribosomal proteins, protein translocases of mitochondrial membranes, and antioxidant enzymes (glutathione S-transferases, thioredoxins, glutaredoxins, and copper/zinc superoxide dismutases).

1. Introduction

The amnesic shellfish poisoning (ASP) toxin, domoic acid, is produced by some species of the genera *Pseudo-nitzschia* and *Nitzschia* [1,2]. The prevalence of domoic acid and toxic diatoms seems to have increased worldwide [1]. Domoic acid is a tricarboxylic amino acid that resembles glutamic acid and is a potent glutamate receptor agonist [3,4]. Bivalve mollusks are filter feeders, and during harmful algal blooms, they can accumulate toxins in their tissues. This is why they are the primary vectors for causing ASP in humans [1,5,6].

Domoic acid depuration time in bivalves is species-specific and can differ largely from one species to another [7]. Mussels of the genus *Mytilus* [8–11] and the oyster *Crassostrea gigas* [9] rapidly eliminate domoic acid, while the king scallop *Pecten maximus* [7] and the razor clam *Siliqua patula* [12] are very slow domoic acid depurators. In mussels and scallops, the digestive gland is the tissue with the highest domoic acid concentration [7,10,13,14]. Mauriz and Blanco [15] suggested that the very low depuration rate of *P. maximus* could be due to the lack of an efficient transmembrane transporter. Unlike the king scallop, in the queen scallop (*Aequipecten opercularis*) the depuration rate is fast [15].

Domoic acid is excitotoxic in the central nervous system of mammals and other vertebrates [3,4], but its putative effects on invertebrates have been less studied. Although it seems that domoic acid-producing organisms are not toxic to shellfish (or at least not highly toxic), they can exert several physiological and sublethal effects on marine bivalves [16–20]. Some of these effects include DNA damage in mussels [16], stress response characterized by shell closure, hemolymph acidosis, hypoxia, an increase in the number and activity of hemocytes in the oyster *C. gigas* [17,18], reduced larval growth in *P. maximus* [19], and negative impacts on growth rate and survival in juvenile king scallops [20]. Some authors have suggested that although several harmful algae toxins do not affect the survival of bivalve mollusks, they provoke oxidative stress [21–23]. However, the molecular mechanisms that cause oxidative stress are poorly understood, and furthermore, domoic acid causes oxidative stress in the vertebrate central nervous system [24–27]. The works cited above [16–21] analyzed several physiological and biochemical parameters after exposure to domoic acid but did not study the gene expression patterns in both exposed and non-exposed bivalves.

There are some publications regarding the gene expression changes associated with exposure to domoic acid in vertebrates [24,28–30]. The transcriptome response was dependent on the dose and the exposure duration; among the differentially expressed genes were those involved in transcription (transcription factors), signal transduction, ion transport, generalized stress response, mitochondrial function, inflammatory response, DNA damage, apoptosis, neurological function, and neuroprotection [24,28–30]. In a previous work, we studied (by RNA-seq) the effects of domoic acid-containing *Pseudo-nitzschia* on gene expression in the mussel *Mytilus galloprovincialis* [31], and to our knowledge, this is the only published work about the transcriptional effects of domoic acid exposure on mollusks. As stated before, among the bivalves there are large interspecific differences in the domoic acid depuration rate [7–12]. It is therefore necessary to carry out gene expression studies on different species.

Understanding the molecular mechanisms of domoic acid uptake and elimination in bivalves and how the toxin (and the toxin-producing species) affects gene expression are two knowledge gaps in this field. The aim of the present work is to contribute to filling these gaps by means of a transcriptomic approach. First, the whole transcriptome of the *A. opercularis* digestive gland was de novo assembled, and then, we analyzed by RNA-seq the transcriptional changes after exposure to domoic acid-producing *Pseudo-nitzschia*. This approach can provide some clues regarding the biological and molecular processes altered by domoic acid. The transcriptomic approach has been successfully employed to uncover the genetic response of bivalves to diarrhetic shellfish poisoning (DSP) and paralytic shellfish poisoning (PSP) toxins and also to identify the genes putatively involved in detoxification processes [32–36].

2. Results

2.1. Domoic Acid Content in the Digestive Gland of A. opercularis

A group of six scallops sampled on April 9 from the tank (group DB) had an average domoic acid content of 1361 ± 804 ng/g digestive gland wet weight, while a group of six scallops sampled on April 17 from the raft (group DA) had an average domoic acid content of 6680 ± 1661 ng/g digestive gland wet weight (Table 1). In the six control scallops sampled on May 12 from the tank (group C), the domoic acid levels were below the limit of quantification (BLOQ, Table 1). The total scallop wet weights and digestive gland (DG) wet weights are shown in Table 1 and Table S1.

Table 1. Domoic acid concentration (ng/g digestive gland wet weight), wet weight (g) of the soft tissues (Total weight), and wet weight (g) of the digestive gland (DG weight) in sampled scallops (*Aequipecten opercularis*).

Group	Sampling Date	Domoic Acid (ng/g)		Total Weight (g)		DG Weight (g)	
		Mean	SD	Mean	SD	Mean	SD
DB	09/04/2015	1361	803.8	3.663	0.739	0.218	0.053
DA	17/04/2015	6680	1611.4	5.102	0.328	0.509	0.076
Control (C)	12/05/2015	BLOQ [1]	BLOQ [1]	2.314	0.489	0.156	0.149

[1] BLOQ: below the limit of quantification; SD: standard deviation.

2.2. Sequencing and de novo Assembly

After the de novo assembly, the transcripts were clustered (homology >90%) to reduce redundancy. Thus, 142,137 unigenes were obtained (Table 2). The minimum, maximum, and mean contig lengths were 200, 17,867, and 1343.9 bp, while the N50 contig length was 1845 bp (Table 2). The raw data are accessible from the NCBI Sequence Read Archive (Project PRJNA508885, sample accession numbers from SAMN10537388 to SAMN10537405).

Table 2. Summary of Illumina transcriptome sequencing and assembly for *A. opercularis* digestive glands.

Summary of Raw Reads Data:	
Total number of filtered reads	968,035,762
Average read length alter filtering (bp)	100
Sequence quality ≥ Q30 (%)	95
Mean quality score	38
GC%	39
Summary of the Assembled Transcriptome	
Number of assembled unigenes	142,137
Contig N50 Length (bp)	1845
Minimum contig length (bp)	200
Maximum contig length (bp)	17,867
Average contig length (bp)	1343.9
Total length in contigs (bp)	191,023,300

2.3. Differential Expression, Functional Annotation, and Functional Enrichment Analysis

A total of 26,932 and 20,608 differentially expressed genes (DEGs) were detected in group DA and in group DB, respectively, when compared to the control (C) group (Figure 1). Genes that were differentially expressed in both groups (the groups that had accumulated domoic acid) and in the same direction (either down- or up-regulation) were selected for further study: 10,144 genes, including 4913 up-regulated and 5231 down-regulated (Figure 1; Tables 3 and 4; Files S1 and S2). The top 25

significantly up-regulated genes are listed in Table 3. Genes coding for fatty acid-binding proteins and cytosolic sulfotransferases were among the top up-regulated genes (Table 3). Most of the top 25 down-regulated genes do not have a Blastx hit (Table 4; File S2).

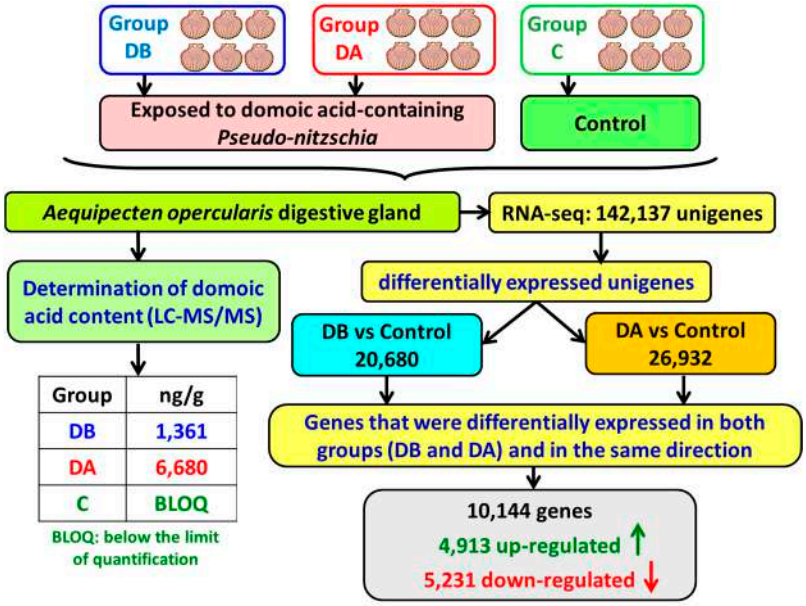

Figure 1. Scheme of the differential expression results obtained in *A. opercularis* digestive glands after exposure to domoic acid-producing *Pseudo-nitzschia*.

A summary of the functional annotation results is shown in Table 5. After functional enrichment performed using the Pfam annotations, 374 domains were found to be significantly (false discovery rate (FDR)-adjusted *p*-value <0.05) enriched in the DEGs (Table 6; File S3). The C-type lectin, the RNA recognition motifs, the major facilitator superfamily, and the cytochrome P450 were among the most enriched Pfam domains whose genes were mostly up-regulated (Table 6). In addition to the cytochromes P-450, several Pfam domains involved in biotransformation (phase I and phase II metabolism of xenobiotics) were functionally enriched and up-regulated: glutathione S-transferases, sulfotransferases, methyltransferases, and aldehyde dehydrogenases (Table 6; File S3). By contrast, most of the genes coding for proteins with C1q domains, immunoglobulin domains, tetratricopeptide repeats, and collagen triple helix repeats were down-regulated (Table 6; File S3).

Significantly enriched gene ontology (GO) terms (Fisher's exact test, FDR-adjusted p-value <0.05) in the biological process (BP), molecular function (MF), and cellular component (CC) categories are displayed in Table 7 (up-regulated DEGs), Table 8 (down-regulated DEGs), and in File S4. A greater number of enriched GO terms was obtained for the up-regulated DEGs (738) than for those down-regulated (229). The analyses identified 426, 198, and 114 enriched GO terms in the BP, MF, and CC categories, respectively, for the up-regulated DEGs (File S4). The top significantly enriched GO terms (classified by FDR) were (Table 7) metabolic process, oxidation-reduction process, and organic substance catabolic process (in the BP category); catalytic activity, oxidoreductase activity and threonine-type peptidase activity (in the MF category); and cytoplasm, proteasome complex, and endopeptidase complex (in the CC category).

On the other hand, the number of enriched GO terms for the down-regulated DEGs (File S4) were 86 (BP), 111 (MF), and 32 (CC). Table 8 shows that the top enriched GO terms were as follows: neurotransmitter transport, regulation of cellular process, and cell communication (in the BP category); neurotransmitter transporter activity, neurotransmitter/sodium symporter activity, and solute/sodium symporter activity (in the MF category); and transcription factor complex, collagen trimer, and cytoskeleton (in the MF category).

Table 3. The top 25 up-regulated genes classified by false discovery rate (FDR)-adjusted p-value (padj) of group DA.

Sequence ID	Description	FC DB	padj DB	FC DA	padj DA
ci | 000048247 | Bact | Sample_DA | 2	fatty acid-binding protein, brain-like	4.02	5.18×10^{-13}	17.42	3×10^{-5}
ci | 000123653 | Bact | Sample_DB | 2	ganglioside-induced differentiation-associated protein 1-like	2.43	1.52×10^{-5}	4.35	2.18×10^{-71}
ci | 000014617 | Bact | Sample_DA | 2	fatty acid-binding protein homolog 5 isoform X2	8.41	1.20×10^{-13}	35.70	1.46×10^{-54}
ci | 000041038 | Bact | Sample_C | 2	fatty acid-binding protein, brain-like	3.82	4.54×10^{-8}	18.21	8.69×10^{-54}
ci | 000053956 | Bact | Sample_C | 2	fatty acid-binding protein, brain-like	3.83	4.61×10^{-9}	17.75	1.17×10^{-53}
ci | 000005112 | Bact | Sample_DB | 2	fatty acid-binding protein homolog 5 isoform X2	6.09	8.48×10^{-13}	26.48	1.16×10^{-49}
ci | 000017145 | Bact | Sample_C | 2	selenoprotein F-like	2.01	4.34×10^{-11}	2.75	5.18×10^{-47}
ci | 000005129 | Bact | Sample_C | 2	uncharacterized protein LOC110453031	2.11	9.79×10^{-13}	3.40	1.02×10^{-45}
ci | 000000144 | Bact | Sample_DA | 2	fatty acid-binding protein, brain-like	4.29	1.10×10^{-11}	18.11	1.02×10^{-45}
ci | 000005171 | Bact | Sample_DB | 2	—NA—	6.89	1.43×10^{-9}	26.37	2.23×10^{-42}
ci | 000069997 | Bact | Sample_DA | 2	acylpyruvase FAHD1, mitochondrial	2.52	3.20×10^{-8}	5.13	1.87×10^{-41}
ci | 000047776 | Bact | Sample_C | 2	sulfotransferase family cytosolic 1B member 1-like	3.33	1.24×10^{-5}	13.03	2.22×10^{-41}
ci | 000033268 | Bact | Sample_DB | 2	arylsulfatase B-like	8.26	3.74×10^{-26}	11.50	6.15×10^{-41}
ci | 000026813 | Bact | Sample_DA | 2	sulfotransferase family cytosolic 1B member 1-like isoform X1	5.10	5.74×10^{-15}	14.18	2.34×10^{-39}
ci | 000049206 | Bact | Sample_C | 2	uncharacterized protein LOC110453031	2.10	6.28×10^{-11}	3.41	2.54×10^{-38}
ci | 000050101 | Bact | Sample_DA | 2	fatty acid-binding protein, brain-like	5.64	2.58×10^{-7}	29.68	3.39×10^{-38}
ci | 000056604 | Bact | Sample_DA | 2	sulfotransferase family cytosolic 1B member 1-like	5.87	2.29×10^{-15}	15.32	3.51×10^{-38}
ci | 000027873 | Bact | Sample_DB | 2	cytochrome b5-like	2.12	5.81×10^{-8}	3.19	2.28×10^{-36}
ci | 000039930 | Bact | Sample_DB | 2	sulfotransferase family cytosolic 1B member 1-like	7.09	9.44×10^{-22}	15.69	3.39×10^{-36}
ci | 000065147 | Bact | Sample_DB | 2	fatty acid-binding protein homolog 5 isoform X2	4.36	1.92×10^{-6}	19.45	2.59×10^{-35}
ci | 000006862 | Bact | Sample_DA | 2	fatty acid-binding protein, brain-like	4.92	1.72×10^{-6}	28.74	1.03×10^{-34}
ci | 000020752 | Bact | Sample_DB | 2	—NA—	8.09	3.57×10^{-32}	7.28	1.07×10^{-34}
ci | 000016532 | Bact | Sample_DA | 2	fatty acid-binding protein, brain-like	5.97	2.32×10^{-8}	30.92	1.21×10^{-34}
ci | 000059056 | Bact | Sample_DA | 2	dimethylaniline monooxygenase [N-oxide-forming] 5-like isoform X1	4.07	7.94×10^{-10}	8.29	1.43×10^{-34}
ci | 000093179 | Bact | Sample_DB | 2	uncharacterized protein LOC110453031	2.67	2.16×10^{-13}	4.31	2.33×10^{-33}

FC: fold change.

Table 4. The top 25 down-regulated genes classified by FDR-adjusted p-value (padj) of group DA.

Sequence ID	Description	FC DB	padj DB	FC DA	padj DA
ci | 000106611 | Bact | Sample_C | 2	—NA—	−57.59	1.68×10^{-42}	−139.49	6.68×10^{-64}
ci | 000007989 | Bact | Sample_C | 2	F-box only protein 33	−7.31	2.69×10^{-11}	−72.56	6.79×10^{-58}
ci | 000015465 | Bact | Sample_C | 2	—NA—	−327.41	8.87×10^{-67}	−438.98	6.31×10^{-54}
ci | 000021112 | Bact | Sample_C | 2	—NA—	−77.85	2.14×10^{-60}	−317.56	7.15×10^{-48}
ci | 000005274 | Bact | Sample_C | 2	—NA—	−371.71	5.02×10^{-52}	−372.69	2.17×10^{-45}
ci | 000028047 | Bact | Sample_C | 2	—NA—	−363.88	3.57×10^{-56}	−393.01	4.76×10^{-45}
ci | 000101976 | Bact | Sample_C | 2	—NA—	−296.03	4.63×10^{-36}	−314.75	3.8×10^{-44}
ci | 000000908 | Bact | Sample_C | 2	—NA—	−28.16	1.34×10^{-23}	−107.94	4.64×10^{-44}
ci | 000036200 | Bact | Sample_DB | 2	probable serine/threonine-protein kinase kinX	−2.76	6.84×10^{-6}	−10.59	5.31×10^{-43}
ci | 000063999 | Bact | Sample_C | 2	—NA—	−544.00	1.59×10^{-52}	−705.51	5.33×10^{-43}
ci | 000012018 | Bact | Sample_DB | 2	zwei Ig domain protein zig-2-like	−6.84	2.58×10^{-13}	−42.34	1.91×10^{-42}
ci | 000012910 | Bact | Sample_C | 2	—NA—	−19.42	2.97×10^{-35}	−199.53	2.71×10^{-42}
ci | 000023297 | Bact | Sample_C | 2	—NA—	−79.85	9.38×10^{-54}	−322.38	4.58×10^{-42}
ci | 000038123 | Bact | Sample_C | 2	—NA—	−80.83	4.63×10^{-47}	−266.21	9.28×10^{-42}
ci | 000020939 | Bact | Sample_C | 2	—NA—	−2.05	3.09×10^{-2}	−58.46	1.05×10^{-39}
ci | 000005202 | Bact | Sample_C | 2	—NA—	−315.71	5.05×10^{-46}	−181.22	4.46×10^{-37}
ci | 000039871 | Bact | Sample_C | 2	neuroglian-like isoform X1	−7.48	3.70×10^{-11}	−44.27	1.65×10^{-35}
ci | 000013710 | Bact | Sample_C | 2	—NA—	−404.07	4.63×10^{-47}	−401.37	1.99×10^{-35}
ci | 000012324 | Bact | Sample_C | 2	—NA—	−163.57	5.05×10^{-46}	−373.00	1.47×10^{-34}
ci | 000023304 | Bact | Sample_DB | 2	gliomedin-like isoform X4	−2.42	2.42×10^{-3}	−5.65	3.18×10^{-33}
ci | 000051151 | Bact | Sample_C | 2	—NA—	−56.53	1.13×10^{-30}	−221.69	1.45×10^{-32}
ci | 000088531 | Bact | Sample_C | 2	—NA—	−55.44	9.80×10^{-33}	−124.60	3.09×10^{-32}
ci | 000072709 | Bact | Sample_C | 2	—NA—	−293.26	3.06×10^{-39}	−243.75	7.51×10^{-32}
ci | 000096728 | Bact | Sample_C | 2	uncharacterized protein LOC110458629	−9.55	9.51×10^{-18}	−20.79	7.51×10^{-32}
ci | 000074174 | Bact | Sample_C | 2	—NA—	−33.35	1.02×10^{-23}	−71.61	2.96×10^{-31}

FC: fold change.

Table 5. Summary of the functional annotation results.

Functional Annotation	Number	%
Differentially expressed unigenes	**10,144**	**100**
With Blastx hit	6081	59.95
With GO terms	3451	34.02
With enzyme code	638	6.29
With KO orthologue	1728	17.03
With PFAM domains	4379	43.17
All unigenes	**142,137**	**100**
With Blastx hit	67,925	47.79
With GO terms	38,825	27.32
With enzyme code	6991	4.92
With KO orthologue	13,978	9.83
With PFAM domains	46,664	32.83

Table 6. The top twenty Pfam families that were significantly (FDR-adjusted p-value <0.05) enriched.

Pfam	Description	N° Genes	UP/DOWN	padj FDR
PF00386.16	C1q domain	13	DOWN	2.08×10^{-137}
PF00059.16	Lectin C-type	27	UP	4.77×10^{-66}
PF14259.1	RNA recognition motif. (RRM_6)	28	UP	8.64×10^{-54}
PF00076.17	RNA recognition motif. (RRM_1	37	UP	5.38×10^{-51}
PF07690.11	Major Facilitator Superfamily	34	UP	5.18×10^{-46}
PF13927.1	Immunoglobulin domain	55	DOWN	7.61×10^{-46}
PF13893.1	RNA recognition motif. (RRM_5)	22	UP	9.46×10^{-44}
PF13414.1	tetratricopeptide repeat	18	DOWN	2.98×10^{-38}
PF00067.17	Cytochrome P450	45	UP	4.06×10^{-38}
PF01391.13	Collagen triple helix repeat (20 copies)	29	DOWN	6.16×10^{-36}
PF12695.2	Alpha/beta hydrolase fold	10	DOWN	2.15×10^{-35}
PF00400.27	WD domain, G-beta repeat;	20	UP	9.61×10^{-35}
PF05721.8	Phytanoyl-CoA dioxygenase (PhyH)	9	UP	1.01×10^{-34}
PF12697.2	Alpha/beta hydrolase fold	6	DOWN	1.07×10^{-34}
PF13424.1	tetratricopeptide repeat	14	DOWN	1.72×10^{-34}
PF00009.22	Elongation factor Tu GTP binding domain	23	UP	5.23×10^{-32}
PF00515.23	tetratricopeptide repeat	16	DOWN	1.52×10^{-31}
PF00531.17	Death domain	18	DOWN	5.62×10^{-31}
PF13181.1	tetratricopeptide repeat	10	DOWN	6.11×10^{-31}
PF07719.12	tetratricopeptide repeat	19	DOWN	7.32×10^{-30}

UP/DOWN indicates if most of the genes in the category were up- or down-regulated.

Table 7. The top 10 enriched gene ontology (GO) terms (classified by FDR) for the up-regulated genes in biological process (BP), molecular function (MF), and cellular component (CC) categories.

GO ID	GO Name	GO Type	padj FDR	Fold Enrichment
GO:0008152	metabolic process	BP	8.55×10^{-165}	2.38
GO:0055114	oxidation-reduction process	BP	3.42×10^{-120}	4.21
GO:1901575	organic substance catabolic process	BP	8.52×10^{-60}	4.89
GO:0044237	cellular metabolic process	BP	3.81×10^{-58}	2.00
GO:0009056	catabolic process	BP	1.89×10^{-54}	4.46
GO:0044248	cellular catabolic process	BP	3.27×10^{-53}	4.74
GO:0071704	organic substance metabolic process	BP	9.09×10^{-53}	1.86
GO:0044238	primary metabolic process	BP	7.05×10^{-49}	1.85
GO:0019752	carboxylic acid metabolic process	BP	1.18×10^{-47}	3.66
GO:0043436	oxoacid metabolic process	BP	2.22×10^{-47}	3.64

Table 7. *Cont.*

GO ID	GO Name	GO Type	padj FDR	Fold Enrichment
GO:0003824	catalytic activity	MF	1.39×10^{-189}	2.53
GO:0016491	oxidoreductase activity	MF	2.06×10^{-134}	4.33
GO:0070003	threonine-type peptidase activity	MF	1.44×10^{-71}	72.62
GO:0004298	threonine-type endopeptidase activity	MF	1.44×10^{-71}	72.62
GO:0016616	oxidoreductase activity, acting on the CH-OH group of donors, NAD or NADP as acceptor	MF	1.21×10^{-48}	14.26
GO:0016614	oxidoreductase activity, acting on CH-OH group of donors	MF	1.13×10^{-44}	9.75
GO:0048037	cofactor binding	MF	8.82×10^{-42}	3.53
GO:0050662	coenzyme binding	MF	6.23×10^{-39}	4.61
GO:0004576	oligosaccharyl transferase activity	MF	3.37×10^{-28}	111.72
GO:0016782	transferase activity, transferring sulfur-containing groups	MF	4.78×10^{-26}	6.61
GO:0005737	Cytoplasm	CC	2.87×10^{-100}	3.60
GO:0000502	proteasome complex	CC	6.28×10^{-82}	30.23
GO:1905369	endopeptidase complex	CC	6.28×10^{-82}	30.23
GO:1905368	peptidase complex	CC	4.48×10^{-78}	25.22
GO:0044424	intracellular part	CC	2.84×10^{-75}	2.37
GO:0005839	proteasome core complex	CC	1.44×10^{-71}	72.62
GO:0044444	cytoplasmic part	CC	4.88×10^{-68}	3.45
GO:0005622	intracellular	CC	2.16×10^{-67}	2.22
GO:0044464	cell part	CC	1.94×10^{-63}	2.15
GO:0005623	Cell	CC	2.00×10^{-62}	2.13

Table 8. The top 10 enriched gene ontology (GO) terms (classified by FDR) for the down-regulated genes in biological process (BP), molecular function (MF), and cellular component (CC) categories.

GO ID	GO Name	GO Type	padj FDR	Fold Enrichment
GO:0006836	neurotransmitter transport	BP	4.01×10^{-34}	17.69
GO:0050794	regulation of cellular process	BP	7.32×10^{-27}	1.98
GO:0007154	cell communication	BP	7.32×10^{-27}	2.45
GO:0023052	Signaling	BP	7.07×10^{-26}	2.42
GO:0050789	regulation of biological process	BP	2.48×10^{-25}	1.93
GO:0007165	signal transduction	BP	3.18×10^{-24}	2.38
GO:0065007	biological regulation	BP	1.39×10^{-18}	1.73
GO:0006468	protein phosphorylation	BP	5.33×10^{-18}	3.02
GO:0050896	response to stimulus	BP	3.98×10^{-17}	1.92
GO:0051716	cellular response to stimulus	BP	1.35×10^{-16}	1.98
GO:0005326	neurotransmitter transporter activity	MF	9.58×10^{-37}	21.66
GO:0005328	neurotransmitter/sodium symporter activity	MF	9.58×10^{-37}	21.66
GO:0015370	solute/sodium symporter activity	MF	9.58×10^{-37}	21.66
GO:0015294	solute/cation symporter activity	MF	4.01×10^{-34}	17.69
GO:0015081	sodium ion transmembrane transporter activity	MF	4.01×10^{-34}	17.69
GO:0015293	symporter activity	MF	2.50×10^{-31}	14.61
GO:0046873	metal ion transmembrane transporter activity	MF	6.68×10^{-30}	8.87
GO:0015291	secondary active transmembrane transporter activity	MF	1.18×10^{-23}	8.72
GO:0003700	DNA-binding transcription factor activity	MF	6.43×10^{-23}	4.26
GO:0015077	monovalent inorganic cation transmembrane transporter activity	MF	2.62×10^{-20}	5.77

Table 8. *Cont.*

GO ID	GO Name	GO Type	padj FDR	Fold Enrichment
GO:0005667	transcription factor complex	CC	3.83×10^{-17}	3.38
GO:0005581	collagen trimer	CC	2.61×10^{-13}	11.58
GO:0005856	cytoskeleton	CC	2.94×10^{-8}	2.24
GO:0099513	polymeric cytoskeletal fiber	CC	8.14×10^{-8}	3.24
GO:0005874	microtubule	CC	1.18×10^{-7}	3.32
GO:0099080	supramolecular complex	CC	2.40×10^{-7}	3.10
GO:0099081	supramolecular polymer	CC	2.40×10^{-7}	3.10
GO:0099512	supramolecular fiber	CC	2.40×10^{-7}	3.10
GO:0030286	dynein complex	CC	4.68×10^{-7}	4.58
GO:0034703	cation channel complex	CC	1.51×10^{-6}	19.63

Among the level-2 enriched GO terms (Figure 2; Table S2), the genes in the categories of metabolic process, cellular process, catalytic activity, structural molecule activity, and transporter activity were mainly up-regulated, while most of the genes in the categories of biological regulation, signaling, immune system process, response to stimulus, and transcription regulator activity were down-regulated. File S5 shows the Kyoto Encyclopedia of Genes and Genomes (KEGG) orthologues (KO) of DEGs and of all unigenes.

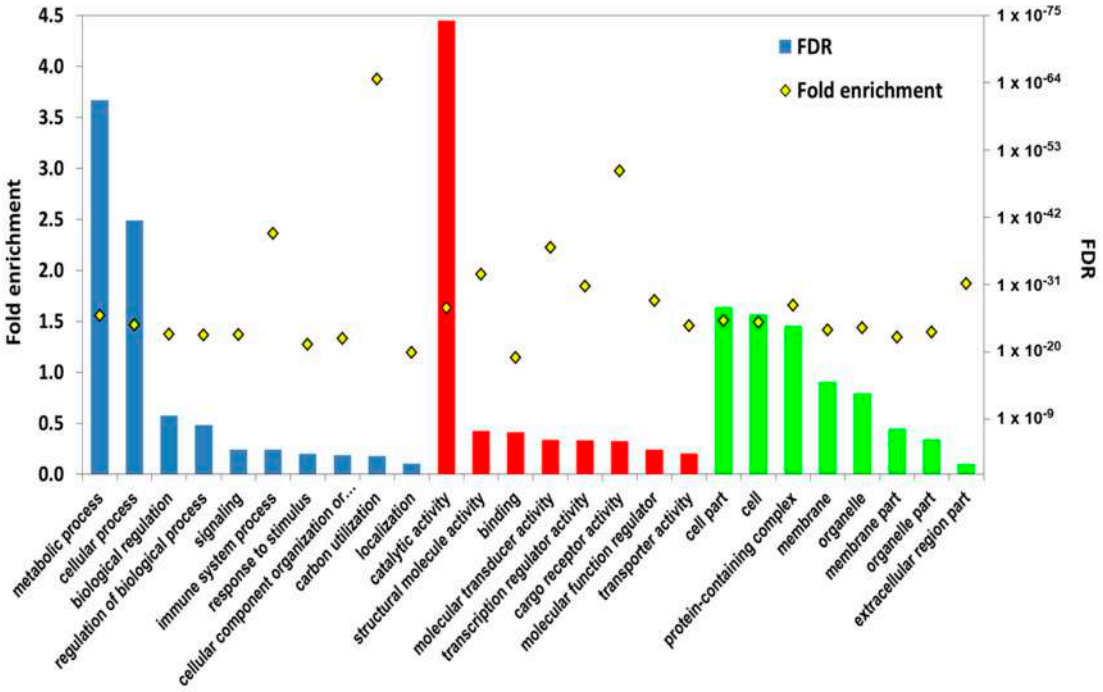

Figure 2. Level-2 enriched gene ontology (GO) terms for the differentially expressed genes in the biological process (BP, blue), molecular function (MF, red), and cellular component (CC, green) categories. FDR: p-value adjusted by FDR. Histograms represent the FDR-adjusted p-value, and the yellow diamonds represent the fold enrichment.

2.4. Protein Network Analysis

Protein–protein interactions can be employed to group and organize all the protein-coding genes in a genome [37]. From the 4913 up-regulated genes, a Blastx search found 931 human homologs in the STRING database. The network obtained in the highest confidence (0.9) mode is enriched in interactions (p-value $<1 \times 10^{-16}$). The results obtained with the up-regulated DEGs showed a small number of highly connected protein nodes. Each group of proteins is involved in specific biological processes (Figure 3; Figure S1; File S6): degradation of proteins (proteasome components), synthesis of

mitochondrial proteins (mitochondrial ribosomal proteins), translocation of cytosolically synthesized mitochondrial preproteins (translocases of outer and inner mitochondrial membrane, TOMMs, and TIMMs), splicing of mRNA (spliceosome components), and phase I and phase II metabolism of xenobiotics (cytochromes P450 and glutathione S-transferases).

From the 5231 down-regulated DEGs, 855 human homologs were found in the STRING database. The network is enriched in interactions (p-value $<1 \times 10^{-16}$). Components of different types of collagen, heat shock proteins, and proteins involved in cytoskeleton dynamics (Figure S2; File S7) were among the proteins that appeared in the network obtained with the down-regulated DEGs.

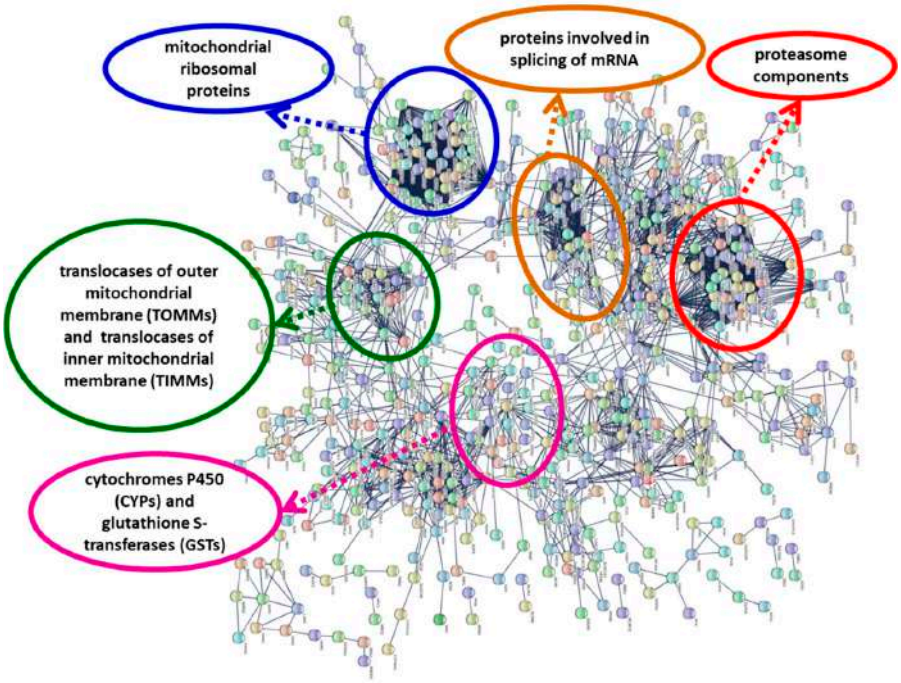

Figure 3. Network showing interactions of proteins coded by genes up-regulated in the present study. Network was constructed using the String 10.5 algorithm and obtained in the highest confidence (0.9) mode. Some highly connected protein nodes are highlighted. Proteins were named according to the human protein name. A full list of protein names is available in Figure S1 and File S6.

2.5. Real Time RT-qPCR

The candidate reference genes (*EIF4EBP2*, *RPS4*, *VAMP7*, *RAP1B*, *DNAJ*, and *MYH9*) (Table 9) were selected for their stable expression based on the RNA-seq data. NormFinder stability values ranged from 0.137 to 0.237 and the geNorm average M from 0.339 to 0.584 (Table 10). The standard deviations (SD) of Cq values calculated with BestKeeper were low (0.53–0.69, Table 10). Pairwise variation (Vn/n+1) [38] was used to determine the optimal number of reference genes for normalization. Figure 4 shows that V5/6 attained the minimum pairwise variation value (0.097); therefore, five reference genes were used for normalization [39]: *EIF4EBP2*, *RPS4*, *VAMP7*, *RAP1B*, and *DNAJ*. The least stable reference gene candidate was *MYH9*.

The normalized gene expression of the five target genes, and the non-selected reference gene (*MYH9*) is displayed in Figure 5. There was good agreement between RT-qPCR (Figure 5, upper panel) and RNA-seq (Figure 5, lower panel). The RNA-seq results showed that *CYP2C14*, *SLC16A12*, *ANT1*, and *SLC16A13* were up-regulated in groups DB and DA in relation to the control; these genes were also up-regulated when the RT-qPCR data were analyzed. The *SLC6A9* gene was down-regulated in groups DB and DA in relation to the control group (Figure 5, lower panel), but the RT-qPCR data showed significant differences only between group DA and the control. The candidate reference gene *MYH9* is not differentially expressed.

Table 9. Genes selected for RT-qPCR: sequence names, description, gene symbols, primers, and amplicon length (bp) for each primer pair and average efficiency (E).

Sequence ID	Description	Symbol	Sense Primer	Antisense Primer	bp	E
ci|000063635|Bact|Sample_C|2	vesicle-associated membrane protein 7-like	*VAMP7*	ACTGACAATCGTAGTGGTGCTG	GCAGTGGTGGTGGTAGTTGATG	84	0.8584
ci|000050253|Bact|Sample_C|2	40S ribosomal protein S4	*RPS4*	AATGGGTTACCGAGGACG	CACCACTCAGTTTGTCCAAC	80	0.7934
ci|000036898|Bact|Sample_DA|2	myosin heavy chain, non-muscle isoform X11-MYOSIN 9	*MYH9*	CGCCATTACAGATGCAGCA	GATTCACCTGTGCAGAGG	75	0.8267
ci|000071167|Bact|Sample_DA|2	eukaryotic translation initiation factor 4E-binding protein 2-like	*EIF4EBP2*	CCAGGAGTAACAGCACCAG	TGTCCATCTCGAACTGTGG	130	0.8659
ci|000071620|Bact|Sample_C|2	molecular chaperone DNAJ/HSP40	*DNAJ*	GCCTATGATAATGCCTCTACG	CTAGGACGTGTGACATATTCC	110	0.8501
ci|000093955|Bact|Sample_DB|2	ras-related protein Rap-1b isoform 1 precursor	*RAP1B*	TGAAGTGGATGGACAACAGTG	TGTGCTGTGATGGAATACACC	129	0.8648
ci|000058258|Bact|Sample_DA|2	cytochrome p450 2c14-like isoform x2	*CYP2C14*	GCCTGGTCCTTCTGGATAC	CTTCAAGCTGAATACGTCACC	115	0.8697
ci|000104366|Bact|Sample_C|2	sodium- and chloride-dependent glycine transporter 1-like	*SLC6A9*	TTCTGAGTCGAATAGCTCTGG	TATCAACCACGGTCGTCTC	80	0.8500
ci|000028690|Bact|Sample_DA|2	monocarboxylate transporter 12-like	*SLC16A12*	CCTGCTATGATTGCTTACGG	CAGTCCAACATCGCTACAG	83	0.9682
ci|000032679|Bact|Sample_DA|2	amino acid transporter antl1-like isoform x1	*ANT1*	AAGCTGGCAGATATACAGTG	TTGGTGTTCCGAACCAGG	189	0.8906
ci|000000293|Bact|Sample_DB|2	monocarboxylate transporter 13-like isoform x1	*SLC16A13*	AAGACATCCAGCCATGAGTTG	CTTCCAAGAACAACGAACCAG	86	0.8463

Table 10. Rank of the six candidate reference genes in quantitative real-time reverse transcription–polymerase chain reaction (RT–qPCR), calculated by geNorm, NormFinder, and BestKeeper analysis.

Rank	GeNorm (Average M)		Normfinder (Stability)		BestKeeper (*r*)		BestKeeper (SD)	
1	*EIF4EBP2-RAP1B*	0.399	*EIF4EBP2*	0.137	*RPS4*	0.92	*DNAJ*	0.53
2	*EIF4EBP2-RAP1B*	0.399	*RPS4*	0.151	*EIF4EBP2*	0.9	*VAMP7*	0.54
3	*RPS4*	0.431	*VAMP7*	0.163	*RAP1B*	0.86	*RPS4*	0.55
4	*VAMP7*	0.487	*RAP1B*	0.192	*VAMP7*	0.79	*EIF4EBP2*	0.55
5	*DNAJ*	0.504	*DNAJ*	0.216	*MYH9*	0.77	*MYH9*	0.63
6	*MYH9*	0.584	*MYH9*	0.237	*DNAJ*	0.68	*RAP1B*	0.69

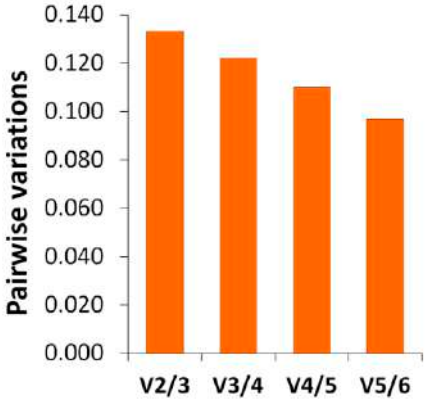

Figure 4. Determination of the optimal number of reference genes for normalization. The pairwise variation (Vn/n+1) was calculated between the normalization factors NFn and NFn+1 (using n or n+1 reference genes respectively) by geNorm software.

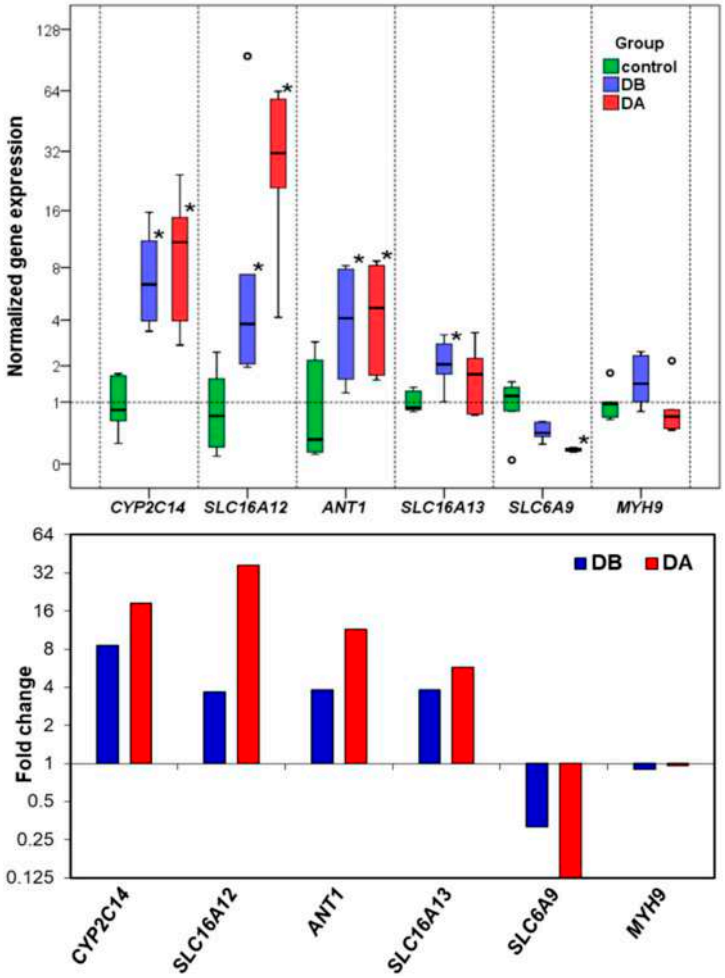

Figure 5. Gene expression. Upper panel: Normalized gene expression in the digestive gland of *A. opercularis* in the presence of domoic acid, as determined by RT-qPCR analyses. The box and whisker plots were obtained using IBM SPSS version 24.0 software. The boxes represent the lower and upper quartiles with medians. The bars represent the ranges for the data ($n = 6$). The circles represent extreme values (more than three box lengths from the end of a box). The statistical analysis was performed using ANOVA and Dunnett's Two-Tailed *t* Test: *$p < 0.05$. Lower panel: Fold change in relation to the control obtained by RNA-seq.

3. Discussion

There are many studies about the mechanisms of the neurotoxicity of domoic acid in vertebrates (especially mammals), but there is very little knowledge about the putative effects of domoic acid on bivalve mollusks. Several publications showed that domoic acid can exert physiological and sublethal effects on marine bivalves [16–20]. Dizer et al. [16] found that in *Mytilus edulis*, DNA damage was significantly increased after the injection of domoic acid and suggested the existence of genotoxic responses in the cells of digestive glands. It is interesting to point out that DNA repair, cellular response to DNA damage stimulus, and cellular response to stress were among the enriched GO terms in the present work for the up-regulated DEGs (File S4). This could be the transcriptomic response of *A. opercularis* to the putative DNA damage provoked by domoic acid. In *C. gigas*, domoic acid provoked a generalized stress response [17] and an increase in the number and activity of hemocytes [18]. Domoic acid induces oxidative stress in the central nervous system and spinal cord in vertebrates [24–27]. Furthermore, harmful algae toxins sometimes provoke oxidative stress in bivalves [21–23], and Prego-Faraldo et al. [40] found that exposure to the toxic dinoflagellate *Prorocentrum lima* induces the differential expression of genes coding for antioxidant enzymes. The glutathione S-transferase, thioredoxin, glutaredoxin, and copper/zinc superoxide dismutase Pfam domains were functionally enriched in queen scallops (File S3), and these genes were, for the most part, up-regulated; these domains are found in proteins involved in protection against reactive oxygen species (ROS).

In a recent work about the effects of environmental stress on gene transcription in oysters, Anderson et al. [41] proposed a consensus model of sub-cellular stress responses in oysters with the involvement of mitochondria and reactive oxygen species (ROS) production. If the anti-oxidant enzymes and molecular chaperones cannot limit the damage caused by ROS, then the consequences are probably cellular dysfunction and apoptosis [41]. In vertebrates, domoic acid causes mitochondrial dysfunction as a consequence of oxidative stress [4,24,26]. Hiolski et al. [24] suggested the existence of compensatory mitochondrial biogenesis in response to mitochondrial dysfunction. Our results (Figure 3; Figure S1; File S2,S6) showed an up-regulation of genes coding for mitochondrial ribosomal proteins and translocases of the outer and inner mitochondrial membrane (proteins involved in mitochondrial biogenesis); in the protein interaction network, these proteins form highly connected protein nodes (Figure 3; Figure S1)

Up-regulation of proteasome subunits (Figure 3; Figure S1; File S2) is also a possible consequence of oxidative stress [42], because the proteasome is responsible for the selective degradation of oxidized proteins [43]. The 26S proteasome is a protease complex, which is responsible for the regulated degradation of proteins in eukaryotic organisms [42]. The proteasome system can be activated to accomplish the destruction of proteins altered by stress conditions [44]. The proteasome complex and proteasome core complex were two of the most enriched GO terms in the cellular component category for the up-regulated DEGs (Table 7), and the proteasome Pfam domain (PF00227) was also enriched (File S3); the genes coding for proteins with this domain were up-regulated in *Pseudo-nitzschia*-exposed scallops (Files S2 and S3). Proteasome proteins form a group of highly connected nodes in the protein–protein interaction network (Figure 3, Figure S1). In *M. galloprovincialis* exposed to the toxin okadaic acid, there is an up-regulation of several mRNAs involved in proteasome activity [45]. Therefore, the results support the hypothesis that exposure to domoic acid-producing *Pseudo-nitzschia* causes oxidative stress and the impairment of the mitochondrial function in *A. opercularis* and that the transcriptional changes are directed, at least in part, to counteract the stress effects.

The metabolism of xenobiotics (such as toxins) has three phases; phase I (functionalization) and phase II (conjugation) are catalyzed by metabolizing enzymes, while phase III consists of the export from the cell by transmembrane transporter proteins. We found that the Pfam domains of some phase I (cytochromes P450 and aldo-keto reductases) and phase II (glutathione S-transferases and sulfotransferases) drug metabolizing enzymes were functionally enriched, and the genes coding for these enzymes were mostly up-regulated. Cytochromes P450 and glutathione S-transferases

constituted a group of highly connected nodes in the protein interaction network (Figure 3, Figure S1). Genes of these families were also up-regulated in mussels (*M. galloprovincialis*) exposed to domoic acid-containing *Pseudo-nitzschia* [31]. Peña-Llopis et al. [46] showed that the treatment of scallops (*P. maximus*) with N-acetylcysteine increased glutathione S-transferase (GST) activity and enabled the scallops to eliminate domoic acid more efficiently. Therefore, it is possible that glutathione S-transferases play a role in domoic acid detoxification. Li et al. [35] found an up-regulation of sulfotransferase genes in the kidney of the Zhikong scallop *Chlamys farreri* after exposure to paralytic shellfish toxin-producing *Alexandrium minutum*. Furthermore, the family of sulfotransferases is significantly expanded in the *C. farreri* genome [35]; the high number of transcripts coding for sulfotransferases in the *A. opercularis* transcriptome is indicative of an expansion of this family in the queen scallop.

The molecular mechanisms of domoic acid absorption and excretion in bivalve mollusks are poorly understood [31]. Mauriz and Blanco [15] found that in the king scallop *P. maximus*, domoic acid is free in the cytosol of the digestive gland and suggested that the low depuration rate of domoic acid in this species could be due to the lack of membrane transporters. Domoic acid is a charged compound and probably needs a transport protein to pass through the plasma membrane, as is the case with glutamic acid [47,48]. This putative transmembrane transporter(s) could therefore play an important role in the absorption and/or the excretion of domoic acid. The results of Kimura et al. [47] suggest that anion exchange transporters are responsible for the transmembrane transport of domoic acid in Caco-2 cell monolayers (which represent the intestinal barrier of mammals); these transporters belong to the solute carrier (*SLC*) superfamily. In *A opercularis*, we found that transmembrane transport and transmembrane transporter activity were two of the enriched GO terms (File S4); furthermore, the major facilitator superfamily (MFS) was one of the most significantly enriched Pfam families (Table 6). Most of the genes belonging to these categories were up-regulated (Table 6; Files S2–S4). MFS is a clan of the SLC superfamily [49], and Hediger et al. [50] reported that the *SLC* gene series included 52 families in the human genome, although it has recently been updated to 65 families [51]. A total of eight *SLC* families (*SLC5*, *SLC16*, *SLC17*, *SLC21*, *SLC22*, *SLC26*, *SLC39*, and *SLC49*) contain up-regulated genes in *A. opercularis* (File S8) and in *M. galloprovincialis* [31] exposed to domoic acid-containing *Pseudo-nitzschia*. The transporter protein(s) putatively involved in the uptake and/or elimination of domoic acid in the digestive gland of bivalve mollusks could be encoded by a gene from one of those families. The families with a higher number of up-regulated genes in both *A. opercularis* and *M. galloprovincialis* were *SLC16* (the monocarboxylate transporters family) and *SLC22* (organic cation/anion/zwitterion transporters). A total of four members of the human *SLC16* gene family encode monocarboxylate transporters, but the substrates of several members are unknown [52]. The *SLC22* family [53] comprises organic cation, zwitterion, and anion transporters (OCTs, OCTNs, and OATs), which participate in the absorption (in the small intestine) and excretion (in the liver and kidney) of xenobiotics and endogenous substances [53]. Unfortunately, the lack of knowledge about the identity of the domoic acid transmembrane transporter(s) in mammals makes it difficult to identify them in bivalve mollusks. Schultz et al. [54] suggested that ATP-binding cassette (ABC) transporters are responsible for the absorption of domoic acid in Dungeness crabs, but in *A. opercularis*, we found only five up-regulated ABC transporters. A similar result was reported by Pazos et al. [31] in *M. galloprovincialis* (with two up-regulated ABC transporters). This contrasts with the high number of up-regulated *SLC* genes found in both bivalves.

Although most of the *SLC* genes differentially expressed in *A. opercularis* were up-regulated, the *SLC6* family (the sodium- and chloride-dependent neurotransmitter transporter family) is an exception, with 48 down-regulated unigenes (File S8). Furthermore, neurotransmitter/sodium symporter activity is one of the most enriched GO terms for the down-regulated genes (Table 8). On the contrary, in *M. galloprovincialis*, two genes from this family were up-regulated and none down-regulated [31]. In *A. opercularis*, the number of genes in this family is very high, and this agrees

with results from Li et al. [35], who found that the *SLC6* family is expanded in the *C. farreri* (a scallop) genome in relation to other bivalves.

Harmful algae and biotoxins exert different effects on the immune systems of bivalve mollusks [23,32,55]. Immune response and immune system process were two of the most enriched GO terms for the down-regulated DEGs (File S4), and Pfam families involved in immunological processes were significantly enriched in *A. opercularis* (Table 6; File S3): the C1q domain-containing proteins, the C-type lectin, the fibrinogen beta and gamma chains C-terminal globular domain, the immunoglobulin domain, and tumor necrosis factors (TNF). Except for the C-type lectins, the genes in these categories were mainly down-regulated (Table 6; Files S2 and S3). Differentially expressed genes from these families have been found in several bivalve mollusks after exposure to different biotoxins [31–34,36,56,57]. Hégaret et al. [23] found that some harmful algae provoked a stimulation of immune function of bivalve hemocytes, while others were immunosuppressive. The C1q domain containing proteins and the C-type lectins are particularly abundant in the digestive glands of bivalves [58,59]. The C1q domain-containing proteins are indispensable in the innate immune systems of invertebrates [60] and could be involved in several functions, such as activation of the complement pathway, cell adhesion, pathogen recognition, response to pollutants, and apoptosis [58,60,61]. An expansion of the genes coding for proteins containing the C1q domain was found in several bivalves [58,61–63]. For example, 321 C1q domain-containing proteins are encoded by the *C gigas* genome [62]; this represents approximately 10-fold more than the Ciq proteins encoded by the *Homo sapiens* genome [62]. Some genes coding for C1q domain-containing proteins were down-regulated in *M. galloprovincialis* fed with toxigenic strains of *Alexandrium minutum* [34]. The C-type lectins are characterized by a calcium-dependent carbohydrate recognition domain and participate in pathogen recognition and in innate immunity in bivalves [59], but they can also perform non-immune functions; for example, a role in efficient food particle sorting (food recognition) was found in the oyster *Crassostrea virginica* [64]. There is a high number of genes coding for C-type lectins in bivalve mollusks [59,65]. Most of the genes coding for C-type lectins were up-regulated in *A opercularis* (Table 6; Files S2 and S3) and *M. galloprovincialis* [31] after exposure to domoic acid-producing *Pseudo-nitzschia*; this agrees with the up-regulation of C-type lectins in *M. chilensis* after exposure to saxitoxin [33,56,57]. On the contrary, these genes were down-regulated in *Argopecten irradians* in response to okadaic acid [32].

One of the most enriched GO terms for the down-regulated DEGs in *A. opercularis* was collagen trimer (Table 8), and collagen triple helix repeat was among the enriched Pfam domains (Table 6). Furthermore, several collagen components form a group of highly connected protein nodes in the network obtained with the down-regulated genes (Figure S2). In *M. galloprovincialis*, after exposure to domoic acid-containing *Pseudo-nitzschia* [31], some collagen genes (7) were down-regulated, although the number of induced genes was greater (13). Collagens are components of the extracellular matrix characterized by the presence of at least one triple-helical domain [66]. They are among the most abundant proteins and have mainly a structural function [66].

Another group of predominantly down-regulated genes (14 up-regulated and 35 down-regulated, File S2) were those coding for heat shock proteins (HSPs). Half of the induced *HSP* genes were mitochondrial forms, and among the repressed ones, the *HSP70* genes predominated. Heat shock proteins are involved in protein folding and can be induced by several types of stress, including high temperature, toxins, pathogens, and hypoxia [67]. Several publications have reported the increased expression of heat shock protein genes in bivalves after exposure to harmful algae toxins [32,57,67–69]. Cheng et al. [67] found an expansion of *Hsp70* (heat shock protein 70 kDa) genes from the *Hspa12* subfamily in *Mizuhopecten yessoensis*. Several of these genes were differentially expressed in response to *Alexandrium catenella* exposure (most of them were induced, but there were also some *Hsp70* genes down-regulated [67]). However, Ryan et al. [29] reported the down-regulation of *Hsp68* (a member of the *Hsp70* family) after domoic acid exposure in mouse brain. Furthermore, the exposure to domoic

acid-producing *Pseudo-nitzschia* provoked a down-regulation of *HSPs* in *M. galloprovincialis* [31]; these results were coincident with those obtained in the present work.

Another result worth highlighting is that some genes coding for glutamate ionotropic receptors, two genes coding for NMDA receptors, and five coding for kainate (KA) receptors, were all down-regulated in the present study (File S2). The zebrafish *gria2* gene (glutamate ionotropic receptor AMPA 2) was down-regulated after two weeks of low-level domoic acid exposure [24], and the authors suggested that this down-regulation is a compensatory response to elevated glutamatergic activity [24]. It is possible that a similar compensatory mechanism takes place in queen scallops after exposure to domoic acid.

The RT-qPCR results confirm the differential gene expression obtained by RNA-seq. The gene expression changes and expression levels (fold change in relation to control) assessed by the two methods (Figure 5) were very similar. In the determination of gene expression by means of RT-qPCR, the validation of the reference genes for each experimental situation is very important [70,71]. The utilization of RNA-seq expression data allowed us to find more suitable candidate reference genes. Thanks to this, their stability values (Table 10), calculated by geNorm and NormFinder, were low (which means that the expression was stable). The selected reference genes performed better than some traditional reference genes, such as *18S rRNA*, *ACTB*, and *EF1A* [70,71].

4. Conclusions

RNA-seq technology was employed to elucidate the transcriptional response triggered by exposure to domoic acid-producing *Pseudo-nitzschia* in the queen scallop *A. opercularis*. A total of 10,144 genes were differentially expressed in the two toxin-exposed groups of scallops in relation to the control group (4913 up-regulated and 5231 down-regulated).

The results obtained are compatible with the hypothesis that exposure to domoic acid-producing *Pseudo-nitzschia* causes oxidative stress in *A. opercularis*. Some consequences of oxidative stress are the impairment of mitochondrial function and oxidation of proteins; therefore, the transcriptional response of the queen scallop tries to counteract these effects with the up-regulation of genes coding for proteins involved in the following: degradation of oxidized proteins (proteasome components), mitochondrial biogenesis (mitochondrial ribosomal proteins, TOMMs, and TIMMs) and antioxidant enzymatic activity (glutathione S-transferases, thioredoxins, glutaredoxins, and copper/zinc superoxide dismutases). The results of the present work and those cited in the literature show that oxidative stress is one of the most common effects of the exposure to toxins and toxin-producing algae, and a part of the harmful effects of the toxins are due to oxidative stress.

A great number of up-regulated genes code for proteins involved in the metabolism of xenobiotics (cytochromes P450, aldo-keto reductases, glutathione S-transferases, and sulfotransferases) and transmembrane transport (solute carriers), while the genes coding for proteins with domains involved in immunological processes (C1q domain, C-type lectins, immunoglobulin domain, fibrinogen beta and gamma chains C-terminal globular domain, and tumor necrosis factors) were mainly down-regulated, with the exception of the C-type lectins.

5. Materials and Methods

The methods employed were the same as those previously described [31] except for minor modifications.

5.1. Animals

Queen scallops (*A. opercularis*) were obtained from a natural bed in the Ría de Arousa in December 2014 and maintained in a 500-L tank, in the Centro de Investigacións Mariñas, (CIMA, Pedras de Corón, Vilanova de Arousa, Spain), with a continuous unfiltered seawater flow (approximate) of 1200 L/h. On April 9, 2015, 2 random samples of the scallops were obtained, and the remaining scallops (control, group C) were maintained in the tank. The scallops in 1 of the samples (group DB)

were analyzed to determine their individual content and concentration of domoic acid. The scallops in the other sample (group DA) were placed in culture baskets and transferred to a raft in the culture area Grove C2 in the Ría de Arousa, where a bloom of *Pseudo-nitzschia* was taking place. The recorded levels of domoic acid in the mussels from that raft showed a maximum of 22 mg DA/kg on April 9 (data obtained from Intecmar, www.intecmar.gal [72]). The scallops were maintained on the raft until April 17, 2015 in order to be exposed to domoic acid-containing *Pseudo-nitzschia*. On that date, the scallops (group DA) were brought back to the laboratory to determine their domoic acid content. The scallops from the control group were sampled on May 12, 2015, after the end of the toxic episode caused by *Pseudo-nitzschia*. From April 9 to May 12, the main characteristics of the seawater, temperature, salinity, light transmission (index of suspended solids), O_2, and fluorescence (index of phytoplankton abundance) in GROVE and in the area of CIMA were very similar (Figure S3). As previously explained by Pazos et al. [31], the experimental approach (animals naturally exposed to domoic acid-producing *Pseudo-nitzschia*) was chosen because of the difficulty of supplying toxic *Pseudo-nitzschia* under controlled conditions in the laboratory due to the relatively low absorption efficiency of the scallops and to the loss of toxicity of the *Pseudo-nitzschia* cultures.

Digestive glands, gills, and the remaining tissues were obtained by dissecting the scallops. Then, 1 part of each digestive gland was used in the determination of the domoic acid content. The second part was stored in RNAlater (ref. AM7021, Ambion, Life Technologies, Carlsbad, CA, USA) at −80°C until RNA extraction.

5.2. Chemicals and Reagents for Toxin Extraction and LC-MS/MS

Methanol for HPLC and formic acid were purchased from RCI Labscan Limited (Bangkok, Thailand) and Sigma-Aldrich (St. Louis, MO, USA), respectively. Ultrapure water was obtained using a Milli-Q Gradient system, coupled with an Elix Advantage 10, both from Millipore (Merck Millipore, Darmstadt, Germany).

5.3. Determination of the Domoic Acid Content

To extract the toxin, each digestive gland was placed in aqueous methanol (50%) in a proportion of 1:2 (w/v) and homogenized with an Ultra-Turrax T25 (IKA, Staufen, Germany). The extract was clarified using centrifugation at 18,000 g at 4 °C for 10 min, retaining a supernatant that was immediately analyzed.

Domoic acid in the obtained extracts was analyzed using LC-MS/MS. The chromatographic separation was carried out using a Thermo Accela chromatographic system (Thermo Fisher Scientific, Waltham, MA, USA), with a high-pressure pump and autosampler. The stationary phase was a solid core Kinetex C18, 50 × 2.1 mm, 2.6 µm particle size, column (Phenomenex, Torrance, CA, USA). An elution gradient, with a flow of 280 µL/min, was used with mobile phase A (formic acid 0.2%) and B (50% MeOH with formic acid 0.2%). The gradient started at 100% A, maintained this condition for 1 min, linearly changed until reaching 55% B in minute 5, was held for 2 min, and then reverted to the initial conditions in order to equilibrate before the next injection. Next, 5 µL of extract, previously filtered through a PES 0.2-µm syringe filter (MFS), were injected.

After the chromatographic separation, domoic acid was detected and quantified by means of a Thermo TSQ Quantum Access MAX triple quadrupole mass spectrometer (Thermo Fisher Scientific, Waltham, MA, USA), equipped with a HESI-II electrospray interface, using positive polarization and SRM mode. The transition 312.18 > 266.18 m/z was used to quantify the response and 312.18 > 248.18 was used for confirmation. The spectrometer was operated under the following conditions: spray voltage 3400 V, capillary temperature 270 °C, HESI-II temperature 110 °C, sheet gas (nitrogen) 20 (nominal pressure), auxiliary gas (nitrogen) 10 (nominal pressure), collision energy of 15 V, and collision gas (argon) pressure of 1.5 mTorr.

Concentrations of domoic acid were obtained by comparing the response of the quantification transition in the sample extracts with that of a reference solution obtained from NRC Canada. The quantification limit of the method for tissue analysis is less than 20 ng/mL of extract.

5.4. RNA Extraction

For digestive gland total RNA isolation, the NucleoSpin RNA kit (ref. 740955, Macherey-Nagel, Düren, Germany) was used following the manufacturer's protocol. Then, RNA was precipitated with 0.5 volumes of Li CL 7.5 M, and the RNA pellet was dissolved in 50 µL of RNA storage solution (ref. AM7000, Ambion, Life Technologies, Carlsbad, CA, USA). To remove DNA contamination, total RNA was treated with DNA-free (ref. AM1907M, Ambion, Life Technologies, Carlsbad, CA, USA). The integrity and quality of the RNA samples were measured using agarose gel electrophoresis, an Agilent 2100 Bioanalyzer (Agilent Technologies, Santa Clara, CA, USA) and a Nanodrop ND-1000 spectrophotometer (NanoDrop Technologies, Wilmington, DE, USA). The quantity of the total RNA was determined using Qubit 2.0 (Invitrogen, Carlsbad, CA, USA).

5.5. Library Preparation and Sequencing

A total of 18 cDNA libraries were generated (Figure 6) from the digestive gland of the scallops (6 obtained from each group: DB, DA, and control). The poly(A) + mRNA fraction was isolated from total RNA, and cDNA libraries were obtained following Illumina's recommendations. Briefly, poly(A) + RNA was isolated on poly-T oligoattached magnetic beads and chemically fragmented prior to reverse transcription and cDNA generation. The cDNA fragments then went through an end repair process, the addition of a single 'A' base to the 3' end, and afterwards, the ligation of the adapters. Finally, the products were purified and enriched with PCR to create the indexed final double-stranded cDNA library. The quality of the libraries was analyzed using a Bioanalyzer 2100 high sensitivity assay; the quantity of the libraries was determined by real-time PCR in a LightCycler 480 (Roche Diagnostics, Mannheim, Germany). Prior to cluster generation in cbot (Illumina), an equimolar pooling of the libraries was performed. The pool of the cDNA libraries was sequenced by paired-end sequencing (100 × 2 bp) on an Illumina HiSeq 2000 sequencer (Illumina, San Diego, CA, USA).

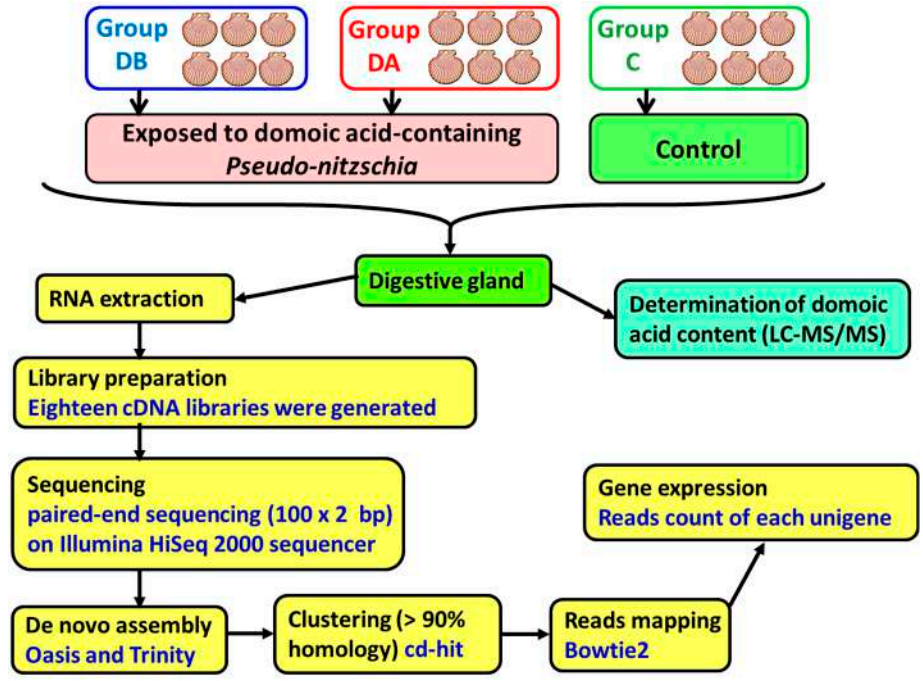

Figure 6. Scheme of the methods employed for sequencing and de novo transcriptome assembly.

5.6. de novo Assembly

Quality control checks of the raw sequencing data were performed with FastQC. The technical adapters were eliminated using Trimgalore software version 0.3.3 (Babraham Bioinformatics, Cambridge, UK) (http://www.bioinformatics.babraham.ac.uk/projects/trim_galore/). Additionally, the reads with a mean Phred score >30 were selected. Subsequently, all the samples were combined, and the complexity of the reads was reduced by removing duplicates. Then, a de novo assembly was performed using the programs Oases, version 0.2.09 [73] and Trinity, version 2.1.1 [74]. The assembled transcripts were clustered (>90% homology) to reduce redundancy using cd-hit software version 4.6. For each sequence, the potential ORFs were detected using Transdecoder software, version 2.0, with standard parameters.

Each sample was then mapped with Bowtie2, version 2.2.6 [75] against the reference transcriptome obtained in the previous step. The good quality reads (Mapping Quality $\geq$20) were selected to increase the resolution of the count expression. Finally, the expression inference was evaluated by means of the counts of properly paired reads in each transcript.

5.7. Differential Expression

The transcriptome expression for each sample was normalized by library size, following the DESeq2 protocols. Considering the whole normalized transcriptome, a study of correlation and Euclidean distance between samples was performed using the statistical software R, version 3.2.3 (www.r-project.org), for identifying possible samples outliers.

Differential gene expression analysis was performed with DESeq2 algorithm, version 1.8.2 (http://www.bioconductor.org/packages/devel/bioc/html/DESeq2.html). The genes with a fold change of less than -2 or greater than 2 and a *p*-value adjusted using the Benjamini and Hochberg [76] method for controlling false discovery rate (FDR) <0.05 were considered differentially expressed (Figure 7).

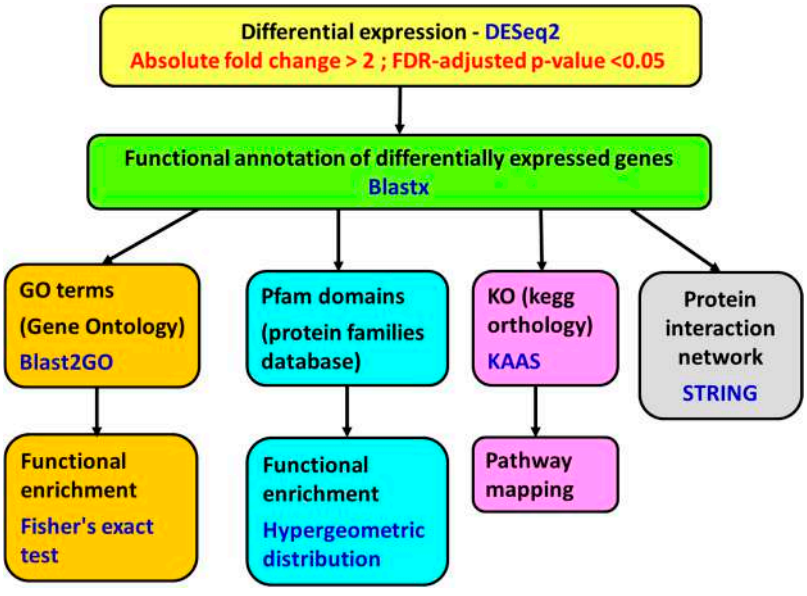

Figure 7. Scheme of the methods employed for differential gene expression analysis, functional annotation, and functional enrichment.

A filtering step was performed with the DEGs to remove the transcripts from *Pseudo-nitzschia*; the contigs were blasted against *Mizuhopecten yessoensis* and *Pseudo-nitzschia multistriata* genomes (*E*-value threshold of 10^{-10}, word size 12):

ftp://ftp.ncbi.nlm.nih.gov/genomes/all/GCF/002/113/885/GCF_002113885.1_ASM211388v2/GCF_002113885.1_ASM211388v2_genomic.fna.gz

ftp://ftp.ncbi.nlm.nih.gov/genomes/all/GCA/900/005/105/GCA_900005105.1_PsnmuV1.4/GCA_900005105.1_PsnmuV1.4_genomic.fna.gz

The contigs that had a lower *E*-value versus *Pseudo-nitzschia* compared with *M. yessoensis* were discarded (approximately 0.7% of the sequences).

5.8. Functional Annotation

The genes were annotated using Blastx [77] against the Uniprot database and Blastn [77] against the NCBI nucleotide database (*E*-value threshold of 10^{-2}). Then, the annotation was expanded by incorporating information from the species, gene name, and functions using gene ontology and protein structure domains associated with the transcript using InterPro (https://www.ebi.ac.uk/interpro/). The genes were also annotated with Blast2GO software version 4.1.9 (BioBam Bioinformatics S.L, Valencia, Spain) [78,79], using local Blastx 2.4.0+ against a database of *Mizuhopecten yessoensis* and *Crassostrea gigas* proteins obtained from NCBI (*E*-value threshold of 10^{-3}):

ftp://ftp.ncbi.nlm.nih.gov/genomes/Mizuhopecten_yessoensis/protein/protein.fa.gz (last modification 19/06/2017)

ftp://ftp.ncbi.nlm.nih.gov/genomes/Crassostrea_gigas/protein/protein.fa.gz (last modification 06/02/2017)

Orthologue assignment and pathway mapping were performed on the KEGG Automatic Annotation Server (KAAS, [80]) using Blast and the bi-directional best hit (BBH) method (http://www.genome.jp/tools/kaas/).

5.9. Functional Enrichment

A functional enrichment study was performed using the Pfam [81] functional information. This study is based on hypergeometric distribution [82] using the statistical software R version 3.2.3 (www.r-project.org). The differentially expressed genes were also subjected to GO enrichment analysis with Blast2GO version 4.1.9. (BioBam Bioinformatics S.L, Valencia, Spain) using Fisher's exact test [83] (up- and down-regulated genes were analyzed separately). The false discovery rate (FDR) adjusted p-value [76] was set at a cutoff of 0.05.

5.10. Protein Network Analysis

To search for the protein–protein interactions, network analyses using the String 10.5 algorithm [84] were performed. The putative human homologues of proteins coded by the up-regulated and the down-regulated genes in the *A. opercularis* digestive gland were identified by means of a Blastx search [85] against the STRING human protein database (9606.protein.sequences.v10.fa), with an E-value threshold of 10^{-5}. The top Blastx search results were used as input in the String program. The up-regulated and the down-regulated genes were analyzed separately.

5.11. Real Time RT-qPCR Validation

cDNA was synthesized from 0.5 µg of total RNA with the iScript™cDNA Synthesis kit (ref. 170-8891, BioRad, Hercules, CA, USA) in a 20-µL reaction volume, and the conditions were 5 min at 25 °C, 30 min at 42 °C, and 5 min at 85 °C.

For the relative quantification of gene expression by means of RT-qPCR, a normalization step must be performed using internal reference genes, whose expression levels are stable [38,86–88]. Suitable reference genes should be selected for each experimental condition to ensure their stable expression [70,89].

A total of 6 reference gene candidates (Table 9), *VAMP7*, *RPS4*, *MYH9*, *EIF4EBP2*, *DNAJ*, and *RAP1B* and 5 target genes (Table 9), *CYP2C14*, *SLC16A12*, *ANT1*, *SLC16A13*, and *SLC6A9*, were used in the gene expression study. The candidate reference genes were selected for their stable

expression based on the RNA-seq data. Oligonucleotide primers were designed with OligoAnalyzer 3.1 (http://eu.idtdna.com/analyzer/Applications/OligoAnalyzer/; Integrated DNA Technologies, Leuven, Belgium) from the sequences in Table 9 and were synthesized by Integrated DNA Technologies (Leuven, Belgium). The primer sequences and amplicon lengths are listed in Table 9. The specificity of the primers was confirmed by the presence of a single peak in the melting curve and by the presence of a single band of the expected size when PCR products were run in a 2% agarose gel. The PCR amplification efficiency (E) of each transcript was determined by means of Real-Time PCR Miner software (Version 4.0; http://www.miner.ewindup.info/ [90]). The mean amplification efficiency (E) of each amplicon (Table 9) was used in the calculation of gene expression.

Real-time qPCR analysis was conducted in technical duplicates and 6 biological replicates, in 96-well reaction plates on an iCycler iQ® Real-Time System (Bio-Rad, Hercules, CA, USA, 2003). The PCR final volume was 20 µL, containing 4 µL of 1:5 diluted cDNA (20 ng of cDNA), 10 µL of SsoFast EvaGreen Supermix (ref. 172-5201, Bio-Rad, Hercules, CA, USA), 400 nM of forward and reverse primers, and 4.4 µL of PCR-grade water. The cycling conditions were as follows: 30 s at 95 °C (initial template denaturation) and 40 cycles of 5 s at 95 °C (denaturation) followed by 10 s at 60 °C (annealing and elongation) and 10 s at 75 °C for fluorescence measurement. At the end of each run, a melting curve was carried out: 95 °C for 20 s and 60 °C for 20 s followed by an increase in temperature from 60 to 100 °C (with temperature increases in steps of 0.5 °C every 10 s). Baseline values were automatically determined for all the plates using Bio-Rad iCycler iQ software V3.1 (IQ™ Real-Time PCR Detection System). The threshold value was set manually at 100 RFU (relative fluorescence units) to calculate the Cq values. Non-reverse transcriptase controls and non-template controls (NTC) were also included in each run.

The gene expression was normalized to reference genes that had stable expression levels [38,86–88]. The gene expression stability of candidate reference genes was analyzed using 3 Microsoft Excel-based software applications, geNorm V3.5 [38], NormFinder V0.953 [86], and BestKeeper V1 [88]. The non-normalized expression (Q) was calculated using the equation $Q = (1 + E)^{-Cq}$. Then, the expression was normalized by dividing it by the normalization factor (the geometric mean of the non-normalized expression of the selected reference genes) [89].

The statistical analyses were performed with the IBM SPSS Statistics 24.0 package (IBM SPSS, Chicago, IL, USA). The data were tested for normality (Shapiro–Wilk test) and for homogeneity of variance (Levene's test). The gene expression was log-transformed (base 2) to meet the requirements of normality and homogeneity of variances. The expression of target genes in domoic acid-exposed scallops (groups DB and DA) in relation to the control group was compared using ANOVA and post hoc Dunnett's *t* test. $p < 0.05$ was considered statistically significant.

Supplementary Materials: The following are available online at http://www.mdpi.com/2072-6651/11/2/97/s1, Table S1: Wet weight and domoic acid content of the queen scallops (*A. opercularis*) in the three groups of the study; Table S2: List of level-2 enriched gene ontology (GO) terms for differentially expressed genes in biological process (BP), molecular function (MF), and cellular component (CC) categories; Figure S1: Network showing interactions (confidence view) of proteins coded by genes up-regulated in the present study; Figure S2: Network showing interactions (confidence view) of proteins coded by genes down-regulated in the present study; Figure S3: Fluorescence (relative units), dissolved oxygen (mL/L), salinity, temperature (°C), and light transmission (%) of the seawater between 1- and 5-m depth between April 9 and May 12, in the area of CIMA (laboratory), and GROVE (transplanted scallops); File S1: Nucleotide sequences of differentially expressed genes (in fasta format); File S2: List of differentially expressed genes in groups DA and DB (in relation to the control group); File S3: Significantly enriched Pfam families among the differentially expressed genes; File S4: Significantly enriched GO terms; File S5: List of KO (KEGG Orthologues) for the differentially expressed genes and for all the genes; File S6: Results of a Blastx search of up-regulated genes against the STRING human protein database (9606.protein.sequences.v10.fa), and list of input proteins in STRING network analysis; File S7: Results of a Blastx search of down-regulated genes against the STRING human protein database (9606.protein.sequences.v10.fa), and list of input proteins in STRING network analysis; and File S8: List of the differentially expressed genes belonging to the solute carriers (*SLC*) superfamily.

Author Contributions: A.J.P., M.L.P.-P., J.B., and J.L.S. conceived of and designed the experiments; J.B. performed the intoxication experiments and the determination of the domoic acid content; J.C.T. performed the de novo assembly and several bioinformatics analyses; P.V., A.J.P, M.L.P.-P., and J.L.S performed the RNA extraction, the RT-qPCR experiments, and several bioinformatics analyses; and P.V., A.J.P., M.L.P.-P., J.B., J.C.T., and J.L.S. wrote the manuscript.

Funding: This work has been supported by the Spanish Ministry MINECO (Ministerio de Economía y Competitividad) and the FEDER Funds (European Regional Development Fund) of the European Union under the project AGL2012-39972-C02.

Acknowledgments: We acknowledge Carmen Mariño and Helena Martín (CIMA) for their technical assistance in toxin determination, and the Biotoxins and Sampling departments of INTECMAR for sharing the information required to choose the place and time to carry out the experiment and for supplying the biological samples. We thank John Souto for his helpful comments on the English version of the manuscript.

Conflicts of Interest: The authors declare no conflicts of interest. The funders had no role in the design of the study; in the collection, analyses, or interpretation of the data; in the writing of the manuscript; or in the decision to publish the results.

References

1. Bates, S.S.; Hubbard, K.A.; Lundholm, N.; Montresor, M.; Leaw, C.P. Pseudo-nitzschia, Nitzschia, and domoic acid: New research since 2011. *Harmful Algae* **2018**, *79*, 3–43. [CrossRef] [PubMed]
2. Bates, S.S.; Bird, C.J.; de Freitas, A.S.W.; Foxall, R.; Gilgan, M.; Hanic, L.A.; Johnson, G.R.; McCulloch, A.W.; Odense, P.; Pocklington, R.; et al. Pennate Diatom Nitzschia pungens as the Primary Source of Domoic Acid, a Toxin in Shellfish from Eastern Prince Edward Island, Canada. *Can. J. Fish. Aquat. Sci.* **1989**, *46*, 1203–1215. [CrossRef]
3. Lefebvre, K.A.; Robertson, A. Domoic acid and human exposure risks: A review. *Toxicon* **2010**, *56*, 218–230. [CrossRef] [PubMed]
4. Pulido, O.M. Domoic Acid Toxicologic Pathology: A Review. *Mar. Drugs* **2008**, *6*, 180–219. [CrossRef] [PubMed]
5. Lelong, A.; Hégaret, H.; Soudant, P.; Bates, S.S. Pseudo-nitzschia (Bacillariophyceae) species, domoic acid and amnesic shellfish poisoning: Revisiting previous paradigms. *Phycologia* **2012**, *51*, 168–216. [CrossRef]
6. Trainer, V.L.; Bates, S.S.; Lundholm, N.; Thessen, A.E.; Cochlan, W.P.; Adams, N.G.; Trick, C.G. Pseudo-nitzschia physiological ecology, phylogeny, toxicity, monitoring and impacts on ecosystem health. *Harmful Algae* **2012**, *14*, 271–300. [CrossRef]
7. Blanco, J.; Acosta, C.P.; Bermúdez De La Puente, M.; Salgado, C. Depuration and anatomical distribution of the amnesic shellfish poisoning (ASP) toxin domoic acid in the king scallop Pecten maximus. *Aquat. Toxicol.* **2002**, *60*, 111–121. [CrossRef]
8. Blanco, J.; de la Puente, M.B.; Arévalo, F.; Salgado, C.; Moroño, Á. Depuration of mussels (Mytilus galloprovincialis) contaminated with domoic acid. *Aquat. Living Resour.* **2002**, *15*, 53–60. [CrossRef]
9. Mafra, L.L., Jr.; Bricelj, V.M.; Fennel, K. Domoic acid uptake and elimination kinetics in oysters and mussels in relation to body size and anatomical distribution of toxin. *Aquat. Toxicol.* **2010**, *100*, 17–29. [CrossRef] [PubMed]
10. Novaczek, I.; Madhyastha, M.S.; Ablett, R.F.; Johnson, G.; Nijjar, M.S.; Sims, D.E. Uptake, disposition and depuration of domoic acid by blue mussels (Mytilus edulis). *Aquat. Toxicol.* **1991**, *21*, 103–118. [CrossRef]
11. Novaczek, I.; Madhyastha, M.S.; Ablett, R.F.; Donald, A.; Johnson, G.; Nijjar, M.S.; Sims, D.E. Depuration of Domoic Acid from Live Blue Mussels (*Mytilus edulis*). *Can. J. Fish. Aquat. Sci.* **1992**, *49*, 312–318. [CrossRef]
12. Trainer, V.L.; Bill, B.D. Characterization of a domoic acid binding site from Pacific razor clam. *Aquat. Toxicol.* **2004**, *69*, 125–132. [CrossRef] [PubMed]
13. Madhyastha, M.S.; Novaczek, I.; Ablett, R.F.; Johnson, G.; Nijjar, M.S.; Sims, D.E. In vitro study of domoic acid uptake by gland tissue of blue mussel (Mytilus L.). *Aquat. Toxicol.* **1991**, *20*, 73–81. [CrossRef]
14. Wright, J.L.C.; Boyd, R.K.; de Freitas, A.S.W.; Falk, M.; Foxall, R.A.; Jamieson, W.D.; Laycock, M.V.; McCulloch, A.W.; McInnes, A.G.; Odense, P.; et al. Identification of domoic acid, a neuroexcitatory amino acid, in toxic mussels from eastern Prince Edward Island. *Can. J. Chem.* **1989**, *67*, 481–490. [CrossRef]
15. Mauriz, A.; Blanco, J. Distribution and linkage of domoic acid (amnesic shellfish poisoning toxins) in subcellular fractions of the digestive gland of the scallop Pecten maximus. *Toxicon* **2010**, *55*, 606–611. [CrossRef] [PubMed]

16. Dizer, H.; Fischer, B.; Harabawy, A.S.A.; Hennion, M.-C.; Hansen, P.-D. Toxicity of domoic acid in the marine mussel Mytilus edulis. *Aquat. Toxicol.* **2001**, *55*, 149–156. [CrossRef]
17. Jones, T.O.; Whyte, J.N.C.; Townsend, L.D.; Ginther, N.G.; Iwama, G.K. Effects of domoic acid on haemolymph pH, PCO2 and PO2 in the Pacific oyster, Crassostrea gigas and the California mussel, Mytilus californianus. *Aquat. Toxicol.* **1995**, *31*, 43–55. [CrossRef]
18. Jones, T.O.; Whyte, J.N.C.; Ginther, N.G.; Townsend, L.D.; Iwama, G.K. Haemocyte changes in the pacific oyster, crassostrea gigas, caused by exposure to domoic acid in the diatom pseudonitzschia pungens f. multiseries. *Toxicon* **1995**, *33*, 347–353. [CrossRef]
19. Liu, H.; Kelly, M.S.; Campbell, D.A.; Dong, S.L.; Zhu, J.X.; Wang, S.F. Exposure to domoic acid affects larval development of king scallop Pecten maximus (Linnaeus, 1758). *Aquat. Toxicol.* **2007**, *81*, 152–158. [CrossRef] [PubMed]
20. Liu, H.; Kelly, M.S.; Campbell, D.A.; Fang, J.; Zhu, J. Accumulation of domoic acid and its effect on juvenile king scallop *Pecten maximus*(Linnaeus, 1758). *Aquaculture* **2008**, *284*, 224–230.
21. González, P.M.; Puntarulo, S. Seasonality and toxins effects on oxidative/nitrosative metabolism in digestive glands of the bivalve Mytilus edulis platensis. *Comp. Biochem. Physiol. A. Mol. Integr. Physiol.* **2016**, *200*, 79–86. [CrossRef] [PubMed]
22. Malanga, G.; González, P.M.; Ostera, J.M.; Puntarulo, S. Oxidative stress in the hydrophilic medium of algae and invertebrates. *Biocell* **2016**, *40*, 35–38.
23. Hégaret, H.; Silva, P.M.; Wikfors, G.H.; Haberkorn, H.; Shumway, S.E.; Soudant, P. In vitro interactions between several species of harmful algae and haemocytes of bivalve molluscs. *Cell Biol. Toxicol.* **2011**, *27*, 249–266. [CrossRef] [PubMed]
24. Hiolski, E.M.; Kendrick, P.S.; Frame, E.R.; Myers, M.S.; Bammler, T.K.; Beyer, R.P.; Farin, F.M.; Wilkerson, H.; Smith, D.R.; Marcinek, D.J.; et al. Chronic low-level domoic acid exposure alters gene transcription and impairs mitochondrial function in the CNS. *Aquat. Toxicol.* **2014**, *155*, 151–159. [CrossRef] [PubMed]
25. Giordano, G.; White, C.C.; McConnachie, L.A.; Fernandez, C.; Kavanagh, T.J.; Costa, L.G. Neurotoxicity of Domoic Acid in Cerebellar Granule Neurons in a Genetic Model of Glutathione Deficiency. *Mol. Pharmacol.* **2006**, *70*, 2116–2126. [CrossRef] [PubMed]
26. Giordano, G.; White, C.C.; Mohar, I.; Kavanagh, T.J.; Costa, L.G. Glutathione Levels Modulate Domoic Acid–Induced Apoptosis in Mouse Cerebellar Granule Cells. *Toxicol. Sci.* **2007**, *100*, 433–444. [CrossRef] [PubMed]
27. Xu, R.; Tao, Y.; Wu, C.; Yi, J.; Yang, Y.; Yang, R.; Hong, D. Domoic acid induced spinal cord lesions in adult mice: Evidence for the possible molecular pathways of excitatory amino acids in spinal cord lesions. *NeuroToxicology* **2008**, *29*, 700–707. [CrossRef] [PubMed]
28. Wang, L.; Liang, X.-F.; Huang, Y.; Li, S.-Y.; Ip, K.-C. Transcriptional responses of xenobiotic metabolizing enzymes, HSP70 and Na+/K+-ATPase in the liver of rabbitfish (Siganus oramin) intracoelomically injected with amnesic shellfish poisoning toxin. *Environ. Toxicol.* **2008**, *23*, 363–371. [CrossRef] [PubMed]
29. Ryan, J.C.; Morey, J.S.; Ramsdell, J.S.; van Dolah, F.M. Acute phase gene expression in mice exposed to the marine neurotoxin domoic acid. *Neuroscience* **2005**, *136*, 1121–1132. [CrossRef] [PubMed]
30. Lefebvre, K.A.; Tilton, S.C.; Bammler, T.K.; Beyer, R.P.; Srinouanprachan, S.; Stapleton, P.L.; Farin, F.M.; Gallagher, E.P. Gene Expression Profiles in Zebrafish Brain after Acute Exposure to Domoic Acid at Symptomatic and Asymptomatic Doses. *Toxicol. Sci.* **2009**, *107*, 65–77. [CrossRef] [PubMed]
31. Pazos, A.J.; Ventoso, P.; Martínez-Escauriaza, R.; Pérez-Parallé, M.L.; Blanco, J.; Triviño, J.C.; Sánchez, J.L. Transcriptional response after exposure to domoic acid-producing Pseudo-nitzschia in the digestive gland of the mussel Mytilus galloprovincialis. *Toxicon* **2017**, *140*, 60–71. [CrossRef] [PubMed]
32. Chi, C.; Giri, S.S.; Jun, J.W.; Kim, S.W.; Kim, H.J.; Kang, J.W.; Park, S.C. Detoxification- and Immune-Related Transcriptomic Analysis of Gills from Bay Scallops (Argopecten irradians) in Response to Algal Toxin Okadaic Acid. *Toxins* **2018**, *10*, 308. [CrossRef] [PubMed]
33. Detree, C.; Núñez-Acuña, G.; Roberts, S.; Gallardo-Escárate, C. Uncovering the Complex Transcriptome Response of Mytilus chilensis against Saxitoxin: Implications of Harmful Algal Blooms on Mussel Populations. *PLoS ONE* **2016**, *11*, e0165231. [CrossRef] [PubMed]

34. Gerdol, M.; Moro, G.D.; Manfrin, C.; Milandri, A.; Riccardi, E.; Beran, A.; Venier, P.; Pallavicini, A. RNA sequencing and de novo assembly of the digestive gland transcriptome in Mytilus galloprovincialis fed with toxinogenic and non-toxic strains of Alexandrium minutum. *BMC Res. Notes* **2014**, *7*, 722. [CrossRef] [PubMed]
35. Li, Y.; Sun, X.; Hu, X.; Xun, X.; Zhang, J.; Guo, X.; Jiao, W.; Zhang, L.; Liu, W.; Wang, J.; et al. Scallop genome reveals molecular adaptations to semi-sessile life and neurotoxins. *Nat. Commun.* **2017**, *8*, 1721. [CrossRef]
36. Prego-Faraldo, M.; Martínez, L.; Méndez, J. RNA-Seq Analysis for Assessing the Early Response to DSP Toxins in Mytilus galloprovincialis Digestive Gland and Gill. *Toxins* **2018**, *10*, 417. [CrossRef]
37. Franceschini, A.; Szklarczyk, D.; Frankild, S.; Kuhn, M.; Simonovic, M.; Roth, A.; Lin, J.; Minguez, P.; Bork, P.; von Mering, C.; et al. STRING v9.1: Protein-protein interaction networks, with increased coverage and integration. *Nucleic Acids Res.* **2013**, *41*, D808–D815. [CrossRef]
38. Vandesompele, J.; De Preter, K.; Pattyn, F.; Poppe, B.; Van Roy, N.; De Paepe, A.; Speleman, F. Accurate normalization of real-time quantitative RT-PCR data by geometric averaging of multiple internal control genes. *Genome Biol.* **2002**, *3*, research0034.1. [CrossRef]
39. Ling, D.; Salvaterra, P.M. Robust RT-qPCR Data Normalization: Validation and Selection of Internal Reference Genes during Post-Experimental Data Analysis. *PLoS ONE* **2011**, *6*, e17762. [CrossRef]
40. Prego-Faraldo, M.V.; Vieira, L.R.; Eirin-Lopez, J.M.; Méndez, J.; Guilhermino, L. Transcriptional and biochemical analysis of antioxidant enzymes in the mussel Mytilus galloprovincialis during experimental exposures to the toxic dinoflagellate Prorocentrum lima. *Mar. Environ. Res.* **2017**, *129*, 304–315. [CrossRef]
41. Anderson, K.; Taylor, D.A.; Thompson, E.L.; Melwani, A.R.; Nair, S.V.; Raftos, D.A. Meta-Analysis of Studies Using Suppression Subtractive Hybridization and Microarrays to Investigate the Effects of Environmental Stress on Gene Transcription in Oysters. *PLoS ONE* **2015**, *10*, e0118839. [CrossRef] [PubMed]
42. Livneh, I.; Cohen-Kaplan, V.; Cohen-Rosenzweig, C.; Avni, N.; Ciechanover, A. The life cycle of the 26S proteasome: From birth, through regulation and function, and onto its death. *Cell Res.* **2016**, *26*, 869–885. [CrossRef] [PubMed]
43. Shang, F.; Taylor, A. Ubiquitin-proteasome pathway and cellular responses to oxidative stress. *Free Radic. Biol. Med.* **2011**, *51*, 5–16. [CrossRef] [PubMed]
44. Dogovski, C.; Xie, S.C.; Burgio, G.; Bridgford, J.; Mok, S.; McCaw, J.M.; Chotivanich, K.; Kenny, S.; Gnädig, N.; Straimer, J.; et al. Targeting the Cell Stress Response of Plasmodium falciparum to Overcome Artemisinin Resistance. *PLOS Biol.* **2015**, *13*, e1002132. [CrossRef] [PubMed]
45. Manfrin, C.; Dreos, R.; Battistella, S.; Beran, A.; Gerdol, M.; Varotto, L.; Lanfranchi, G.; Venier, P.; Pallavicini, A. Mediterranean Mussel Gene Expression Profile Induced by Okadaic Acid Exposure. *Environ. Sci. Technol.* **2010**, *44*, 8276–8283. [CrossRef] [PubMed]
46. Peña-Llopis, S.; Serrano, R.; Pitarch, E.; Beltrán, E.; Ibáñez, M.; Hernández, F.; Peña, J.B. N-Acetylcysteine boosts xenobiotic detoxification in shellfish. *Aquat. Toxicol.* **2014**, *154*, 131–140. [CrossRef] [PubMed]
47. Kimura, O.; Kotaki, Y.; Hamaue, N.; Haraguchi, K.; Endo, T. Transcellular transport of domoic acid across intestinal Caco-2 cell monolayers. *Food Chem. Toxicol.* **2011**, *49*, 2167–2171. [CrossRef]
48. Smith, Q.R. Transport of glutamate and other amino acids at the blood-brain barrier. *J. Nutr.* **2000**, *130*, 1016S–1022S. [CrossRef]
49. Hoglund, P.J.; Nordstrom, K.J.V.; Schioth, H.B.; Fredriksson, R. The Solute Carrier Families Have a Remarkably Long Evolutionary History with the Majority of the Human Families Present before Divergence of Bilaterian Species. *Mol. Biol. Evol.* **2011**, *28*, 1531–1541. [CrossRef]
50. Hediger, M.A.; Clémençon, B.; Burrier, R.E.; Bruford, E.A. The ABCs of membrane transporters in health and disease (SLC series): Introduction. *Mol. Aspects Med.* **2013**, *34*, 95–107. [CrossRef]
51. SLC Tables. Available online: http://slc.bioparadigms.org/ (accessed on 15 December 2018).
52. Halestrap, A.P. The SLC16 gene family—Structure, role and regulation in health and disease. *Mol. Aspects Med.* **2013**, *34*, 337–349. [CrossRef] [PubMed]
53. Koepsell, H. The SLC22 family with transporters of organic cations, anions and zwitterions. *Mol. Aspects Med.* **2013**, *34*, 413–435. [CrossRef] [PubMed]
54. Schultz, I.R.; Skillman, A.; Sloan-Evans, S.; Woodruff, D. Domoic acid toxicokinetics in Dungeness crabs: New insights into mechanisms that regulate bioaccumulation. *Aquat. Toxicol.* **2013**, *140*, 77–88. [CrossRef] [PubMed]

55. Chi, C.; Giri, S.S.; Jun, J.W.; Kim, H.J.; Yun, S.; Kim, S.G.; Park, S.C. Marine Toxin Okadaic Acid Affects the Immune Function of Bay Scallop (Argopecten irradians). *Molecules* **2016**, *21*, 1108. [CrossRef] [PubMed]
56. Astuya, A.; Carrera, C.; Ulloa, V.; Aballay, A.; Núñez-Acuña, G.; Hégaret, H.; Gallardo-Escárate, C. Saxitoxin Modulates Immunological Parameters and Gene Transcription in Mytilus chilensis Hemocytes. *Int. J. Mol. Sci.* **2015**, *16*, 15235–15250. [CrossRef] [PubMed]
57. Núñez-Acuña, G.; Aballay, A.E.; Hégaret, H.; Astuya, A.P.; Gallardo-Escárate, C. Transcriptional responses of Mytilus chilensis exposed in vivo to saxitoxin (STX). *J. Molluscan Stud.* **2013**, *79*, 323–331. [CrossRef]
58. Gerdol, M.; Venier, P.; Pallavicini, A. The genome of the Pacific oyster Crassostrea gigas brings new insights on the massive expansion of the C1q gene family in Bivalvia. *Dev. Comp. Immunol.* **2015**, *49*, 59–71. [CrossRef] [PubMed]
59. Gerdol, M.; Venier, P. An updated molecular basis for mussel immunity. *Fish Shellfish Immunol.* **2015**, *46*, 17–38. [CrossRef] [PubMed]
60. Leite, R.B.; Milan, M.; Coppe, A.; Bortoluzzi, S.; dos Anjos, A.; Reinhardt, R.; Saavedra, C.; Patarnello, T.; Cancela, M.L.; Bargelloni, L. mRNA-Seq and microarray development for the Grooved carpet shell clam, Ruditapes decussatus: A functional approach to unravel host -parasite interaction. *BMC Genomics* **2013**, *14*, 741. [CrossRef] [PubMed]
61. Gerdol, M.; Manfrin, C.; De Moro, G.; Figueras, A.; Novoa, B.; Venier, P.; Pallavicini, A. The C1q domain containing proteins of the Mediterranean mussel Mytilus galloprovincialis: A widespread and diverse family of immune-related molecules. *Dev. Comp. Immunol.* **2011**, *35*, 635–643. [CrossRef] [PubMed]
62. Zhang, L.; Li, L.; Guo, X.; Litman, G.W.; Dishaw, L.J.; Zhang, G. Massive expansion and functional divergence of innate immune genes in a protostome. *Sci. Rep.* **2015**, *5*, 8693. [CrossRef] [PubMed]
63. Philipp, E.E.R.; Kraemer, L.; Melzner, F.; Poustka, A.J.; Thieme, S.; Findeisen, U.; Schreiber, S.; Rosenstiel, P. Massively Parallel RNA Sequencing Identifies a Complex Immune Gene Repertoire in the lophotrochozoan Mytilus edulis. *PLoS ONE* **2012**, *7*, e33091. [CrossRef] [PubMed]
64. Espinosa, E.P.; Allam, B. Reverse genetics demonstrate the role of mucosal C-type lectins in food particle selection in the oyster Crassostrea virginica. *J. Exp. Biol.* **2018**, *221*, jeb-174094. [CrossRef] [PubMed]
65. Zhang, G.; Fang, X.; Guo, X.; Li, L.; Luo, R.; Xu, F.; Yang, P.; Zhang, L.; Wang, X.; Qi, H.; et al. The oyster genome reveals stress adaptation and complexity of shell formation. *Nature* **2012**, *490*, 49–54. [CrossRef] [PubMed]
66. Ricard-Blum, S. The Collagen Family. *Cold Spring Harb. Perspect. Biol.* **2011**, *3*. [CrossRef] [PubMed]
67. Cheng, J.; Xun, X.; Kong, Y.; Wang, S.; Yang, Z.; Li, Y.; Kong, D.; Wang, S.; Zhang, L.; Hu, X.; et al. Hsp70 gene expansions in the scallop Patinopecten yessoensis and their expression regulation after exposure to the toxic dinoflagellate Alexandrium catenella. *Fish Shellfish Immunol.* **2016**, *58*, 266–273. [CrossRef] [PubMed]
68. Cao, R.; Wang, D.; Wei, Q.; Wang, Q.; Yang, D.; Liu, H.; Dong, Z.; Zhang, X.; Zhang, Q.; Zhao, J. Integrative Biomarker Assessment of the Influence of Saxitoxin on Marine Bivalves: A Comparative Study of the Two Bivalve Species Oysters, Crassostrea gigas, and Scallops, Chlamys farreri. *Front. Physiol.* **2018**, *9*. [CrossRef] [PubMed]
69. Mello, D.F.; De Oliveira, E.S.; Vieira, R.C.; Simoes, E.; Trevisan, R.; Dafre, A.L.; Barracco, M.A. Cellular and Transcriptional Responses of Crassostrea gigas Hemocytes Exposed in Vitro to Brevetoxin (PbTx-2). *Mar. Drugs* **2012**, *10*, 583–597. [CrossRef] [PubMed]
70. Volland, M.; Blasco, J.; Hampel, M. Validation of reference genes for RT-qPCR in marine bivalve ecotoxicology: Systematic review and case study using copper treated primary Ruditapes philippinarum hemocytes. *Aquat. Toxicol.* **2017**, *185*, 86–94. [CrossRef] [PubMed]
71. Martínez-Escauriaza, R.; Lozano, V.; Pérez-Parallé, M.L.; Pazos, A.J.; Sánchez, J.L. Validation of Reference Genes in Mussel Mytilus galloprovincialis Tissues under the Presence of Okadaic Acid. *J. Shellfish Res.* **2018**, *37*, 93–101. [CrossRef]
72. Intecmar, Xunta de Galicia. Available online: http://www.intecmar.gal/ (accessed on 15 December 2018).
73. Schulz, M.H.; Zerbino, D.R.; Vingron, M.; Birney, E. Oases: Robust de novo RNA-seq assembly across the dynamic range of expression levels. *Bioinformatics* **2012**, *28*, 1086–1092. [CrossRef]
74. Grabherr, M.G.; Haas, B.J.; Yassour, M.; Levin, J.Z.; Thompson, D.A.; Amit, I.; Adiconis, X.; Fan, L.; Raychowdhury, R.; Zeng, Q.; et al. Full-length transcriptome assembly from RNA-Seq data without a reference genome. *Nat. Biotechnol.* **2011**, *29*, 644–652. [CrossRef] [PubMed]

75. Langmead, B.; Salzberg, S.L. Fast gapped-read alignment with Bowtie 2. *Nat. Methods* **2012**, *9*, 357–359. [CrossRef] [PubMed]
76. Benjamini, Y.; Hochberg, Y. Controlling the False Discovery Rate: A Practical and Powerful Approach to Multiple Testing. *J. R. Stat. Soc. Ser. B Methodol.* **1995**, *57*, 289–300. [CrossRef]
77. Altschul, S.F.; Gish, W.; Miller, W.; Myers, E.W.; Lipman, D.J. Basic local alignment search tool. *J. Mol. Biol.* **1990**, *215*, 403–410. [CrossRef]
78. Conesa, A.; Götz, S.; García-Gómez, J.M.; Terol, J.; Talón, M.; Robles, M. Blast2GO: A universal tool for annotation, visualization and analysis in functional genomics research. *Bioinformatics* **2005**, *21*, 3674–3676. [CrossRef] [PubMed]
79. Götz, S.; García-Gómez, J.M.; Terol, J.; Williams, T.D.; Nagaraj, S.H.; Nueda, M.J.; Robles, M.; Talón, M.; Dopazo, J.; Conesa, A. High-throughput functional annotation and data mining with the Blast2GO suite. *Nucleic Acids Res.* **2008**, *36*, 3420–3435. [CrossRef]
80. Moriya, Y.; Itoh, M.; Okuda, S.; Yoshizawa, A.C.; Kanehisa, M. KAAS: An automatic genome annotation and pathway reconstruction server. *Nucleic Acids Res.* **2007**, *35*, W182–W185. [CrossRef]
81. Finn, R.D.; Coggill, P.; Eberhardt, R.Y.; Eddy, S.R.; Mistry, J.; Mitchell, A.L.; Potter, S.C.; Punta, M.; Qureshi, M.; Sangrador-Vegas, A.; et al. The Pfam protein families database: Towards a more sustainable future. *Nucleic Acids Res.* **2016**, *44*, D279–D285. [CrossRef]
82. Johnson, N.L.; Kotz, S.; Kemp, A.W. *Univariate Discrete Distributions*, 2nd ed.; John Wiley & Sons: New York, NY, USA.
83. Fisher, R.A. On the Interpretation of $\chi 2$ from Contingency Tables, and the Calculation of P. *J. R. Stat. Soc.* **1922**, *85*, 87–94. [CrossRef]
84. Szklarczyk, D.; Franceschini, A.; Wyder, S.; Forslund, K.; Heller, D.; Huerta-Cepas, J.; Simonovic, M.; Roth, A.; Santos, A.; Tsafou, K.P.; et al. STRING v10: Protein–protein interaction networks, integrated over the tree of life. *Nucleic Acids Res.* **2015**, *43*, D447–D452. [CrossRef] [PubMed]
85. Altschul, S.F.; Madden, T.L.; Schäffer, A.A.; Zhang, J.; Zhang, Z.; Miller, W.; Lipman, D.J. Gapped BLAST and PSI-BLAST: A new generation of protein database search programs. *Nucleic Acids Res.* **1997**, *25*, 3389–3402. [CrossRef] [PubMed]
86. Andersen, C.L.; Jensen, J.L.; Ørntoft, T.F. Normalization of Real-Time Quantitative Reverse Transcription-PCR Data: A Model-Based Variance Estimation Approach to Identify Genes Suited for Normalization, Applied to Bladder and Colon Cancer Data Sets. *Cancer Res.* **2004**, *64*, 5245–5250. [CrossRef] [PubMed]
87. Bustin, S.A.; Benes, V.; Garson, J.A.; Hellemans, J.; Huggett, J.; Kubista, M.; Mueller, R.; Nolan, T.; Pfaffl, M.W.; Shipley, G.L.; et al. The MIQE Guidelines: Minimum Information for Publication of Quantitative Real-Time PCR Experiments. *Clin. Chem.* **2009**, *55*, 611–622. [CrossRef] [PubMed]
88. Pfaffl, M.W.; Tichopad, A.; Prgomet, C.; Neuvians, T.P. Determination of stable housekeeping genes, differentially regulated target genes and sample integrity: BestKeeper—Excel-based tool using pair-wise correlations. *Biotechnol. Lett.* **2004**, *26*, 509–515. [CrossRef]
89. Mauriz, O.; Maneiro, V.; Pérez-Parallé, M.L.; Sánchez, J.L.; Pazos, A.J. Selection of reference genes for quantitative RT-PCR studies on the gonad of the bivalve mollusc Pecten maximus L. *Aquaculture* **2012**, *370–371*, 158–165. [CrossRef]
90. Zhao, S.; Fernald, R.D. Comprehensive Algorithm for Quantitative Real-Time Polymerase Chain Reaction. *J. Comput. Biol. J. Comput. Mol. Cell Biol.* **2005**, *12*, 1047–1064. [CrossRef] [PubMed]

A1.3 TRANSCRIPTIONAL RESPONSE IN THE DIGESTIVE GLAND OF THE KING SCALLOP (PECTEN MAXIMUS) AFTER THE INJECTION OF DOMOIC ACID

A1.3.1 Características de la publicación

Estado: Publicado
Título: Transcriptional response in the digestive gland of the king scallop (Pecten maximus) after the injection of domoic acid
Nombre de la revista: Toxins
Editorial: MDPI
Autores: Ventoso Pablo, Antonio J. Pazos, Juan Blanco, M. Luz Pérez-Parallé, Juan C. Triviño, y José L. Sánchez
Contribución específica del doctorado: Investigación, redacción (revisión y edición)
Año publicación: 2021
Volumen: 13 (339)
DOI: https://doi.org/10.3390/toxins13050339
Autorización de la revista: No es necesaria autorización de la editorial y/o revista. Al tratarse de una revista de acceso abierto se permite su uso para la elaboración de tesis doctorales. (https://www.mdpi.com/openaccess)

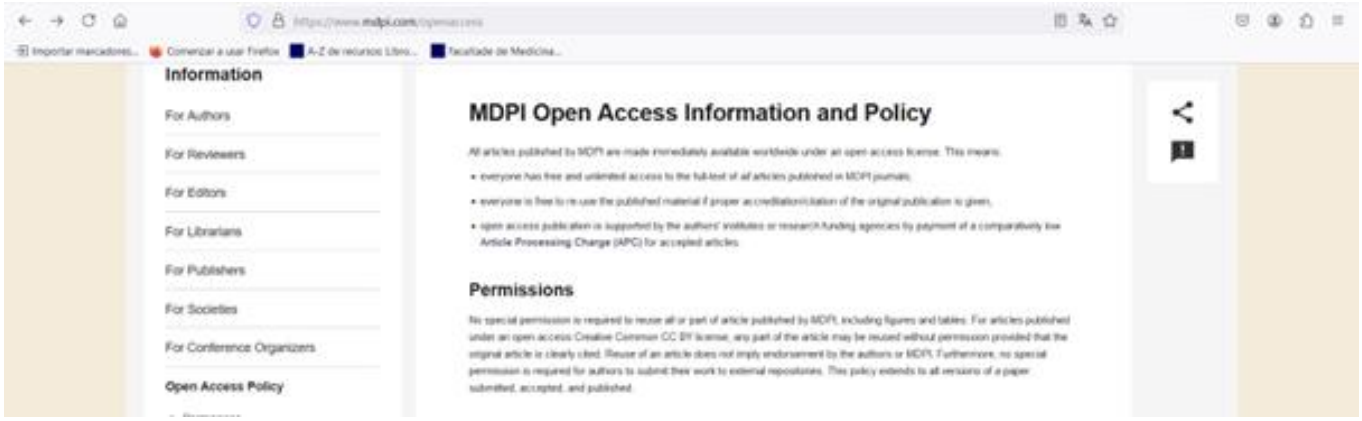

A1.3.2 Indicios de calidad de la revista

Scientific Journal Rankings (SJR): 0,884
Cuartil (2021): 1 - Área: Health, Toxicology and Mutagenesis; Toxicology
Journal Impact Factor (JIF): 5,075
Cuartil (2021): 1 - Área: Food Science & Technology; Toxicology
Journal Citation Indicator (JCI): 0,96
Cuartil (2021): 1 - Área: Food Science & Technology; Toxicology

A1.3.3 Impacto de la publicación

Citas: Citas: 10 (Scopus), 13 (Google Scholar), 10 (Web of Science)

toxins

MDPI

Article

Transcriptional Response in the Digestive Gland of the King Scallop (*Pecten maximus*) After the Injection of Domoic Acid

Pablo Ventoso [1], Antonio J. Pazos [1,*], Juan Blanco [2], M. Luz Pérez-Parallé [1], Juan C. Triviño [3] and José L. Sánchez [1]

[1] Departamento de Bioquímica y Biología Molecular, Instituto de Acuicultura, University of Santiago de Compostela, 15782 Santiago de Compostela, Spain; pabloventoso24@hotmail.com (P.V.); luz.perez-paralle@usc.es (M.L.P.-P.); joseluis.sanchez@usc.es (J.L.S.)
[2] Centro de Investigacións Mariñas, Xunta de Galicia, Pedras de Corón s/n Apdo. 13, 36620 Vilanova de Arousa, Spain; juan.carlos.blanco.perez@xunta.gal
[3] Sistemas Genómicos, Ronda G. Marconi 6, Paterna, 46980 Valencia, Spain; jc.trivino@sistemasgenomicos.com
* Correspondence: antonioj.pazos@usc.es

Abstract: Some diatom species of the genus *Pseudo-nitzschia* produce the toxin domoic acid. The depuration rate of domoic acid in *Pecten maximus* is very low; for this reason, king scallops generally contain high levels of domoic acid in their tissues. A transcriptomic approach was used to identify the genes differentially expressed in the *P. maximus* digestive gland after the injection of domoic acid. The differential expression analysis found 535 differentially expressed genes (226 up-regulated and 309 down-regulated). Protein–protein interaction networks obtained with the up-regulated genes were enriched in gene ontology terms, such as vesicle-mediated transport, response to stress, signal transduction, immune system process, RNA metabolic process, and autophagy, while networks obtained with the down-regulated genes were enriched in gene ontology terms, such as response to stress, immune system process, ribosome biogenesis, signal transduction, and mRNA processing. Genes that code for cytochrome P450 enzymes, glutathione S-transferase theta-1, glutamine synthase, pyrroline-5-carboxylate reductase 2, and sodium- and chloride-dependent glycine transporter 1 were among the up-regulated genes. Therefore, a stress response at the level of gene expression, that could be caused by the domoic acid injection, was evidenced by the alteration of several biological, cellular, and molecular processes.

Keywords: amnesic shellfish poisoning (ASP); bivalves; RNA-seq; transcriptome; differential expression; DEGs; injection

Key Contribution: The results show that some processes were altered in the digestive gland of *Pecten maximus*, probably due to the action of domoic acid. Thus, vesicle-mediated transport, response to stress, signal transduction, immune system process, RNA metabolic process, autophagy, and oxidoreductase activity were terms enriched in the protein interaction network obtained with the up-regulated genes, whereas that response to stress, immune system process, ribosome biogenesis, signal transduction, mRNA processing, and oxidoreductase activity were terms enriched in the down-regulated genes. Some effects of domoic acid may be mediated by glutamate receptors since we found the mRNA expression of genes coding for putative glutamate receptors in the digestive gland of *Pecten maximus*.

check for updates

Citation: Ventoso, P.; Pazos, A.J.; Blanco, J.; Pérez-Parallé, M.L.; Triviño, J.C.; Sánchez, J.L. Transcriptional Response in the Digestive Gland of the King Scallop (*Pecten maximus*) After the Injection of Domoic Acid. *Toxins* **2021**, *13*, 339. https://doi.org/10.3390/toxins13050339

Received: 26 March 2021
Accepted: 5 May 2021
Published: 7 May 2021

1. Introduction

Some diatom species of the genus *Pseudo-nitzschia* produce domoic acid, a toxin that can cause amnesic shellfish poisoning (ASP) in humans [1–5]. During harmful algae blooms the bivalves accumulate the toxins in their tissues and therefore they can act as vectors of ASP [1–3]. The accumulation of biotoxins in shellfish can cause harvesting closures and thus it has adverse economic impacts. In recent years there has been an increase in the

number of toxigenic *Pseudo-nitzschia* blooms worldwide [2,6]. Domoic acid, an amino acid structurally similar to glutamate and kainic acid, is a glutamate receptor agonist that binds mainly to two subtypes of ionotropic receptors (α-amino-3-hydroxy-5-methylisoxazole-4-propionate, AMPA, and kainate receptors [4,7,8]) and exerts excitotoxic effects in the central nervous system of vertebrates [4,7,8].

The king scallop *Pecten maximus* is a valuable fisheries resource in Europe [9]. Unlike mussels and oysters [10–13], with high domoic acid depuration rates, in the king scallop (*Pecten maximus*) the depuration rate of domoic acid is very low [14,15]. Due to the blooms of domoic acid-producing species of the genus *Pseudo-nitzschia* and the low depuration rate of *P. maximus* [14,15], the domoic acid concentration in this scallop is usually above the regulatory limits (20 μg of domoic acid g^{-1}) in many areas [16]. There are other scallop species (*Placopecten magellanicus* and *Argopecten purpuratus*) that do not show this slow domoic acid depuration [17,18].

Domoic acid in bivalves is mostly unmetabolized and is excreted unchanged [10]. In many bivalves, including the king scallop, the digestive gland is the main organ of accumulation of domoic acid [10,14,15,17,19,20]. In the digestive gland of *P. maximus*, domoic acid was found to be present in the cytosol in soluble form [21], therefore Mauriz and Blanco [21] suggested that the lack of an efficient membrane transporter could be the cause of the low depuration rate. In a recent work, Blanco et al. [16] showed that this toxin, in the digestive gland, is mainly accumulated in large cells (digestive cells) and the concentration was lower in small cells (secretory cells).

Several publications have described the physiological effects of domoic acid and domoic acid-producing organisms on marine bivalves: transient DNA damage in *Mytilus edulis* after de injection of domoic acid [22], mild respiratory alkalosis in *Mytilus californianus* after the exposure to domoic acid-producing *Pseudo-nitzschia* [23], transient respiratory acidosis, hypoxia, and increase in the activity and number of haemocytes in *Crassostrea gigas* following the exposure to domoic acid-producing *Peseudo-nitzschia* [23,24], negative impacts on survival and growth rate in juvenile *Pecten maximus* exposed to domoic acid-spiked feed [25], negative effects on growth and survival in *Pecten maximus* larvae exposed to dissolved domoic acid [26], impairment of immune functions and oxidative stress in *Argopecten irradians* exposed to dissolved domoic acid [27,28]. In two previous works, we studied the transcriptional effects of domoic acid-containing *Pseudo-nitzschia* in the digestive gland of the mussel *Mytilus galloprovincialis* [29] and the queen scallop *Aequipecten opercularis* [30] by means of RNA-seq technology. The results obtained showed the differential expression of genes involved in protection against oxidative stress, the metabolism of xenobiotics (detoxification), transmembrane transport, and immunological processes [29,30]. Oxidative stress is one of the principal effects caused by exposure to domoic acid in vertebrates [31–34], and also in invertebrates [35,36], including marine bivalves (*Argopecten irradians* [28] and *Aequipecten opecularis* [30]), and can play an important role in domoic acid induced toxicity. In the present work, a transcriptomic approach (RNA-seq) has been used to identify the genes differentially expressed in the digestive gland of the king scallop *P. maximus* after the injection of domoic acid, in order to uncover dysregulated biological and molecular processes and contribute to the knowledge of detoxification mechanisms in bivalves.

2. Results

2.1. Domoic Acid Content in the Tissues of P. maximus

Table 1 and Figure 1 display the domoic acid concentration (μg g^{-1}wet weight) and burden (μg) in different *P. maximus* tissues. Due to the low depuration rate of *P. maximus* [14,15], and the blooms of toxigenic *Pseudo-nitzschia*, the king scallops collected in Galicia (NW Spain) have high levels of domoic acid in their body tissues. This explains why domoic acid concentration in the digestive gland (DG) is high in control and treated scallops (2222.9 and 1987.0 μg g^{-1} wet weight, respectively). The domoic acid burden in the digestive gland of control and treated animals was 3690.2 μg and 3884.8 μg, respectively.

The domoic acid content in the digestive gland accounted for 84% of the total domoic acid burden in the body tissues of *P. maximus*, despite the fact that the digestive gland only represented about 7% of the total weight of soft tissues.

Table 1. Domoic acid concentration (μg g^{-1} wet weight) and domoic acid burden (μg) in control and treated scallops (*Pecten maximus*). DG, digestive gland; AM, adductor muscle; Other, remaining tissues.

	Domoic Acid Concentration (μg g^{-1} Wet Weight): Mean ± SD					
	DG	**Kidney**	**Gonad**	**AM**	**Gill**	**Other**
Control	2222.9 ± 551.7	370.7 ± 238.2	39.0 ± 27.2	35.1 ± 44.9	3.9 ± 3.1	14.4 ± 7.0
Treated	1987.0 ± 406.5	1226.3 ± 1037.3	42.9 ± 17.7	22.9 ± 17.0	6.1 ± 6.9	14.7 ± 8.8
	Domoic Acid Burden (μg): Mean ± SD					
	DG	**Kidney**	**Gonad**	**AM**	**Gill**	**Other**
Control	3690.2 ± 1002.5	88.8 ± 48.2	51.2 ± 31.4	385.6 ± 526.9	8.7 ± 6.5	114.2 ± 56.6
Treated	3884.8 ± 988.6	329.0 ± 293.3	64.9 ± 30.8	262.4 ± 191.2	13.2 ± 12.7	123.8 ± 62.6

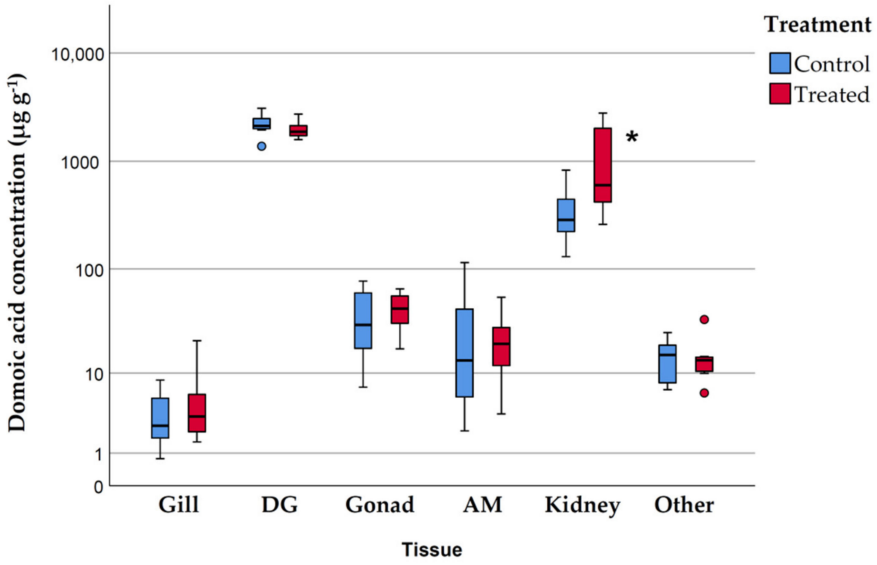

Figure 1. Box plots showing the domoic acid concentration (μg g^{-1} wet weight) in control and treated scallops (*Pecten maximus*). DG, digestive gland; AM adductor muscle; Other, remaining tissues. * significant difference from control (*t*-test, $p < 0.05$).

The kidney (Table 1 and Figure 1) is the only organ that shows a clear increase in the concentration of domoic acid (and in the domoic acid burden) in treated animals (1226.34 μg g^{-1} wet weight) in relation to the control (370.70 μg g^{-1} wet weight). In absolute terms, the greatest increases in the domoic acid burden were found in the kidney followed by the digestive gland (Table 1). Significant differences between control and treated animals were found only in the concentration of domoic acid in the kidney (log10 transformed to meet the assumptions of normality and homoscedasticity; t-test, $p = 0.041$).

Although the experiment was not designed to see the effect of domoic acid on the behavior of scallops, we have observed that the scallops treated with domoic acid maintained a larger valve opening than those injected with seawater, but no mortality was recorded.

2.2. Sequencing and De Novo Assembly

The reads obtained by means of paired-end sequencing in the Illumina Hiseq 2000 platform were de novo assembled with Trinity and Oasis. Then, to reduce redundancy, the assembled transcripts were clustered (homology > 90%), thus 72,673 unigenes were obtained (Table 2). Mean contig length and N50 contig length were 1481 bp and 1883 bp respectively (Table 2). The raw data are accessible from the NCBI Sequence

Read Archive (BioProject ID PRJNA704533, BioSample accessions: SAMN18043529 to SAMN18043540).

Table 2. Summary of the transcriptome assembly for *P. maximus* digestive gland (bp).

Contig N50 Length	1883 bp
Minimum contig length	450 bp
Maximum contig length	18,874 bp
Average contig length	1481 bp
Total length in contigs	107,645,527 bp
Number of assembled unigenes	72,673

A BUSCO analysis of completeness of the de novo assembly identified 82.29% complete orthologs (45.6% single-copy and 36.69% duplicated), 3.88% fragmented orthologs and 13.83% missing orthologs (Table S1). The BUSCO results indicate that our de novo transcriptome assembly is of high quality, and although we only sequenced one tissue (digestive gland) the assembly has a completeness of 86.2%.

2.3. Differential Expression and Functional Annotation

A representation of the differentially expressed genes (DEGs) is displayed in a MA plot (Supplementary Figure S1) and a volcano plot (Supplementary Figure S2). The number of genes with absolute fold change > 1.5 and adjusted *p*-value < 0.05 (DEGs) was 535, of which 226 were up-regulated and 309 down-regulated (Supplementary Files S1 and S2). Tables 3 and 4 display the top 20 significantly up-regulated genes and the top 20 significantly down-regulated genes, respectively.

Table 3. Top 20 up-regulated genes classified by FDR adjusted *p*-value (padj). Only genes with Blastx result are displayed. FC: fold change.

Sequence ID	Description	FC	padj
ci|000200864|proj|Sample_C_D|2	cytochrome P450 2D10-like	16.57	5.88×10^{-6}
ci|000249823|proj|Sample_C_D|2	probable proline iminopeptidase	14.85	1.33×10^{-5}
ci|000199464|proj|Sample_C_D|2	pyrroline-5-carboxylate reductase 2-like	2.68	1.57×10^{-5}
ci|000262059|proj|Sample_C_D|2	integumentary mucin C.1-like	16.32	2.09×10^{-5}
ci|000180736|proj|Sample_C_D|2	exocyst complex component 4-like	2.67	2.82×10^{-5}
ci|000220117|proj|Sample_C_D|2	multiple epidermal growth factor-like domains protein 10	14.30	7.17×10^{-5}
ci|000029875|proj|Sample_C_D|2	cytochrome P450 4F6-like isoform X1	2.48	1.23×10^{-4}
ci|000033337|proj|Sample_C_D|2	uncharacterized protein LOC117330985	4.40	1.90×10^{-4}
ci|000031940|proj|Sample_C_D|2	retinol dehydrogenase 7-like isoform X2	2.51	2.59×10^{-4}
ci|000050118|proj|Sample_C_D|2	4-coumarate–CoA ligase 1-like	2.34	3.48×10^{-4}
ci|000208120|proj|Sample_C_D|2	46 kDa FK506-binding nuclear protein-like	10.84	3.73×10^{-4}
ci|000199228|proj|Sample_C_D|2	cholecystokinin receptor-like	11.25	4.78×10^{-4}
ci|000033677|proj|Sample_C_D|2	ectonucleotide pyrophosphatase/phosphodiesterase family member 5-like isoform X2	8.80	7.96×10^{-4}
ci|000181387|proj|Sample_C_D|2	sodium- and chloride-dependent glycine transporter 1-like	11.00	8.03×10^{-4}
ci|000193220|proj|Sample_C_D|2	uncharacterized protein LOC117327200	10.18	1.27×10^{-3}
ci|000201571|proj|Sample_C_D|2	uncharacterized protein LOC117327200	10.47	1.27×10^{-3}
ci|000216669|proj|Sample_C_D|2	NPC intracellular cholesterol transporter 2-like	9.15	1.48×10^{-3}
ci|000211651|proj|Sample_C_D|2	CD109 antigen-like isoform X1	3.45	1.89×10^{-3}
ci|000199247|proj|Sample_C_D|2	uncharacterized protein LOC117331788	5.65	1.93×10^{-3}
ci|000027261|proj|Sample_C_D|2	zygotic DNA replication licensing factor mcm3-like	2.31	2.16×10^{-3}

Table 4. Top 20 down-regulated genes classified by FDR adjusted *p*-value (padj). Only genes with blastx result are displayed. FC: fold change.

Sequence ID	Description	FC	padj
ci|000057484|proj|Sample_C_D|2	uncharacterized protein LOC110456411 isoform X5	−56.49	1.06×10^{-16}
ci|000056978|proj|Sample_C_D|2	uncharacterized protein LOC110456411 isoform X4	−53.9	7.97×10^{-16}
ci|000094075|proj|Sample_C_D|2	pinin-like	−29.78	2.37×10^{-11}
ci|000008473|proj|Sample_C_D|2	uncharacterized protein LOC117340902	−3.381	3.65×10^{-7}
ci|000008352|proj|Sample_C_D|2	uncharacterized protein LOC117325809 isoform X1	−4.911	3.83×10^{-7}
ci|000077317|proj|Sample_C_D|2	uncharacterized protein LOC117338873	−11.63	4.35×10^{-7}
ci|000097219|proj|Sample_C_D|2	serine protease inhibitor Cvsi-1-like	−16.21	3.09×10^{-6}
ci|000161872|proj|Sample_C_D|2	uncharacterized protein LOC117338873	−14.53	2.04×10^{-5}
ci|000090287|proj|Sample_C_D|2	innexin unc-7-like	−5.491	2.04×10^{-5}
ci|000055679|proj|Sample_C_D|2	putative nuclease HARBI1	−15.75	2.44×10^{-5}
ci|000057152|proj|Sample_C_D|2	uncharacterized protein LOC117338914	−11.88	3.84×10^{-5}
ci|000193936|proj|Sample_C_D|2	uncharacterized protein LOC117332862, partial	−7.373	7.17×10^{-5}
ci|000071556|proj|Sample_C_D|2	serine/threonine-protein kinase PINK1, mitochondrial-like	−13.21	1.65×10^{-4}
ci|000038909|proj|Sample_C_D|2	sphingomyelin synthase-related protein 1-like	−4.889	2.27×10^{-4}
ci|000061087|proj|Sample_C_D|2	uncharacterized protein LOC110461911 isoform X1	−10.47	2.35×10^{-4}
ci|000058655|proj|Sample_C_D|2	apoptosis-stimulating of p53 protein 1-like	−3.122	3.73×10^{-4}
ci|000104877|proj|Sample_C_D|2	uncharacterized protein LOC117339040	−9.715	3.90×10^{-4}
ci|000017126|proj|Sample_C_D|2	uncharacterized protein LOC117326392	−3.294	4.56×10^{-4}
ci|000019333|proj|Sample_C_D|2	selenoprotein N-like isoform X1	−1.813	5.94×10^{-4}
ci|000009958|proj|Sample_C_D|2	uncharacterized protein LOC117345233	−2.103	6.09×10^{-4}

Among the top up-regulated genes (Table 3, Supplementary File S1) were genes involved in the metabolism of xenobiotics (cytochromes P450, glutathione S-transferase) a gene (*SLC6A9*) coding for a sodium- and chloride-dependent glycine transporter (a solute carrier of the *SLC6* family [37]) and two genes coding for enzymes involved in the metabolism of glutamate and proline (glutamine synthetase and pyrroline-5-carboxylate reductase 2). Pinin, serine protease inhibitor Cvsi-1, innexin UNC-7, serine/threonine-protein kinase PINK1 and apoptosis-stimulating of p53 protein 1 were among the top down-regulated genes (Table 4). Many of the top down-regulated genes code for uncharacterized proteins (Table 4).

It is worth pointing out that we have found 19 transcripts that code for putative glutamate receptors in the digestive gland of *P. maximus*, 10 of them for ionotropic receptors and 9 for metabotropic receptors (Table 5 and Supplementary File S3), but none of these genes were differentially expressed.

Table 5. List of transcripts coding for putative glutamate receptors in the digestive gland of *Pecten maximus*. FC: fold change; padj: FDR adjusted *p*-value.

Sequence ID	Description	Type	FC	padj
ci|000016850|proj|Sample_C_D|2	XP_033740949.1 metabotropic glutamate receptor 1-like [*Pecten maximus*]	Metabotropic	2.938	0.278
ci|000042484|proj|Sample_C_D|2	XP_033740949.1 metabotropic glutamate receptor 1-like [*Pecten maximus*]	Metabotropic	1.309	0.937
ci|000199286|proj|Sample_C_D|2	XP_033740949.1 metabotropic glutamate receptor 1-like [*Pecten maximus*]	Metabotropic	2.566	0.288
ci|000235714|proj|Sample_C_D|2	XP_033740949.1 metabotropic glutamate receptor 1-like [*Pecten maximus*]	Metabotropic	1.575	NA
ci|000005744|proj|Sample_C_D|2	XP_033744387.1 glutamate receptor-like [*Pecten maximus*]	Ionotropic	1.504	0.714
ci|000012480|proj|Sample_C_D|2	XP_033744387.1 glutamate receptor-like [*Pecten maximus*]	Ionotropic	1.567	0.765

Table 5. *Cont.*

Sequence ID	Description	Type	FC	padj
ci|000178783|proj|Sample_C_D|2	XP_033744387.1 glutamate receptor-like [*Pecten maximus*]	Ionotropic	3.428	0.123
ci|000194581|proj|Sample_C_D|2	XP_033744387.1 glutamate receptor-like [*Pecten maximus*]	Ionotropic	1.655	0.845
ci|000000691|proj|Sample_C_D|2	XP_033760483.1 glutamate receptor 3-like [*Pecten maximus*]	Ionotropic	1.242	0.945
ci|000077591|proj|Sample_C_D|2	XP_033760483.1 glutamate receptor 3-like [*Pecten maximus*]	Ionotropic	−1.006	0.998
ci|000108874|proj|Sample_C_D|2	XP_033760483.1 glutamate receptor 3-like [*Pecten maximus*]	Ionotropic	−1.199	0.968
ci|000219160|proj|Sample_C_D|2	XP_033760483.1 glutamate receptor 3-like [*Pecten maximus*]	Ionotropic	−1.319	0.937
ci|000054856|proj|Sample_C_D|2	XP_033760586.1 glutamate receptor U1-like [*Pecten maximus*]	Ionotropic	−1.100	0.970
ci|000106439|proj|Sample_C_D|2	XP_033760586.1 glutamate receptor U1-like [*Pecten maximus*]	Ionotropic	−1.447	0.912
ci|000013492|proj|Sample_C_D|2	XP_033763623.1 metabotropic glutamate receptor 7-like isoform X3 [*Pecten maximus*]	Metabotropic	1.042	0.985
ci|000015386|proj|Sample_C_D|2	XP_033763623.1 metabotropic glutamate receptor 7-like isoform X3 [*Pecten maximus*]	Metabotropic	1.066	NA
ci|000028888|proj|Sample_C_D|2	XP_033763623.1 metabotropic glutamate receptor 7-like isoform X3 [*Pecten maximus*]	Metabotropic	1.169	0.937
ci|000048793|proj|Sample_C_D|2	XP_033763623.1 metabotropic glutamate receptor 7-like isoform X3 [*Pecten maximus*]	Metabotropic	1.161	0.928
ci|000191381|proj|Sample_C_D|2	XP_033763623.1 metabotropic glutamate receptor 7-like isoform X3 [*Pecten maximus*]	Metabotropic	1.348	0.937

The functional annotation results are shown in Table 6 and in Supplementary Files S4 and S5.

Table 6. Summary of the functional annotation results.

Functional Annotation	Number	%
Differentially expressed unigenes	**535**	**100**
With Blastx hit	286	53.5
With GO terms	259	48.4
With enzyme code	129	24.1
With KO ortholog	102	19.1
With PFAM domains	188	35.1
All unigenes	**72,673**	**100**
With Blastx hit	35,583	49.0
With GO terms	32,203	44.3
With enzyme code	16,429	22.6
With KO ortholog	7657	10.5
With PFAM domains	24,810	34.1

2.4. Protein Network Analysis

Differentially expressed protein-coding genes can be grouped by means of the protein-protein interactions [38]. A Blastx search of the sequences of the 226 up-regulated and the 309 down-regulated genes found 88 and 93 human homologs in the STRING database, respectively. The networks obtained with up-regulated (Figure 2 and Supplementary File S6) and down-regulated (Figure 3 and Supplementary File S7) genes were enriched in interac-

tions (p-values 5.31×10^{-6} and 0.0152, respectively). Up-regulated genes (Figure 2 and Supplementary File S6) were involved in biological processes, such as the metabolism of xenobiotics, stress response, immune response, lysosomal degradation, autophagy, apoptosis, RNA processing, and exocytosis. On the other hand, down-regulated genes (Figure 3 and Supplementary File S7) were involved in biological processes such as RNA processing, ribosome formation, apoptosis, immune and inflammatory responses.

The up-regulated genes that code for proteins that showed interactions in the protein network analysis were enriched in gene ontology (GO) terms (Supplementary File S8) such as vesicle-mediated transport, response to stress, signal transduction, immune system process, RNA metabolic process, autophagy, lysosome and oxidoreductase activity. The down-regulated genes that code for proteins that showed interactions in STRING analysis were enriched in GO terms (Supplementary File S8) such as response to stress, immune system process, ribosome biogenesis, signal transduction, mRNA processing, and oxidoreductase activity.

2.5. Real Time RT-qPCR

Four candidate reference genes (*GAPDH*, *EF1A*, *COX1* and *NDUFA7*, Table 7) were selected based on a previous work on *P. maximus* [39]. Table 8 shows the results obtained with the three algorithms (geNorm, NormFinder and BestKeeper) employed to test the stable expression of these genes. *GAPDH*, and *COX1* were the best ranked genes and therefore selected as reference genes.

The comparison of gene expression results of the six target genes (*MRP7*, *CYP2B4*, *P5CR*, *SLC6A9*, *FERRITIN*, *CYP2U1*, Table 7) obtained with RT-qPCR and RNA-seq is displayed in Figure 4. The log2 FC values achieved by the two methods were very similar and showed good correlation ($r = 0.969$; $r^2 = 0.939$).

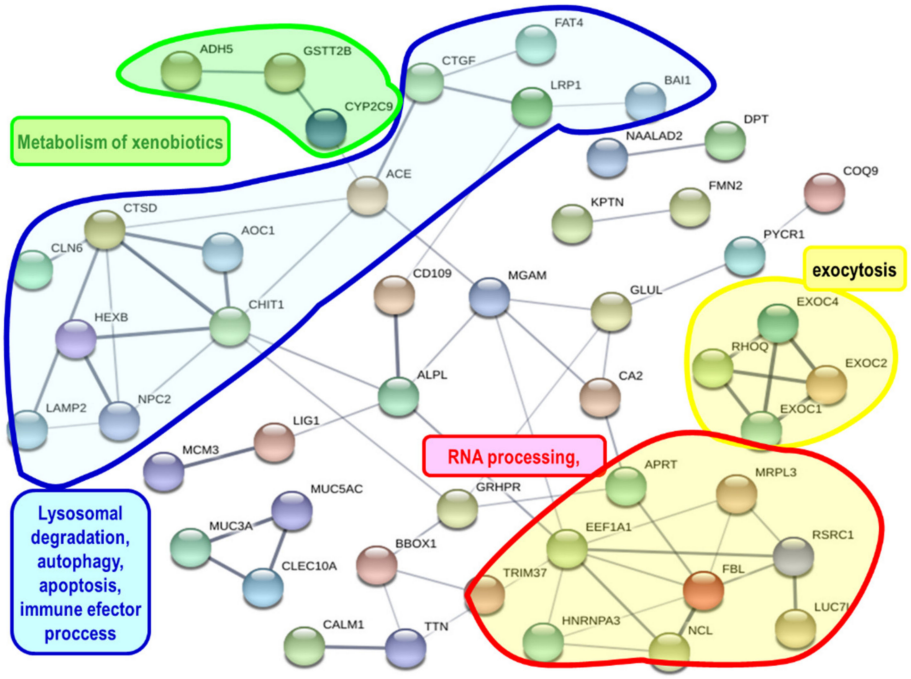

Figure 2. Network showing interactions of proteins coded by genes up-regulated in the present study. The network was constructed using the String 10.5 algorithm. Some connected protein nodes are highlighted showing some of the processes in which these proteins participate. Proteins were named according to the human protein name. A full list of protein names is available in Supplementary File S6.

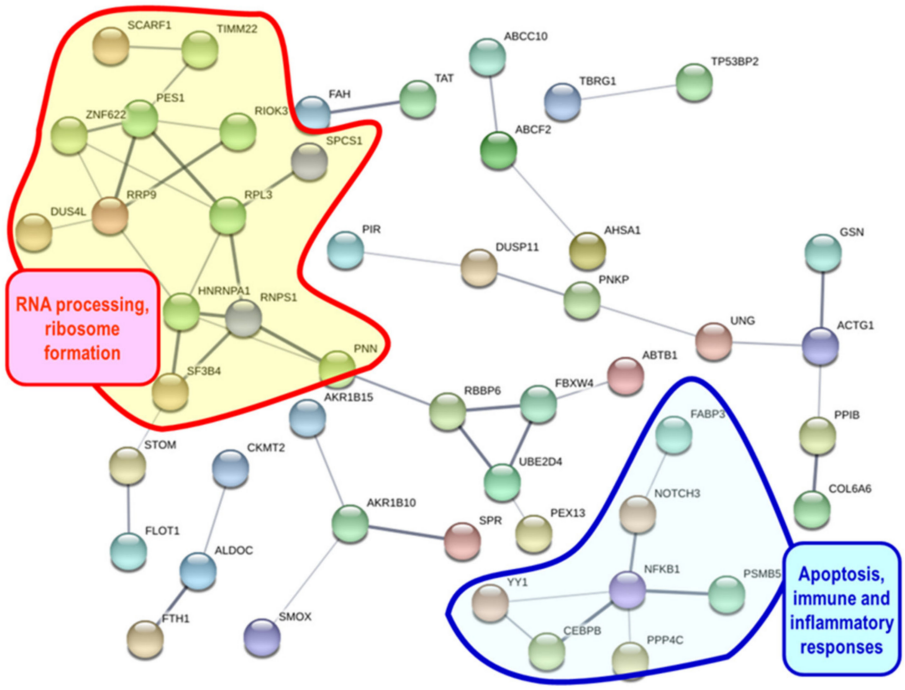

Figure 3. Network showing interactions of proteins coded by genes down-regulated in the present study. The network was constructed using the String 10.5 algorithm. Some connected protein nodes are highlighted showing some of the processes in which these proteins participate. Proteins were named according to the human protein name. A full list of protein names is available in Supplementary File S7.

Table 7. Genes selected for RT-qPCR: sequence names, description, gene symbols, primers, amplicon length (bp) for each primer pair and average efficiency (E).

Sequence Name	Description	Symbol	Sense Primer	Antisense Primer	bp	E
ci|000200326|proj|Sample_C_D|2	glyceraldehyde-3-phosphate dehydrogenase	*GAPDH*	TCCGGATGTGTCTGTTGTTGAC	TTCAGATCTCCATCAGCTGCAC	102	0.8465
ci|000017232|proj|Sample_C_D|2	eukaryotic translation elongation factor 1 alpha	*EF1A*	AGGGCTCCTTCAAGTATGCCTG	TGAGCGGTCTCGAACTTCCAC	100	0.8275
ci|000019926|proj|Sample_C_D|2	cytochrome c oxidase subunit 1	*COX1*	AGTGGAGAACTATTGGGTGTGC	AGACCTAGGCCGATTTCCAAAC	119	0.8525
ci|000005190|proj|Sample_C_D|2	NADH dehydrogenase (ubiquinone) 1 alpha subcomplex subunit 7	*NDUFA7*	ATTACACACGAGATGGACGCTG	ACATCAGAGCTGGCTGTTTCAG	115	0.8043
ci|000002411|proj|Sample_C_D|2	multidrug resistance-associated protein 7	*MRP7*	CGGATGGTGGCTAACTCATT	CGATGCACCCATACACTGTC	200	0.8594
ci|000062123|proj|Sample_C_D|2	cytochrome p450 2b4-like	*CYP2B4*	CATGCGAAGGACTACGACAAG	GAACAAAATGGCCCAAAGAAG	183	0.8314
ci|000199464|proj|Sample_C_D|2	pyrroline-5-carboxylate reductase 2-like	*P5CR*	CCTCACATCATCACTCCA GTCC	GACGGGAGCAGATTCTCCTC	119	0.8547
ci|000181387|proj|Sample_C_D|2	sodium- and chloride-dependent glycine transporter 1-like	*SLC6A9*	GACGGTACTGGGCATTTCTG	ATCAGCAAGGCCGTAAGGAG	183	0.8539
ci|000018690|proj|Sample_C_D|2	ferritin 2	*FERRITIN*	CCATGCTGAAACCGAGGCTG	CAATCCTGCCTCCTCTCTTG	206	0.8547
ci|000200864|proj|Sample_C_D|2	cytochrome p450 2u1-like	*CYP2U1*	CATCGACGCCTTCCAGTTCG	GATAGTCAGCCATCGTGGGT	233	0.8753

Table 8. Rank of four candidate reference genes in quantitative real-time reverse transcription–polymerase chain reaction (RT–qPCR), calculated by geNorm, NormFinder, and BestKeeper analysis.

Rank	geNorm (Average M)		NormFinder (Stability)		BestKeeper (*r*)		BestKeeper (SD)	
1	*GAPDH-COX1*	0.78	*GAPDH*	0.105	*COX1*	0.858	*GAPDH*	0.724
2	*GAPDH-COX1*	0.78	*COX1*	0.196	*GAPDH*	0.782	*NDUFA7*	0.781
3	*EF1A*	1.01	*EF1A*	0.244	*EF1A*	0.662	*COX1*	0.838
4	*NDUFA7*	1.34	*NDUFA7*	0.386	*NDUFA7*	−0.243	*EF1A*	0.861

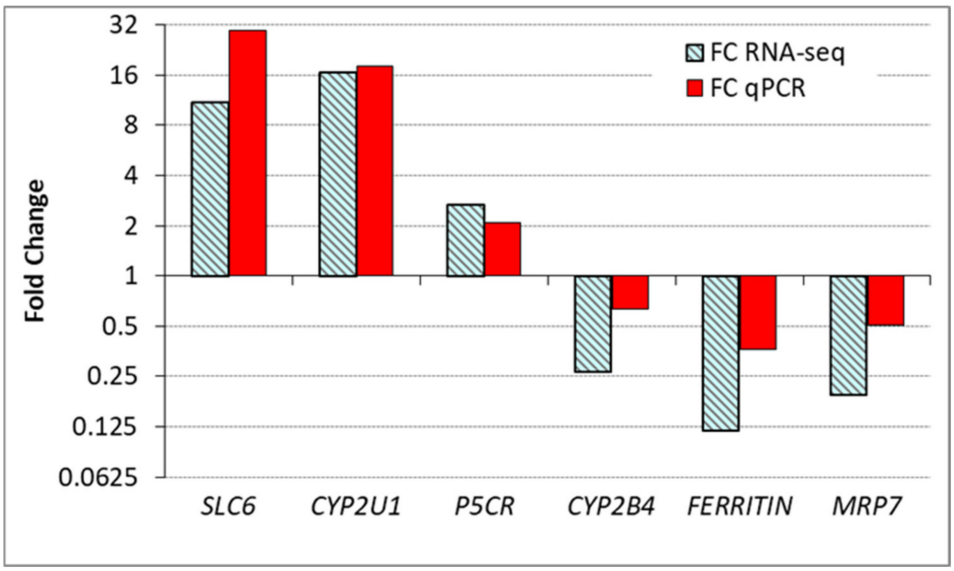

Figure 4. Gene expression (fold change in relation to control) in the digestive gland of *P. maximus* as determined by RT-qPCR analyses and RNA-seq. FC qPCR = geometric mean of the normalized gene expression in treated samples/geometric mean of the normalized gene expression in control samples.

3. Discussion

Several authors have shown [14–16] that the digestive gland in the king scallop *P. maximus* accumulates most of the domoic acid. This agrees with the results obtained in the present work that found that domoic acid content in the digestive gland accounts for 84% of the total domoic acid burden in the body tissues of *P. maximus* (Table 1). The total amount of domoic acid injected was 3000 µg per animal, but only a mean difference of 339 µg between treated and control animals was found. These results suggest that part of the administered domoic acid was depurated. After the injection into the adductor muscle, the domoic acid enters into the circulatory system, through the hemolymph sinuses [40]. In scallops, urine formation takes place through hemolymph filtration into the pericardial cavity, which in turn is connected to the kidneys through the reno-pericardial ducts [40]. Therefore, part of the domoic acid is probably filtered from the hemolymph into the kidneys and only a part of the injected domoic acid was distributed to the digestive gland. In kidneys, we have found a significant difference in domoic acid concentration between control and treated animals (Figure 1). It is important to emphasize that in the natural environment the scallops obtain the toxin from the food-chain through the digestive system.

We found 535 DEGs (226 up-regulated and 309 down-regulated, Supplementary File S1) in the digestive gland of *P. maximus* after the injection of domoic acid, therefore the toxin might have an effect on the gene expression in the digestive gland. The analysis of gene expression found the alteration of some processes at the biological, cellular, and molecular level (Figures 2 and 3, Supplementary File S8), that could be due to the effects of domoic acid. Thus, genes involved in xenobiotic metabolism, immune response, response to stress, signal transduction, apoptosis, RNA processing, ribosome biogenesis, lysosomal

degradation, autophagy, and regulated exocytosis were differentially expressed. Scallops injected with domoic acid showed a behavior different (maintained a clearly larger valve opening) to the ones to which only seawater was injected. This reveals that domoic acid probably had an effect at the level of the central nervous system. There are three ways, not mutually exclusive, that can explain how domoic acid exerts its effects on the digestive gland of *P. maximus*: (a) the interaction of domoic acid with different biomolecules (mainly proteins) after the entry of domoic acid into the cells of the digestive gland; (b) the binding of domoic acid to glutamate receptors present on the plasma membrane of the cells of the digestive gland (we found that there is expression of mRNA that codes for glutamate receptors, both ionotropic and metabotropic, in the digestive gland of *P. maximus*, Table 5 and Supplementary File S3); and (c) the binding of domoic acid to glutamate receptors present in the central nervous system (cerebral, pedal, and parietovisceral ganglia) of the scallop (the actions triggered in these ganglia could be transmitted to the digestive gland through the nervous and neuroendocrine systems). Dizer et al. [22] also found an effect (increased DNA damage) of the intramuscular injection of domoic acid on digestive gland cells of a bivalve, *Mytilus edulis*.

In vertebrates, domoic acid is a potent neurotoxin [4,8,41–43], and the response to domoic acid includes genes involved in transcription (transcription factors), signal transduction, ion transport, generalized response to stress, mitochondrial function, inflammatory response, response to DNA damage, apoptosis, neurological function and neuroprotection [31,41,44,45]. Although there are fewer studies on the effects of domoic acid on invertebrates than vertebrates, this toxin also exerts effects on marine bivalves at the physiological and gene expression levels [22–26,28–30]. In two previous studies [29,30] we showed that exposure to domoic acid containing *Pseudo-nitzschia* alters the transcriptomic profile of the digestive gland of the mussel *Mytilus galloprovincialis* and of the queen scallop *Aequipecten opercularis*. The results obtained by Ventoso et al. [30] suggest that exposure to domoic acid-producing organisms causes oxidative stress and mitochondrial dysfunction in *A. opercularis*, thus the transcriptional response of the queen scallop is involved in the protection against oxidative stress. This agrees with the results obtained by Song et al. [28] that showed that domoic acid induces oxidative stress and impairs defence mechanisms in bay scallops (*Argopecten irradians*). The contribution of oxidative stress to the effects and toxicity of domoic acid has been highlighted by several authors [6,28,31–33,35,36].

A consequence of oxidative stress, if the protective anti-oxidant mechanisms cannot limit the damage, is cellular dysfunction and apoptosis [46], and domoic acid can induce apoptosis [32,47–49]. Cathepsin D, a lysosomal aspartic acid protease that initiates caspase-8-dependent apoptosis [50], was up-regulated in *P. maximus* (Figure 2 and Supplementary File S1), and also in *A. opercularis* [30] and *M. galloprovincialis* [29] after exposure to domoic acid containing *Pseudo-nitzschia*. Several genes coding for proteins putatively involved in apoptosis were differentially expressed in *P. maximus* (CTSD, AOC1, LRP1, BAI1, NFKB1, NOTCH3, PPP4C, RBBP6, Figures 2 and 3).

One of the effects of domoic acid in *P. maximus* was the down-regulation of genes involved in RNA processing, ion transport, immune response, metabolic process and signal transduction (Supplementary File S8); this agrees with the results of Lefebvre et al. [41] with zebrafish, after low-level domoic acid exposures, that found the down-regulation of genes involved in those same biological processes.

Genes coding for several phase I (cytochromes P450) and phase II (glutathione S-transferases and sulfotransferases) drug metabolizing enzymes were up-regulated in *P. maximus* (Table 3, Figure 2 and Supplementary File S1), these types of genes were also up-regulated in *A. opercularis* [30] and *M. galloprovincialis* [29] following exposure to domoic acid-producing *Pseudo-nitzschia*.

Several authors have shown that glutamate receptors are expressed not only in the central nervous system but also in other types of tissues or organs (intestine, liver, kidney, stomach, etc.) [51–53]. Therefore, glutamate and glutamate receptor agonists could participate in the regulation of several physiological processes in peripheral organs [51–53]. We

have found 19 genes that code for possible glutamate receptors in the digestive gland of *P. maximus*, 10 of them for ionotropic receptors and 9 for metabotropic receptors (Table 5 and Supplementary File S3). Some of the effects of domoic acid on the cells of the digestive gland may be mediated by these receptors. None of the genes coding for these receptors were differentially expressed in *P. maximus* (Table 5 and Supplementary File S3). In *A. opercularis*, some genes coding for glutamate ionotropic receptors were down-regulated [30] in the digestive gland of animals exposed to domoic acid-containing *Pseudo-nitzschia*. This may be due to a compensatory response to elevated glutamatergic activity, thus Hiolski et al. [31] found this type of compensatory response in zebrafish after domoic acid exposure.

Glycine, in addition to acting as an inhibitory neurotransmitter, is also a co-agonist at N-methyl-D-aspartate (NMDA) glutamate receptors [54]. In the central nervous system of vertebrates, the glycine transporter 1 (sodium- and chloride-dependent glycine transporter 1) regulates the binding of glycine to NMDA receptors [54], because the action of glycine is terminated through the reuptake mediated by sodium- and chloride-dependent glycine transporters [55]. The up-regulation of the *SLC6A9* gene (coding for sodium and chloride-dependent glycine transporter 1) could prevent or reduce NMDA receptor activation. The *SLC6A9* gene was among the top up-regulated genes in *P. maximus* (Table 3). There was another gene of this family (*SLC6*) that was downregulated in *P.maximus* (Supplementary File S1). Although both genes code for putative sodium- and chloride-dependent glycine transporters, they share only 52% sequence identity at the amino acid level. Genes of this family (*SLC6*) were up-regulated in *M. galloprovincialis* [29] and down-regulated in *A. opercularis* [30] after exposure to domoic acid-producing *Pseudo-nitzschia*. A gene of the *SLC6* family was up-regulated in *Pseudo-nitzschia multiseries* under toxin-producing conditions [56], and this gene was also up-regulated in a domoic acid-producing *Pseudo-nitzschia* species in relation to two *Pseudo-nitzschia* species that do not produce domoic acid [57]. The *SLC6* family is expanded in the genome of the scallops *Chlamys farreri and Patinopecten yessoensis* [58,59], in relation to other bivalves. In the *A. opercularis* [30] and in *P. maximus* digestive gland transcriptome, the number of transcripts belonging to this family is also very high (we found 58 in *P. maximus*).

One of the up-regulated genes in *P. maximus*, glutamine synthetase (Supplementary File S1), might play a neuroprotective role against glutamate neurotoxicity in neural tissues [60,61], because it catalyzes the transformation of glutamate to glutamine. Glutamate and glutamate receptor agonists increased glutamine synthetase expression and glutamine synthetase activity in cultured astrocytes [62,63]. Glutamine synthetase also participates in the production of GABA (gamma-aminobutyric acid), an inhibitory neurotransmitter. GABA has been shown to be able to prevent, at least partially, the effects of domoic acid in rat glial cells [64]. Therefore, the overexpression of this gene could have a protective effect against domoic acid. Another gene involved in the metabolism of amino acids (glutamate and proline) is up-regulated in *P. maximus*. This gene codes for the enzyme pyrroline-5-carboxylate reductase 2 that catalyzes the conversion of pyrroline-5-carboxylate to proline, and proline has a protective effect against oxidative stress [65]. Kenny et al. [66] suggested that mutations in the sodium channel gene, *Neuron Navigator 1* (*Nav1*), could protect against the effects of domoic acid in *P. maximus*. We have not found transcripts of the *Nav1* gene in the digestive gland of *P. maximus*, therefore the sodium channel is likely expressed in nervous tissue but not in the digestive gland.

The immune system of marine bivalves is sensitive to toxins and harmful algae [67,68]. Several harmful algae can provoke a stimulation of immune functions, while others cause inhibition [68]. Chi et al. [27] found that exposure to domoic acid impaired immune functions in the bay scallop *A. irradians*. In *P. maximus*, the immune system process was one of the enriched terms in the proteins coded by DEGs that showed interaction in STRING (Figures 2 and 3, Supplementary Files S6–S8). C-type lectins are calcium-dependent carbohydrate-binding proteins and participate in innate immunity in bivalves [67,69]. In bivalve mollusks there is a high number of genes coding for C-type lectins [69,70]. Three

transcripts coding for putative C-type lectins were up-regulated in the *P. maximus* digestive gland (Supplementary File S1). This agrees with the results obtained with *A. opercularis* [30] and *M. galloprovincialis* [29] after exposure to domoic acid-producing *Pseudo-nitzschia*, where most of the genes coding for C-type lectins were up-regulated.

Heat shock proteins (HSP) can be induced by several types of stress (high temperature, hypoxia, toxins, or pathogens) and they are involved in protein folding [71]. There is an expansion of *Hsp70* (heat shock protein 70 kDa) genes from the *Hspa12* subfamily in *Mizuhopecten yessoensis* [71], and a gene of this subfamily (*heat shock 70 kDa protein 12A-like*) was up-regulated in *P. maximus* (Supplementary File S1). A up-regulation of *HSP* genes after exposure to harmful algae toxins (including domoic acid) has been found in several bivalves [27,28,71–75], although in *A. opercularis*, after exposure to domoic acid-producing *Pseudo-nitzschia*, HSP genes were both up- and down-regulated [30].

The digestive gland of *Pecten maximus* contains principally two types of cells, secretory cells and digestive cells [16,40,76,77]. Vesicle-mediated transport and regulated exocytosis were enriched biological processes identified in protein networks obtained with the up-regulated genes (Figure 2 and Supplementary File S8), therefore the activity of secretory cells in the digestive gland may be stimulated by domoic acid. These cells may be involved in the secretion of digestive enzymes [40,76,77].

Collagens are structural components of the extracellular matrix [78]. Components of collagen and proteins involved in cytoskeleton dynamics were among the proteins that appeared in the network obtained with the down-regulated genes in *A. opercularis* after exposure to domoic acid-producing *Pseudo-nitzschia* [30]. In the present work, several collagen genes were down-regulated (File S1) and cytoskeleton (Supplementary File S8) is one of the enriched cellular components in the down-regulated genes coding for proteins that showed interactions in the protein network analysis.

4. Conclusions

The domoic acid injected might have an effect on the gene expression in the digestive gland as reflected in the 535 DEGs found (226 up-regulated and 309 down-regulated). Some genes that code for putative glutamate receptors were expressed in the digestive gland of *P. maximus*, therefore part of the effects of domoic acid may be mediated by these receptors. A stress response at the level of gene expression, that could be caused by the domoic acid injection, was evidenced by the alteration of several biological, cellular, and molecular processes. Thus, protein networks obtained with the up-regulated genes were enriched in gene ontology (GO) terms, such as vesicle-mediated transport, response to stress, signal transduction, immune system process, RNA metabolic process, autophagy, lysosome, and oxidoreductase activity. On the other hand, networks obtained with the down-regulated genes were enriched in terms, such as response to stress, immune system process, ribosome biogenesis, signal transduction, mRNA processing, and oxidoreductase activity. In future research, it would be interesting investigate the domoic acid effects on gene expression in the kidneys and in the central nervous system (cerebral, pedal, and parietovisceral ganglia) of *P. maximus*.

5. Materials and Methods

The methods employed were similar as those previously described [29,30] except for minor modifications.

5.1. Animals

King scallops were obtained from the Ría de Arousa (Galicia, NW Spain) and maintained for a week in a 500 L tank, with a continuous unfiltered seawater flow (approximate) of 1200 $L \cdot h^{-1}$. No domoic acid was detected in the routine monitoring of mollusks from the area and no toxic *Pseudo-nitzschia* cells were present in the area neither during the experiment nor during the previous month. All scallops, notwithstanding, contained domoic acid. It was impossible to obtain individuals free of toxin from the study area (and even

from other European Countries) because the very low depuration rate of this species [14] makes easy their re-contamination. In the data obtained by the monitoring system run by Intecmar during the last 25 years in Galicia, it has been observed that the prevalence of domoic acid in the king scallop was 100%, and the same happened in other areas, such as Scotland [79]. The experimental approach was conditioned by this limitation, so we try to induce a response in the scallops by increasing the domoic acid levels that, in natural conditions, only undergo the progressive and slow changes derived from the depuration process. Fourteen scallops, with average height 10.98 ± 0.16 cm and 24.9 ± 1.3 g of soft tissues weight, were randomized into two groups: seven scallops as a control group and the other seven as a treated (with toxin injections) group. The scallops in the treated group were subjected to repeated injections of domoic acid (ABCAM) dissolved in filtered seawater and those in the control group, to equivalent injections of filtered seawater. One injection was made into the adductor muscle of each scallop every other day, for a period of 12 days. A volume of 62.5 µL of filtered seawater with a concentration of 8 µg domoic acid μL^{-1} was used for each injection (500 µg domoic acid in each injection). The total amount of domoic acid injected was 3000 µg per animal. The same volume of filtered seawater was injected into the scallops in the control group. When the scallops spontaneously opened the valves, a silicone stopper was placed between them to maintain them opened, and the injection was carried out.

After the injection, each scallop (treatment and control) was placed into a 5 L beaker, with 4 L of seawater water, with aeration, and maintained there for 24 h. After that period, the scallops were transferred to a 500 L tank with running seawater for one day. Following that, the injection process was repeated. Twenty-four hours after the last injection the scallops were dissected into digestive gland, gill, kidney, gonad, adductor muscle and remaining tissues. The dissected tissues were used for the determination of domoic acid content using liquid chromatography-tandem mass spectrometry (LC–MS/MS). A portion of the digestive gland was treated with RNAlater (ref. AM7021, Ambion, Life Technologies) and stored at −80 °C until the RNA extraction.

5.2. Determination of the Domoic Acid Content

Methanol for HPLC and formic acid were purchased from Labscan (Bangkok, Thailand) and Sigma Aldrich (St. Louis, MO, USA), respectively. Ultrapure water was obtained using a Milli-Q Gradient system, coupled to an Elix Advantage 10, both from Millipore (Merck Millipore, Darmstadt, Germany).

To extract the toxin, each digestive gland was placed in aqueous methanol (50%) in a proportion of 1:2 *w:v* and homogenized with an Ultraturax T25 (IKA, Staufen, Germany). The extract was clarified using centrifugation at 18,000× *g* at 4 °C for 10 min, retaining the supernatant that was immediately analyzed.

Domoic acid in the obtained extracts was analyzed using LC–MS/MS. The chromatographic separation was carried out using a Thermo Accela chromatographic system (Thermo Fisher Scientific, Waltham, MA, USA), with a high-pressure pump and autosampler. The stationary phase was a solid core Kinetex C18, 50 × 2.1 mm 2.6 µm column (Phenomenex, Torrance, CA, USA). An elution gradient, with a flow of 280 µL min^{-1}, was used with mobile phase A (formic acid 0.2%) and B (50% MeOH with formic acid 0.2%). The gradient started at 100% A, maintained this condition for one minute, linearly changed until reaching 55% B in minute 5, held for 2 min, and reverted to the initial conditions to equilibrate before the next injection. Five microliters of extract, previously filtered through a PES 0.2 µm syringe filter (MFS), were injected.

After the chromatographic separation, domoic acid was detected and quantified by means of a Thermo TSQ Quantum Access MAX triple quadrupole mass spectrometer (Thermo Fisher Scientific, Waltham, MA, USA), equipped with a HESI-II electrospray interface, using positive polarization and SRM mode. The transition 312.18 > 266.18 *m/z* was used to quantify the response and 312.18 > 248.18 for confirmation. The spectrometer was operated under the following conditions: spray voltage 3400 V, capillary temperature

270 °C, HESI-II temperature 110 °C, sheet gas (Nitrogen) 20 (nominal pressure), auxiliary gas (Nitrogen) 10 (nominal pressure), collision energy of 15 V and collision gas (Argon) pressure of 1.5 mTorr.

Concentrations of domoic acid were obtained by comparing the response of the quantification transition in the sample extracts with that of a reference solution obtained from NRC Canada. The quantification limit of the method for tissue analysis is less than 20 ng/mL of extract.

5.3. RNA Extraction

Twelve scallops (six obtained from the control group and six from the treated group) were subjected to RNA-seq analysis. A NucleoSpin RNA kit (ref. 740955, Macherey-Nagel, Düren, Germany) was used for digestive gland total RNA isolation. Then an RNA precipitation step with 0.5 volumes of Li CL 7.5 M was performed and the RNA pellet was dissolved in 50 µL of RNA storage solution (ref. AM7000, Ambion, Life Technologies, Carlsbad, CA, USA). Total RNA was treated with DNA-free (ref. AM1907M, Ambion, Life Technologies, Carlsbad, CA, USA) to remove DNA contamination. The integrity and quality of the RNA samples were measured using agarose gel electrophoresis, an Agilent 2100 Bioanalyzer (Agilent Technologies, Santa Clara, CA, USA) and a Nanodrop ND-1000 spectrophotometer (NanoDrop Technologies, Wilmington, DE, USA). The quantity of the total RNA was determined using Qubit 2.0 (Invitrogen, Carlsbad, CA, USA).

5.4. Library Preparation and Sequencing

Twelve cDNA libraries were generated. The poly(A)+ mRNA fraction was isolated from total RNA and cDNA libraries were obtained following Illumina's recommendations. Briefly, poly(A)+ RNA was isolated on poly-T oligo-attached magnetic beads and chemically fragmented prior to reverse transcription and cDNA generation. The cDNA fragments then went through an end repair process, the addition of a single 'A' base to the 3′ end and afterwards the ligation of the adapters. Finally, the products were purified and enriched with PCR to create the indexed final double stranded cDNA library. The quality of the libraries was analyzed using a Bioanalyzer 2100 (Agilent Technologies, Santa Clara, CA, USA) high sensitivity assay; the quantity of the libraries was determined by real-time PCR in LightCycler 480 (Roche Diagnostics, Mannheim, Germany). Prior to cluster generation in cbot (Illumina), an equimolar pooling of the libraries was performed. The pool of the cDNA libraries was sequenced by paired-end sequencing (100 × 2 bp) on an Illumina HiSeq 2000 sequencer (Illumina, San Diego, CA, USA).

5.5. De Novo Assembly

Quality control checks of raw sequencing data were performed with FastQC. The technical adapters were eliminated using Trimgalore software version 0.3.3 (Trim Galore. Available Online: http://www.bioinformatics.babraham.ac.uk/projects/trim_galore/ (accessed on 10 March 2021)). Additionally, the reads with a mean Phred score > 30 were selected. Subsequently, the twelve samples were combined, and the complexity of the reads was reduced by removing duplicates. Then, a de novo assembly was performed using the programs Oasis, version 0.2.09 [80] and Trinity, version 2.1.1 [81]. The assembled transcripts were clustered (>90% homology) to reduce redundancy using cd-hit software version 4.6. For each sequence, the potential ORFs were detected using Transdecoder software, version 2.0, with standard parameters. The completeness of the de novo assembly was evaluated with BUSCO [82] in OmicsBox software (BioBam Bioinformatics—2019, Valencia, Spain. OmicsBox—Version 1.4.11.) [83,84], using the Metazoa database (metazoa_odb10) [85], with a total of 954 orthologs (Blast E-value < 10^{-3}).

Each sample was then mapped with Bowtie2, version 2.2.6 [86] against the reference transcriptome obtained in the previous step. The good quality reads (Mapping Quality ≥ 20) were selected to increase the resolution of the count expression. Finally, the expression inference was evaluated by means of the counts of properly paired reads in each transcript.

5.6. Differential Expression

The transcriptome expression for each sample was normalized by library size, following the DESeq2 protocols. Differential gene expression analysis of treated versus control samples was performed with DESeq2 algorithm version 1.8.2 (DESeq2. Available online: http://www.bioconductor.org/packages/devel/bioc/html/DESeq2.html (accessed on 10 March 2021)). The genes with a fold change of less than −1.5 or greater than 1.5, and a *p*-value adjusted using the Benjamini and Hochberg [87] method for controlling false discovery rate (FDR) < 0.05 were considered differentially expressed.

5.7. Functional Annotation

Genes were annotated with OmicsBox software (BioBam Bioinformatics—2019. OmicsBox—Version 1.4.11.) [83,84], using local Blastx 2.10.0+ [88], (E-value threshold of 10^{-3}) against a database of *Pecten maximus* [66], *Mizuhopecten yessoensis* [89], *Crassostrea gigas* [70] and *SwissProt* proteins obtained from NCBI and UNIPROT:

https://ftp.ncbi.nlm.nih.gov/genomes/refseq/invertebrate/Pecten_maximus/latest_assembly_versions/GCF_902652985.1_xPecMax1.1/GCF_902652985.1_xPecMax1.1_protein.faa.gz (accessed on 28 April 2020)

https://ftp.ncbi.nlm.nih.gov/genomes/archive/old_refseq/Mizuhopecten_yessoensis/protein/protein.fa.gz (accessed on 19 July 2017)

https://ftp.ncbi.nlm.nih.gov/genomes/archive/old_refseq/Crassostrea_gigas/protein/protein.fa.gz (accessed on 06 February 2017)

https://ftp.uniprot.org/pub/databases/uniprot/current_release/knowledgebase/complete/uniprot_sprot.fasta.gz (accessed on 03 October 2020)

Then, annotations were expanded by incorporating information from gene names and functions using gene ontology (GO) and protein structure domains associated with the transcript using InterPro (InterPro. Available online: https://www.ebi.ac.uk/interpro/ (accessed on 15 March 2021)).

Ortholog assignment and pathway mapping were performed on the KEGG Automatic Annotation Server (KAAS, [90]) using Blast and the BBH (bi-directional best hit) method (KAAS—KEGG Automatic Annotation Server. Available online: http://www.genome.jp/tools/kaas/ (accessed on 15 March 2021)).

5.8. Protein Network Analysis

To search for the protein-protein interactions, network analyses using the String 10.5 algorithm [91] were performed. The putative human homologs of proteins coded by the up- and down-regulated genes in the *P. maximus* digestive gland were identified by means of a Blastx search [92] against the STRING human protein database (9606.protein.sequences.v10.fa), with an E-value threshold of 10^{-5}. The top Blastx search results were used as input in the String program. The up-regulated and the down-regulated genes were analyzed separately.

The genes that code for proteins that showed protein-protein interactions were subjected to GO enrichment analysis with OmicsBox using Fisher's exact test [93] (up- and down-regulated genes were analyzed separately). The false discovery rate (FDR) adjusted *p*-value [87] was set at a cutoff of 0.05.

5.9. Technical Validation of RNA-seq data by RT-qPCR

cDNA was synthesized from 0.5 µg of total RNA with the iScript™cDNA Synthesis kit (ref. 170-8891, BioRad, CA, USA) in a 20 µL reaction volume, and the conditions were 5 min at 25 °C, 30 min at 42 °C and 5 min at 85 °C.

A normalization step using reference genes was performed for the relative expression of gene expression by means of RT-qPCR [94–97]. Only genes which show stable expression must be employed [39,98].

Four reference gene candidates (Table 7), *GAPDH*, *EF1A*, *COX1*, *NDUFA7*, and six target genes randomly selected (Table 7), *MRP7*, *CYP2B4*, *P5CR*, *SLC6A9*, *FERRITIN*,

CYP2U1, were used in the gene expression study. The candidate reference genes have been successfully employed previously in *P. maximus* [39]. Oligonucleotide primers (Table 7) were synthesized by Integrated DNA Technologies. The specificity of the primers was confirmed by the presence of a single peak in the melting curve and by the presence of a single band of the expected size when PCR products were run in a 2% agarose gel. The PCR amplification efficiency (E) of each transcript was determined by means of Real Time PCR Miner software (Real-time PCR Miner. Available online: http://www.miner.ewindup.info/ (accessed on 15 March 2021) [99]). The mean amplification efficiency (E) of each amplicon (Table 7) was used in the calculation of gene expression.

Real-time qPCR analysis was conducted in technical duplicates and 6 biological replicates, in 96-well reaction plates on an iCycler iQ® Real-time System (BioRad, CA, USA). The PCR final volume was 20 µL, containing 4 µL of 1:5 diluted cDNA (20 ng of cDNA), 10 µL of SsoFast EvaGreen Supermix (ref. 172-5201, Bio-Rad), 400 nM of forward and reverse primers, and 4.4 µL of PCR-grade water. The cycling conditions were: 30 s at 95 °C (initial template denaturation), and 40 cycles of 5 s at 95 °C (denaturation) followed by 10 s at 60 °C (annealing and elongation) and 10 s at 75 °C for fluorescence measurement. At the end of each run a melting curve was carried out: 95 °C for 20 s and 60 °C for 20 s followed by an increase in temperature from 60 to 100 °C (with temperature increases in steps of 0.5 °C every 10 s). Baseline values were automatically determined for all plates using Bio-Rad iCycler iQ software V3.1 (IQ™ Real-Time PCR Detection System). The threshold value was set manually at 100 RFU to calculate the Cq values. Non-reverse transcriptase controls and non-template controls (NTC) were also included in each run.

Gene expression was normalized to reference genes that had stable expression levels [94–97]. The gene expression stability of candidate reference genes was analyzed using three Microsoft Excel based software applications, geNorm V3.5 [97], NormFinder V0.953 [94] and BestKeeper V1 [96]. The non-normalized expression (Q) was calculated using the equation $Q = (1 + E)^{-Cq}$. Then the expression was normalized by dividing it by the normalization factor (the geometric mean of the non-normalized expression of the selected reference genes) [39].

5.10. Statistical Analyses

The data were log-transformed to meet the requirements of normality and homogeneity of variances. The domoic acid concentration and domoic acid burden in control and treated scallops was compared using Student's *t*-test. The normalized expression of target genes (log2-transformed) in treated scallops, in relation to the control group, was also compared using Student's *t*-test. $p < 0.05$ was considered statistically significant. Statistical analyses were carried out with the IBM SPSS Statistics 24.0 package.

Supplementary Materials: The following are available online at https://www.mdpi.com/article/10.3390/toxins13050339/s1, Table S1: Summary of BUSCO analysis results obtained in the transcriptome of *Pecten maximus* digestive gland using the Metazoa database (metazoa_odb10), Figure S1: MA plot showing log2 fold-change as a function of mean log expression level. The red dots represent genes with adjusted *p*-value < 0.05 and FC > 1.5 or <−1.5 (DEGs); the grey dots represent non-DEGs, Figure S2. Volcano plot. The red dots represent genes with adjusted *p*-value < 0.05 and FC > 1.5 or <−1.5 (DEGs); the grey dots represent non-DEGs, Figure S3: Species distribution of the top Blastx hits, File S1: List of differentially expressed genes. Sequence name, description, fold change (FC), FDR adjusted *p*-value (padj) and annotation results are shown, File S2: Nucleotide sequences of differentially expressed genes (in fasta format), File S3: List of transcripts coding for putative glutamate receptors in the digestive gland of *Pecten maximus*, File S4: Annotation of the transcripts expressed in the digestive gland of *P. maximus*. File S5: List of KO (KEGG Orthologs) for the differentially expressed genes and for all genes, File S6: Results of a Blastx search of up-regulated genes against the STRING human protein database (9606.protein.sequences.v10.fa), and list of input proteins in STRING network analysis, File S7: Results of a Blastx search of down-regulated genes against the STRING human protein database (9606.protein.sequences.v10.fa), and list of input proteins in STRING network analysis, File S8: Significantly enriched GO terms in the genes that code for

proteins that showed interactions in the protein network analysis. The first two spreadsheets list the enriched GO terms for the up-regulated and the down-regulated genes respectively, the next two spreadsheets show the enriched GO terms after GO slim.

Author Contributions: Conceptualization, A.J.P., J.B., M.L.P.-P. and J.L.S.; investigation, P.V., A.J.P., J.B., M.L.P.-P., J.C.T., and J.L.S.; data curation, J.C.T.; writing—original draft preparation, A.J.P., J.B., M.L.P.-P. and J.L.S.; writing—review and editing, P.V., A.J.P., J.B., M.L.P.-P., J.C.T., and J.L.S.; funding acquisition, J.B., A.J.P., M.L.P.-P. and J.L.S. All authors have read and agreed to the published version of the manuscript.

Funding: This work has been supported by the Spanish Ministry MINECO (Ministerio de Economía y Competitividad) and FEDER Funds (European Regional Development Fund) of the European Union under the project AGL2012-39972-C02.

Institutional Review Board Statement: Not applicable.

Informed Consent Statement: Not applicable.

Data Availability Statement: The data presented in this study are openly available in the NCBI Sequence Read Archive (BioProject ID PRJNA704533, BioSample accessions: SAMN18043529 to SAMN18043540) and in the Supplementary Materials.

Acknowledgments: We acknowledge Carmen Mariño and Helena Martín (CIMA) for their technical assistance in toxin determination. We thank John Souto for his helpful comments on the English version of the manuscript. We thank INTECMAR for providing the information about the routine monitoring of molluscs and the presence *Pseudo-nitzschia* cells in Galicia (http://www.intecmar.gal (accessed on 15 March 2021)).

Conflicts of Interest: The authors declare no conflict of interest.

References

1. Bates, S.S.; Bird, C.J.; de Freitas, A.S.W.; Foxall, R.; Gilgan, M.; Hanic, L.A.; Johnson, G.R.; McCulloch, A.W.; Odense, P.; Pocklington, R.; et al. Pennate Diatom Nitzschia pungens as the Primary Source of Domoic Acid, a Toxin in Shellfish from Eastern Prince Edward Island, Canada. *Can. J. Fish. Aquat. Sci.* **1989**, *46*, 1203–1215. [CrossRef]
2. Bates, S.S.; Hubbard, K.A.; Lundholm, N.; Montresor, M.; Leaw, C.P. Pseudo-Nitzschia, Nitzschia, and domoic acid: New research since 2011. *Harmful Algae* **2018**, *79*, 3–43. [CrossRef] [PubMed]
3. Lelong, A.; Hégaret, H.; Soudant, P.; Bates, S.S. Pseudo-Nitzschia (Bacillariophyceae) species, domoic acid and amnesic shellfish poisoning: Revisiting previous paradigms. *Phycologia* **2012**, *51*, 168–216. [CrossRef]
4. Pulido, O.M. Domoic Acid Toxicologic Pathology: A Review. *Mar. Drugs* **2008**, *6*, 180–219. [CrossRef]
5. Trainer, V.L.; Bates, S.S.; Lundholm, N.; Thessen, A.E.; Cochlan, W.P.; Adams, N.G.; Trick, C.G. Pseudo-Nitzschia physiological ecology, phylogeny, toxicity, monitoring and impacts on ecosystem health. *Harmful Algae* **2012**, *14*, 271–300. [CrossRef]
6. Zabaglo, K.; Chrapusta, E.; Bober, B.; Kaminski, A.; Adamski, M.; Bialczyk, J. Environmental roles and biological activity of domoic acid: A review. *Algal Res.* **2016**, *13*, 94–101. [CrossRef]
7. Costa, L.G.; Giordano, G.; Faustman, E.M. Domoic acid as a developmental neurotoxin. *NeuroToxicology* **2010**, *31*, 409–423. [CrossRef]
8. Lefebvre, K.A.; Robertson, A. Domoic acid and human exposure risks: A review. *Toxicon* **2010**, *56*, 218–230. [CrossRef]
9. Duncan, P.F.; Brand, A.R.; Strand, Ø.; Foucher, E. Chapter 19—The European Scallop Fisheries for Pecten maximus, *Aequipecten opercularis*, *Chlamys islandica*, and *Mimachlamys varia*. In *Developments in Aquaculture and Fisheries Science*; Shumway, S.E., Parsons, G.J., Eds.; Elsevier: Amsterdam, The Netherlands, 2016; Volume 40, pp. 781–858.
10. Novaczek, I.; Madhyastha, M.; Ablett, R.; Johnson, G.; Nijjar, M.; Sims, D. Uptake, disposition and depuration of domoic acid by blue mussels (*Mytilus edulis*). *Aquat. Toxicol.* **1991**, *21*, 103–118. [CrossRef]
11. Novaczek, I.; Madhyastha, M.S.; Ablett, R.F.; Donald, A.; Johnson, G.; Nijjar, M.S.; Sims, D.E. Depuration of Domoic Acid from Live Blue Mussels (*Mytilus edulis*). *Can. J. Fish. Aquat. Sci.* **1992**, *49*, 312–318. [CrossRef]
12. Blanco, J.; de la Puente, M.B.; Arévalo, F.; Salgado, C.; Moroño, Á. Depuration of Mussels (*Mytilus galloprovincialis*) Con-taminated with Domoic Acid. *Aquat. Living Resour.* **2002**, *15*, 53–60. [CrossRef]
13. Mafra, L.L., Jr.; Bricelj, V.M.; Fennel, K. Domoic acid uptake and elimination kinetics in oysters and mussels in relation to body size and anatomical distribution of toxin. *Aquat. Toxicol.* **2010**, *100*, 17–29. [CrossRef]
14. Blanco, J.; Acosta, C.P.; Bermúdez de la Puente, M.; Salgado, C. Depuration and Anatomical Distribution of the Amnesic Shellfish Poisoning (ASP) Toxin Domoic Acid in the King Scallop *Pecten* Maximus. *Aquat. Toxicol.* **2002**, *60*, 111–121. [CrossRef]
15. Blanco, J.; Acosta, C.P.; Mariño, C.; Muñiz, S.; Martín, H.; Moroño, Á.; Correa, J.; Arévalo, F.; Salgado, C. Depuration of domoic acid from different body compartments of the king scallop *Pecten maximusgrown* in raft culture and natural bed. *Aquat. Living Resour.* **2006**, *19*, 257–265. [CrossRef]

16. Blanco, J.; Mauríz, A.; Álvarez, G. Distribution of Domoic Acid in the Digestive Gland of the King Scallop Pecten maximus. *Toxins* **2020**, *12*, 371. [CrossRef]
17. Álvarez, G.; Rengel, J.; Araya, M.; Álvarez, F.; Pino, R.; Uribe, E.; Díaz, P.A.; Rossignoli, A.E.; López-Rivera, A.; Blanco, J. Rapid Domoic Acid Depuration in the Scallop *Argopecten purpuratus* and Its Transfer from the Digestive Gland to Other Organs. *Toxins* **2020**, *12*, 698. [CrossRef]
18. Douglas, D.J.; Kenchington, E.R.; Bird, C.J.; Pocklington, R.; Bradford, B.; Silvert, W. Accumulation of domoic acid by the sea scallop (*Placopecten magellanicus*) fed cultured cells of toxic *Pseudo-Nitzschia multiseries*. *Can. J. Fish. Aquat. Sci.* **1997**, *54*, 907–913. [CrossRef]
19. Madhyastha, M.; Novaczek, I.; Ablett, R.; Johnson, G.; Nijjar, M.; Sims, D. In vitro study of domoic acid uptake by gland tissue of blue mussel (*Mytilus* L.). *Aquat. Toxicol.* **1991**, *20*, 73–81. [CrossRef]
20. Wright, J.L.C.; Boyd, R.K.; de Freitas, A.S.W.; Falk, M.; Foxall, R.A.; Jamieson, W.D.; Laycock, M.V.; McCulloch, A.W.; McInnes, A.G.; Odense, P.; et al. Identification of domoic acid, a neuroexcitatory amino acid, in toxic mussels from eastern Prince Edward Island. *Can. J. Chem.* **1989**, *67*, 481–490. [CrossRef]
21. Mauriz, A.; Blanco, J. Distribution and linkage of domoic acid (amnesic shellfish poisoning toxins) in subcellular fractions of the digestive gland of the scallop *Pecten maximus*. *Toxicon* **2010**, *55*, 606–611. [CrossRef]
22. Dizer, H.; Fischer, B.; Harabawy, A.; Hennion, M.-C.; Hansen, P.-D. Toxicity of domoic acid in the marine mussel *Mytilus edulis*. *Aquat. Toxicol.* **2001**, *55*, 149–156. [CrossRef]
23. Jones, T.; Whyte, J.; Townsend, L.; Ginther, N.; Iwama, G. Effects of domoic acid on haemolymph pH, PCO2 and PO2 in the *Pacific oyster*, *Crassostrea gigas* and the *California mussel*, *Mytilus californianus*. *Aquat. Toxicol.* **1995**, *31*, 43–55. [CrossRef]
24. Jones, T.O.; Whyte, J.N.; Ginther, N.G.; Townsend, L.D.; Iwama, G.K. Haemocyte changes in the pacific oyster, crassostrea gigas, caused by exposure to domoic acid in the diatom *Pseudo-Nitzschia pungens* f. multiseries. *Toxicon* **1995**, *33*, 347–353. [CrossRef]
25. Liu, H.; Kelly, M.S.; Campbell, D.A.; Fang, J.; Zhu, J. Accumulation of Domoic Acid and Its Effect on Juvenile King Scallop<I> Pecten Maximus (Linnaeus, 1758). *Aquaculture* **2008**, *284*, 224–230.
26. Liu, H.; Kelly, M.S.; Campbell, D.A.; Dong, S.L.; Zhu, J.X.; Wang, S.F. Exposure to domoic acid affects larval development of king scallop *Pecten maximus* (Linnaeus, 1758). *Aquat. Toxicol.* **2007**, *81*, 152–158. [CrossRef]
27. Chi, C.; Zhang, C.; Liu, J.; Zheng, X. Effects of Marine Toxin Domoic Acid on Innate Immune Responses in Bay Scallop *Argopecten irradians*. *J. Mar. Sci. Eng.* **2019**, *7*, 407. [CrossRef]
28. Song, J.A.; Choi, C.Y.; Park, H.-S. Exposure to domoic acid causes oxidative stress in bay scallops *Argopecten irradians*. *Fish. Sci.* **2020**, *86*, 701–709. [CrossRef]
29. Pazos, A.J.; Ventoso, P.; Martínez-Escauriaza, R.; Pérez-Parallé, M.L.; Blanco, J.; Triviño, J.C.; Sánchez, J.L. Transcriptional response after exposure to domoic acid-producing Pseudo-Nitzschia in the digestive gland of the mussel *Mytilus galloprovincialis*. *Toxicon* **2017**, *140*, 60–71. [CrossRef]
30. Ventoso, P.; Pazos, A.J.; Pérez-Parallé, M.L.; Blanco, J.; Triviño, J.C.; Sánchez, J.L. RNA-Seq Transcriptome Profiling of the Queen Scallop (Aequipecten Opercularis) Digestive Gland after Exposure to Domoic Acid-Producing Pseudo-Nitzschia. *Toxins* **2019**, *11*, 97. [CrossRef]
31. Hiolski, E.M.; Kendrick, P.S.; Frame, E.R.; Myers, M.S.; Bammler, T.K.; Beyer, R.P.; Farin, F.M.; Wilkerson, H.-W.; Smith, D.R.; Marcinek, D.J.; et al. Chronic low-level domoic acid exposure alters gene transcription and impairs mitochondrial function in the CNS. *Aquat. Toxicol.* **2014**, *155*, 151–159. [CrossRef]
32. Giordano, G.; White, C.C.; Mohar, I.; Kavanagh, T.J.; Costa, L.G. Glutathione Levels Modulate Domoic Acid–Induced Apoptosis in Mouse Cerebellar Granule Cells. *Toxicol. Sci.* **2007**, *100*, 433–444. [CrossRef]
33. Giordano, G.; White, C.C.; McConnachie, L.A.; Fernandez, C.; Kavanagh, T.J.; Costa, L.G. Neurotoxicity of Domoic Acid in Cerebellar Granule Neurons in a Genetic Model of Glutathione Deficiency. *Mol. Pharmacol.* **2006**, *70*, 2116–2126. [CrossRef]
34. Xu, R.; Tao, Y.; Wu, C.; Yi, J.; Yang, Y.; Yang, R.; Hong, D. Domoic acid induced spinal cord lesions in adult mice: Evidence for the possible molecular pathways of excitatory amino acids in spinal cord lesions. *NeuroToxicology* **2008**, *29*, 700–707. [CrossRef]
35. Cabrera, J.; González, P.M.; Puntarulo, S. The Phycotoxin Domoic Acid as a Potential Factor for Oxidative Alterations Enhanced by Climate Change. *Front. Plant. Sci.* **2020**, *11*, 576971. [CrossRef]
36. Tian, D.; Zhang, G. Toxic Effects of Domoic Acid on Caenorhabditis elegans and the Underlying Mechanism. *Int. J. Biol.* **2019**, *11*, v11n3p1. [CrossRef]
37. Pramod, A.B.; Foster, J.; Carvelli, L.; Henry, L.K. SLC6 transporters: Structure, function, regulation, disease association and therapeutics. *Mol. Asp. Med.* **2013**, *34*, 197–219. [CrossRef]
38. Franceschini, A.; Szklarczyk, D.; Frankild, S.; Kuhn, M.; Simonovic, M.; Roth, A.; Lin, J.; Minguez, P.; Bork, P.; von Mering, C.; et al. STRING v9.1: Protein-protein interaction networks, with increased coverage and integration. *Nucleic Acids Res.* **2012**, *41*, D808–D815. [CrossRef]
39. Mauriz, O.; Maneiro, V.; Pérez-Parallé, M.L.; Sanchez, J.L.; Pazos, A.J. Selection of reference genes for quantitative RT-PCR studies on the gonad of the bivalve mollusc *Pecten maximus* L. *Aquaculture* **2012**, *370-371*, 158–165. [CrossRef]
40. Beninger, P.G.; Le Pennec, M. Chapter 3—Scallop Structure and Function. In *Developments in Aquaculture and Fisheries Science*; Shumway, S.E., Parsons, G.J., Eds.; Elsevier: Amsterdam, The Netherlands, 2016; Volume 40, pp. 85–159.

41. Lefebvre, K.A.; Tilton, S.C.; Bammler, T.K.; Beyer, R.P.; Srinouanprachan, S.; Stapleton, P.L.; Farin, F.M.; Gallagher, E.P. Gene Expression Profiles in Zebrafish Brain after Acute Exposure to Domoic Acid at Symptomatic and Asymptomatic Doses. *Toxicol. Sci.* **2008**, *107*, 65–77. [CrossRef]
42. Pérez-Gómez, A.; Tasker, R.A. Domoic Acid as a Neurotoxin. In *Handbook of Neurotoxicity*; Kostrzewa, R.M., Ed.; Springer: New York, NY, USA, 2014; pp. 399–419.
43. Jeffery, B.; Barlow, T.; Moizer, K.; Paul, S.; Boyle, C. Amnesic shellfish poison. *Food Chem. Toxicol.* **2004**, *42*, 545–557. [CrossRef]
44. Ryan, J.; Morey, J.; Ramsdell, J.; van Dolah, F. Acute phase gene expression in mice exposed to the marine neurotoxin domoic acid. *Neuroscience* **2005**, *136*, 1121–1132. [CrossRef] [PubMed]
45. Wang, L.; Huang, Y.; Liang, X.-F.; Li, S.-Y.; Ip, K.-C. Transcriptional responses of xenobiotic metabolizing enzymes, HSP70 and Na+/K+-ATPase in the liver of rabbitfish (*Siganus oramin*) intracoelomically injected with amnesic shellfish poisoning toxin. *Environ. Toxicol.* **2008**, *23*, 363–371. [CrossRef] [PubMed]
46. Anderson, K.; Taylor, D.A.; Thompson, E.L.; Melwani, A.R.; Nair, S.V.; Raftos, D.A. Meta-Analysis of Studies Using Suppression Subtractive Hybridization and Microarrays to Investigate the Effects of Environmental Stress on Gene Transcription in Oysters. *PLoS ONE* **2015**, *10*, e0118839. [CrossRef]
47. Tsunekawa, K.; Kondo, F.; Okada, T.; Feng, G.-G.; Huang, L.; Ishikawa, N.; Okada, S. Enhanced expression of WD repeat-containing protein 35 (WDR35) stimulated by domoic acid in rat hippocampus: Involvement of reactive oxygen species generation and p38 mitogen-activated protein kinase activation. *BMC Neurosci.* **2013**, *14*, 4. [CrossRef]
48. Pinto-Silva, C.R.C.; Moukha, S.; Matias, W.G.; Creppy, E.E. Domoic acid induces direct DNA damage and apoptosis in Caco-2 cells: Recent advances. *Environ. Toxicol.* **2008**, *23*, 657–663. [CrossRef]
49. Giordano, G.; Klintworth, H.; Kavanagh, T.; Costa, L. Apoptosis induced by domoic acid in mouse cerebellar granule neurons involves activation of p38 and JNK MAP kinases. *Neurochem. Int.* **2008**, *52*, 1100–1105. [CrossRef]
50. Lein, P.J.; Supasai, S.; Guignet, M. Chapter 9—Apoptosis as a Mechanism of Developmental Neurotoxicity. In *Handbook of Developmental Neurotoxicology*, 2nd ed.; Slikker, W., Paule, M.G., Wang, C., Eds.; Academic Press: Cambridge, MA, USA, 2018; pp. 91–112. ISBN 978-0-12-809405-1.
51. Kirchgessner, A.L. Glutamate in the enteric nervous system. *Curr. Opin. Pharmacol.* **2001**, *1*, 591–596. [CrossRef]
52. Storto, M.; Vairetti, M.P.; Sureda, F.X.; Riozzi, B.; Bruno, V.; Nicoletti, F. Expression and Function of Metabotropic Glutamate Receptors in Liver. In *Glutamate Receptors in Peripheral Tissue: Excitatory Transmission Outside the CNS*; Gill, S., Pulido, O., Eds.; Springer US: Boston, MA, USA, 2007; pp. 211–217.
53. Du, J.; Li, X.-H.; Li, Y.-J. Glutamate in peripheral organs: Biology and pharmacology. *Eur. J. Pharmacol.* **2016**, *784*, 42–48. [CrossRef]
54. Zafra, F.; Ibáñez, I.; Bartolomé-Martín, D.; Piniella, D.; Arribas-Blázquez, M.; Giménez, C. Glycine Transporters and Its Cou-pling with NMDA Receptors. In *Glial Amino Acid Transporters*; Advances in Neurobiology; Ortega, A., Schousboe, A., Eds.; Springer International Publishing: Cham, Switzerland, 2017; pp. 55–83. ISBN 978-3-319-55769-4.
55. Aragón, C.; López-Corcuera, B. Glycine transporters: Crucial roles of pharmacological interest revealed by gene deletion. *Trends Pharmacol. Sci.* **2005**, *26*, 283–286. [CrossRef]
56. Boissonneault, K.R.; Henningsen, B.M.; Bates, S.S.; Robertson, D.L.; Milton, S.; Pelletier, J.; Hogan, D.A.; E Housman, D. Gene expression studies for the analysis of domoic acid production in the marine diatom *Pseudo-Nitzschia multiseries*. *BMC Mol. Biol.* **2013**, *14*, 25. [CrossRef]
57. Di Dato, V.; Musacchia, F.; Petrosino, G.; Patil, S.; Montresor, M.; Sanges, R.; Ferrante, M.I. Transcriptome sequencing of three Pseudo-Nitzschia species reveals comparable gene sets and the presence of Nitric Oxide Synthase genes in diatoms. *Sci. Rep.* **2015**, *5*, 12329. [CrossRef]
58. Li, Y.; Sun, X.; Zhihui, Y.; Xun, X.; Zhang, J.; Guo, X.; Jiao, W.; Zhang, L.; Liu, W.; Wang, J.; et al. Scallop genome reveals molecular adaptations to semi-sessile life and neurotoxins. *Nat. Commun.* **2017**, *8*, 1–11. [CrossRef]
59. Xun, X.; Cheng, J.; Wang, J.; Li, Y.; Li, X.; Li, M.; Lou, J.; Kong, Y.; Bao, Z.; Hu, X. Solute carriers in scallop genome: Gene expansion and expression regulation after exposure to toxic dinoflagellate. *Chemosphere* **2020**, *241*, 124968. [CrossRef]
60. Vardimon, L.; Ben-Dror, I.; Avisar, N.; Shiftan, L.; Kruchkova, Y.; Oren, A. Regulation of glutamine synthetase in normal and injured neural tissues. *Gene Funct. Dis.* **2001**, *2*, 83–88. [CrossRef]
61. Zou, J.; Wang, Y.-X.; Dou, F.-F.; Lü, H.-Z.; Ma, Z.-W.; Lu, P.-H.; Xu, X.-M. Glutamine synthetase down-regulation reduces astrocyte protection against glutamate excitotoxicity to neurons. *Neurochem. Int.* **2010**, *56*, 577–584. [CrossRef]
62. Fleischer-Lambropoulos, E.; Kazazoglou, T.; Geladopoulos, T.; Kentroti, S.; Stefanis, C.; Vernadakis, A. Stimulation of glutamine synthetase activity by excitatory amino acids in astrocyte cultures derived from aged mouse cerebral hemispheres may be associated with non-n-methyl-d-aspartate receptor activation. *Int. J. Dev. Neurosci.* **1996**, *14*, 523–530. [CrossRef]
63. Lehmann, C.; Bette, S.; Engele, J. High extracellular glutamate modulates expression of glutamate transporters and glutamine synthetase in cultured astrocytes. *Brain Res.* **2009**, *1297*, 1–8. [CrossRef]
64. Hogberg, H.T.; Bal-Price, A.K. Domoic Acid-Induced Neurotoxicity Is Mainly Mediated by the AMPA/KA Receptor: Comparison between Immature and Mature Primary Cultures of Neurons and Glial Cells from Rat Cerebellum. *J. Toxicol.* **2011**, *2011*, 543512. [CrossRef]
65. Krishnan, N.; Dickman, M.B.; Becker, D.F. Proline modulates the intracellular redox environment and protects mammalian cells against oxidative stress. *Free Radic. Biol. Med.* **2008**, *44*, 671–681. [CrossRef]

66. Kenny, N.J.; McCarthy, S.A.; Dudchenko, O.; James, K.; Betteridge, E.; Corton, C.; Dolucan, J.; Mead, D.; Oliver, K.; Omer, A.D.; et al. The gene-rich genome of the scallop *Pecten maximus*. *GigaScience* **2020**, *9*, 9. [CrossRef]
67. Gerdol, M.; Gomez-Chiarri, M.; Castillo, M.G.; Figueras, A.; Fiorito, G.; Moreira, R.; Novoa, B.; Pallavicini, A.; Ponte, G.; Roumbedakis, K.; et al. Immunity in Molluscs: Recognition and Effector Mechanisms, with a Focus on Bivalvia. In *Advances in Comparative Immunology*; Springer International Publishing: Cham, Switzerland, 2018; pp. 225–341. ISBN 978-3-319-76768-0.
68. Hégaret, H.; da Silva, P.M.; Wikfors, G.H.; Haberkorn, H.; Shumway, S.E.; Soudant, P. In vitro interactions between several species of harmful algae and haemocytes of bivalve molluscs. *Cell Biol. Toxicol.* **2011**, *27*, 249–266. [CrossRef]
69. Gerdol, M.; Venier, P. An updated molecular basis for mussel immunity. *Fish. Shellfish. Immunol.* **2015**, *46*, 17–38. [CrossRef]
70. Zhang, G.; Fang, X.; Guo, X.; Li, L.; Luo, R.; Xu, F.; Yang, P.; Zhang, L.; Wang, X.; Qi, H.; et al. The oyster genome reveals stress adaptation and complexity of shell formation. *Nat. Cell Biol.* **2012**, *490*, 49–54. [CrossRef]
71. Cheng, J.; Xun, X.; Kong, Y.; Wang, S.; Yang, Z.; Li, Y.; Kong, D.; Wang, S.; Zhang, L.; Hu, X.; et al. Hsp70 gene expansions in the scallop *Patinopecten yessoensis* and their expression regulation after exposure to the toxic dinoflagellate *Alexandrium catenella*. *Fish. Shellfish. Immunol.* **2016**, *58*, 266–273. [CrossRef]
72. Chi, C.; Giri, S.S.; Jun, J.W.; Kim, S.W.; Kim, H.J.; Kang, J.W.; Park, S.C. Detoxification- and Immune-Related Transcriptomic Analysis of Gills from Bay Scallops (*Argopecten irradians*) in Response to Algal Toxin Okadaic Acid. *Toxins* **2018**, *10*, 308. [CrossRef]
73. Núñez-Acuña, G.; Aballay, A.E.; Hégaret, H.; Astuya, A.P.; Gallardo-Escárate, C. Transcriptional responses of Mytilus chilensis exposed in vivo to saxitoxin (STX). *J. Molluscan Stud.* **2013**, *79*, 323–331. [CrossRef]
74. Cao, R.; Wang, D.; Wei, Q.; Wang, Q.; Yang, D.; Liu, H.; Dong, Z.; Zhang, X.; Zhang, Q.; Zhao, J. Integrative Biomarker Assessment of the Influence of Saxitoxin on Marine Bivalves: A Comparative Study of the Two Bivalve Species Oysters, *Crassostrea gigas*, and *Scallops*, *Chlamys farreri*. *Front. Physiol.* **2018**, *9*, 1173. [CrossRef]
75. Mello, D.F.; de Oliveira, E.S.; Vieira, R.C.; Simões, E.; Trevisan, R.; Dafre, A.L.; Barracco, M.A. Cellular and Transcriptional Responses of Crassostrea gigas Hemocytes Exposed in Vitro to Brevetoxin (PbTx-2). *Mar. Drugs* **2012**, *10*, 583–597. [CrossRef]
76. Pennec, G.L.; Pennec, M.L.; Beninger, G. Seasonal Digestive Gland Dynamics of the Scallop Pecten Maximus in the Bay of Brest (France). *J. Mar. Biol. Assoc. UK* **2001**, *81*, 663–671. [CrossRef]
77. Henry, M.; Boucaud-Camou, E.; Lefort, Y. Functional micro-anatomy of the digestive gland of the scallop *Pecten maximus* (L.). *Aquat. Living Resour.* **1991**, *4*, 191–202. [CrossRef]
78. Ricard-Blum, S. The Collagen Family. *Cold Spring Harb. Perspect. Biol.* **2011**, *3*, a004978. [CrossRef] [PubMed]
79. Stobo, L.A.; Lacaze, J.-P.; Scott, A.C.; Petrie, J.; Turrell, E.A. Surveillance of algal toxins in shellfish from Scottish waters. *Toxicon* **2008**, *51*, 635–648. [CrossRef] [PubMed]
80. Schulz, M.H.; Zerbino, D.R.; Vingron, M.; Birney, E. Oases: Robust de novo RNA-seq assembly across the dynamic range of expression levels. *Bioinformatics* **2012**, *28*, 1086–1092. [CrossRef] [PubMed]
81. Grabherr, M.G.; Haas, B.J.; Yassour, M.; Levin, J.Z.; Thompson, D.A.; Amit, I.; Adiconis, X.; Fan, L.; Raychowdhury, R.; Zeng, Q.; et al. Full-length transcriptome assembly from RNA-Seq data without a reference genome. *Nat. Biotechnol.* **2011**, *29*, 644–652. [CrossRef] [PubMed]
82. Seppey, M.; Manni, M.; Zdobnov, E.M. BUSCO: Assessing Genome Assembly and Annotation Completeness. In *Gene Prediction: Methods and Protocols*; Methods in Molecular Biology; Kollmar, M., Ed.; Springer: New York, NY, USA, 2019; pp. 227–245. ISBN 978-1-4939-9173-0.
83. Conesa, A.; Götz, S.; García-Gómez, J.M.; Terol, J.; Talón, M.; Robles, M. Blast2GO: A universal tool for annotation, visualization and analysis in functional genomics research. *Bioinformatics* **2005**, *21*, 3674–3676. [CrossRef] [PubMed]
84. Götz, S.; García-Gómez, J.M.; Terol, J.; Williams, T.D.; Nagaraj, S.H.; Nueda, M.J.; Robles, M.; Talón, M.; Dopazo, J.; Conesa, A. High-throughput functional annotation and data mining with the Blast2GO suite. *Nucleic Acids Res.* **2008**, *36*, 3420–3435. [CrossRef] [PubMed]
85. Kriventseva, E.V.; Kuznetsov, D.; Tegenfeldt, F.; Manni, M.; Dias, R.; A Simão, F.; Zdobnov, E.M. OrthoDB v10: Sampling the diversity of animal, plant, fungal, protist, bacterial and viral genomes for evolutionary and functional annotations of orthologs. *Nucleic Acids Res.* **2019**, *47*, D807–D811. [CrossRef]
86. Langmead, B.; Salzberg, S.L. Fast gapped-read alignment with Bowtie 2. *Nat. Methods* **2012**, *9*, 357–359. [CrossRef]
87. Benjamini, Y.; Hochberg, Y. Controlling the False Discovery Rate: A Practical and Powerful Approach to Multiple Testing. *J. R. Stat. Soc. Ser. B* **1995**, *57*, 289–300. [CrossRef]
88. Altschul, S.F.; Gish, W.; Miller, W.; Myers, E.W.; Lipman, D.J. Basic local alignment search tool. *J. Mol. Biol.* **1990**, *215*, 403–410. [CrossRef]
89. Wang, S.; Zhang, J.; Jiao, W.; Li, J.; Xun, X.; Sun, Y.; Guo, X.; Huan, L.; Dong, B.; Zhang, L.; et al. Scallop genome provides insights into evolution of bilaterian karyotype and development. *Nat. Ecol. Evol.* **2017**, *1*, 120. [CrossRef]
90. Moriya, Y.; Itoh, M.; Okuda, S.; Yoshizawa, A.C.; Kanehisa, M. KAAS: An automatic genome annotation and pathway reconstruction server. *Nucleic Acids Res.* **2007**, *35*, W182–W185. [CrossRef]
91. Szklarczyk, D.; Franceschini, A.; Wyder, S.; Forslund, K.; Heller, D.; Huerta-Cepas, J.; Simonovic, M.; Roth, A.; Santos, A.; Tsafou, K.P.; et al. STRING v10: Protein–protein interaction networks, integrated over the tree of life. *Nucleic Acids Res.* **2015**, *43*, D447–D452. [CrossRef]
92. Altschul, S.F.; Madden, T.L.; Schäffer, A.A.; Zhang, J.; Zhang, Z.; Miller, W.; Lipman, D.J. Gapped BLAST and PSI-BLAST: A new generation of protein database search programs. *Nucleic Acids Res.* **1997**, *25*, 3389–3402. [CrossRef]

93. Fisher, R.A. On the Interpretation of χ 2 from Contingency Tables, and the Calculation of P. *J. R. Stat. Soc.* **1922**, *85*, 87. [CrossRef]
94. Andersen, C.L.; Jensen, J.L.; Ørntoft, T.F. Normalization of Real-Time Quantitative Reverse Transcription-PCR Data: A Model-Based Variance Estimation Approach to Identify Genes Suited for Normalization, Applied to Bladder and Colon Cancer Data Sets. *Cancer Res.* **2004**, *64*, 5245–5250. [CrossRef]
95. Bustin, S.A.; Benes, V.; Garson, J.A.; Hellemans, J.; Huggett, J.; Kubista, M.; Mueller, R.; Nolan, T.; Pfaffl, M.W.; Shipley, G.L.; et al. The MIQE Guidelines: Minimum Information for Publication of Quantitative Real-Time PCR Experiments. *Clin. Chem.* **2009**, *55*, 611–622. [CrossRef]
96. Pfaffl, M.W.; Tichopad, A.; Prgomet, C.; Neuvians, T.P. Determination of stable housekeeping genes, differentially regulated target genes and sample integrity: BestKeeper—Excel-based tool using pair-wise correlations. *Biotechnol. Lett.* **2004**, *26*, 509–515. [CrossRef]
97. Vandesompele, J.; de Preter, K.; Pattyn, F.; Poppe, B.; van Roy, N.; de Paepe, A.; Speleman, F. Accurate normalization of real-time quantitative RT-PCR data by geometric averaging of multiple internal control genes. *Genome Biol.* **2002**, *3*. [CrossRef]
98. Volland, M.; Blasco, J.; Hampel, M. Validation of reference genes for RT-qPCR in marine bivalve ecotoxicology: Systematic review and case study using copper treated primary *Ruditapes philippinarum* hemocytes. *Aquat. Toxicol.* **2017**, *185*, 86–94. [CrossRef]
99. Zhao, S.; Fernald, R.D. Comprehensive Algorithm for Quantitative Real-Time Polymerase Chain Reaction. *J. Comput. Biol. J. Comput. Mol. Cell Biol.* **2005**, *12*, 1047–1064. [CrossRef] [PubMed]

ANEXO II PERMISOS PARA PUBLICAR LAS FIGURAS

Las figuras de la Introducción de esta tesis (Figuras 1.1 a 1.8) han sido obtenidas de PubChem y pueden utilizarse sin ningún tipo de permiso especial siempre que se citen adecuadamente, como se indica en https://pubchem.ncbi.nlm.nih.gov/docs/citation-guidelines y se puede ver en la imagen siguiente:

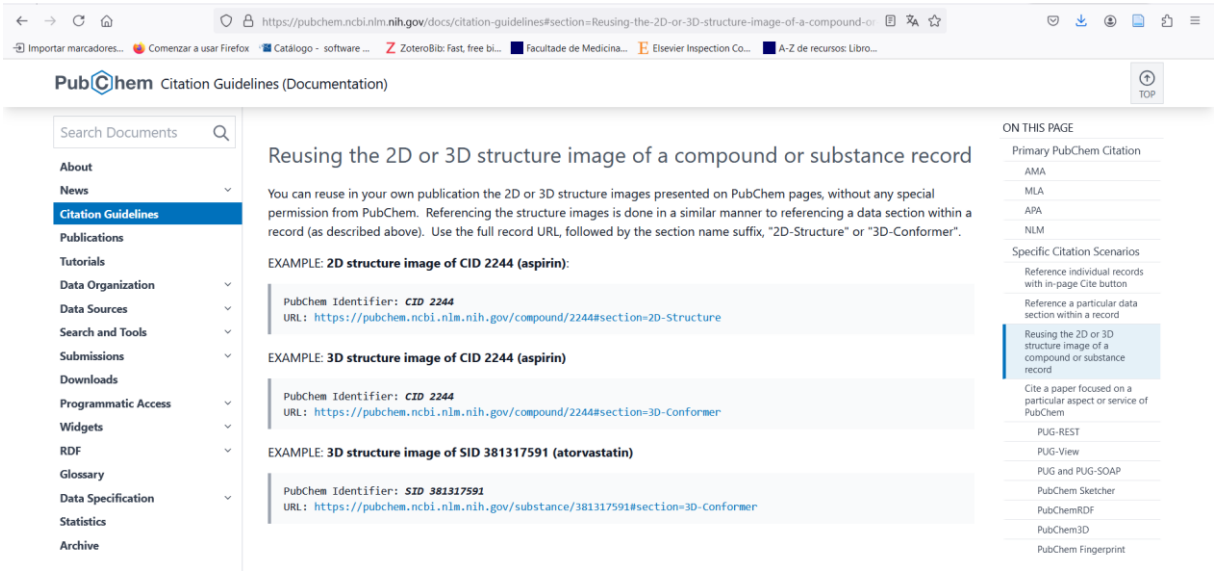

La intoxicación amnésica por mariscos (ASP) es causada por diatomeas del género *Pseudo-nitzschia*, que producen la toxina ácido domoico. El conocimiento de los efectos y los mecanismos moleculares implicados en la captación y excreción del ácido domoico es limitado en moluscos bivalvos.
Para ayudar a esclarecer estos procesos, se ha empleado un enfoque transcriptómico basado en la secuenciación y ensamblaje de novo del RNA en la glándula digestiva de 3 especies de moluscos bivalvos (*M. galloprovincialis*, *A. opercularis* y *P. maximus*) y la determinación de la expresión diferencial en condiciones de exposición al ácido domoico o a *Pseudo-nitzschia* productora de ácido domoico.